

Temporal Dynamics of Amygdalar Norepinephrine During Pavlovian Threat Conditioning

by

Walter Thomas Piper

A dissertation submitted in partial fulfillment

of the requirements for the degree of

Doctor of Philosophy

Center for Neural Science

New York University

September 2020

Advisor, Joseph E. LeDoux, Ph.D.

© Walter Thomas Piper

All Rights Reserved, 2020

DEDICATION

Dedicated to my partner and best friend, Meredith LaBouff

Also, to my parents, Colleen Fehely Piper and Brian Piper

ACKNOWLEDGMENTS

To all my mentors and advisors throughout my educational journey.

I would especially like to acknowledge my dissertation advisor, Joe LeDoux.

Others in my lab who got me where I am today include Rob Sears, Claudia Farb, Mian Hou, Will Chang, Rodrigo Triana-Del Río, José Oliveira da Cruz, Lorenzo Díaz-Mataix, Vinn Campese, Lauren Branigan, Clark Roberts, Javiera Oyarzun, Justin Moscarello, Rob Simmons, Rebecca Cohen, and many others.

I also must thank my previous advisors including my Masters degree advisor, Sarina Rodrigues Saturn, who helped me rise above so much before I arrived at New York University, and my rotation advisors Chiye Aoki and Dayu Lin.

ABSTRACT

In Pavlovian threat conditioning (PTC), a widely used paradigm for studying implicit threat learning, a previously neutral conditioned stimulus (CS) acquires threatening valence after it co-occurs in time with a painful unconditioned stimulus (US). Acquisition of PTC memory is mediated by lateral amygdala (LA) and expression of PTC memory is mediated by central amygdala (CeA). Acquisition and expression are enhanced by norepinephrine (NE) acting through β -adrenergic receptors (β -ARs), but the naturalistic triggers and temporal dynamics of these effects are unclear, and the anatomical locus of the NE effect on expression is unknown.

First, systemic β -AR blockade was used as a probing strategy to identify triggering stimuli that recruit β -ARs to boost PTC acquisition. Baseline NE levels were insufficient to engage β -ARs in single-trial PTC or excessively spaced multi-trial PTC (40 minutes), but footshocks, signaled by a CS or unsignaled, opened a transient window of β -AR priming for subsequent CS-US pairings. Second, bidirectional NE and β -AR manipulations in CeA robustly modulated PTC expression, but this was not observed in LA, demonstrating the specificity of CeA for PTC expression. Finally, fiber photometry measurements in LA and CeA using fluorophore-conjugated NE receptors revealed temporal dynamics of NE reactions to be largely consistent across stimulus types and across amygdala subnuclei, although the NE reactions were larger and more consistent for footshocks than tones and were larger for the first presentation of a given stimulus compared with later trials of the same stimulus in that session.

Altogether, these observations point to circuitry differences in LA versus CeA downstream from NE release as the point of divergence in NE effects on acquisition versus expression, respectively. Stimulus response dynamics of NE levels, which appeared consistent between LA and CeA, are discussed in relation to theoretical roles of NE.

TABLE OF CONTENTS

| | |
|-----------------------|-----|
| Dedication | iii |
| Acknowledgements | iv |
| Abstract | v |
| List of Figures | vii |
| List of Abbreviations | x |
| List of Appendices | xii |
| Chapter 1 | 1 |
| Chapter 2 | 23 |
| Chapter 3 | 42 |
| Chapter 4 | 65 |
| Chapter 5 | 95 |
| Appendix A | 104 |
| Appendix B | 167 |
| Appendix C | 177 |
| References | 179 |

LIST OF FIGURES

| | |
|--|-----|
| <i>Figure 1.1.</i> General configuration of active defense mechanisms | 105 |
| <i>Figure 1.2.</i> Pavlovian Threat Conditioning | 106 |
| <i>Figure 1.3.</i> Circuits mediating acquisition of associative memory between a nociceptive unconditioned stimulus and an auditory conditioned stimulus | 107 |
| <i>Figure 1.4.</i> Circuits mediating expression of conditioned responses to an auditory conditioned stimulus | 109 |
| <i>Figure 2.1.</i> Long-term threat memory (LTM) is impaired by pretraining propranolol (10 mg/kg) in animals conditioned with 2 CS-US pairing trials but not in animals that received 1 CS-US trial. | 110 |
| <i>Figure 2.2.</i> The enhancement of freezing during long-term memory test induced by the preexposure to an unsignaled footshock (U-US) before single-trial weak conditioning is prevented by pretraining propranolol. | 112 |
| <i>Figure 2.3.</i> The norepinephrine enhancement of acquisition of long-term threat memory depends on the length of ITI during training. | 114 |
| <i>Figure 3.1</i> Norepinephrine β -AR activity is required for CS-elicited freezing responses. | 116 |
| <i>Figure 3.2</i> Chemogenetic inhibition of LC-NE signaling decreases CS-elicited freezing in threat-conditioned animals | 118 |
| <i>Figure 3.3</i> Chemogenetic activation of LC-NE signaling increases CS-elicited freezing in threat-conditioned animals | 120 |
| <i>Figure 3.4</i> CeA blockade of β -ARs or chemogenetic inhibition of LC-NE axon terminals in the CeA decreases CS-elicited freezing | 122 |
| <i>Figure 3.5</i> Chemogenetic activation of LC-NE terminals in CeA increases CS-elicited freezing behavior and is blocked by β -AR antagonist | 124 |

| | |
|--|-----|
| <i>Supplementary Figure 3.1.</i> Virus and CeA cannulation targeting for all experiments ... | 126 |
| <i>Supplementary Figure 3.2.</i> Representative image of DBH+ and HA co-localization in hM3Dq/hM4Di LC rats | 128 |
| <i>Supplementary Figure 3.3.</i> Experiments using axon terminal manipulations require longer incubation periods | 130 |
| <i>Supplementary Figure 3.4.</i> β -ARs are required for Pavlovian defensive responses, regardless of US intensity or memory age | 132 |
| <i>Supplementary Figure 3.5.</i> Control experiments to validate DREADD functionality and rule out noradrenergic BLA contributions to expression of conditioned freezing | 134 |
| <i>Figure 4.1.</i> Schematic of fiber photometry system | 136 |
| <i>Figure 4.2.</i> Surgical and experimental timeline | 137 |
| <i>Figure 4.3.</i> Visualization of the applied markers | 139 |
| <i>Figure 4.4.</i> Representative recordings at photodetectors | 140 |
| <i>Figure 4.5.</i> Demonstration of dual lock-in amplification | 141 |
| <i>Figure 4.6.</i> Least Squares optimization was effective for separating superimposed sinusoids. | 143 |
| <i>Figure 4.7.</i> Examples of extracted amplitude signals | 144 |
| <i>Figure 4.8.</i> Preliminary analysis of sessions after only 3 weeks viral incubation. | 146 |
| <i>Figure 4.9.</i> Demodulated data from UUS trial | 148 |
| <i>Figure 4.10.</i> Representative recordings of Yohimbine- vs. Saline-treated animals | 150 |
| <i>Figure 4.11.</i> Yohimbine experiment comparison between channels within subjects | 152 |
| <i>Figure 4.12.</i> Yohimbine experiment comparison between treatments | 153 |
| <i>Figure 4.13.</i> ARIMAX-model forecasted baseline | 154 |
| <i>Figure 4.14.</i> NE reactions to unsignaled footshocks | 155 |
| <i>Figure 4.15.</i> NE reactions to conditioned tones | 156 |

| | |
|---|-----|
| <i>Figure 4.16.</i> NE dynamics during discriminative PTC | 157 |
| <i>Figure 4.17.</i> Output coordinates from DeepLabCut (DLC) are Bayesian-likelihood-weighted image coordinates | 158 |
| <i>Figure 4.18.</i> Estimated position of a single animal's head points in a 1080p resolution video of the conditioning context | 159 |
| <i>Figure 4.19.</i> Correcting for asymmetric artifacts through identification of novel exogenous variables | 160 |
| <i>Figure 4.20.</i> Manually generated anticorrelated artifact | 162 |
| <i>Figure 4.21.</i> Discriminative PTC reveals conditioned-arousal-like effects in the dynamics of NE responses to tone over trials. | 163 |
| <i>Figure 4.22.</i> Discriminative LTM shows a continuation of conditioned-arousal-like effects. | 165 |
| <i>Figure B.1.</i> Histological samples from animal #95. | 169 |
| <i>Figure B.2.</i> Histological samples from animal #96. | 170 |
| <i>Figure B.3.</i> Histological samples from animal #98. | 171 |
| <i>Figure B.4.</i> Histological samples from animal #99. | 172 |
| <i>Figure B.5.</i> Histological samples from animal #00. | 173 |
| <i>Figure B.6.</i> Histological samples from animal #01. | 174 |
| <i>Figure B.7.</i> Histological samples from animal #05. | 175 |
| <i>Figure B.8.</i> Histological samples from animal #06. | 176 |
| <i>Figure C.1.</i> Serotonergic 1A/1B agonism in CeA modulates conditioned freezing. | 178 |

LIST OF ABBREVIATIONS

| | |
|---------------|--|
| ACh | Acetylcholine |
| BA | Basal Amygdala |
| BL | Baseline |
| CeA | Central Amygdala |
| CeC | Capsular part of Central Amygdala |
| CeL | Lateral part of Central Amygdala |
| CeM | Medial part of Central Amygdala |
| CNO | Clozapine-N-oxide |
| CS | Conditioned Stimulus |
| DREADD | Designer receptor exclusively activated by designer drug |
| GFP | Green fluorescent protein |
| hM3Dq | G_q -coupled excitatory DREADD |
| hM4Di | $G_{i/o}$ -coupled inhibitory DREADD |
| LA | Lateral Amygdala |
| LC | Locus coeruleus |
| LTM | Long-term memory |
| NE | Norepinephrine |
| NE2h | GFP-conjugated α_2 -AR |
| PTC | Pavlovian Threat Conditioning |
| PTSD | Post-traumatic stress disorder |
| US | Unconditioned Stimulus |

| | |
|---------------------------------|-----------------------------------|
| U-US | Unsignaled Unconditioned Stimulus |
| α_1-AR | Alpha-1 adrenergic receptor |
| α_2-AR | Alpha-2 adrenergic receptor |
| β-AR | Beta adrenergic receptor |

LIST OF APPENDICES

| | |
|--|-----|
| Appendix A - Figures and Figure captions | 104 |
| Appendix B - Microscope Images for Fiber Photometry Animals from Chapter 4 | 167 |
| Appendix C - Additional Works | 177 |

CHAPTER 1

Threat learning and the brain

The ability to avoid harm is critical for all organisms. From a functional perspective, this is obvious. Many threats are existential; the failure to avoid them equals death. Over evolutionary timescales, natural selection favors the accumulation of numerous defense mechanisms (LeDoux, 2019). Passive defense mechanisms, such as plasma membranes or animal skin, are ubiquitous, but so are active defense mechanisms. Active mechanisms require, at a minimum, detection of a threat and deployment of a response. This is just as true for plants or microbes as it is for animals, and within animals it is equally true for the immune system and the nervous system.

In animals, the most rapid defense mechanisms typically utilize nervous systems. Neurons are optimized to propagate electrical and chemical signals to other cells on a timescale on the order of milliseconds, and these neural signals are delivered with incredibly high spatial and temporal specificity (Squire et al., 2012). Neurons arranged in circuits can act as coherent populations in order to drive functions that are both consistent and flexible. Sensory circuits collect and process information about the immediate environment. Effector circuits include motor circuits that drive muscular responses, but they also include circuits that inhibit movement or that modulate internal physiology (LeDoux, 1996). In many cases, intermediate circuits between sensory and effector circuits allow modification of the response or changes in the sensory inputs required to trigger the response.

The complexity of the intermediate circuits in active defense mechanisms varies widely.

Consider a relatively simple case: the withdrawal reflex. Nociceptive neurons in the periphery detect potentially damaging stimuli and transmit signals via axonal projections to the spinal cord where they innervate motor neurons and interneurons (Derderian & Tadi, 2020). The direct innervation of motor neurons enables rapid movement of a limb away from the nociceptive stimulus, and the innervation of interneurons allows flexible recruitment of additional muscles and provision of pain signals to the brain for further processing.

More complex defense mechanisms require information processing within the brain. Large-scale networks, such as the so-called cognitive networks in the forebrain can enable carefully planned responses to environmental or internal stimuli, integrating both external stimuli and complex internal processes. On the other hand, numerous specialized integrative circuits have evolved to fulfill specific needs. The latter can be called survival circuits (LeDoux, 2012), due to their central role in fulfilling the basic functions of life: consuming food, avoiding danger, reproduction, thermoregulation, et cetera. The specialized nature of survival circuits is optimal for active defense mechanisms, which require reliable detection of threats and rapid responses. Neuromodulators can tune and adjust the properties of specialized circuits, leading to greater adaptation over time within individuals. Neural plasticity in survival circuits enables implicit learning to occur largely independent of high-level networks.

Without any prior experience, survival circuits can rely on innate neural arrangements (LeDoux, 2012; Silva et al., 2016). Some active defense strategies are entirely innate, such as the withdrawal reflex (Derderian & Tadi, 2020) or the reflex to flinch away from a quickly approaching visual stimulus (Ball & Tronick, 1971). In these cases, an innate reflex is triggered by specific types of sensory signals that are recognized by almost all members of a species, regardless of individual experience. However, these purely innate reflexes require a highly

predictive danger signal, lest they waste metabolic resources responding to false alarms, and a danger signal that is both highly predictive and innately recognized typically does not arrive until the organism is already very close to harm.

Fortunately, learning and memory mechanisms allow organisms to react defensively to arbitrary cues that were previously associated with an innate danger signal (LeDoux, 1996). By remembering the significance of such stimuli, the organism can respond sooner, before harm is imminent. In addition to learning the significance of new stimuli, some animals can learn entirely new behaviors through a variety of mechanisms. It must be noted that countless types of learning have been described, especially in vertebrates (B. R. Moore, 2004), but a select few are especially relevant to threat processing.

In summary, survival of a species depends on that species' capacity to avoid harm. This need can be met with passive defense mechanisms or active defense mechanisms, the latter of which requires recognition of a threat and deployment of a response. Numerous survival circuits have evolved to recognize and respond to biologically significant stimuli to fulfill specific needs, including defense, without depending on high-level cognitive circuits (LeDoux, 2012, 2014; LeDoux & Pine, 2016; Mobbs & LeDoux, 2018). In some species, especially animals, learning mechanisms expand the threat recognition and response repertoire beyond innate capabilities. In general, mammals can detect both innately recognized threats and learned threats and respond with either innate reactions or learned actions. The philosophical relationships between threat detection and defensive behavior and between innate and learned processes are illustrated in Figure 1.1.

Types of threat learning

Obviously, humans have unique learning capabilities that rely on advanced cognition.

Our capacities for symbolic communication and logical reasoning enable us to learn from story-telling, semantic knowledge, or logical operations on semantic knowledge (Olsson & Phelps, 2007). Our frontal, parietal, and temporal cortex regions are especially advanced compared to most other animals (Eichenbaum, 2000). Nevertheless, we humans still have implicit memory systems that operate non-consciously in ways that can be independent from or informed by explicit memory (LeDoux, 2019). While explicit understanding of stimuli might be achieved by higher-order networks, explicit understanding is not required for implicit memory to trigger defensive reactions (LeDoux, 1996). In contrast to the circuits mediating conscious awareness, the circuits mediating implicit threat learning are highly conserved across mammalian species (LeDoux, 2019).

The evolutionary proliferation of learning systems in the mammalian brain complicates any attempt to be both accurate and complete in describing all possible threat learning mechanisms (B. R. Moore, 2004). However, a handful of learning systems are especially reliable under threat, with some systems able to produce robust behavioral changes with as little as 1 trial of learning.

Pavlovian Conditioning

One well-studied learning paradigm that flexibly recruits multiple neural systems is Pavlovian conditioning (Pavlov, 1927). In this paradigm, a conditioned stimulus (CS) is introduced immediately before or coincident with an innately recognized unconditioned stimulus (US), and associative learning causes future presentations of the CS to trigger reactions relevant to the US (Fig. 1.2). It was originally conceived of as a pure stimulus-stimulus substitution, with the CS gaining control of the exact effectors that the US recruited, but this was inaccurate (Rescorla, 1988). For example, an electric shock, being a US, triggers rapid

withdrawal and escape behavior, but an auditory or visual CS previously associated with the US will trigger freezing, a different behavior altogether. Furthermore, the exact behaviors triggered by a CS are flexible, and temporal or contextual factors like perceived imminence of the US can change the responses being made (Fanselow, 2018). Instead, Pavlovian conditioning is better described as learning an association between events (Rescorla, 1988), or as a change in the meaning of the CS (LeDoux, 2014).

The neural circuits for Pavlovian conditioning are quite diverse. Different subtypes of Pavlovian conditioning are mediated by different circuits, and widely distributed neural systems cooperate to manage the dynamics of conditioning. For example, eyeblink classical conditioning, in which the US is an air puff to the eye or a shock to the eyelid, engages plasticity in the cerebellum to acquire the CS-US association (Thompson & Steinmetz, 2009). In contrast, most subtypes that use a nociceptive US, such as a footshock, engage plasticity in the amygdala (Blair et al., 2001; Grewe et al., 2017; Quirk et al., 1997). The medial prefrontal cortex provides inputs to amygdala that modulate threat learning and facilitate extinction learning (Giustino & Maren, 2015; Maren & Quirk, 2004; Morgan et al., 1993; Uematsu et al., 2017). The hippocampus, which is adjacent to the amygdala, is necessary for conditioning a spatial CS (Anagnostaras et al., 2001; Phillips & LeDoux, 1992) or if a time gap is inserted between CS and US (Bangasser et al., 2006). Hippocampal connections with the amygdala allow a hybrid memory that recruits both amygdalar and hippocampal memory systems (Anagnostaras et al., 2001; LeDoux, 2000).

Instrumental Conditioning

Instrumental conditioning is a form of learning about successful actions through associations with outcomes (B. R. Moore, 2004). The striatum is necessary for learning action-

outcome associations (Schönberg et al., 2007). CS-action-outcome relationships (CS-triggered action to avoid a threatening outcome) also recruit the striatum through amygdalar projections from basal amygdala (BA) (Ramirez et al., 2015). In a distinct process, a separately trained Pavlovian CS can invigorate the expression of an action-outcome memory via functional connections of the central amygdala (CeA) with the striatum, if the paired Pavlovian US was the same stimulus that was used to train the instrumental action-outcome association (Campese et al., 2013, 2014, 2017).

Explicit Memory Systems

Explicit (consciously accessible) memory in humans is known to be mediated by the temporal cortex. A lack of language in non-human animals means that the “hard problem” of animal consciousness is fundamentally unanswerable, making the label of explicit memory inappropriate for non-humans (Mobbs et al., 2019). Nevertheless, temporal cortex circuits in non-human mammals are known to mediate some similar memory phenomena, including object recognition and the mapping of relationships between stimuli in a spatiotemporal context. Patterns of neural connectivity in the temporal cortex are somewhat different between species (Manns & Eichenbaum, 2006), although the impact of these differences are not entirely known.

Mechanistic study of threat processing requires precise language

This dissertation focuses on a form of Pavlovian conditioning that pairs an auditory CS with a nociceptive US. Although Pavlovian conditioning is a non-conscious process, published works on the topic has often been misinterpreted as a conscious emotional process (LeDoux, 2014). Before advancing further, it is important to address this controversy as it regards terminology. Traditionally, Pavlovian conditioning with a threatening US has been called ‘fear conditioning’. Despite the use of the word ‘fear’, the conceptualization of the paradigm does not

include a subjective experience of fear. To avoid confusing language, this document will use an alternative term, ‘Pavlovian threat conditioning’ (PTC) (LeDoux, 2014).

Emotional language in science is ambiguous because there is no universal agreement on the definitions of emotion and consciousness (LeDoux, 2017). Scientists use different definitions, and this often leads to differing psychological constructs being used under the same name. Some of the most common theoretical perspectives on emotion, consciousness, and motivated behavior are incompatible with each other. Some scientists still prefer the old behaviorist perspective that emotion and consciousness can be safely ignored (Fanselow & Pennington, 2018). Other scientists pursue basic emotion theory, the view that human neurobiology necessitates a consistent set of basic emotions that are nearly identical in all humans, regardless of individual socialization and culture (Sauter et al., 2010). Others engage with various cognitive frameworks with various hypotheses about the interaction of body and mind (Damasio & Carvalho, 2013; Gendron & Feldman Barrett, 2009). In the hands of a skilled neuroscientist, any framework could be used, provided the constructs are thoroughly explained. All too often, however, constructs like ‘fear’ are not explicitly defined.

Vague theoretical descriptions and terms can encourage readers to fill in the gaps with their own beliefs. Even if emotional language is avoided entirely, there are plenty of other terms like ‘cognition’ and ‘motivation’ that are vague when not presented with a precise definition.

In addition, fundamental barriers in our ability to observe consciousness (aside from one’s own) are problematic because many of the disagreements about emotion regard its relationship to consciousness. Both emotion and consciousness sit so close to high-level mental functions like explicit memory, language, attention, perception, and deliberation, and the neural circuits known to facilitate these are also closely connected to some of the nonconscious

learning systems in question. The related inability to establish reciprocal causality between consciousness and physiology prevent the reliable use of evolutionary logic, which is usually so important in biology. Some philosophers have made evolutionary arguments about concrete roles of consciousness (Pierson & Trout, 2017), but these hypotheses might never be confirmed by empirical research.

These blind spots are problematic when researchers study complex processes that combine neural networks underlying learning, inference of stimulus relationships, behavior, and allostatic physiological responses. because relevant definitions and unspoken assumptions often get left out for the sake of brevity. The words ‘fear’ and ‘emotion’ are left unclear when the underlying frameworks are not divulged in every publication.

Therefore, I will clearly state here what conceptual frameworks I am using. My overall scientific perspective is based on the laws of thermodynamics and the basic rules of logic. Evolution of complex systems, including life and nervous systems, is explainable through thermodynamics and logic (Buzsáki, 2006; Gleick, 1988; Schreiber & Gimbel, 2010). I seek to be agnostic about nature of human consciousness, except that it exists. I am completely agnostic about the existence of non-human animal consciousness, because I do not expect any empirical observations on non-human animal consciousness to be made, given the lack of advanced symbolic language outside the species *Homo sapiens*.

My use of ‘threat’ instead of ‘fear’ is consistent with a conceptualization of PTC as a process of implicitly making and remembering an inference regarding the predictive meaning of a CS, without making claims about downstream mental and perceptual functions beyond those immediately involved in representing the CS and US. I believe using the word ‘fear’ for operationalized constructs would presuppose a theoretical conclusion that has not been

reached. Mindful of all these uncertainties, I wish to minimize confusion by avoiding the use of emotional language as much as possible.

I do not reject the idea that implicit threat processing circuits might interact with conscious experience. On the contrary, our detailed knowledge of neural circuits in humans and other mammals is poised open this avenue of investigation. There is no shortage of plausible candidate circuits for interactions between subjective experience and implicit threat processing. For example, connections between amygdalar and hippocampal/parahippocampal circuits could be examined by relating existing literature on human episodic memory to the extensive literature on spatiotemporal contextual representations in threat learning.

I choose to use the concept of ‘survival circuits’ because mounting evidence suggests that integrative neural circuits mediating innately defined behavioral and physiological reactions are largely distinct from subjective experience circuits (LeDoux, 2012, 2014, 2020; LeDoux & Pine, 2016; Mobbs & LeDoux, 2018), as opposed to a contrasting framework in which both phenomena are two manifestations of one neural process. This is not a trivial controversy. Strictly speaking, the entire central nervous system is one network, and plenty of neural circuits are candidates for bridging the two processes. On the other hand, no current theory of emotion would claim that subjectively experienced emotion is exact same process as emotional behavior or autonomic reactions, although there may be interactions between these processes.

Interestingly, a new basic emotion theory recently proposed (Scarantino, 2018) uses an opposing philosophical and semantic approach but ends up at a very similar two-system framework where the activation of nonconscious threat-responsive circuits is called ‘basic fear’. ‘Feelings of fear’ is a term to describe the subjective experience of fear. The only substantial difference between the two-systems model with ‘survival circuits’ (LeDoux & Pine, 2016) and the

two-systems model with ‘basic emotions’ (Scarantino, 2018) is in how ‘emotion’ is semantically defined. Scarantino (2018) argues emotional language should be used for both systems because colloquial language uses the same words for emotional behaviors as for subjectively experienced emotion.

I disagree and would argue that colloquial use of the same words to describe multiple distinct concepts is reason to avoid those words in mechanistic research. In my view, nonconscious processes should be described primarily in physiological terms, with functional explanations withheld unless they can be thoroughly supported. Appeals to mental states should be reserved solely for the contents of human consciousness.

None of the research presented in this document is on subjective experience, so I will make no further mention of consciousness, emotion, or fear, except when citing human research. Existing literature on ‘fear conditioning’ will be introduced as ‘Pavlovian Threat Conditioning’ (PTC), as the latter term was introduced for the express purpose of replacing the former without changing the underlying construct (LeDoux, 2014).

Neural motifs for Pavlovian threat conditioning

Biological significance can be associated with a neural representation of a CS by neural plasticity in circuits that integrate general sensory inputs with inputs that represent innately recognized stimuli, and in doing so are implicitly making predictive or causal inferences. In associative threat learning, the optimal circuits would selectively induce plasticity in CS-specific sensory inputs that are active coincidentally with a threat-specific teaching signal, which could be a representation of the US or something activated by the US. One unique structure that fits this description is the amygdala, a subcortical temporal lobe structure with multiple relevant subnuclei (LeDoux, 2000, 2007). The lateral subnucleus of the amygdala (LA) receives

extensive weak inputs from the visual, auditory, and somatosensory systems and receives strong nociceptive inputs that act as a teaching signal (Ozawa & Johansen, 2018). The basal subnucleus of the amygdala (BA) and intercalated cell groups of the amygdala (ITC) act as integrative hubs, flexibly recruiting other neural structures as needed. The central subnucleus of the amygdala (CeA) serves as an output structure for coordinating a repertoire of innate reactions to threat.

Plasticity in LA is especially critical for acquisition of the CS-US associative memory. As the CS representations in LA shift to resemble the US representation in LA (Blair et al., 2001; Grewel et al., 2017; Johansen et al., 2010; Rodrigues, Schafe, et al., 2004), ascending nociceptive signals are inhibited by a negative feedback pathway from central amygdala (CeA) to ventrolateral periaqueductal gray (vIPAG) to the rostroventral medulla (Ozawa et al., 2017). This property allows for asymptotic learning, which is a key property of Pavlovian conditioning (Rescorla & Wagner, 1972).

The relative functions of LA/BLA versus CeA are also observed in human neuroimaging (Michely et al., 2020), where CeA activity was elevated by shock US regardless of expectations, and LA/BLA activity tracked expectations, increasing after unexpected shocks and decreasing after omitted expected shocks. Important contributions of prefrontal cortex are also consistent between humans and other model species (Schiller et al., 2013). The dynamics of the human amygdala has in itself become a fascinating model for understanding the amygdala across species (Phelps & LeDoux, 2005).

This initial associative plasticity in LA is soon followed by distributed learning in other brain regions, which undergo memory-related plasticity on a slower time scale than LA. This includes CeA, sensory cortex areas, and thalamic areas previously identified as relays for the

relevant sensory signals (J. H. Han et al., 2008; McEchron et al., 1996).

Thus, these survival circuits are ideally located for plasticity mechanisms to establish robust threat learning. Neural plasticity in these critical nodes must lead to a selective receptivity to the learned danger signal in the future.

Learning and remembering the CS-US association requires multi-step processes with distinct functions and coordinated molecular mechanisms (Bauer et al., 2002; Johansen et al., 2010; Rodrigues, Farb, et al., 2004; Schiff et al., 2017). Acquisition mechanisms are required at the time of CS-US pairing to encode the associative memory. Consolidation mechanisms must then stabilize the CS-US association into long-term memory, which typically requires new RNA and protein synthesis. When the CS is presented alone later, retrieval mechanisms enable defensive reactions, but the associative memory then becomes labile, and reconsolidation mechanisms must restabilize it (Dębiec & LeDoux, 2004; Nader et al., 2000). Disrupting any of these steps can impair defensive reactions to the CS, although experimental separation of these processes is possible through appropriate research design (Rodrigues, Schafe, et al., 2004).

PTC is critically dependent on the amygdala

In mammals and other vertebrates, a survival circuit in the amygdala mediates PTC (LeDoux, 1996). This was discovered when two areas of research on Pavlovian conditioning converged on the amygdala, one finding the CeA to mediate CS-triggered autonomic reactions (Kapp et al., 1979), and the other finding a critical role for auditory thalamus to LA projections in memory formation of CS-US associations (LeDoux et al., 1984, 1986; LeDoux, Cicchetti, et al., 1990; LeDoux, Farb, et al., 1990). It soon became clear that the LA served as a major sensory interface, receiving inputs from multiple sensory systems, and that acquisition of CS-US associations depended on the LA.

In a simplified model of the amygdala PTC circuit, the LA transmits CS- and US-related signals to the basolateral subnucleus of the amygdala (BLA), which in turn transmits to central amygdala (CeA) to trigger innate behavioral reactions like freezing via efferents to the periaqueductal gray and physiological changes via efferents to multiple hypothalamic circuits (LeDoux et al., 1988). Alternatively, the BLA can transmit to the striatum in order to trigger learned instrumental actions to avoid a threat (Ramirez et al. 2015) (Fig. 1.3).

In rats, stimulus representations are sent to the LA from sensory processing regions of the thalamus or cerebral cortex (Fig. 1.3). The LA responds to aversive stimuli by recruiting downstream circuits that drive defensive reactions. When the stimulus is a US, the amygdala can trigger defensive reactions without prior learning. When a CS and US are paired, neurons in the LA undergo synaptic plasticity, causing future presentations of the CS to evoke downstream defensive reactions (Fig. 1.4).

It must be noted that the central amygdala (CeA) also experiences some plasticity during PTC (Paré et al., 2004; Wilensky et al., 2006), although the architecture and development of CeA is much different from LA (Swanson & Petrovich, 1998). While CeA is striatum-like and operates like a switchboard with multiple layers of inhibitory neurons (S. Lee et al., 2013; Ressler & Maren, 2019), the LA consists of 80% excitatory neurons in a mesh of inhibitory interneurons (Krabbe et al., 2018). This LA arrangement allows robust ensemble encoding by recruiting the most excitable principal neurons into coherent memory traces (F. Feng et al., 2016). The CeA has a medial part, which is the primary source of outputs to many other circuits, and a lateral part with PKC-delta+ interneurons (OFF cells) that inhibit the medial part, and somatostatin+ interneurons (ON cells) that inhibit the OFF cells (Ciocchi et al., 2010).

Encoding of CS representations in distributed circuits

Naturally, the ability to learn CS-US associations and the potentially lifelong stability of the resulting memory have provoked much research on molecular and cellular mechanisms. Perhaps the most straight-forward explanation is calcium-mediated associative plasticity in LA (Blair et al., 2001). This builds on the theory of synaptic plasticity first postulated by Hebb (1949) and later confirmed by electrophysiological evidence in the hippocampus (Andersen et al., 1977; Bliss & Lomo, 1973; Lynch et al., 1977; Mcnaughton et al., 1978). This synapse-specific plasticity was later observed in LA in vivo (Clugnet & LeDoux, 1990) and in vitro (Weisskopf et al., 1999), and in relation to PTC (Rogan et al., 1997; Rogan & LeDoux, 1995). This LTP was shown to follow the same stimulus contingencies as PTC learning (Bauer et al., 2001). Numerous proteins and receptors linked to calcium signaling were shown to be critical for amygdala function, including calcium/calmodulin-dependent protein kinase II (Rodrigues, Farb, et al., 2004), NMDA receptors and L-type voltage gated calcium channels (Bauer et al., 2002), and downstream activation of extracellular signal-regulated kinase (Schafe et al., 2000). More recently, cell-type-specific LTP was explored in LA using active neuron tagging techniques to optogenetically harness the exact thalamic and cortical inputs that represented the CS (Kim & Cho, 2017), and in BA after contextual conditioning (Kim & Cho, 2020).

Huang and Kandel (1998) demonstrated these Hebbian principles in the external capsule fibers that terminate in LA, which represents the cortical inputs to LA rather than the thalamic inputs. LTP at these cortico-amygdala synapses was shown to be mediated through post-synaptic mechanisms including calcium entry through NMDA receptors and pre-synaptic mechanisms including the kinase protein PKA and its associated cAMP. Interestingly, Weisskopf and colleagues (1999) discovered that LTP at the thalamo-amygdala synapses did not require NMDA receptors. Thalamo-amygdala LTP still depended on calcium, but the calcium at these synapses entered primarily through L-type voltage-gated calcium channels (L-VGCC).

The framework that these LTP studies cumulatively built was expanded upon as an explanation of CS-US learning in LA (Blair et al., 2001). To briefly paraphrase, the neural impulses that represent the US can depolarize LA neurons that also receive CS-related impulses, forming an arrangement that is ideal for synapse-specific associative plasticity. Before conditioning, the CS signals only cause small excitatory post-synaptic potentials (EPSP) that are unable to induce large calcium influx into dendritic spines on their own. When the post-synaptic neuron is depolarized because of a US, a back-propagating action potential can meet with the slight depolarization of the CS-triggered EPSP, which opens NMDA receptors and L-VGCC, causing a strong influx of calcium at the CS synapse and inducing LTP.

An important distinction between the early LTP studies and the reality of learning and memory is the persistence of LTP. When McNaughton and colleagues (1978) examined LTP for long enough, they found that LTP fades away in less than 1 day. In contrast, CS-US associative memory can last a lifetime. Much research in recent decades has examined the transition from the early LTP (E-LTP) in those first hours to late LTP (L-LTP) that does not typically fade simply due to the passage of time (Huang et al., 2000). Many mechanisms are known to affect this process, but the ultimate effect is new protein synthesis, often implicating extracellularly regulated kinase (ERK) and various other kinases and transcription factors (D. Y. Chen et al., 2012; Ota et al., 2010; Schiff et al., 2017). This can be accomplished through calcium influx or metabotropic mechanisms. L-VGCC and NR2B subunit of NMDA receptors are candidate molecule that allows calcium currents to initiate robust intracellular signaling (Rodrigues et al., 2001; Weisskopf et al., 1999). The same research group later found that β -adrenergic receptors (β -AR) could stabilize LTP and CS-US associative memory via interactions with associative plasticity mechanisms (Johansen et al., 2014).

Norepinephrine and adrenergic receptors

A complete discussion of synaptic plasticity in mammals should include norepinephrine (NE). NE is a neuromodulator with three major classes of receptors (α_1 -, α_2 -, and β -adrenergic receptors), all of which are coupled to G-proteins (O'Donnell et al., 2012). Of these, β -adrenergic receptors (β -AR's) have the lowest affinity for NE, making them responsive to higher concentrations of NE (Giustino & Maren, 2018). The β -AR's play a major role in synaptic plasticity, as their associated intracellular signaling cascades (through G_s proteins) can downregulate postsynaptic calcium-activated potassium channels (Faber et al., 2008) and upregulate calcium-permeable AMPA receptors and ERK-/CREB-mediated gene expression (Schiff et al., 2017). α_2 -AR's also participate in plasticity by suppressing inhibitory interneurons in LA, effectively disinhibiting projection neurons and gating long-term potentiation (Tully et al., 2007). It must be noted, however, that the cellular distribution of β -AR's and α_2 -AR's is somewhat promiscuous, with β -AR's expressed in a variety of cell types and subcellular locations (Farb et al., 2010) and α_2 -AR's localized to some projection neurons in addition to interneurons (Buffalari & Grace, 2007).

An interesting property of β -AR dynamics in LA is that the memory enhancing effects are specific to the acquisition phase (and reconsolidation), but not the consolidation phase (Bush et al., 2010; Dębiec & LeDoux, 2004; Schiff et al., 2017). Infusion of propranolol, a β -AR antagonist, disrupts learning if administered to LA immediately before, but not immediately after PTC training (Bush et al., 2010). Later findings illustrated that β -AR engagement at the time of acquisition activates an ERK/CREB pathway that drives consolidation (Schiff et al., 2017). The requisite temporal order of NE activation before CS-US pairing is not trivial. With cued PTC, β -AR's enable coincidence detection on a timescale that differs from the more canonical Hebbian

plasticity.

NE neurons in the central nervous system primarily originate in the brainstem. The brainstem contains several NE source nuclei, the most well-known of which is the locus coeruleus (LC). The LC innervates much of the central nervous system with NE projections with both synaptic release and volume transmission release (Luppi et al., 1995). Originally thought to be functionally homogenous with a global broadcast motif, the LC is now known to contain functional modules that innervate specific circuits for functional control of learning processes (Uematsu et al., 2015, 2017). For example, optogenetically manipulating NE release in BA/LA and in medial prefrontal cortex (mPFC) revealed that NE release in BA/LA during a footshock US will enhance conditioning, while NE release in mPFC during a CS presentation will enhance extinction (Uematsu et al., 2017). Notably, these researchers found that the LC module projecting the BA/LA also projects to CeA.

Norepinephrine responses to stimuli and enhancement of arousal and learning

Broadly speaking, the LC/NE system functions as a stress-response system that enhances arousal (Valentino & Van Bockstaele, 2008) and learning (O'Donnell et al., 2012) and can trigger orienting to unexpected stimuli (Sara & Bouret, 2012). NE release can be triggered by stressors of numerous kinds, including innately recognized threats including footshock, restraint, hypotension, social stress, and water stress (Quirarte et al., 1998; Valentino & Van Bockstaele, 2008), primary rewards and their conditioned associations (Bouret & Sara, 2005), and unexpected stimuli that may indicate a context change or state change within a context (A. J. Yu & Dayan, 2005). Following footshock, NE extracellular concentrations in the amygdala remain elevated for up to 15-30 minutes (Galvez et al., 1996; Hatfield et al., 1999; Quirarte et al., 1998).

Activation of the LC/NE system is associated with enhanced arousal and enhanced learning, effects that are at least in part attributable to NE effects on neuronal receptive fields, which includes a transient and broad amplification of tuning curves in the short-term and an enduring narrowing of tuning curves in the long-term (Martins & Froemke, 2015). NE primes neurons for learning by binding to β -AR's and α_1 -AR's on principal neurons (O'Donnell et al., 2012). Although α_2 -AR's are inhibitory and oppose some of the actions of the other AR's (Buffalari & Grace, 2007), α_2 -AR's on interneurons can have a disinhibition effect, allowing principal neurons to be recruited into memory traces (Estrade et al., 2019). The β -AR's are especially important, as they trigger intracellular processes that boost excitability of neurons and capacity for plasticity (Schiff et al., 2017). β -AR's have been shown to stabilize Hebbian plasticity that underlies PTC learning (Johansen et al., 2014).

Considering the various activators of the LC/NE system and the downstream effects on arousal and learning, it's quite possible that daily stressors can modulate nonconscious threat learning in humans through an LC/NE mechanism. This should be investigated, as illuminating these potential links could lead to a better quality of life for humans, given that stress, wakefulness, and learning are all in the realm of volitional lifestyle choices. Additional benefits could be realized by clinical populations. NE-targeted pharmacotherapies are already in use for multiple disorders related to stress, anxiety, and attention. Prazosin, a α_1 -AR antagonist, reduces nightmares in patients with post-traumatic stress disorder (PTSD) (Seda et al., 2015). Clonidine, an α_2 -AR agonist, has efficacy for treating attention-deficit hyperactivity disorder (Connor et al., 1999). Propranolol, a β -AR antagonist, treats stage fright (Brantigan et al., 1982) and has been tested with mixed results for disrupting the negative impacts of traumatic stress (Argolo et al., 2015).

Some hoped for NE-therapies have not been as successful as anticipated. Key discoveries about disrupting the reconsolidation of amygdala-based memories with pharmacological agents (e.g. Dębiec & LeDoux, 2004; Nader et al., 2000) sparked much research into treat PTSD with drug-facilitated exposure therapy. In fact, a recent meta-analysis showed propranolol can block consolidation and reconsolidation of emotional memory in humans (Lonergan et al., 2013). This led many to question if propranolol could be used to disrupt traumatic memories related to PTSD (Argolo et al., 2015). This disorder, the onset of which can be triggered by traumatic experiences, includes many symptoms, some of which are of hypervigilance, severe anxiety, and flashbacks that are often triggered by external stimuli (Jorge, 2015). Because several symptoms are consistent with expression of PTC memory and dysregulated NE activity, propranolol was expected to work well for PTSD. However, according to a meta-analysis that examined the use of propranolol in-hospital immediately post-trauma, the only symptoms reduced by this treatment were physiological arousal symptoms (Argolo et al., 2015).

The activity of β -AR's in the amygdala turned out to be more complex than anticipated. For example, propranolol impairs consolidation of contextual PTC (Abrari et al., 2008), but not cued PTC (Dębiec & LeDoux, 2004). Propranolol treatment does not impair reconsolidation of contextual PTC, but it does impair reconsolidation of cued PTC (Muravieva & Alberini, 2010). Another study found that propranolol has the side effect of impairing declarative memory up to 24 hours after administration (Kroes et al., 2010). Clearly a more nuanced understanding of NE, stress, and traumatic stress is needed. The diverging results on propranolol were likely due to differential roles of overlapping neural circuits recruited by the different types of threat conditioning because contextual conditioning recruits the hippocampus and amygdala, while cued conditioning (without a time gap between CS offset and US onset) recruits the amygdala

but not the hippocampus (LeDoux, 2012). If there is a gap in time between CS offset and US onset, then the hippocampus is recruited, possibly due to the hippocampus's role as a predictive map through its capacity for successor representations (Dayan, 1993; Stachenfeld et al., 2017). These are just a few examples of the complexity of these integrative circuits. Clearly more research is needed before optimal pharmacological strategies can be implemented.

Because the stage of learning (acquisition vs. consolidation vs. recall vs. reconsolidation & extinction) is differentially affected by β -AR blockade (Rodrigues et al., 2009; Rodrigues, Schafe, et al., 2004), and sensitivity to β -AR blockade is different for cued and contextual conditioning (Muravieva & Alberini, 2010), it is clear that temporal dynamics of NE and β -AR activity in the amygdala are complex and important to elucidate more clearly.

Overview of experiments

The research presented in the coming chapters sought to identify specific naturalistic triggers of NE activity during PTC, to characterize temporal dynamics of the associated NE signals, and to form a stronger understanding of the consequences of amygdalar NE and β -AR signals for the acquisition and expression of PTC.

The first set of experiments, in Chapter 2, used systemic propranolol treatment to probe the β -AR dependence of various specialized CS-US pairing protocols, thereby identifying protocol components necessary for enhancement of PTC acquisition by β -AR's (Díaz-Mataix et al., 2017). We established a model in which low-affinity β -AR's are not engaged by baseline NE levels, but the acquisition-enhancing effect of β -AR's is activated by the additional NE release triggered by footshocks. Furthermore, this footshock-induced priming of acquisition fades with time, fully disappearing before 40 minutes post footshock. Although this systemic propranolol study did not directly study the amygdala, many past experiments from our lab have linked

similar acquisition effects to β -AR's in the LA (Bush et al., 2010; Dębiec & LeDoux, 2004; Johansen et al., 2014; Schiff et al., 2017).

The second study used bidirectional chemogenetic manipulations of LC/NE projections to CeA or LA and pharmacological manipulations of β -AR's in CeA during long-term memory (LTM) testing (Gu et al., 2020). Expression of LTM for cued PTC was highly sensitive to bidirectional NE and β -AR manipulations in CeA, but insensitive to NE manipulations in LA/BA. This revealed a previously unknown link between LC/NE projections to CeA and the expression of conditioned defensive reactions.

To get measurements of NE in amygdala with sub-second temporal resolution, the third and final study used a fiber photometry preparation with a bioengineered fluorescent α_2 -AR conjugated to a green fluorescent protein (GFP) intracellular domain whose brightness is modulated by NE binding. We observed NE increases in and around LA and CeA. The NE reactivity was most pronounced in response to footshocks but were also observed during some tone CS presentations. Interestingly, the NE reactivity to a given type of stimulus tended to be strongest on the first presentation of that stimulus. Theories of NE function were discussed in Chapters 4 and 5 in relation to the fiber photometry findings.

The observed temporal patterns of NE fluctuations are remarkably similar in LA and CeA, suggesting their differential roles in enhancing acquisition and expression, respectively, are products of how their unique neural circuitry respond to NE and affect downstream structures rather than any obvious difference in NE influx. Overall, these findings reveal NE dynamics not previously seen, namely the necessity of NE-activating stimuli before β -AR engagement in cued PTC acquisition (Chapter 2), the central amygdala as a locus for NE-modulation of conditioned defensive reactions (Chapter 3), and the generic temporal dynamics

of NE reactions that are at least somewhat consistent between LA and CeA and between multiple types of stimuli.

CHAPTER 2

Characterization of the amplificatory effect of norepinephrine in the acquisition of Pavlovian threat associations

Lorenzo Díaz-Mataix,^{1,2,4} Walter T. Piper,^{1,4} Hillary C. Schiff,^{1,3} Clark H. Roberts,¹

Vincent D. Campese,¹ Robert M. Sears,^{1,2} and Joseph E. LeDoux^{1,2}

¹Center for Neural Science, New York University, New York, New York 10003, USA;

²Emotional Brain Institute, Nathan Kline Institute for Psychiatric Research, Orangeburg, New York 10962, USA;

³Department of Neurobiology and Behavior, The State University of New York-Stony Brook, Stony Brook, New York 11794, USA

⁴These authors contributed equally to this work.

Published in Learning & Memory at <https://doi.org/10.1101/lm.044412.116>

Abstract

The creation of auditory threat Pavlovian memory requires an initial learning stage in which a neutral conditioned stimulus (CS), such as a tone, is paired with an aversive one (US), such as a shock. In this phase, the CS acquires the capacity of predicting the occurrence of the US and therefore elicits conditioned defense responses. Norepinephrine (NE), through β -adrenergic receptors in the amygdala, enhances threat memory by facilitating the acquisition of the CS-US association, but the nature of this effect has not been described. Here we show that NE release, induced by the footshock of the first conditioning trial, promotes the subsequent enhancement of learning. Consequently, blocking NE transmission disrupts multitrial but not one-trial conditioning. We further found that increasing the time between the conditioning trials

eliminates the amplificatory effect of NE. Similarly, an unsignaled footshock delivered in a separate context immediately before conditioning can enhance learning. These results help define the conditions under which NE should and should not be expected to alter threat processing and fill an important gap in the understanding of the neural processes relevant to the pathophysiology of stress and anxiety disorders.

Introduction

Pavlovian aversive conditioning (PTC) (Pavlov, 1927) is a widely used behavioral paradigm to study a basic and universal form of associative learning. In this paradigm, which will be referred to here as Pavlovian threat conditioning (LeDoux, 2014), a neutral conditioned stimulus (CS), a tone in the case of auditory conditioning, is paired with an innately aversive unconditioned stimulus (US), usually a mild footshock. The CS then acquires predictive value over the delivery of the US and can elicit conditioned defensive responses (CRs), such as freezing. Quantification of the time the animal freezes during CS presentations provides an objective and noninvasive measure of the degree of threat learning and memory induced by pairing of the CS and US (LeDoux, 2000).

During learning, neural signals encoding the sensory representations of the CS and the US converge in the lateral nucleus of the amygdala (LA) (LeDoux, 2007). Neurons in this region respond to both stimuli, and the CS-US pairing induces increased single-unit activity, potentiated auditory-evoked field potentials, activation of molecular cascades, and morphological changes that eventually underlie the consolidation of the learning as a long-term memory (LTM) (Bauer et al., 2001; Doyère et al., 2003; Johansen et al., 2011; Maren & Quirk, 2004; Ostroff et al., 2010; Weisskopf et al., 1999). These changes are the result of a combination of Hebbian and neuromodulatory mechanisms (Bailey et al., 2000; Johansen et al., 2014; McGaugh et al., 2002; Pawlak et al., 2010; Tully & Bolshakov, 2010).

Norepinephrine (NE), which is released widely in the brain during situations involving stress, emotional arousal, attention, and alertness (for reviews, see Raio & Phelps, 2015; Rodrigues et al., 2009; Sara & Bouret, 2012) is one of the key neuromodulators that regulate the degree of learning and memory (Joëls et al., 2011; McEwen, 2012; Roozendaal et al., 2009). The amygdala receives direct noradrenergic innervation from the locus coeruleus (LC) (Uematsu et al., 2015), and β -adrenergic receptors (β ARs) are highly expressed in LA (Farb et al., 2010). The standard view of the effect of NE in the amygdala, largely based on studies using inhibitory avoidance, is that NE acting through β ARs potentiates the consolidation of the learning (McGaugh, 2000, 2015; McGaugh et al., 2002; Packard & Wingard, 2004; Roozendaal & McGaugh, 2011) without having any effect on the acquisition of the association itself. However, we have recently reported that NE, also acting through β ARs, must be present during the initial CS-US training (acquisition) to create robust memory of the CS-US association (Johansen et al., 2014; Sears et al., 2013). In line with these results, our laboratory and others have found that the blockade of β ARs by propranolol disrupts long-term memory when infused into the LA before the training session (acquisition) but not immediately after (Bush et al., 2010; Dębiec & LeDoux, 2004; H. J. Lee et al., 2001; Miserendino et al., 1990; Schiff et al., 2017). This suggests that the action of NE in LA results in an enhanced memory of the CS-US by facilitating the acquisition of the association.

How might NE achieve these effects on acquisition? The NE system projects widely throughout the brain (Swanson & Hartman, 1975). It is involved in many adaptive physiological and pathophysiological processes, being released in response to a large variety of stimuli (Benarroch, 2009). While tones and shocks both activate LC and elicit NE release, shock is a particularly effective stimulus (Aston-Jones et al., 1996; Sara, 2009). In the present study, we explore the possibility that the footshock US is the trigger responsible for an increase of the NE

release during acquisition. This hypothesis leads to the prediction that the basal release of NE has no influence on the first pairing trial of multitrial learning, but should affect subsequent trials, provided the presentation of these trials occur before NE levels return to baseline.

Results

NE facilitates learning only when conditioning involves multiple trials

We previously reported that NE, acting through β ARs in the LA, is involved in the acquisition but not in the consolidation of cued threat memories, as long-term memory is only reduced when the β AR-antagonist propranolol is infused into the LA before training but not after training (Bush et al., 2010). In accordance, systemic injection of propranolol after training does not affect LTM (Dębiec & LeDoux, 2004; H. J. Lee et al., 2001). However, to our knowledge, the effect of a pretraining systemic administration of a β AR-blocker in rodents has never been reported.

We tested whether pretraining systemic propranolol administration would similarly diminish acquisition of PTC. Rats were randomly administered an intraperitoneal (i.p.) injection of propranolol (10 mg/kg) or its vehicle (saline 1 mL/kg) 30 min before the beginning of the conditioning session (Fig. 2.1A). To account for the possibility that NE activity could differ depending on prior exposure to the CS-US pairing, during the training session half of the animals received a single CS-US presentation (1Trial group) while the other half were presented with a second CS-US 2 min after the first one (2Trial group). All animals stayed a total duration of 9 min in the conditioning box (Fig. 2.1A).

The freezing to the context was assessed by measuring the freezing during the 30 sec immediately before the first CS-US pairing in the conditioning session or the first CS presentation in the long-term memory test. For all the described experiments, no significant difference was observed between saline and propranolol treatment or between behavioral

manipulations, therefore detailed contextual freezing data is not shown. Instead only the statistics and the average contextual freezing of all rats in each experiment are shown.

Baseline freezing to the conditioning context before CS-US1 did not differ among the four conditions ($F(3,38) = 1.37, P = 0.27$), and freezing in all conditions was low (combined average: $1.5 \pm 0.5\%$, mean \pm SEM). A one-way ANOVA with six levels compared freezing during CS-US1 and CS-US2 across the four conditions. The six levels included freezing to CS-US1 for all four conditions and freezing to CS-US2 for the two conditions that received the second trial. (Fig. 2.1B) This ANOVA showed a significant effect ($F(5,54) = 14.21, P < 0.01$). Post hoc Sidak tests showed no pairwise differences between conditions in freezing to CS-US1 (adjusted P values: Sal 1Trial versus Prop 1Trial $P = 0.99$; Sal 1Trial versus Sal 2Trial $P > 0.99$; Sal 1Trial versus Prop 2Trial $P = 0.74$; Prop 1Trial versus Sal 2Trial $P = 0.93$; Prop 1Trial versus Prop 2Trial $P > 0.99$; Sal 2Trial versus Prop 2Trial $P = 0.55$). Conditioning was effective in the 2Trial group, as shown by Sidak tests comparing freezing to the first tone with freezing to the second tone in both Sal 2Trial and Prop 2Trial (both $P < 0.01$). Interestingly, Prop 2Trial animals showed significantly less freezing than Sal 2Trial to the CS-US2 presentation ($P < 0.01$). These results indicate that propranolol reduced freezing to CS-US2, but did not affect freezing to CS-US1 or to the context prior to CS-US1. This suggests that propranolol may be selectively affecting the brain processing of the first CS-US presentation or affecting freezing only to a learned CS, rather than decreasing freezing behavior in general.

Long-term memory was tested 2 d later by 10 CS-alone presentations in a modified context (Fig. 2.1A). A two-way ANOVA comparing treatment (Propranolol or Saline) and groups (1Trial or 2Trial) revealed no difference in the contextual freezing level (Treatment effect: $F(1,38) = 1.51, P = 0.23$; Group effect: $F(1,38) = 0.01, P = 0.93$; Interaction: $F(1,38) = 0.63, P = 0.43$) and conditioning did not induce freezing to the context since averaged pre-CS freezing of

all tested animals ($5.0 \pm 1.3\%$) was negligible. A two-way ANOVA test comparing average freezing across the 10 CS presentations (Fig. 2.1C) showed an interaction between treatment and group ($F(1,38) = 4.21, P < 0.05$), a main effect of the treatment ($F(1,38) = 12.17, P < 0.01$) and a main effect of the group ($F(1,38) = 4.70, P < 0.05$). As expected, Sal 2Trial animals showed significantly more freezing than Sal 1Trial ($P < 0.05$). However, Prop 2Trial animals displayed significantly less freezing than Sal 2Trial ($P < 0.05$), while the freezing of Prop 1Trial animals did not differ from their controls ($P = 0.86$).

Two-way ANOVAs comparing the average freezing per treatment during each of the 10 tones (Fig. 2.1D) for the 1Trial group (left graph) showed an overall effect of the CS trial ($F(9,220) = 4.44, P < 0.01$), no effect of treatment ($F(1,220) = 0.16, P = 0.69$) nor a treatment by trial interaction ($F(9,220) = 0.68, P = 0.73$). This confirms that NE activity at β ARs is not required for learning in the single-trial group. In contrast, the animals conditioned with two CS-US trials (Fig. 2.1D, right) showed a significant effect of treatment ($F(1,160) = 101.10, P < 0.01$) and trial ($F(9,160) = 5.54, P < 0.01$) but no treatment by trial interaction ($F(9,220) = 0.64, P = 0.77$). This indicates that the animals treated with propranolol on conditioning day showed reduced freezing on test day. There was a main effect of Trial in both panels (Fig. 2.1) indicating no difference in extinction over the 10 CSs regardless of the number of trials on conditioning day. Similarly, the lack of interaction indicates that within-session extinction was unaffected by pretraining drug administration.

Overall the above results reveal that (1) the first conditioning trial affects the following trial within the conditioning session (Fig. 2.1B); (2) when tested for LTM, saline-treated animals conditioned with two trials show higher freezing than the ones conditioned with a single trial (Fig. 2.1C); (3) propranolol diminishes the freezing response only for the animals that experienced the second CS-US (Fig. 2.1C,D). This pattern of results suggests that the first

conditioning trial induces an increase in the release of NE that strengthens the learning of the following CS-US presentation.

An unsignaled footshock before acquisition enhances learning through a mechanism involving β-adrenergic receptors

Several studies using in vivo microdialysis have reported that the release of NE in the Amygdala is increased by the presentation of an unsignaled footshock (Galvez et al., 1996; Hatfield et al., 1999; Quirarte et al., 1998). According to these findings, the concentration of NE remains elevated for nearly 30 min. Given this evidence, we hypothesize that the footshock delivered with the first CS-US presentation is the necessary trigger that, by increasing the release of NE, facilitates learning on following trials.

To test this idea, we designed an experiment in which rats were exposed to an unsignaled footshock (U-US) before conditioning (Fig. 2.2A). The U-US was delivered in a different context (shuttlebox in a different room) than the one used for conditioning to prevent contextual freezing. Rats were assigned randomly to one of four experimental groups (Fig. 2.2A). In a control group, “No U-US”, rats were placed in the shuttlebox and did not experience a U-US. “High U-US” and “Early U-US” received a 1-mA intensity footshock with a duration of 5 sec, while the shock presented to the “Low U-US” group had the same intensity (1 mA) but only 1 sec duration (Fig. 2.2A). Thirty minutes before the presentation of the U-US, the animals were injected with propranolol or saline. After the unsignaled shock, “Early U-US” rats spent 40 min in their home cages before conditioning, while the three other groups were conditioned immediately in the new context for a single CS-US conditioning trial.

Pre-CS freezing for both the conditioning session and the LTM test showed no group or treatment effect nor an interaction between group and treatment (Conditioning: $F(3,75) = 1.83$, $P = 0.35$; $F(1,75) < 0.01$, $P = 0.95$; $F(3,75) = 1.1$, $P = 0.34$. LTM test: $F(3,75) = 2.40$, $P = 0.07$;

$F(1,75) = 3.30, P = 0.07$; $F(3,75) = 0.79, P = 0.50$). The averaged pre-CS freezing was $4.0 \pm 1\%$ (Conditioning) and 6.9 ± 1.3 (LTM test). All animals were conditioned with a single CS-US trial. The intensity of the footshock was 0.4 mA with the aim of inducing weak learning in the animals, which is ideal for detecting increases in freezing due to manipulations when decreases relative to the control condition are not expected. Freezing to the CS presented during conditioning was unaffected by drug treatment and the U-US precondition, and there was no interaction between the two as shown by a two-way ANOVA (Fig. 2B) (U-US: $F(3,75) = 1.92, P = 0.13$; Drug: $F(1,75) = 0.54, P = 0.47$; U-US \times Drug $F(3,75) = 0.50, P = 0.68$). Thus, neither systemic propranolol administration nor prior exposure to a U-US in a distinct context affected freezing in response to a novel auditory cue (the CS).

In contrast, the comparison of the averaged freezing across the 10 CSs presented to test LTM 48 h after conditioning (Fig. 2.2C) showed a main effect of group ($F(3,75) = 3.20, P < 0.05$). There was no main effect of treatment ($F(1,75) = 0.80, P = 0.37$) and no group by treatment interaction ($F(3,75) = 1.07, P = 0.37$). In the saline condition, only the animals that were exposed to the high intensity U-US and conditioned immediately after (High U-US) froze significantly more than the animals that were not exposed to the U-US before training (post hoc Sidak pairwise test $P < 0.05$). This finding indicates that prior exposure to an unsignaled shock in a distinct context can enhance one-trial learning, perhaps relying on a similar mechanism as that recruited by two-trial learning.

The analysis of the effect of propranolol in each U-US condition was performed comparing the mean percent freezing scores across each test trial (Fig. 2.2D). The animals that were exposed to high intensity U-US and treated with propranolol exhibited significantly less freezing than their vehicle controls ($F(1,210) = 26.87, P < 0.01$). Interestingly, only animals that did not experience the conditioning session immediately after the U-US (Early U-US condition)

showed significant within-session extinction over the course of 10 CS presentations ($F(9,180) = 3.51, P < 0.01$). No interactions between treatment and CS trial were significant for any of the groups.

These results indicate that an unsignaled footshock, depending on its intensity, potentiates learning when conditioning occurs close in time. The effect of the unsignaled footshock is prevented by propranolol, providing further evidence for the hypothesis that the first shock during conditioning can be the trigger of the NE-induced facilitation of learning.

The enhancement of learning induced by NE depends on the time interval between training trials

If the initial shock during the threat conditioning session is what induces the release of NE that further enhances the acquisition of the CS-US association, then we predict that this facilitative effect must be circumscribed to the temporal window in which NE concentration is increased in the LA (Galvez et al., 1996; Hatfield et al., 1999; Quirarte et al., 1998). To test this, 30 min after systemic propranolol or saline, rats underwent two-trial conditioning with ITIs of 2 or 40 min (Fig. 2.3A). All animals stayed in the conditioning context for a total time of 60 min.

Pre-CS freezing for both the conditioning session and LTM test showed no main effect of ITI group or drug treatment, nor was there an interaction (conditioning, one-way ANOVA: $F(3,38) = 2.21, P = 0.10$; LTM test, two-way ANOVA: group: $F(1,38) = 0.24, P = 0.63$; treatment: $F(1,38) = 1.73, P = 0.20$; interaction: $F(1,38) = 0.02, P = 0.89$). The averaged pre-CS freezing of all conditions together was $1.2 \pm 0.3\%$ (Conditioning) and $6.6 \pm 2.4\%$ (LTM test). During training, a one-way ANOVA on the freezing response of each group to CS-US1 (Fig. 2.3B) showed no significant difference among conditions in their response to the tone before it was paired with a shock ($F(3,38) = 1.66, P = 0.19$). Next, a two-way ANOVA including the four conditions as a between-subjects factor and CS-US trial as the other factor revealed a significant effect of CS-

US trial ($F(1,76) = 173.90, P < 0.01$), indicating that after a single CS-US presentation, subjects were conditioned. In addition, a significant interaction suggests that this conditioning varied in strength between different conditions ($F(3,76) = 5.38, P < 0.01$). There was also a main effect of condition ($F(1,76) = 6.51, P < 0.01$; Fig. 3B). Post hoc Sidak testing revealed that Prop Short ITI animals froze significantly less during the second CS compared with their vehicle controls ($P < 0.05$), confirming our previous finding with two-trial conditioning (Fig. 2.1B).

During LTM, we observed a main effect of group ($F(1,38) = 14.05, P < 0.01$) on freezing (Fig. 2.3C). There was no overall effect of the treatment ($F(1,38) = 3.00, P = 0.09$), nor was there a significant group by treatment interaction ($F(1,38) = 1.91, P = 0.17$). Sidak's post hoc tests along the group dimension revealed a difference between ITI group only for the propranolol treatment (Prop Short ITI versus Prop Long ITI; $P < 0.01$), while saline-treated animals did not differ significantly (Sal Short ITI versus Sal Long ITI; $P = 0.19$).

The effect of treatment across the 10 CS presentations of the LTM session was assessed with a separate treatment-by-CS trial ANOVA for each group (Fig. 2.3D). Both Short ITI and Long ITI groups experienced a significant effect of CS trial ($F(9,200) = 7.11, P < 0.01$; $F(9,180) = 2.04, P < 0.05$, respectively). Within the Short ITI group, propranolol-treated animals exhibited significantly lower freezing than their saline controls ($F(1,200) = 64.95, P < 0.01$), while the freezing in the long ITI group was not affected by treatment ($F(1,180) = 0.11, P > 0.99$). Neither group showed a treatment by CS trial interaction (short ITI: $F(9,200) = 0.95, P = 0.49$; long ITI: $F(9,180) = 0.31, P = 0.58$). This result indicates that propranolol only affects memory formation when the second CS-US pairing occurs within a certain time following the first CS-US pairing.

Discussion

The results obtained here confirm that the NE transmission greatly contributes to the

acquisition of Pavlovian threat associations. Building on this, the studies presented here show that the NE-induced facilitation of learning is governed by precise temporal dynamics initiated by an increase in the NE release triggered by the footshock presented as part of the first conditioning association.

Few studies have used systemic administration of propranolol and other β ARs antagonist in rats or mice to study the role of NE transmission in memory formation during auditory threat conditioning. In those reports, the drug was only administered immediately after training (Dębiec & LeDoux, 2004; H. J. Lee et al., 2001; Miserendino et al., 1990). Their conclusion, based on the lack of effect observed during the short-term memory and/or long-term memory tests, was that β AR activity is not involved in the consolidation of learning. When applied directly to the LA through local administration, blockade of β ARs with propranolol reduces acquisition (Bush et al., 2010), but whether systemic propranolol would have the same effect was unknown. Here we show that systemic propranolol similarly reduces acquisition, indicating that NE, acting through β ARs, serves to enhance memory formation by modulating acquisition processes. This suggests that NE effects observed here occur in the LA and supports the conclusion that the LA is a critical site for PTC learning. Using threat-potentiated startle, Davis and his collaborators have reported contradictory results since systemic pretraining propranolol disrupted the expression of cued potentiated startle in rats (Walker & Davis, 2002); however, this was not replicated in humans (Grillon et al., 2004).

This study provides evidence that NE must already be present at the time of a CS-US pairing in order to play its modulatory role in acquisition. The amount of freezing during the memory test was not modified by propranolol in the animals exposed to only one CS-US. In contrast, in the animals that were exposed to a second conditioning trial, propranolol diminished the CS-evoked freezing during the second CS-US presentation and the freezing when long-

term memory was tested 48 h later. This implies that NE is not involved when learning occurs after a single CS-US pairing.

Pavlovian learning is instructed by expectation, or rather, by violation of expectation.

This prediction error can be the direct result of an unexpected US (Rescorla & Wagner, 1972) or indirectly caused by the CS after the first CS-US presentation since this second CS commands more attention (Mackintosh, 1975). Hence, the learning of the first CS-US association might be governed by different learning rules instructed by different brain areas and neurotransmitters. As an example, μ -opioid receptors in the ventrolateral quadrant of the midbrain periaqueductal gray mediate learning by altering the brain's processing of the US while having no effect on the CS attentional teaching signal (Cole & McNally, 2007). Since NE blockade attenuates two-trial but not one-trial learning (Fig. 2.1), it is possible that NE facilitates learning by enhancing the attentional strength of the CS as a teaching signal. However, the facilitation of learning induced by the U-US is suggestive of an arousal mechanism, since in this case the facilitation of learning happens after only one CS-US presentation. The interval between a U-US or CS-US and a future CS-US seems to determine NE dependence, also consistent with an arousal mechanism.

We have not tested the effect of propranolol after single-trial learning; however, a previous article reported, using the same protocol and drug dose we use here, that after conditioning with 1 CS-US pairing neither systemic nor intra-LA propranolol impaired memory when tested 48 h later (Dębiec & LeDoux, 2004). Together, these findings strongly suggest that NE is not necessary for single-trial learning.

The present results show that increased NE levels potentiate learning and this NE release can come from the US in the first CS-US pairing. However, learning is also potentiated in a β -AR-dependent manner when one-trial conditioning is preceded by an unsignaled US, indicating that the first CS-US pairing can be replaced by an unsignaled shock, or perhaps any

strong enough stressor. We observed that long-term memory was strengthened only by preexposure to a long-duration unsignaled footshock immediately before conditioning and not by the short-duration one (Fig. 2.2), and this effect was prevented by propranolol. Confirming our prediction that was based on previous reports of a time-limited increase in NE release after an electrical shock (Galvez et al., 1996; Hatfield et al., 1999; Quirarte et al., 1998), the effect of the U-US did not occur if conditioning was delayed by 40 min. This temporal constraint on the NE-induced enhancement of learning was also observed when the interval between two consecutive conditioning trials was increased from 2 to 40 min (Fig. 2.3). The intensity of the U-US was not identical to the intensity of the US during conditioning. We chose the parameters of the unsignaled shock based on previous publications measuring the release of NE after the delivery of an unsignaled footshock (Galvez et al., 1996; Hatfield et al., 1999; Quirarte et al., 1998). Since we were not directly measuring NE release, and we wanted to be sure that in our paradigm were inducing an increase in NE we increased the intensity of the footshock from 0.6 to 1 mA. Of note, 1 mA, 1-sec U-US did not induce an effect on long-term memory while 1 mA, 5 sec did. An unsignaled shock increases the NE levels, but since the rodents in experiment 2 are exposed to the CS for the first time after the unsignaled shock, its salience is not comparable to the salience of the CS when it is presented in a second trial. This could explain the necessity of higher intensity of the U-US to facilitate learning.

It must be noted that the two-trial learning with a long ITI was robust despite the apparent lack of NE-dependence. Perhaps the same mechanisms that underlie single-trial learning have, over the 40 min ITI, induced an intermediate phase of memory formation that acts as scaffolding for further conditioning. It is also possible that other neuromodulators are involved that accomplish similar effects on a different time scale. For example, dopamine and

serotonin have been shown to increase in the amygdala for well over an hour following tone–footshock pairings (Yokoyama et al., 2005).

Extensive evidence indicates that NE released into the amygdala from neurons in the LC has a direct and indirect (mediating the effects of other hormones and neurotransmitters) role in regulating stress effects on memory by acting through activation of β -adrenergic receptors (Morilak et al., 2005; Rodrigues et al., 2009; Roozendaal et al., 2009; Schwabe et al., 2012). Creating adaptive explicit and implicit memories during stress is vital for confronting future threats (Yehuda et al., 2010). We previously showed that NE, acting through β ARs, enhances memory formation with temporally specific actions on extracellular regulated kinase (ERK) and AMPA receptor subunits within the LA (Schiff et al., 2017). Since unsignaled electrical shocks are used to generate stress responses, it is possible that the effect of the U-US is mediated by such mechanisms, priming the system for subsequent memory formation. Nonetheless, if the U-US facilitation of learning observed in the present experiments is a stress response remains to be evaluated by using other type of acute stressors.

Another question that comes out of our findings is whether prior U-US exposure could similarly enhance expression of a previously trained conditioned threat memory. According to our findings, the brain levels of NE would be elevated to levels that are capable of enhancing subsequent learning, but would it also enhance expression?

Pavlovian conditioning contributes to disorders like PTSD (Cain et al., 2012; Mahan & Ressler, 2012; Rau & Fanselow, 2009). Using this task, we have found that NE enhances memory by acting during learning. Our findings are consistent with clinical studies demonstrating that while β AR blockade does not prevent the consolidation of traumatic memory, it improves symptoms of stage fright (Dubovsky, 1990). The description of the dynamics by which NE facilitates the acquisition of Pavlovian threat memories suggests that the timing in

which NE agents are used to treat PTSD and related psychiatric conditions must be reevaluated for therapeutic success.

Materials and Methods

Subjects

Subjects were 167 male Sprague-Dawley rats (Hilltop Laboratory Animals; Scottdale, PA, USA) weighing 225–400 g at the beginning of the experiments. The animals were single housed in an environment that was temperature- and humidity-controlled and maintained on a 12/12 light–dark cycle. Rats had ad libitum access to food and water. All conditions and procedures followed the National Institutes of Health *Guide for the Care and Use of Experimental Animals* and all procedures were approved by the New York University Animal Care and Use Committee.

Drug injections

(±) Propranolol hydrochloride (Sigma-Aldrich) was freshly prepared on each conditioning day. All rats were injected i.p. with 10 mg/mL of propranolol or its vehicle (saline). The volume was 1 mL/kg. For experiments 1 and 3, the treatments were administered 30 min before conditioning procedure. For experiment 2, the treatments were administered 30 min before the delivery of the U-US. This dose is commonly used in PTC experiments (Dębiec & LeDoux, 2004; Rodriguez-Romaguera et al., 2009). All injections were done by the same experimenter.

Apparatus and stimuli

All experiments were conducted using a Habitest Linc system controlled by Graphic State 2 software. Conditioning boxes (Model H10-11R-TC; Coulbourn Instruments; 30 cm width, 25 cm depth, 30 cm height) were placed in sound-isolating cubicles (Model H10-24A; Coulbourn Instruments). For experiment 2, shuttleboxes were also used (Model H10-11R-SC; Coulbourn Instruments; 50 cm width, 25 cm depth, 30 cm height.) Every box had a rod flooring connected

to shock generators (Model H13-15; Coulbourn Instruments), a house light, a speaker connected to a tone generator (Model A12-33; Coulbourn Instruments), and infrared cue lights.

The CS was a continuous tone (30 sec duration; 5 kHz; 80 dB). The US consisted of a mild electrical footshock (1 sec, 0.4 or 0.6mA depending on the experiment). For experiment 2, we also used an unsignaled footshock (U-US; 1 or 5 sec, 1 mA) delivered in the shuttle boxes. During conditioning the US coterminated with the CS.

Behavioral procedures

On day 1, rats were habituated to the conditioning context by placing them in the conditioning boxes for 30 min. Twenty-four hours later the rats were weighed and randomly assigned to be injected i.p. with either propranolol (Prop) or saline vehicle (Sal) 30 min before the conditioning session (or 30 min before U-US delivery in experiment 2). Forty-eight hours later, long-term memory (LTM) was tested by presenting 10 unreinforced CS's in a modified context with a variable ITI ranging from 90 to 140 sec (mean ITI was 112 sec). The first CS was preceded by a 3-min acclimation period. This was in the same box as the conditioning session, but with peppermint odor, a smooth black plastic floor covering the rod flooring, and a dim red light instead of the usual house light. All sessions of all procedures were run for six rats at a time.

Experiment 1

In the conditioning session on day 2 (Fig. 2.1A), rats received either 1 or 2 CS-US pairing trials. A footshock (0.6 mA, 1 sec) was given during the final second of a 30 sec tone. The acclimation period was 5 min, and rats were in the conditioning context for 9 min total. For the rats that received 2 CS-US pairings, the ITI was 2 min. (Group sizes were Sal 1Trial: $N = 12$; Prop 1Trial: $N = 12$; Sal 2Trial: $N = 9$; Prop 2Trial: $N = 9$).

Experiment 2

Rats were exposed to an unsignaled 1.0-mA footshock in a shuttlebox before the conditioning session on day 2 (Fig. 2.2A). Four behavioral conditions were used: “No U-US” group was placed in the shuttlebox for the same duration as the other three groups but did not receive any footshock. After 3 sec, the other three groups were subjected to either 1 sec (Low U-US) or 5 sec (High U-US and Early U-US) of a 1.0-mA footshock. After this unsignaled shock procedure, rats were transferred to the conditioning context (No U-US, Low U-US, and High U-US groups) for the conditioning session, or returned to the home cage (Early U-US group) for a 40 min rest period before transfer to the conditioning session. (Group sizes were Sal No U-US: $N = 10$; Prop No U-US: $N = 10$; Sal Low U-US: $N = 10$; Prop Low U-US: $N = 10$; Sal High U-US: $N = 11$; Prop High U-US: $N = 12$; Sal Early U-US: $N = 10$; Prop Early U-US: $N = 10$)

For the conditioning procedure in experiment 2, a single CS–US trial was given, consisting of a weak footshock (0.4 mA) delivered during the last second of a 30-sec tone presentation. This trial was after 5 min of acclimation to context. Twenty seconds after the CS–US offset, animals were removed from the conditioning context and returned to the vivarium.

Experiment 3

Two CS–US pairings were delivered with an ITI that was either short (2 min; “Short ITI” group) or long (40 min; “Long ITI” group) (Fig. 2.3A). The pairings consisted of a 30-sec tone coterminating with a 1-sec 0.6-mA footshock. All rats were in the conditioning context for a total of 60 min, including a 3-min acclimation period, CS–US pairings with the ITI between, and a continued context-exposure period after the second pairing that brought the total length to 60 min. (Group sizes were Sal Short ITI: $N = 11$; Prop Short ITI: $N = 11$; Sal Long ITI: $N = 10$; Prop Long ITI: $N = 10$)

Assessment of freezing

Videos recorded during conditioning sessions and LTM test sessions were analyzed for freezing by at least one rater who was blind to drug treatment condition. Freezing was defined as cessation of all movement other than respiration. Freezing during each CS presentation was timed with a digital stopwatch and presented as a percentage of the CS duration. Baseline freezing in conditioning and test contexts was established by scoring the 30-sec period before the first CS.

Statistical analysis

The freezing in the conditioning session (Figs. 2.1B, 2.2B, 2.3B) was analyzed differently between experiments because the nature of the manipulations differed. First, we used one-way analysis of variance (ANOVA) tests to check for differences (freezing during Pre-CS and CS-US1) before behavioral manipulations. This was done in experiments 1 and 3. We then confirm effectiveness of conditioning by analyzing increases in the percentage of freezing from CS-US1 to CS-US2. In experiment 1, only the 2Trial group was exposed to CS-US2, so in this case the one-way ANOVA included the freezing to the CS-US2 to simplify analysis. In experiment 3, a two-way ANOVA is used, one factor being CS-US1 or CS-US2 and the other factor being the combination of treatment and behavioral group. Given that the acquisition of learning is reflected in part by within-session change, we include CS-US1 in all ANOVAs involving CS-US2. We examined group and treatment effects on CS-US2 with post hoc Sidak tests. Experiment 2 involved only one CS-US pairing, and this was analyzed with a two-way group-by-treatment ANOVA because the manipulation resulting in the four groups occurred before conditioning. Pre-CS freezing is also analyzed by a two-way ANOVA in this case because it is also after behavioral manipulations.

Analysis of the long-term memory test was the same in all experiments. First, we performed a two-way ANOVA with group and treatment as factors and the average of all 10

freezing-to-CS measures for each rat as the dependent variable (Figs. 2.1C, 2.2C, 2.3C) followed by a Sidak post hoc test analyzing the biologically relevant factors depending on the experiment. To further analyze the effect of treatment we analyzed each group separately and including CS-presentation trial as a second variable in a treatment-by-CS two-way ANOVA.

Acknowledgments

This work was supported by a grant from the National Institute for Mental Health to J.E.L. (R01 MH046516).

CHAPTER 3

A brainstem-central amygdala circuit underlies defensive responses to learned threats

Yiran Gu,^{1,2,3} Walter T. Piper,² Lauren A. Branigan,² Elena M. Vazey,⁴ Gary Aston-Jones,⁵

Longnian Lin,¹ Joseph E. LeDoux,^{1,2,6} Robert M. Sears^{2,6,7}

¹ Shanghai Key Laboratory of Brain Functional Genomics (Ministry of Education), Institute of Brain Functional Genomics, School of Life Science, NYU-ECNU Institute of Brain and Cognitive Science, East China Normal University, Shanghai, China

² Center for Neural Science, New York University, New York, NY, USA

³ Department of Psychiatry, McLean Hospital, Harvard Medical School, Belmont, MA, USA

⁴ Department of Biology, University of Massachusetts, Amherst, MA, USA

⁵ Brain Health Institute, Rutgers University/Rutgers Biomedical and Health Sciences, Piscataway, NJ, USA

⁶ Emotional Brain Institute, The Nathan Kline Institute, Orangeburg, NY, USA

⁷ Department of Child and Adolescent Psychiatry, New York University Langone School of Medicine, New York, NY, USA

Published in Molecular Psychiatry at <https://doi.org/10.1038/s41380-019-0599-6>

Abstract

Norepinephrine (NE) plays a central role in the acquisition of aversive learning via actions in the lateral nucleus of the amygdala (LA) (Bush et al., 2010; Schiff et al., 2017). However, the function of NE in expression of aversively-conditioned responses has not been established. Given the role of the central nucleus of the amygdala (CeA) in the expression of such behaviors (Fadok et al., 2018; Keifer et al., 2015; B. Li, 2019), and the presence of NE

axons projections in this brain nucleus (Y.-W. Chen et al., 2019), we assessed the effects of NE activity in the CeA on behavioral expression using receptor-specific pharmacology and cell- and projection-specific chemogenetic manipulations. We found that inhibition and activation of locus coeruleus (LC) neurons decreases and increases freezing to aversively conditioned cues, respectively. We then show that locally inhibiting or activating LC terminals in CeA is sufficient to achieve this bidirectional modulation of defensive reactions. These findings support the hypothesis that LC projections to CeA are critical for the expression of defensive responses elicited by conditioned threats.

Introduction

Much of the work describing the neural and behavioral mechanisms of defensive behavior and threat processing has used Pavlovian threat conditioning (PTC) (LeDoux, 2014). This research has shown that the amygdala plays a crucial role in defensive reactions initiated by environmental threats (Davis, 1992; Herry & Johansen, 2014). PTC and the amygdala have both been implicated in fear and anxiety disorders (Fenster et al., 2018; Herry & Johansen, 2014), as has the neuromodulator norepinephrine (NE). In the present study, we explore the contribution of NE in the amygdala to the expression of amygdala controlled defensive behavior. During PTC, a neutral conditioned stimulus (CS; e.g., an acoustic tone) is paired with a noxious unconditioned stimulus (US; e.g., an electric foot shock) so that later presentation of the CS alone results in expression of defensive behaviors (the conditioned response; e.g., freezing). CS and US signals converge in both the lateral nucleus of the amygdala (LA) and the central nucleus of the amygdala (CeA) (S. Han et al., 2015; Herry & Johansen, 2014; Wilensky et al., 2006; K. Yu et al., 2016). The LA communicates directly with CeA (H. Li et al., 2013) and indirectly via the basal amygdala (BA) (H. Li et al., 2013; Pitkänen et al., 1997; K. Yu et al., 2016). As a major output nucleus of the amygdala, the CeA coordinates defensive behavioral

reactions and supports physiological adjustments in response to threatening stimuli via divergent projections to the midbrain (Ciocchi et al., 2010; Fadok et al., 2018; LeDoux et al., 1988; Ozawa et al., 2017; Tovote et al., 2016), lateral/paraventricular hypothalamus (PVN) (Carter et al., 2010; LeDoux et al., 1988; Vazey et al., 2018), and medulla (Keifer et al., 2015; Sikha Saha et al., 2005; Tovote et al., 2016).

NE is also implicated in fear and anxiety (Giustino & Maren, 2018; Rodrigues et al., 2009). Aversive stimuli and stress increase levels of NE in the brain, including the amygdala (F. J. Chen & Sara, 2007), largely through activation of the brain stem locus coeruleus (LC) (McCall et al., 2015; Uematsu et al., 2017). LC stimulation or noxious stimuli (e.g., footshock) modulate the basolateral region of the amygdala (BLA), which consists of LA and BA (F. J. Chen & Sara, 2007; Johansen et al., 2014; Uematsu et al., 2017), and studies suggest that this is through direct NE activity at β -adrenergic receptors (β -ARs) (Buffalari & Grace, 2007; Cahill et al., 1994; Ferry & McGaugh, 2000; Quirarte et al., 1998; Schiff et al., 2017). Notably, β -ARs in the LA are critical for initial acquisition (and indirectly for consolidation processes (Schiff et al., 2017)), but not expression of Pavlovian threat memories (Bush et al., 2010; Schiff et al., 2017), and in BLA, for conditioned place aversion and anxiety-like behaviors (McCall et al., 2017). Although much work on the role of NE in the amygdala has focused on the BLA, the CeA also receives significant NE inputs from the LC (Fallon et al., 1978; B. E. Jones & Yang, 1985; R. Y. Moore & Bloom, 1979; Uematsu et al., 2015). Despite this anatomical evidence, few studies have examined the contribution of NE inputs to CeA to the expression of defensive responses elicited by conditioned threats.

Here we describe the role of NE in the expression of Pavlovian threat memories and uncover key components of the underlying brain circuitry. We first show that CS-elicited defensive responses (freezing) decreased following systemic injection of the β -AR antagonist

(propranolol), while injection of β 2-AR agonist (procaterol) increased freezing. To test the role of LC in these adrenergic effects on behavioral expression, we used adeno-associated virus (AAV) vectors expressing DREADDs (Armbruster et al., 2007) and engineered to target NE-expressing neurons in the LC (NE-LC) (Vazey et al., 2018; Vazey & Aston-Jones, 2014). Systemic Clozapine-N-oxide (CNO) injections administered prior to testing reduced or enhanced behavioral expression, by inhibiting (hM4Di) or activating (hM3Dq) NE-LC neurons, respectively. To test the hypothesis that CeA mediates these effects, we directly infused propranolol into the CeA, which also reduced freezing. To test the role of a specific NE-LC→CeA circuit in expression, we directly inhibited or activated LC axon terminals by infusing CNO into the CeA prior to the expression test. Consistent with the pharmacology and NE-LC DREADD studies, we found that inhibition and activation of LC terminals in CeA bidirectionally modulated freezing behavior. Finally, to test a requirement for β -AR activation in the circuit-specific hM3Dq results, propranolol was co-infused with CNO in CeA. As predicted, propranolol attenuated CNO-induced enhancement of freezing. Taken together, these studies demonstrate that NE released from LC terminals in CeA enhances the expression of defensive responses elicited by learned threats.

Methods

Subjects

We used adult male Sprague-Dawley rats (Hilltop Laboratory Animals, Inc.; Scottdale, PA, USA), weighing 250–275 g (~60–70 days old) upon arrival. All animals were naive and allowed at least 1 week of acclimation to the vivarium before surgery and conditioning. Rats were individually housed in transparent plastic high-efficiency particulate absorption (HEPA)-filtered cages and maintained on a 12/12 h light/dark cycle (7:00 A.M.–7:00 P.M.) within a temperature- and humidity-controlled environment. Food and water were available *ad libitum*

throughout the duration of the experiments. All experiments were conducted during the light cycle. All procedures were conducted in accordance with the *National Institutes of Health Guide for the Care and Use of Experimental Animals* and were approved by the *New York University Animal Care and Use Committee*.

Stereotaxic surgery

Rats were anesthetized with a mixture of ketamine (100 mg/kg, i.p.) and xylazine (10 mg/kg, i.p.), and placed in a stereotaxic apparatus (David Kopf Instruments, Tujunga, CA, USA). Supplemental doses of the mixture were given as needed to maintain a deep level of anesthesia. Brain areas were targeted using coordinates from Paxinos and Watson (2005). Following surgery, rats were administered three daily doses of ketoprofen (5.0 mg/kg) as analgesic.

For CeA/BLA infusion experiments, rats were implanted bilaterally with stainless steel guide cannulae (22 gauge; Plastics One, Roanoke, VA, USA). Guide cannulae were lowered to CeA (stereotaxic coordinates from bregma: anterior–posterior (AP) –2.8 mm, medial–lateral (ML) ± 4.3 mm, dorsal–ventral (DV) –7.0mm from skull) or BLA (stereotaxic coordinates from bregma: anterior–posterior (AP) –2.8mm, medial–lateral (ML) ± 5.2 mm, dorsal–ventral (DV) –7.0mm from skull) and secured to the skull using surgical screws and acrylic dental cement (Ortho-jet; Lang Dental Manufacturing Co.). Dummy cannulae (28 gauge) extending 0.2mm from the guides were inserted to prevent clogging. Internal cannulae (28 gauge) extending 1.5mm beyond the guides were used for drug infusions. Results of cannula targeting are shown in Supplementary Fig. 3.1.

For LC viral injection experiments (Supplementary Fig. 3.2), DREADD virus was bilaterally injected (stereotaxic coordinates from lambda: anterior–posterior (AP) –0.8 mm, medial–lateral (ML) ± 1.35 mm, dorsal–ventral (DV) –7.5 mm from skull) to a volume of 1.4

μ l/side using a 5.0 μ l Hamilton Neuros syringe (Hamilton Co.). After 3 weeks for LC soma manipulations or 6–8 weeks for LC axon manipulations in CeA or BLA, animals were handled and subjected to behavioral conditioning as described below.

Apparatus

For behavioral experiments, rats underwent threat conditioning in one of six identical chambers (Rat Test Cage; Coulbourn Instruments, Allentown, PA, USA) constructed of aluminum and Plexiglas walls, with metal stainless steel rod flooring that was attached to a shock generator (Model H13-15; Coulbourn Instruments). Each chamber was enclosed within a sound isolation cubicle (Model H10-24A; Coulbourn Instruments). A computer, installed with Graphic State 2 software and connected to the chambers via the Habitest Linc System (Coulbourn Instruments), delivered tone and shock stimuli during behavioral sessions. During habituation and threat conditioning, the chambers were lit with a single house light (context A). Expression tests took place in a modified context which consisted of red lighting, smooth black plastic flooring, a mild peppermint, or lavender scent and a striped pattern on the Plexiglas door (context B or context C), a mild almond scent or a mild citrus scent and a striped pattern on the Plexiglas door (context D or context E). An infrared digital camera mounted on top of each chamber was used to videotape behavioral procedures.

Viral vectors

Excitatory (hM3Dq: AAV9/PRS \times 8-HA-hM3Dq-SV40-PolyA), inhibitory (hM4Di: AAV9/PRS \times 8-HA-hM4Di-SV40-PolyA) and control vectors (Control: AAV9/PRS \times 8-mCherry-WPRE-rBG) were subcloned by Dr. Elena M. Vazey from Gary Aston-Jones' lab and packaged by the University of Pennsylvania Vector Core. The synthetic PRS \times 8 promoter was used to restrict expression of the hM3Dq/hM4Di DREADDs to noradrenergic neurons in the LC (see Supplementary Fig. 3.2).

Drug preparation and Infusion

(\pm)-Propranolol hydrochloride and procaterol hydrochloride (Sigma-Aldrich Co. St. Louis, MO, USA) were freshly dissolved in 0.9% sterile saline immediately prior to injections. For intraperitoneal (IP) injection experiments, concentrations for propranolol and procaterol were 10 mg/kg and 300 μ g/kg, respectively. For CeA microinfusion experiments, propranolol was dissolved in 0.9% sterile saline and administered at 1.0 μ g/0.3 μ l. CNO for IP experiments (5.0 mg/kg for hM4Di inhibition, 1.0 mg/kg for hM3Dq activation) was obtained from the NIH as part of the Rapid Access to Investigative Drug Program funded by the NINDS and prepared in a 7% DMSO + 0.9% sterile saline, which was also used for vehicle. For c-Fos experiments, CNO was obtained from RTI International (Batch ID: 13662-18; MH No. C-929). For intracranial CeA or BLA infusions, CNO (Sigma-Aldrich) was dissolved in 0.9% sterile saline (1.0 mM, 0.3 μ l per side) (Mahler et al., 2014).

For all intracranial infusions, infusion cannulae were attached to 10 μ l Hamilton syringes via 0.015 in. \times 0.043 in. \times 0.014 in. polyethylene tubing obtained from A-M Systems, Inc. (Carlsborg, WA, USA). Tubing and syringes were backfilled with distilled water, and a small air bubble was introduced to separate the water from the infusate. Rats were bilaterally infused with 0.3 μ l using an infusion pump (PHD 2000; Harvard Apparatus) at a constant rate of 0.1 μ l/min. Animals were allowed to move freely in their home cage during infusions. After infusion was complete, cannulae were left in place for an additional 1–2 min to allow drug diffusion away from the cannula tip.

For infusions to estimate spread of drugs in CeA, a fluorophore-conjugated propranolol (CA200693 CellAura fluorescent β 2 antagonist [(S)-propranolol-green], Hello Bio Inc., Princeton, NJ, USA) was dissolved at a concentration of 0.5 μ g/ μ l in a vehicle of 5% DMSO, 25% TWEEN

80, and 70% by volume of saline. Animals were infused as described above and were perfused with 4% paraformaldehyde 30 min after fluorophore infusion.

Pavlovian threat conditioning and testing procedures

Rats were habituated to the conditioning box (context A) for 30 min and returned to the colony room. Twenty-four hours following habituation (Day 2) animals were threat conditioned in the same context. Following an initial 5-min acclimation period, rats were subject to three conditioning trials consisting of a 30-s, 5 kHz, 80 dB SPL sine-wave tone CS co-terminating with a 1-s footshock US (a 0.4 mA weak footshock US, a 0.6 mA standard footshock US, or a 1.0 mA strong footshock (see Supplementary Fig. 3.4)). Expression testing for CS-elicited freezing responses was conducted 1 day after conditioning in the modified context (context B). After the 5-min acclimation period, rats were presented with five CS presentations without the footshock US. The mean inter-trial interval was 4 min (2–6 min range) for both conditioning and testing sessions. On Day 4, 2 days after conditioning, drug-free testing for CS-elicited freezing was conducted in a modified context (context C) using the same procedure as the previous expression test. Behavior was recorded and freezing scored as described below.

Measurement of freezing behavior

Freezing was used to measure the conditioned threat response and was defined as the cessation of all movement with the exception of respiration-related movement and non-aware or resting body posture (McAllister et al., 1971). Behavior was recorded and scored offline as the time spent freezing during each 30-s tone CS. Pre-CS freezing was also scored during the 30-s interval prior to the initial tone onset and was used as a measure of non-specific freezing to the context. Two experimenters, blind to drug group allocation scored freezing and the data were averaged.

c-Fos experiments to confirm DREADD activity

Some animals used for DREADD experiments were injected IP with CNO or saline to validate the functionality of DREADDs (Supplementary Fig. 3.5a and 3.5b). Animals expressing excitatory hM3Dq receptors were injected IP with either CNO (1.0 mg/kg) or saline, then perfused 90 minutes later with 4% paraformaldehyde (PFA) as described in the histology section below. Animals expressing inhibitory hM4Di were injected IP with CNO (5.0 mg/kg) or saline, then 30 minutes later exposed to footshocks by running the CS-US conditioning procedure again (to increase baseline c-Fos levels) and perfused 85 minutes after completion of the three tone-footshock pairings. Brain sections and microscope images were prepared as described below for c-Fos counts of cell nuclei in LC.

Histology and immunohistochemistry

Following behavior experiments, animals were overdosed with 25% chloral hydrate or a mixture of ketamine (100 mg/kg, i.p.) and xylazine (10 mg/kg, i.p.) and transcardially perfused with either 10% formalin for histology to assess cannula placement or 4% PFA in 0.1M phosphate buffer (PB) for immunohistochemistry (IHC).

Tissue processed for cannula placement was post-fixed in 10% formalin at 4 °C until prepared for histological staining. For IHC, some brains were cryoprotected in a 30% sucrose–4% PFA solution for at least 1 day and then stored in 0.01M PBS at 4 °C before being sectioned on a freezing microtome (Leica). Other brains were post-fixed in 4% PFA, blocked coronally, and cut on a Vibratome (Leica).

For histological verification of cannula targeting, tissue was cut at a thickness of 50 µm and kept in 0.01M PBS + 0.05% sodium azide (NaAz) until mounted on gelatin-coated slides and dried overnight. After standard Nissl staining and coverslipping, sections were examined on a light microscope for injector tip localization in the CeA or BLA. Only data from rats with bilateral injector placements localized to the CeA or BLA were included in the study.

For IHC, tissue was cut at 35 or 40 µm, rinsed in 0.01M PBS, and blocked in 1% BSA in 0.01M PBS for 30–60 min at room temperature (RT). Immunohistochemical detection was achieved in primary antibody solutions containing 1% BSA, 0.2% Triton-X 100, and 0.05% NaAz.

DREADD-injected brain sections were incubated overnight at RT in rabbit anti-HA (for detection of HA-Tag; 1:500; cat. # 3724s; Cell Signaling Technology, MA) and mouse anti-dopamine beta hydroxylase (DBH; 1:2000; cat. # MAB308; EMD Millipore, MA) antibodies for verification of viral expression in LC neurons, long-projection terminals in CeA, and cell specificity of viral expression. Viral control animal brain sections were incubated overnight at RT in rabbit anti-DsRed (for detection of mCherry; 1:500; cat # 632496; Clontech Laboratories, CA) and anti-DBH (DBH; 1:2000; cat. # MAB308; EMD Millipore, MA) antibodies. For c-Fos experiments, guinea pig anti-c-Fos (1:1000; cat. # 226-005; Synaptic Systems, Goettingen, Germany) was used to detect c-Fos in LC cell nuclei.

Following primary antibody incubation, sections were rinsed with agitation three times for 5 min in 0.01M PBS at RT. Sections were then incubated in Alexa Fluor goat anti-rabbit 594 (1:200; cat. # A-11012; Life Technologies, CA) or goat anti-mouse 488 secondary antibody (1:200; cat. # A-11001; Life Technologies, CA) in 0.01M PBS at RT. For c-Fos experiments, secondary antibodies were Alexa Fluor goat anti-rabbit 488 (1:400; Thermo Fisher Scientific, MA) to label HA, Alexa Fluor goat anti-mouse 555 (1:800; Thermo Fisher Scientific, MA) to label DBH, and Alexa Fluor goat anti-guinea pig 647 (1:400; cat. # A-21450; Thermo Fisher Scientific, MA, USA) to label c-Fos. Sections were rinsed three times for 5 min in PBS, mounted on gelatin-coated slides, and allowed to dry for several hours, followed by a brief wash in deionized H₂O to remove excess salt (PBS), coverslipped in aqueous mount (ProLong Gold Antifade Reagent; cat. #3P6930 or #3P6931; Life Technologies, CA), and allowed to cure overnight at

RT. Sections were imaged using a Leica TCS SP8 confocal microscope (Leica) or Olympus VS120 fluorescent microscope (Olympus). Imaging data were processed and analyzed with ImageJ software (NIH). For all experiments, animals were excluded from analysis if virus-expression was insufficient or cannulae targeting was outside the areas of interest.

c-Fos and HA-expressing cells in LC were quantified by two raters blind to experimental condition. Images were prepared by importing confocal z-stacks into ImageJ software, which were then partially collapsed to project 10 z-planes to produce an image representing a 6.8 μ m thick plane of LC. The measure of interest was the ratio of HA + c-Fos double-labeled cells over HA cells in LC.

Statistics

Rats were randomly allocated to groups prior to surgery and behavioral testing. Previous studies using similar techniques guided our estimates of sample size. Out of 382 total animals, 103 were removed for these reasons, leaving 279 animals for analysis. Animals were excluded from the study if (1) virus expression was absent unilaterally or bilaterally, (2) if cannulae missed their target (bilaterally or unilaterally) and (3) if baseline freezing was not significantly different from CS-elicited freezing, indicating contextual generalization. For experiments with two groups, an unpaired Student's *t* test (two-tailed) was used to analyze freezing levels (baseline or CS-elicited freezing). One-way ANOVA was used for comparing more than two groups followed by a Tukey's multiple comparison tests. Mean CS freezing data between drug treatment days and drug-free days were analyzed using repeated measures ANOVAs followed by Sidak multiple comparisons tests. For all experiments, normal distribution was assumed. A Brown–Forsythe test for equal variances was used for one-way ANOVAs, whereas the *F* test was used for the Student's *t* test to confirm that variances were not significantly different in compared groups. Where unequal variances were revealed by *F* test, data was reanalyzed using a Mann–Whitney

U test. All behavioral results were replicated in multiple groups or runs for each experiment.

Error bars in all figures represent \pm SEM. Data were analyzed using GraphPad Prism.

Results

We first investigated the contribution of β -AR activity to the expression of Pavlovian conditioned defensive responses. Rats were administered the β -AR antagonist propranolol (10 mg/kg, $n = 12$) or saline ($n = 12$) 24 h following cued threat conditioning and tested for freezing responses to the CS (Fig. 1a). Consistent with another report [43], propranolol significantly attenuated CS-evoked freezing levels ($t(22) = 3.894$, *** $p = 0.0008$), and slightly reduced baseline freezing ($t(22) = 2.348$, * $p = 0.0283$) (Fig. 3.1b, left panel), effects that were not observed during a drug-free test in the same animals (Fig. 3.1b, center panel). In separate groups of animals, propranolol still reduced freezing with stronger training (Supplementary Fig. 3.4a, 3.4b, $n = 11$ /group, 1.0 mA shock training ($t(20) = 2.129$, * $p = 0.0459$)) and during a remote memory test (Supplementary Fig. 3.4c, 3.4d, $n = 9$ /group, 1 month after conditioning (BL freezing: Student's t test, $t(16) = 2.297$, * $p = 0.0354$, CS freezing: $t(16) = 5.930$, **** $p < 0.0001$).

To assess the effects of β_2 -AR activation on memory expression, two groups of rats were administered systemic injections of the β_2 -AR agonist procaterol (300 μ g/kg, $n = 8$) or vehicle ($n = 8$) prior to the expression test. Procaterol significantly increased CS-evoked freezing levels (Fig. 1c left panel, 300 μ g/kg, ($t(14) = 2.625$, * $p = 0.0200$)), with no difference observed between groups when the drug was not onboard (Fig. 3.1c, center panel). Collectively, these data reveal that β -ARs positively modulate the expression of defensive responses regardless of memory strength or time since memory formation, and blockade or activation does not have long-term effects on behavioral plasticity.

Chemogenetic inhibition of LC attenuates freezing to a conditioned cue

LC neurons send NE efferents throughout the brain, including the amygdala (Fallon et al., 1978; B. E. Jones & Yang, 1985; R. Y. Moore & Bloom, 1979; Uematsu et al., 2015). We therefore tested whether LC-NE activity modulates the expression of defensive responses. Using AAV vectors expressing DREADDs (hM4Di) or a fluorescent reporter (mCherry) under the control of a synthetic promoter (PRS × 8) (Hwang et al., 2001; Vazey et al., 2018; Vazey & Aston-Jones, 2014), we observed expression restricted to NE (dopamine β hydroxylase (DBH)-positive) neurons in LC (Fig. 3.2b). Following bilateral AAV injections in LC, an hM4Di group ($n=9$) and an mCherry ($n=7$) group were trained using a moderate protocol (3 CS-US pairings, 0.6mA US), while a third hM4Di group ($n=7$) received three CS presentations without footshock to control for nonspecific effects on freezing behavior. All animals received systemic injections of CNO (5.0mg/kg) prior to the expression test (Fig. 3.2a). CNO significantly attenuated CS-elicited freezing levels only in conditioned animals expressing hM4Di compared to conditioned animals expressing mCherry alone (CS freezing: One-way ANOVA $F(2, 20) = 126.4$, **** $p < 0.0001$, Tukey's MCT: hM4Di untrained versus mCherry trained, **** $p < 0.0001$, hM4Di untrained versus hM4Di trained, **** $p < 0.0001$, mCherry trained versus hM4Di trained, ** $p < 0.01$), with no effect observed in the untrained behavioral controls expressing hM4Di (Fig. 3.2c, left panel). No significant effect was observed between trained groups in freezing levels during a CNO-free test and freezing remained negligible in the untrained group (Fig. 3.2c, center panel). In a separate analysis, c-Fos expression showed a trend, but no significant reduction in HA-expressing DBH neurons following CNO expression and training (Supplementary Fig. 3.5a). These data suggest that LC-NE activity positively modulates the expression of learned threat reactions.

Chemogenetic activation of LC enhances freezing to a conditioned cue

Next, excitatory DREADDs (hM3Dq) were used to determine how stimulation of LC-NE activity would affect CS-elicited freezing. hM3Dq- and mCherry-immunopositive neurons were observed to co-localize with the DBH-positive neurons in LC (Vazey et al., 2018; Vazey & Aston-Jones, 2014), red fluorescence was detected throughout the entire LC but not in neighboring regions (Fig. 3.3b, Supplementary Fig. 3.2), which showed that viral targeting was LC specific. An hM3Dq group ($n=9$) and an mCherry group ($n=7$) were trained using a weak protocol (to avoid ceiling effects, three CS-US pairings, 0.4mA shock), and a third hM3Dq group ($n=7$) received three CS-alone presentations without footshock to control for unconditioned freezing behaviors. Systemic CNO (1.0mg/kg) significantly increased CS-elicited freezing levels in trained hM3Dq-expressing animals compared with mCherry-expressing animals ($F(2, 20)=69.54$, **** $p < 0.0001$, Tukey's MCT: hM3Dq untrained versus mCherry trained, **** $p < 0.0001$, hM3Dq untrained versus hM3Dq trained, **** $p < 0.0001$, mCherry trained versus hM3Dq trained, *** $p < 0.001$), with minimal CS-elicited freezing responses observed in the untrained control group (Fig. 3.3c, left panel). No significant effects were observed between trained groups during a CNO-free test (Fig. 3.3c, center panel). In a separate group of animals, c-Fos expression in HA-expressing DBH neurons was significantly increased by CNO (* $p < 0.05$; Supplementary Fig. 3.5b). Taken together, these and the hM4Di data (Fig. 3.2) suggest that LC activity positively modulates CS-elicited freezing.

Pharmacological blockade of β-ARs in CeA attenuates freezing

We found that pharmacological and chemogenetic manipulations of brain NE activity bidirectionally modulated behavioral expression. We next tested the hypothesis that NE activity in the CeA positively modulates CS-elicited freezing. Rats received bilateral microinjections of the β-AR antagonist propranolol or vehicle in the CeA prior to the expression test. Results show that propranolol (1.0 µg/0.3 µL/side) significantly attenuated CS-elicited freezing levels

compared with vehicle controls ($n=7/\text{group}$, $t(12)=5.324$, $***p=0.0002$) (Fig. 3.4a, right panel). Therefore, β -AR activity specifically in CeA mediates the expression of responses to learned threats.

Chemogenetic inhibition of LC terminals in CeA attenuates freezing

We have shown that NE neurons in LC and β -AR activity in CeA play a critical role in defensive responses. To test the LC→CeA circuit, we combined targeted expression of hM4Di in LC-NE with direct CNO infusions to block axon terminal activity in CeA (Fig. 3.4b). Six weeks following surgery, animals were trained using a standard conditioning protocol (Fig. 3.4c) and memory tested the subsequent day. Pre-test infusion of CNO in CeA (1.0 mM/0.3 $\mu\text{l}/\text{side}$) in hM4Di-expressing animals ($n = 15$) significantly attenuated freezing levels compared with mCherry controls (Fig. 3.4d left panel, $n = 7$, Mann–Whitney U test, $**p = 0.0015$). During a CNO-free test, intra-CeA infusion of vehicle did not significantly affect freezing behavior between groups (Fig. 3.4d, center panel). To control for drug spread affecting the adjacent BLA, some animals were infused with CNO directly in BLA (Supplementary Fig. 3.5c). Consistent with previous reports (Bush et al., 2010; Vetere et al., 2013), no effect was observed on behavioral expression. These data support the hypothesis that LC→CeA, but not LC→BLA circuit activity is necessary for the expression of conditioned threat reactions.

Chemogenetic activation of LC-NE terminals in CeA enhances CS-elicited freezing

To further confirm a role for a LC→CeA circuit in defensive responses, we combined targeted expression of hM3Dq in LC-NE with direct CNO infusions to activate axon terminals in CeA. Six weeks following surgery, animals were trained using a weak conditioning protocol followed by an expression test the next day (Fig. 3.5c). Following bilateral microinjections of CNO in CeA (1.0 mM/0.3 $\mu\text{l}/\text{side}$), we found that CNO significantly increased freezing levels in hM3Dq animals compared with the mCherry control group (Fig. 3.5c, left panel, $n = 8–10/\text{group}$,

$t(16) = 3.114$, ** $p = 0.0067$). In a subsequent CNO-free test, CS-elicited freezing was not different between groups (Fig. 3.5c, center panel). To control for CNO effects on adjacent regions, some animals received CNO in BLA (Supplementary Fig. 3.5d). As with the BLA infusion control in hM4Di-expressing animals, no effect was observed on CS-elicited freezing behavior.

Enhancement of CS-elicited freezing by chemogenetic activation of the LC→CeA circuit requires β-AR activity in CeA

Next, we determined if chemogenetic enhancement of CS-elicited freezing requires NE activity at β-ARs in CeA. Prior to the expression test, hM3Dq rats were administered bilateral microinjections of either CNO alone (1.0 mM/0.3 µl/side) or a cocktail of propranolol (1.0 µg/0.3 µl/side) and CNO (1.0 mM/0.3 µl/side) in CeA. An mCherry group was also administered the propranolol-CNO cocktail. Results showed that CNO alone significantly enhanced CS-elicited freezing in hM3Dq animals, whereas inhibition of β-ARs in CeA significantly reduced this effect (one-way ANOVA: $F(2, 24) = 23.77$, **** $p < 0.0001$, Tukey's MCS: mCherry (CNO + Prop) versus hM3Dq (CNO + Prop), n.s., mCherry (CNO + Prop) versus hM3Dq (CNO), **** $p < 0.0001$, hM3Dq (CNO + Prop) versus hM3Dq (CNO), **** $p < 0.0001$) (Fig. 3.5e, $n = 7$ –10/group). No difference was observed between hM3Dq (CNO + Prop) and mCherry (CNO + Prop) groups. These data suggest that freezing reactions require NE release from LC terminals in CeA.

Discussion

Here we establish the neural underpinnings of noradrenergic modulation of Pavlovian defensive reactions. First, we found that propranolol-mediated blockade of β-ARs significantly reduced behavioral expression of PTC (Rodriguez-Romaguera et al., 2009) (Fig. 3.1b, Supplementary Fig. 3.4b, 3.4d), whereas systemic activation of β2-ARs using procaterol

enhanced it (Fig. 3.1c). Chemogenetic reduction (Fig. 3.2c) or enhancement (Fig. 3.3c) of noradrenergic LC activity confirmed the role of endogenous noradrenergic activity in behavioral expression. Furthermore, blockade of β -ARs in the CeA, the major output nucleus of the amygdala mediating defensive reactions (Fig. 3.4a) or inhibition of the LC→CeA circuit (Fig. 3.4d) yielded results consistent with systemic propranolol (Fig. 3.1b) and chemogenetic LC inhibition (Fig. 3.2c). As with procaterol injections (Fig. 3.1c) and LC activation (Fig. 3.3c), stimulation of LC→CeA inputs enhanced CS-elicited freezing (Fig. 3.5c). This enhancement was blocked by direct infusion of propranolol, suggesting that NE released from LC axons acts through β -ARs in CeA (Fig. 3.5e). Consistent with previous work (Bush et al., 2010; Vetere et al., 2013), our control studies (Supplementary Fig. 3.5c, 3.5d) found no effect of BLA DREADD manipulations on the expression of defensive responses, suggesting that other targets of the NE system, e.g., CeA are responsible. Taken together, these data suggest that LC→CeA axonal projections release NE into the CeA where β -AR activation positively modulates the degree of CS-elicited freezing.

Noradrenergic LC neurons phasically respond to salient stimuli (learned or novel) in all sensory modalities (Aston-Jones & Bloom, 1981; Foote et al., 1980). NE may improve selectivity or increase the magnitude of neuronal responses to sensory stimulation (Vazey & Aston-Jones, 2014) and promote synaptic transmission and plasticity in threat processing circuits of the amygdala (Tully et al., 2007). Indeed, NE signaling through β -ARs in LA and/or BLA can regulate the acquisition (Bush et al., 2010; Johansen et al., 2014; Schiff et al., 2017), consolidation (Quirarte et al., 1998; Schiff et al., 2017), reconsolidation (Dębiec & LeDoux, 2004, 2006), and extinction (Berlau & McGaugh, 2006; Dębiec et al., 2011) of memory. However, neither propranolol nor DREADD-mediated inhibition or activation at axon terminals in

BLA during an expression test affected CS-elicited freezing (Bush et al., 2010; Vetere et al., 2013) (also see Supplementary Fig. 3.5c, 3.5d).

A recent study showed that sustained (10–15 s) high-frequency (10 Hz) photostimulation of LC can lead to reversible ‘behavioral arrest’ (Carter et al., 2010). However, this strong stimulation decreased cortical release of NE, suggesting that brain-wide depletion of NE may be responsible for the observed effects on behavior. On the other hand, DREADD-mediated LC excitation, which we used here (Fig. 3.3), was shown to tonically increase LC neuronal firing at physiological frequencies (~5 Hz) (Vazey & Aston-Jones, 2014). Indeed, using this same viral vector, Kane et al. did not observe behavioral arrest, but did find a disruption in a foraging behavior task (Kane et al., 2017), possibly due to ‘decision noise’ created by persistent LC activity. This is perhaps consistent with our previous study showing that the invigorating effects of a CS on an avoidance task (Pavlovian-to-instrumental transfer, PIT) were disrupted by hM3Dq-mediated excitation of LC (Campese et al., 2017). Notably, baseline shuttling behavior (before the CS) was not affected, suggesting that the PIT deficit was due to an inability of the CS to motivate responding. Taken together, these results suggest that conditioned aversive arousal modulates both Pavlovian and instrumental responses and are consistent with the theory that phasic activation of NE neurons of the LC, and NE release in CeA, could permit rapid behavioral adaptation to changing environmental imperatives (Aston-Jones & Waterhouse, 2016; Bouret & Sara, 2005; Vazey et al., 2018).

Studies using other aversive learning paradigms such as inhibitory avoidance also find an important role for NE activity in amygdala, although there are discrepancies when compared with PTC (Berlau & McGaugh, 2006; Cahill et al., 1994; Ferry & McGaugh, 2000; Quirarte et al., 1998). For example, NE signaling in the LA and/or BLA is required for memory acquisition in PTC but not for inhibitory avoidance (Berlau & McGaugh, 2006; Bush et al., 2010; Cahill et al.,

1994; Ferry & McGaugh, 2000; Quirarte et al., 1998; Schiff et al., 2017). These differences suggest that distinct behavioral and neural processes may underlie each task. Indeed, inhibitory avoidance involves contextual and instrumental learning that are not required for cued PTC (Berlau & McGaugh, 2006; Cahill et al., 1994; Ferry & McGaugh, 2000; Quirarte et al., 1998; Schiff et al., 2017). Moreover, a recent study showed that low, tonic optogenetic stimulation (5 Hz for 20min) of LC-NE neurons innervating the BLA can increase anxiety-like behaviors and conditioned aversion, the latter of which shares similarities to inhibitory avoidance (McCall et al., 2017). In contrast to LA/BLA, very little is known about NE activity in CeA in both inhibitory avoidance and PTC. A single study looking at NE signaling in CeA found no role in the consolidation of inhibitory avoidance memory but did not test for expression effects (Quirarte et al., 1998).

While the NE LC→CeA circuit modulated conditioned memory expression, it did not affect unconditioned freezing (Figs. 3.2c, 3.3c). Although pre-CS freezing was slightly reduced in two experiments (by systemic propranolol (Fig. 3.1b) and systemic injections of CNO in LC hM4Di animals (Fig. 3.2c)), CNO infusion in CeA in hM4Di animals did not change pre-CS freezing levels (Fig. 3.4d). Also, baseline freezing was not affected in any of the excitatory manipulations, including the potentiation of β 2-AR activity with procaterol (Fig. 3.1c) or hM3Dq-mediated enhancement of LC (Fig. 3.3c) and LC→CeA activity (Fig. 3.5c, e). Changes in pre-CS freezing levels would be expected if brain manipulations of NE activity affected unconditioned freezing.

We used chemogenetic manipulations for many of our studies. There has been recent controversy over the use of CNO, which can be metabolically converted into the atypical antipsychotic clozapine (Gomez et al., 2017). We attempted to circumvent this caveat in several ways. First, we chose systemic doses of CNO that were low enough to minimize this effect

(MacLaren et al., 2016; Mahler & Aston-Jones, 2018), and we used mCherry controls that received the same CNO treatments as experimental groups. Furthermore, we supplemented systemic CNO injection studies with direct, intracranial infusion of CNO to bypass the peripheral metabolism of CNO to clozapine.

The experimental group of animals expressing inhibitory DREADD receptors and treated with intra-CeA CNO (Fig. 3.4d) displayed unusually high individual variability in freezing levels on the day they received CNO. The same animals did not exhibit high individual variability on the drug-free test day. Separate groups of animals expressing inhibitory DREADD and treated with systemic CNO did not exhibit high individual variability in freezing levels (Fig. 3.2d). The LC of animals sacrificed 90 minutes after a footshock, which was 30 minutes after CNO treatment, exhibited c-Fos counts that were not highly variable, but were also not fully effective at suppressing c-Fos in DREADD-expressing neurons (Supplementary Fig. 3.4a). In fact, the trend of systemic CNO suppressing LC c-Fos after footshock was non-significant.

Thus, the most likely explanation for the high individual variability in inhibitory DREADD animals after intra-CeA CNO infusion is an inability of the $G_{i/o}$ -coupled hM4Di DREADD to completely suppress NE release from axonal release sites. This could be highly variable between animals for a few reasons. The DREADD constructs required substantial incubation time to express adequately in axons (Supplementary Fig. 3.3). Different animals probably differed substantially in hM4Di expression levels at the axon terminals, so equal CNO treatment would produce differing levels of inhibition. Another possibility regards the highly heterogenous nature of CeA, with many distinct cell types in various subdivisions, the individual variability might arise from inconsistent surgical placement of the cannula, leading to differential adrenergic receptor activation on different functional modules. However, the same explanation could be extended to excitatory DREADD animals, which is not consistent with our results.

Alternatively, there might be genetic differences leading to individual variation in the intracellular milieu of axon terminals and varicosities, causing different animals to be differentially sensitive to artificial G_{i/o} activity disrupting neurotransmitter release.

Although LC is a major source of NE to the forebrain (Aston-Jones & Cohen, 2005; B. E. Jones & Moore, 1977; Sara, 2009), NE cell groups in the medulla and subcoeruleus region also send strong projections throughout the brain (Rinaman, 2011). Much existing evidence shows A2 adrenergic neurons (located in the dorsal vagal complex, including the nucleus of the solitary tract (NTS)), also project to CeA (Y.-W. Chen et al., 2019; Rinaman, 2011; Robertson et al., 2013; S Saha et al., 2002). Our chemogenetic inhibitory studies with hM4Di show subtle but significant effects, which may suggest that other sources of NE, e.g., A2, summate with LC-NE in the CeA to positively modulate CS-elicited freezing. Indeed, one study showed that A2 neurons are activated by threat-conditioned stimuli (Zhu & Onaka, 2002), and a more recent study shows that neurons from the NTS can negatively regulate anxiety-like behavior (Y.-W. Chen et al., 2019). It is also possible that DREADD-mediated neuromodulatory inhibition is not sufficient to fully shunt excitatory responses in NE cells (see Supplementary Fig. 3.5a). Future work delineating the relative contribution of other NE inputs to defensive responses is therefore warranted.

Given the canonical role of the CeA in expression, in the current studies we focused on this particular phase of conditioning. However, there is some evidence that the CeA itself can mediate Pavlovian memory formation (memory acquisition and/or consolidation) (Goosens & Maren, 2003; H. Li et al., 2013; Wilensky et al., 2006; K. Yu et al., 2017). Recent work exploring the mechanisms underlying this phenomenon suggests that the CeA may convey information about the unconditioned stimulus to the LA during learning (K. Yu et al., 2017). Further studies are needed to determine if NE modulates CeA during the acquisition phase.

Our studies describe the LC→CeA projection, but a reciprocal CeA→LC projection has also been reported (Valentino & Van Bockstaele, 2008). This circuit is modulated by corticotrophin releasing factor (CRF), which is enhanced by stress and may represent a feedforward excitatory mechanism for the LC-NE-mediated responses to threat. If and how this reciprocal circuit is involved in defensive reactions is an important subject of future research.

Symptoms of fear and anxiety disorders involve exaggerated responses to stimuli, whether or not it is a threatening (Parsons & Ressler, 2013), and studies in humans and animals suggest this may be due to dysfunction of the amygdala, the LC (Naegeli et al., 2018) and NE activity in amygdala (Bremner et al., 1996; Davis, 1992; Díaz-Mataix et al., 2017; Fenster et al., 2018; Geraciotti et al., 2001; Giustino et al., 2016; Giustino & Maren, 2018; Ronzoni et al., 2016; Southwick et al., 1997). Together with previous studies, our findings suggested the systemic propranolol treatment can temper the expression of defensive responses (McAllister et al., 1971). Indeed, this models the efficacy of propranolol to quell the symptoms of stage fright or memory retrieval in PTSD patients (Giustino & Maren, 2018). Notably, we do not replicate previous findings showing that systemic propranolol given during the expression test can impair reconsolidation (Dębiec & LeDoux, 2004, 2006) as determined by CS-elicited freezing levels in a second expression test. However, as has been highlighted by others (Giustino & Maren, 2018), the strength of training may determine the efficacy of this manipulation on reconsolidation. Indeed, for our experiments we used three CS-US pairings as opposed to one pairing used in these other studies (Dębiec & LeDoux, 2004, 2006).

The current findings suggest a mechanism for emotional regulation in health and disease. Specifically, the LC→CeA circuit may underlie exaggerated reactions to stimuli and may explain the efficacy of β-AR antagonists like propranolol in fear and anxiety disorders (Cain et al., 2012; Hurlemann et al., 2010; Pitman et al., 2002).

Acknowledgements

We thank Claudia R. Farb and Mian Hou for technical assistance, Dr. Vinod K. Yaragudri for assistance with imaging, Dr. Hillary C. Schiff, Justin Chu, Dylan W. Brown for assistance with behavioral experiments, Dr. Justin M. Moscarello for discussions during the course of this work, and Dr. Vadim Bolshakov for advice and comments on the manuscript. We thank the University of Pennsylvania Vector Core for packaging the AAV vectors. This study was funded by National Institute of Mental Health (NIMH) grants R01-MH046516 and R01-MH38774, National Institute on Drug Abuse (NIDA) grant DA029053, The Vulnerable Brain Project (JEL), and the National Natural Science Foundation of China (Grant 31661143038) (LL).

Open Access

Two paragraphs were added to the original article in preparation of this dissertation. These added paragraphs were inserted after the 6th paragraph of the discussion section and regarded inhibitory DREADD receptors. This change is acknowledged here in accordance with the Creative Commons Attribution 4.0 International License.

This article is licensed under a Creative Commons Attribution 4.0 International License, which permits use, sharing, adaptation, distribution and reproduction in any medium or format, as long as you give appropriate credit to the original author(s) and the source, provide a link to the Creative Commons license, and indicate if changes were made. The images or other third party material in this article are included in the article's Creative Commons license, unless indicated otherwise in a credit line to the material. If material is not included in the article's Creative Commons license and your intended use is not permitted by statutory regulation or exceeds the permitted use, you will need to obtain permission directly from the copyright holder.

To view a copy of this license, visit <http://creativecommons.org/licenses/by/4.0/>.

CHAPTER 4

Direct observations of amygdalar norepinephrine responses to CS and US

Abstract

Fiber photometry, a technique to measure fluorescent reporters in vivo, was combined with a bioengineered norepinephrine (NE) sensor (NE2h) to track changes in NE extracellular concentrations in amygdala during PTC or LTM testing. This enabled the continuous recording of NE dynamics in amygdala subnuclei during tones and footshocks. Specifically, the possibilities that NE release dynamics differ between lateral amygdala (LA) and central amygdala (CeA) and between auditory tones and footshocks were examined. Finally, the characteristics of the stimuli that triggered the strongest NE responses were discussed in relation to theoretical roles of NE.

In general, there were no obvious differences in NE release between LA and CeA. Footshocks triggered more robust and reliable NE reactions than tones, but some NE reactions to tones were also robust, and NE reactions to conditioned tones were more reliable than to neutral tones. Thus, presence of a perceived threat may be a key driver of amygdala NE activity during PTC. Another consistent pattern observed across all stimulus types was a tendency of the first presentation to produce a larger NE reaction than subsequent presentations of the same stimulus within the same recording session. This is in keeping with the idea that NE activity signals unexpected changes in state or context (A. J. Yu & Dayan, 2005).

Given the novel methodology, many technical points were also addressed, including the

time course of viral incubation, the use of a stable fluorophore (mCherry) on an alternate photometry channel as an artifact control strategy, the identification and characterization of a type of artifact that undermines that artifact control strategy by unequally affecting photometry channels at differing wavelengths, the use of unsignaled footshocks as a positive control to demonstrate NE reactivity, the stabilization of NE₂h with an antagonist (yohimbine) to validate the sensor, and the creation of a regression model to estimate NE signal.

Introduction

Norepinephrine (NE), a neuromodulator that enhances multiple types of learning and is a critical component of acute stress responses, facilitates multiple phases of Pavlovian Threat Conditioning (PTC) (Díaz-Mataix et al., 2017; Gu et al., 2020; Johansen et al., 2014; Rodrigues et al., 2009; Schiff et al., 2017).

The findings in Chapter 2 suggest that NE is mainly involved in PTC acquisition only after a prior unconditioned stimulus (US) induces a temporal window of heightened NE activity (Díaz-Mataix et al., 2017). The neural circuitry underlying stimulus-triggered NE-enhancement of PTC acquisition has not been confirmed, but the neural locus for the artificial disruption of acquisition by antagonizing NE's low affinity β-adrenergic receptors (β-ARs) has consistently been shown to be the lateral amygdala (LA) (Bush et al., 2010; Dębiec & LeDoux, 2004; Johansen et al., 2014; Schiff et al., 2017). Synaptic plasticity underlying this memory formation is driven by both glutamate-dependent and NE-dependent mechanisms (Johansen et al., 2014; Tully et al., 2007). The main sources of NE input to amygdala are the NE-releasing axons originating from the locus coeruleus (LC) (Aston-Jones & Cohen, 2005; B. E. Jones & Moore, 1977; Sara, 2009), although the nucleus of the solitary tract (NTS) also sends NE-projections to central amygdala (CeA) (Y.-W. Chen et al., 2019; Rinaman, 2011; Robertson et al., 2013; S

Saha et al., 2002). The CeA also plays a role in PTC acquisition (Wilensky et al., 2006), although the role of the CeA in acquisition is less understood than the LA's role. These observations illustrate the need for observations of localized NE activity to supplement the inferences gained from carefully controlled manipulation studies.

In contrast, the PTC expression findings from Chapter 3 showed NE in the CeA to modulate conditioned freezing through β -ARs, while NE in LA had no effect on expression (Gu et al., 2020). This raises the question of whether NE release in CeA is triggered by the same types of stimuli and circumstances as NE release in LA.

Based on our previous findings (Díaz-Mataix et al., 2017), a footshock prior to a CS-US pairing should trigger a PTC-enhancing release of NE in LA. With this in mind, we sought to directly observe this NE surge with continuous measurements (12,190 Hz). We utilized a recently developed family of genetically encoded NE sensors called 'NE_GRAB' sensors (J. Feng et al., 2019). NE_GRAB sensors consist of an α_2 -adrenergic receptor conjugated to an intracellular green fluorescent protein domain. This sensor is capable of reporting fluctuations in NE activity when monitored through fiber photometry or other fluorescent recording methods. Specifically, we used a newly developed version of the NE_GRAB sensor called 'NE2h'. We exploited this to directly measure NE signaling in and around LA and CeA.

The opportunity to observe endogenous NE activity is especially critical for understanding NE's role in stress related maladies, as NE tends to be recruited by stressful stimuli (Rodrigues et al., 2009; Sara & Bouret, 2012). However, the term 'stress' can be vague. More precise conceptualizations have been proposed with respect to the LC and NE, mainly using frameworks that place their functions in the realm of cognitive flexibility and behavioral adaptations to unforeseen circumstances (Sara, 2016; A. J. Yu & Dayan, 2005). Under such a

framework, the effect of a large surge of NE would be disengagement from previous assumptions and increased openness to new sources of information.

This does not reject the understanding of NE as mediating arousal (Sara & Bouret, 2012) or in responding to painful stimuli (Ozawa & Johansen, 2018), nor does it reject the possibility of NE underlying conditioned arousal (Sokolov, 1963). Rather, it complements these other perspectives and encourages the decomposition of all possible triggers of NE activity into a few types of environment-responsive schemes without the need to appeal to the vague concept of ‘stress’.

Obtaining a clear picture of amygdala NE dynamics post-footshock will illuminate an area of research uncovered in Chapter 2 and somewhat at odds with traditional learning theory, which is the ability of an U-US to strengthen Pavlovian conditioning. The canonical view is that an U-US presentation will weaken Pavlovian learning due to degradation of CS-US contingency, but our recent research contradicts this (Díaz-Mataix et al., 2017). The experiments proposed here will help reconcile neurobiological knowledge of NE’s role in facilitating synaptic plasticity with Pavlovian learning theory. The controversy comes down to this question: If a U-US has the effects of degrading a CS-US contingency (which should decrease conditioned responding), but also of raising NE levels (priming plasticity), will the resulting threat learning be stronger or weaker than if no U-US was administered? While we found that the U-US enhances learning through a NE-dependent mechanism (Díaz-Mataix et al., 2017), this fiber photometry work will go further by enabling clear characterizations of temporal dynamics and stimulus response tendencies.

Specifically, I predicted that NE signaling in amygdala would rapidly increase during and immediately after US or U-US delivery, then would taper off gradually after US or U-US offset (within 2 to 10 minutes, based on our acquisition time window experiments in Chapter 2, (Díaz-

Mataix et al., 2017)). Due to our findings in Chapter 3 on NE-regulation of conditioned freezing (Gu et al., 2020), I predicted that auditory tones would elicit moderate NE response that would be less robust than footshock-induced surges.

The target brain regions were the lateral amygdala (LA) and central amygdala (CeA), which are critical for PTC learning and expression, respectively (Blair et al., 2001; Grewe et al., 2017; Gu et al., 2020; Johansen et al., 2011; Kim & Cho, 2017). The observational nature of fiber photometry allowed continuous measurements throughout entire protocols, giving opportunities to examine immediate NE responses to stimuli as well as the characteristics of sustained NE elevation after stimulus-offset. learning dynamics and effects on future behavior. Long-term memory for the association between the CS and US is stored within LA. Aside from learning dynamics, NE is known to respond to stressful and painful experiences, often serving as a critical mediator of stress reactivity (Rodrigues et al., 2009).

In addition to the aforementioned research questions, the high-frequency fluorescent measurement of neuromodulators is still a relatively new suite of methods, so this work provided ample opportunity to study the technical parameters involved in preparing the model system for data collection and to develop new quantitative approaches for data analysis. For example, I used a neutral fluorophore (mCherry) on a separate photometry channel in the same animals in order to separate NE_{2h} fluctuations that match fluctuations in the mCherry channel and are probably artifacts from fluctuations that are only on the NE_{2h} and therefore more likely to be the true NE signal. The mCherry channel later served as an exogenous regressor onto the NE_{2h} channel in a time-series model that produced a single output variable representing NE.

Methods

Sample

Male Sprague-Dawley rats (n=10) were prepared for fiber photometry by unilaterally

injecting viral vectors expressing NE2h and mCherry and implanting fiberoptic cannulas into lateral amygdala (n=7) or central amygdala (n=3). All 10 animals were habituated to conditioning context and initially conditioned the next day with 5 CS-US (tone-shock) pairings. Six animals (n=3 LA and n=3 CeA) were given a long-term memory test (LTM) 24 hours later followed by a relatively strong unsignaled unconditioned stimulus (U-US), while four animals (n=4 LA) were given the LTM/U-US session 11 weeks later in order to allow a longer viral incubation period. The purpose of the U-US at the end of the LTM session was to generate a strong NE increase in order to test the visibility of NE reactions and thereby assess the adequacy of the viral incubation period leading up to that recording session.

Reagents and Equipment

Fiber Photometry.

The dual-channel single-site fiber photometry system was designed by Doric Lenses for simultaneous sampling of Green Fluorescent Proteins (GFP) and Red Fluorescent Proteins (RFP) (Ordering code: FPS_1S_GFP/RFP_400-0.57) (Fig. 4.1). The GFP channel was used for NE2h (channel of interest) and the RFP channel was used for mCherry (control channel). Briefly, a central console sent analog sine waves at characteristic frequencies (NE2h channel: 208.616Hz, mCherry channel: 572.205Hz) to a two-channel LED driver connected to two LED's (NE2h channel: $465\pm12.5\text{nm}$, mCherry channel: $560\pm50\text{nm}$) both oscillating between 0.92mW and 4.6mW of output power. This sinusoidal modulation allowed detection based on lock-in amplification, which is a robust signal encoding and decoding strategy for eliminating noise from a signal with a known reference frequency (Zurich Instruments, 2016).

The LED-generated photons traveled through a filter mini-cube with dichroic mirrors and through a patch cord with a 400 μm core and numerical aperture of 0.57 (Doric Lenses Inc.: Mono Fiberoptic Patchcord – Low AutoFluorescence – Item# D207-1402-0.76, Ordering Code:

MFP_400/430/1100-0.57_0.76m_FCM_MF_LAF) to the implanted fiberoptic cannula into the brain. Light absorbed by fluorophores was then emitted at higher wavelengths (lower energy) and traveled back up the fiberoptic cable and through the dichroic mirrors and bandpass filters to arrive at photodetectors. The resulting analog-to-digital converted signal is collected at approximately 12,190Hz and is saved in the form of a time series of voltage measurements (either at full temporal resolution or with a decimation factor of 4 or 25 to average data points and reduce file size)

(Researcher Note: My first day of data was collected with a decimation factor of 25, but this proved limiting for later computations on frequency information. On the flip side, uncompressed files upwards of 1GB (~12 kHz resolution for approximately 30 minutes of recording) caused some computer memory problems when processing the data at full temporal resolution. I have found that a decimation factor of 4 (~3 kHz resolution with file size ~300MB for 30 minutes) strikes a balance of preservation of frequency information with manageable file sizes.)

The Doric system automatically generated a digitally demodulated data stream that is obtained through dual lock-in detection (explained in a later subsection in Methods). After each experimental session, the data were saved in comma-separated-values (.csv) data files with columns for time points (in seconds), raw photodetector signal from each of the 2 channels, an automatically frequency-demodulated stream for each of 2 channels, a column for digital input from the Arduino-based behavior control system, and 2 columns with binary entries indicating the channel is active at each time point. The last 2 columns were not needed because the channels never spontaneously deactivated.

When further data processing was conducted, a 200Hz down-sampled copy of the file was saved to allow easier batch processing with smaller file sizes.

Behavior apparatus.

A single-chamber Pavlovian test cage (Coulbourn Instruments: Item# H10-11R-TC; Dimensions: width 30cm * depth 25cm * height 30cm) was used for all sessions. A low-light infrared camera (Wyze Cam Pan) was mounted on top of the cage ceiling. Infrared LED's inside the cage served as indicator lights to record in video records when tones or shocks were on. Sessions utilized rod flooring. During conditioning sessions, this rod flooring was connected to an electric shock generator (Coulbourn Instruments: Item# H13-15). A speaker near the top of the cage was connected to a tone generator (Coulbourn Instruments: Item# A12-33). No house lights were used in order to minimize the risk of artifacts caused by ambient light infiltrating fiberoptic patchcords.

The expression test days of PTC protocols typically use modifications to the conditioned chamber in order to separate the test context from the conditioning context, which theoretically increases the CS-triggered conditioned freezing and decreases spontaneous freezing to context (Johansen et al., 2011). Therefore, expression test sessions included a black plastic floor that was placed on top of the floor rods (tactile modification of context) or papers with solid black lines that were taped against the plexiglass walls facing inward (visual modification of context).

The timing of stimuli in behavioral sessions was managed by a hybrid custom set-up of Arduino-based circuitry with a laptop-based timer guided by Python scripts. The Arduino sent 5V square pulses to the tone generator and shock generator to deliver stimuli, as well as to the infrared LED and the Doric fiber photometry console in order to synchronize timing between video records and fiber photometry records. (Examples of Arduino and Python scripts for equipment control during behavioral protocols are posted on Github at <https://github.com/WalterPiTheScienceGuy/PiperPiTry>).

Fiberoptic implants.

Fiber optic cannulas (ThorLabs Item# CFMC54L10) had a 400 μ m-diameter glass fiber core (0.50 numerical aperture) held in a 2.5mm-diameter ceramic ferrule. Grooves were cut in the outside of the ceramic ferrule with a small diamond wheel (Dremel 545) to ensure the cannula could be firmly held by dental cement. Implants were autoclaved prior to surgery (257°F / 125°C for 15 minutes) to minimize risk of infection.

Viral Vectors.

All viral vectors were adeno-associated viruses (AAV). The NE sensor AAV9-hSyn-NE2h was a gift from Yulong Li and Jessie Feng and was prepared by Vigene Biosciences (Vigene Item# YL10074-AV9), and AAV5-hSyn-mCherry was obtained from Addgene as a gift from Karl Deisseroth (Addgene viral prep # 114472-AAV5). Before injection, AAV9-hSyn-NE2h was mixed with AAV5-hSyn-mCherry to a 2:1 titer ratio (Final titer: AAV9-hSyn-NE2h=1.304E+13 GC/mL; AAV5-hSyn-mCherry=6.519E+12 GC/mL).

Surgery

Animals (300-350g at time of surgery) were anesthetized with ketamine+xylazine ((100mg+10mg)/kg) or isoflurane. Once animals were non-responsive to a moderate tail-pinch, the rat's head hair was shaved over the incision site and the animal was placed in ear bars in a stereotaxic frame. For surgeries conducted with isoflurane, a nose cone delivered a continuous flow to maintain adequate depth of anesthesia. If ketamine/xylazine was used, booster shots were given as need. With animals in the stereotaxic frame, the scalp was scrubbed with ethanol and betadine, then an incision was made so that bregma and lambda points on the skull could be measured to ensure a flat orientation (less than 0.2mm difference in depth between bregma and lambda). Relative to bregma, LA coordinates were Anterior-Posterior (AP) = -3.0mm , Medial-Lateral (ML) = +/-5.2mm, Dorsal-Ventral (DV) = -8.0mm. CeA coordinates were AP= -2.3mm, ML= +/-4.0mm, DV= -8.3mm . A stereotaxic-mounted drill penetrated the skull directly

over the injection/implantation sites. Autoclave-sterilized screws were applied to other areas of the skull to anchor the dental cement headcap.

Virus was injected using a 5 μ L Hamilton syringe or with a glass-pulled pipette on a Nanoject II (Drummond Scientific Company: Item# 3-000-204). 300nL of the AAV virus mixture (titer of 2.44e13 GC/mL NE2h and 1.40e13 GC/mL mCherry) was injected at a speed of 50nL/minute. The injector tip was left in place for 5 minutes after injection to ensure adequate diffusion of virus mixture in region of interest. After injector tip was removed, a fiber optic implant (ThorLabs: Item# CFMC54L10) with grooves cut in the ceramic ferrule (cut using a Dremel 545 diamond wheel) was implanted at a depth 0.1mm above the virus injection site. Dental cement was then poured onto the skull surface to lock the preparation in place by gripping the implant's ferrule, the ferrule grooves, and the skull-anchored screws.

Ketoprofen (5 mg/kg once daily for 3 days) was injected s.c. as post-operative analgesia. Once dental cement was dry, the animal was removed from the stereotaxic frame and placed in a warmed cage with a heating pad underneath. The surgeon stayed with the animal until it regained consciousness and a healthy appearance.

Histology

Perfusions were carried out using ketamine+xylazine ((200mg+20mg)/kg) as anesthetic. Once rats were unresponsive to tail-pinch, the abdominal and thoracic cavities were opened, a perfusion needle was inserted into the left ventricle, and if possible, clamped in the upper aorta. A small opening was cut in the right atrium and a flow of 100mL phosphate-buffered saline (PBS) was started. This was followed by 300mL of 4% paraformaldehyde (PFA). The brain was then removed and placed in a scintillation vial containing more PFA. At least 48 hours later, 50 μ m-thick floating sections were collected on a vibratome.

Native fluorescent signal from mCherry was typically strong and did not need

amplification. However, although some native signal from NE2h was usually apparent, a clear delineation of expression required antibody staining for GFP (Life Technologies – rabbit anti-GFP at 1:2000 dilution). The immunohistochemistry procedure consisted of a 30 minutes block with bovine-serum-albumin. The anti-GFP primary antibody incubated with free-floating sections and 0.2% Triton-X overnight on a shaker, followed by fluorophore-conjugated secondary antibodies (Invitrogen Molecular Probes #A11034 Lot#702323 - Alexa Fluor 488 anti-rabbit IgG (H+L) highly cross-adsorbed) for approximately 30 minutes at 1:500 dilution. Samples were triple-rinsed with phosphate-buffered saline after each stage of the immunolabeling procedure.

The most informative microscope images were obtained on a VS120 scanning microscope (Olympus Life Science Solutions) with 2x lens for brightfield imaging and 10x lens for fluorescent imaging with a ‘FITC’ channel with 75ms exposure for the NE2h/anti-GFP imaging and a ‘mCherry’ channel with 100ms exposure for the mCherry imaging. Notes from these images are displayed in Table 4.1

Procedure

Behavioral Sessions.

Habituation.

Before this first session, animals were habituated to conditioning context for 30 minutes. No stimuli were delivered, and no measures were taken.

Pavlovian Threat Conditioning (PTC)

After a 10-minute acclimation period, a series of 5 tone-shock (CS-US) pairings were delivered. The conditioned stimulus (CS) was a pure tone (5kHz, 80 dB, 30 second duration), and the unconditioned stimulus was a footshock (0.7mA, 1 second duration) with an onset 1 second before the end of the CS and an offset that co-terminated with the CS. The mean intertrial interval was 210 seconds (range: 180-240 seconds). Following the 5th CS-US pairing, a

300 second cooldown period was given before recording was ended and the animal was returned to its home cage. The total length of the conditioning session was 31.5 minutes.

Digital 5V pulses sent from the Arduino to the fiber photometry console marked events in time for synchronization with photometry data. This square wave indicates the start and end of the PTC session, the onset and offset of the tone CS, and the onset and offset of the shock US.

Long-term memory (LTM) test and U-US

After a 5-minute acclimation period, 5 tone CS trials were delivered, followed by 1 unpaired shock (unpaired unconditioned stimulus; U-US) of relatively high intensity and duration (1.0mA, 5 second duration). The intertrial intervals between CS trials had a mean of 180 seconds (range: 150-200 seconds). The interval between the 5th CS trial and the U-US was 150 seconds. Following the U-US, there was a cooldown of 150 seconds, leading to a total length for the LTM/U-US session of 24 minutes 35 seconds.

Digital square pulses from Arduino to the fiber photometry console marked the start and end of the LTM/U-US session, the onset and offset for the tone CS, and the onset and offset of the 5 second U-US.

Yohimbine-validation sessions

These were identical to the LTM sessions with 5 CS trials, but there were 3 U-US trials at the end instead of 1 U-US trial. The additional U-US trials were spaced approximately 2 minutes apart.

Discriminative PTC

Three months after the previous LTM session (and six months post-surgery), a discriminative conditioning procedure was administered. This session gave, in alternating order that was counterbalanced between animals, 5 CS⁺-US pairings interspersed with 5 tone-only CS⁻ presentations. The US was a 0.7mA, 1 second footshock. The identity of the CS⁺ was either

a 2 kHz, 20 second tone or a 10 kHz, 20 second tone, with the CS⁻ being the other tone, and this was counterbalanced between animals.

Discriminative LTM

One day after discriminative PTC, animals were tested with a block of 3 CS⁺ tone-only presentations or a block of 3 CS⁻ tone-only presentations, followed by the other block of 3 for counterbalancing. The animals were then presented with 2 trials of the original CS (5 kHz, 30 second tone), followed by alternating blocks of 2 novel (and non-conditioned) auditory tones of 1 kHz or 14 kHz. However, for the sake of brevity, only the CS⁺ and CS⁻ trials will be examined in this chapter.

Data Processing and Statistics

Data processing required multiple phases of preprocessing and artifact correction. Data processing and analysis was done almost exclusively with the Python programming language, relying heavily on the NumPy (Oliphant, 2006) and SciPy (E. Jones et al., 2001) modules for generic vector/matrix operations and specialized digital signal processing techniques, respectively, as well as on the Statsmodels module (Seabold & Perktold, 2010) for ARIMAX modeling and student t-tests (within-subjects and between-subjects).

Principles of Time Series Analysis

A time series is defined as a discrete multidimensional dataset with a time dimension (independent variable) and a dimension for each measured variable (dependent variable(s)). It is often convenient to represent time series in vector, matrix, or tensor terms. At a minimum, it can be represented as a 2-by- N matrix,

$$\begin{bmatrix} x_0 & x_1 & \dots & x_N \\ t_0 & t_1 & \dots & t_N \end{bmatrix} = \begin{bmatrix} \vec{x} \\ \vec{t} \end{bmatrix} \quad (4.1)$$

where N is the number of time points, and the 2 row vectors are measurements of a variable \vec{x}

(or an ordered set of variables \mathbf{X}) at time \vec{t} .

The most straightforward techniques for digital signal processing may be the sliding window functions. The mathematics can be expressed as vector or matrix operations, in which a smaller kernel with fewer elements is repeatedly applied to consecutive, overlapping stretches of a larger vector or matrix. These techniques generally fall under convolution theory. A simple example is a moving average, which repeatedly takes a dot product of a uniform vector (where all elements sum to one) with consecutive and overlapping time series data. More complex examples include finite impulse response filters, which produce frequency-based transformations as they slide across the data set.

It must be noted that the process of convolving a discrete kernel with a discrete dataset is an index-based process. Accuracy of a convolution method is compromised if time points are not equidistant, because convolving across an inconsistent time dimension will cause unintentional warping of the time dimension. This can be addressed by first interpolating equidistant data points using cubic spline interpolation (E. Jones et al., 2001) before any convolution operations are conducted.

Nature of measured signal

Given that endeavors with such new technologies often lead to exploratory analysis, I prepared by thinking deeply about the nature of the signals that we sought to rely on. Briefly, the variable of interest, being the change in amygdala NE concentration over time under the tip of the fiberoptic cannula, is encoded in the amplitude of sine waveforms emitted by the stimulation LED's and received at photodetectors with some noise. Given two photodetectors and two characteristic frequencies, the signal of interest was expected to be measurable as increased activity at the NE2h channel's photodetector relative to the amplitude at the mCherry channel's photodetector.

Advanced artifact considerations

Broadly speaking, we had two sets of goals with our data analysis. The first was to clarify the appearance of true NE signal. This was our rationale in using mCherry. We expected that artifacts should show up in similar ways on both channels. From the beginning, the expected artifacts were photobleaching (a gradual process of exponential decay), potential leakage of ambient light, and general movement artifacts that would be symmetric with the control channel in the sense that the perturbation on the mCherry channel would be directly proportional to the perturbation of the NE2h channel.

As we will discuss in detail later, the expectation that signal processing would be easily executed proved to be naïve. In fact, the characterization of and correction for artifacts and sources of noise became a focus in its own right. For the most part (at least after ample viral incubation time), the signal between NE2h and mCherry channels was highly correlated (most measured Pearson r coefficients were above 0.85). Generally, our working definition of an artifact was an unexpected perturbation in the signal of one or both channels (usually both) with consistent quantitative parameters (even if those parameters are hidden or obscured) and a qualitatively identifiable cause. Eventually, I resorted to creative tactics (adding new data streams extracted from videos of behavior sessions) to investigate and characterize a recurring artifact that was asymmetric between channels.

The second goal was to characterize temporal relationships of NE to stimulus presentations (tones, shocks), and to behavior (primarily freezing, as it is a consistent defensive behavior in rats), as well as time-lagged relationships between NE and future changes in behavior, or conversely, changes in behavior that predicted future NE levels.

Some of the most intense NE responses should be verifiable by standard comparison of means methods. Based on our previous work (Díaz-Mataix et al., 2017), I expected footshocks,

especially 5-second-long footshocks would trigger robust endogenous NE surges. For some preliminary analysis, comparing mean NE2h signal before versus after stimulus onset was adequate for extracting meaningful insights. However, other techniques are more amenable to complex time series.

I must note that for the first round of analysis for the 3-month post-surgery sessions, I subtracted a mean estimate of background patchcord autofluorescence from the photometry channels before further processing. I did this by recording from the patchcord without an animal tethered to the cord, which I did before and after each animal to obtain a mean of background signal on the NE2h channel and mCherry channel.

ARIMAX modeling

In the present work, I explored many processing and discovery techniques. To improve the accuracy of the putative NE signal, I expanded my statistical repertoire to include time series modeling methods. The formal statistical models that I implemented fall under the autoregressive and moving average (ARMA) family of models, along with extensions that remove consistent long-term trends and influence of exogenous variables (all together constituting the ARIMAX family of models). The Akaike information criterion (AIC) was then used as a cost function and minimized in order to find the best fitting ARIMAX model order, which consistently turned out to (0,1,1) when the mCherry channel was included as an exogenous regressor, meaning there was no autoregressive term, there was a single application of differencing in order to extract changes from time point to time point, and there was a single moving average term. Once a ARIMAX model output establishes a reliable forecast as a baseline, then NE events can be examined as NE2h channel deviations from a forecast that suppresses most artifacts by taking into account the fluctuations of the neutral mCherry channel.

Early statistical analysis consisted of within-sample t-tests comparing NE2h signal before versus during/after stimulus delivery. However, my focus on time series methods eventually led me to the ARIMAX model family, with flexible options to reject artifacts by including exogenous regressors that capture the artifacts to be removed. The implemented ARIMAX model contained the mCherry channel as an exogenous regressor, but that channel was inadequate for tracking artifacts that were not consistently correlated in their effects on the NE2h vs mCherry channels. For those “anti-correlated artifacts” or “non-correlated artifacts”, video-based data streams could be analyzed with computer vision deep learning methods to identify physical causes of artifacts. Although these latter ARIMAX models for advanced artifact rejection were not implemented, a carefully designed recurrent neural network architecture could theoretically be used to make an algorithm learn the approximate patterns in fiber photometry and video data streams that would be indicative of poorly behaved artifacts and then classify these patterns with the end goal of removing their influence on the NE2h and mCherry channels.

Once a model was created capable of computing a baseline substantially more valid than a flat baseline, the model’s output was taken as a reliable index of NE activity at the implantation site, if histological analysis confirmed expression of the NE2h sensor. (Ultimately, two animals were rejected because we could not detect expression post-mortem)

Lock-in Detection

Digital dual lock-in detection was employed to estimate amplitude of sinusoidal oscillations at specific frequencies over time. This is not a trivial calculation, as it involves extraction of frequency dependent information while maintaining temporal flow, regardless of phase offset. However, relevant techniques have existed since the mid-20th century. Lock-in detection describes a family of techniques in which a reference signal is multiplied by a

measurement signal. Sinusoidal reference signals are advantageous because they are approximately orthogonal to all other functions, except for other sinusoidal functions with the same frequency and phase shift. The product of the reference with a recording that does not contain the reference frequency will theoretically cancel to zero over enough periods of oscillation. Thus, it is also advantageous to use a rapidly oscillating frequency, in order to average over many periods within a short time window.

If the phase shift can be discarded without hindering the intended purpose, as is often the case when the variable of interest is encoded in the amplitude, an orthogonal copy of the reference signal can be obtained with a 90° phase shift in order to capture the out-of-phase, or quadrature, component. In this scenario, a sine function and cosine function are individually multiplied by the recorded signal to obtain in-phase and quadrature components. This generates noise at twice the frequency of the reference, so these components are each passed through a lowpass filter. Finally, a Euclidian norm of the two components at each time point is taken to represent the amplitude-encoded signal.

The purpose of this for our use case is to demodulate the rapidly oscillating voltage data from photodetectors into a relatively stable form that captures changes in fluorescent intensity. This is done with computations implemented by the proprietary Doric Lenses system, but the lock-in amplification calculations will also be replicated to ensure we are using the best possible approaches. The demodulated data represents the activity of the fluorescent sensors that we injected into rats' brains during surgery.

Video Data Analysis

Recorded video of the behavior session was entered into a computer-vision-based analysis process and transformed into distinct time series data channels. We used a convolutional neural network software package called DeepLabCut (Mathis et al., 2018; Nath et

al., 2019) that is designed for animal researchers. It iteratively fits a deep neural net to experimenter-labeled images of rat anatomy. In this case, approximately 400 frames were labeled with seven points on the head and the surgical implant (tip of nose, both eyes, both ears, one at the base of the fiberoptic implant, and one at the top of the ferrule where it connects to the patch cord), two on the back, three on the tail, two additional labels for the infrared LED array (to detect on versus off configuration) to allow automated determination of time-syncing signals, another additional label on the patch cord about an inch from the animal's head. (This last point was used to study artifacts).

This software used a transfer learning approach by stacking untrained layers on top of a 50-layer deep 'ResNet50' pre-trained network that is specialized for visual pattern recognition. Artificial neural nets such as this are designed to find approximations of gradients through iterative changing of weights by alternating back-propagating with forward calculations. The model we used for automated behavior analysis was trained with 400,000 iterations. The magnitude of each iterative adjustment is dictated by parameters called learning rates. We adjusted the learning rate only three times during training. (10,000 iterations at a learning rate of 0.005, then 220,000 iterations at a 0.02 learning rate, then 100,000 iterations at 0.002, and ending with 70,000 iterations at 0.001). These learning rates can be thought of as step sizes, where an initial phase of relatively rough approximations encouraged diverse solutions and was eventually followed with lower learning rates to fine-tune the optimal strategies. While steps are taking to reduce overfitting, there are bound to be noticeable instances. For example, a human accidentally labeling an incorrect anatomical location just a few times will lead to a model that also mislabels that location. However, placing so many points on the head, a generally rigid structure, gives us redundant tools for tracking the head during behavior.

Results

Initial Signal Validation

To ensure the operability of the fiber photometry equipment, we first used a Fast Fourier Transform (FFT) on the raw photodetector voltage data from each session and at various window sizes, ranging from 20 seconds to entire recording sessions of approximately 35 to 40 minutes. We consistently saw precise frequency peaks at the expected frequencies. Figure 4.4 shows time domain (top) and frequency domain (bottom) for NE2h (left) and mCherry (right) channels. The frequency domain was computed by transforming 2^{22} time points over 344 seconds at a sampling rate of 12,190Hz. Other than very low frequencies (<1Hz), the only substantial frequency signals were very narrow peaks at the characteristic frequencies ($\text{NE2h}_{\text{char.freq.}} = 208.616\text{Hz}$, $\text{mCherry}_{\text{char.freq.}} = 572.212\text{Hz}$). The NE2h waveform appeared to contain a dominant sinusoid at $\text{NE2h}_{\text{char.freq.}}$ with only slight noise visible in the time domain. There was no indication of the $\text{mCherry}_{\text{char.freq.}}$ infiltrating the NE2h channel. However, there was a clear $\text{NE2h}_{\text{char.freq.}}$ component on the mCherry channel. This was clear in the time and frequency domains. Thus, we paid close attention to our initial signal processing steps.

Lock-in demodulation is a popular and well-established technique to selectively filter out frequencies that are not close to the reference signal. Figure 4.5 displays my work on applying this method. Unfortunately, the unwelcome $\text{NE2h}_{\text{char.freq.}}$ could not be completely eliminated with this approach. My attempt to implement this method resulted in outputs with residual oscillations at the $\text{NE2h}_{\text{char.freq.}}$. This was probably due to a non-optimal choice of low-pass finite-impulse response filter.

Fortunately, I discovered that a least squares sinusoid fitting approach is highly effective at checking the work of the proprietary automated demodulation (Fig. 4.6). Temporal segments less than 20ms in width could be quickly fit to either one or two sinusoids of known frequencies, which required least squares estimation of a total of three or six estimated parameters

(amplitude, phase shift, and DC-offset (i.e. a constant)). The amplitude estimate could then be taken as the measure of interest without further processing. Our least squares approach also measured the 208.6Hz signal that was contaminating the mCherry channel. In fact, once the Least Squares-derived pure 208.6Hz reference was subtracted from the mCherry channel, the remaining waveform closely resembled a pure sine wave of the expected mCherry_{char.freq.} of 572.2Hz (Figure 4.6). Nevertheless, I subsequently discovered that the amplitude estimate precisely mirrors the results of the Doric console's automatic demodulation (Fig. 4.7). Because the Doric method was automated and appeared consistent with least-squares-based amplitude estimation, I used the Doric-demodulated signal rather than continuing to extract amplitude with the least-squares method.

I did encounter one example of a saturation artifact on the mCherry channel so intense that, even without amplifier gain, the sinusoid was truncated by the photodetector's upper limit of just under 5V. In this example, Doric's demodulation algorithm miscalculated increased amplitude as decreased amplitude because the increased DC offset crunched the waveform against the photodetector's ceiling. This extreme artifact only occurred in a single animal, and that was after more than 6 months of viral incubation with mCherry. In this case, the utility of frequency methods would be contaminated by the truncated peaks. A careful application of least squares to the bottom of the sinusoid might recover some of the mCherry signal from this animal's recordings. Alternatively, using a carefully designed periodic sampling function such as a Dirac comb (Bertolim et al., 2016) is probably the optimal approach.

Early Behavior Experiments and Analysis of Viral Incubation Dynamics

Approximately three weeks after surgery, all animals underwent one session of Pavlovian threat conditioning consisting of five CS-US pairings with a 30 second CS (5kHz tone) that co-terminates with a 1 second US (0.7mA footshock). The next day, six of the ten animals

were exposed to long-term memory (LTM) testing followed by a single 5-second-long footshock to test for NE responses.

Little to no structured signal was observed, so we decided to postpone further testing to allow more time for viral expression. Eventually, some exploratory analysis detected possible trial-averaged and group-averaged NE2h response to footshock in both of these early sessions (Fig. 4.8) after standardizing the photometry signals (Z-scoring; i.e. subtracting an animal's measurements by its mean signal and then dividing by that animal's standard deviation). Although we expected to normalize the mean, we did not expect to standardize any measure of variance. Standardizing variance might have boosted the signal of weakly expressed NE_GRAB sensors, but an alternative explanation is that it boosted the impact of artifacts that in effect gave a false positive. Furthermore, the NE signal in this exploration was estimated by dividing the NE2h channel by the mCherry channel. This operation assumes the effect of artifacts on the two channels will always be correlated, and we now know this to be a false assumption.

Although these results are consistent across both early experiment sessions (and their averaged duration of signal resembles our later observation), they should be viewed as secondary to our later results. The possibility that Z-scoring enhanced weak NE_GRAB signal is certainly plausible, but Z-scoring also boosts any irregular fluctuations caused by artifacts of unknown source if they are larger magnitude than most other sources of variation.

As we closely examined the photometry data and video recordings, we became aware of various sources of noise. For example, despite the use of connecting sleeves with black covers, ambient light from a standard cage house light still interfered with the signal when the rat reared up near the light. We therefore ceased using lights during recording sessions (with the exception of infrared LEDs).

NE dynamics are revealed by longer viral incubation

Approximately three months after surgery, rats were tested again, with some tested for LTM for the first time (Fig. 4.9). This revealed stronger viral expression that made visible substantial NE2h responses. The following day's session was especially relevant to validating the NE2h approach to directly recording NE signal, so I shall highlight that data below.

The NE2h sensor, as well as other lines of the NE_GRAB sensors, are modified forms of α_2 -adrenergic receptors (J. Feng et al., 2019). This subtype of adrenergic receptor was selected by Feng and colleagues (2019) because it showed the best surface expression of the GFP-conjugated adrenergic receptor variants. Yohimbine is a naturally occurring antagonist at the α_2 -adrenergic receptor, and this is also true for the GFP-conjugated NE_GRAB sensors (J. Feng et al., 2019). The effect of blocking the NE-binding site has the effect of stabilizing the fluorescent intensity of the NE2h's GFP domain. The fluorescent intensity should remain constant, similar to the mCherry channel, while significant concentrations of yohimbine are present. Thus, this is an ideal experiment to confirm that the fluctuations that appear to be true NE2h signal are indeed a product of NE binding to NE2h.

The procedure on this day was similar to the LTM sessions with 5 tone CS presentations that were followed with a U-US, except there were 3 U-US trials instead of 1 trial. While this is likely to drive contextual threat learning, the signal of interest is the immediate NE reaction to strong U-US presentations. This provides a starting point from which to examine NE dynamics under other circumstances in the future. This aim is similar to the series of studies in the 90s that measured amygdalar NE through microdialysis after footshocks (Galvez et al., 1996; Hatfield et al., 1999; Quirarte et al., 1998). However, the fiber photometry method gives temporal resolution that is only limited by the clarity of the measurements, which makes for a much more open-ended and accessible data set for exploring NE temporal dynamics.

Preliminary analysis on this data set was first undertaken with visual examination of

NE2h versus mCherry channels in individual U-US trials and of group-averaged visualizations (Fig. 4.10). Within-subjects t-tests then demonstrated significant differences between NE2h and mCherry channels during U-US and some CS trials in vehicle-treated animals, while showing only one significant difference for the yohimbine-treated animals (Fig. 4.11). Between-subject t-tests on the NE2h channel showed a markedly elevated NE2h response to all 3 U-US trials in vehicle animals compared to yohimbine-treated animals (Fig. 4.12, top). Importantly, no significant differences were apparent on the mCherry control channel (Fig. 4.12, bottom). This was a critical validation of the NE2h sensor, essentially showing that NE2h reactivity is in fact due to NE reactivity.

ARIMAX model findings

An iterative model search minimizing AIC using NE2h data from the 3-month post-surgery LTM/U-US sessions with the mCherry channel as an exogenous regressor consistently selected a model order of (0,1,1), meaning no autoregressive term, a single differencing operation to extract changes from time point to time point, and a single moving average term, combined with a linear regression term from the mCherry data after a single differencing operation. For each trial, this model was fit on the 60 seconds of data preceding stimulus onset, then forecast for the next 30 seconds in order to establish an artifact-aware baseline surrounded by a 95% confidence interval that can be compared to the actual observed NE2h signal. If desired, the difference between the forecasted baseline and actual NE2h signal can be extracted as a univariate estimate of fluctuations in NE concentration. Figure 4.13 shows the ARIMAX-forecasted baseline and actual signal for a single LA-targeted animal for the first CS presentation (top) and the single U-US presentation (middle), along with estimated NE signal for that U-US presentation (bottom).

Representative images of 3 animals show NE dynamics with U-US presentations (Fig.

4.14). NE estimated signal during U-US is characterized by a steep, steady increase in NE during the entirety of the footshock, followed by a highly variable gradual decline after U-US offset. Representative images from 2 animals comparing first CS trials to last CS trials (Fig. 4.15) show a substantially more robust response to first CS (top) than last CS (bottom). These were recordings from the 3-month post-surgery LTM/U-US session.

Three months later (6-months post-surgery), a discriminative PTC procedure was administered. In general, auditory tones (especially on the first trial of each tone) boost NE signal, and signal is boosted again with the footshock US at the end of the CS (Fig. 4.16). One consistent pattern we found was a sustained elevation after prolonged footshocks of 5 seconds, which may represent heightened tonic activity that lasts approximately 40 seconds to 2 minutes, whereas elevated signal from 1 second footshocks and auditory tones were more transient, often fading within 20 seconds.

Another pattern apparent from the 2 best animals from these later sessions (Figs. 4.21, 4.22) was that in discriminative PTC and discriminative LTM sessions, the conditioned tone (CS^+) consistently produced a NE response, but NE responses to the neutral tone (CS^-) quickly habituated.

Advanced artifact analysis

I am hesitant to conduct summary statistics on the sessions 6-months post-surgery due to the unpredictable presence of an artifact that affects the photometry channels differently, with inter-channel correlations that rapidly change with time in a manner that at first glance is stochastic. However, by watching animal videos and extracting anatomical positions over time (Figs. 4.17, 4.18, 4.19), I identified the source of this artifact. My hypothesis was that horizontal tension force or torque was corrupting the fiber photometry signal in a way that was uneven between wavelengths.

This was likely because the medium of the brain is non-homogenous, possibly creating prism-like dynamics inside the brain that are wavelength-dependent. Perhaps there is some other wavelength-dependent optical effect relating to internal reflection or the optical interface between the patch cord and the fiberoptic cannula, but it seems to depend on the medium that the fiber tip is in. My justification for that statement is built on Figure 4.20, in which I present a photometry recording in which I was able to manually replicate that artifact, which is characterized by strong anticorrelated movements on the NE2h and mCherry channels. The only way I could generate the anticorrelated effect was to hold the fiber tip tightly between two loosely gloved latex-covered fingers while pulling the cord horizontally away with my other hand. If the fiber tip faced an orthogonal surface, such as facing the palm of my hand, the simulated artifact was never anticorrelated between channels.

A proper path forward from here would be to build a classifier to identify instances where this artifact occurs during animal recordings, then develop an algorithm to remove the influence of the artifact. Unfortunately, time is limited. The proof on concept put forth in Figures 4.19 and 4.20 must suffice.

Late data recordings

Eventually, five of the animals were run through additional sessions 6-months post-surgery, including an attempt at counterbalancing the yohimbine experiment (unfortunately, only one of the surviving animals was in the vehicle group in the previous round, so the experiment ended up as $N_{\text{vehicle}}=4$ and $N_{\text{Yohimbine}}=1$, which makes it difficult to draw inferences. In addition, the previously mentioned artifact seemed stronger and more frequent in these later sessions. One reason for this was an experimenter error on one day, namely failing to secure the area where the patch cord entered the conditioning chamber, so it slipped out of place and entered the cage through a crack over the door, increasing the potential for horizontal tension, which

seems to be the cause of that artifact.

Another round of Pavlovian threat conditioning was conducted, in which NE2h responses to footshocks were consistently observed. Auditory tones also appeared to trigger NE responses, albeit of a smaller magnitude. However, persistent appearances of artifacts discouraged attempts at statistical inferences in favor of identifying the actual cause of the artifact, which I demonstrated in Figures 4.19 and 4.20.

Discussion

Technical insights

This research is important for a number of reasons. Fiber photometry clearly has potential to explore nuanced temporal profiles of intracranial processes with relevance to behavior and psychology. The experiences here were only a taste of that potential. There are many forms of methods that address similar issues. For example, many researchers index norepinephrine simply by measuring pupil dilation. An astute understanding of how internal physiological dynamics are reflected externally can itself be a fundamental and powerful tool.

This research also utilized computer vision and machine learning, with an end result of non-video visualizations that capture time series dynamics of animal motion, as in Figures 4.17, 4.18, 4.19. Aside from any designs on benefits for the current NE research, it is helpful for scientists in general to expand their visualization repertoire and their access to resources that automate analysis when appropriate.

My work here lays out many of the arduous technical troubleshooting processes required to start using fiber photometry. Others in my lab are picking up on these skills. Fiber photometry and automated video analysis both provide data sets with file sizes measured in gigabytes. Experience with managing such large datasets has turned out to be extremely important, as integrating roughly 100 large files for a single integrated data exploration is not a trivial task.

This means algorithms must be written in ways that are relatively easy to understand and to apply to new data.

As a technical summary, the work presented in this chapter demonstrated the utility of fiber photometry and computer vision techniques based on convolutional neural networks in researching intricate subcortical molecular processes. The exact temporal parameters that were observed may be new information, and as such, should be estimated and reported. The extent to which NE in the amygdala is reactive to tones, whether conditioned, neutral, or novel, will be important to flesh out in as much detail as possible. An open-ended but important project would be to keep dissecting putative NE signals to identify reliable components and noisy components. Over time, fiber photometry researchers may be able to improve the clarity of the NE signals to the point of finding new effects and new detail never before observed at the level of direct NE measurements in real time.

Theoretical insights

There are at least three theoretical frameworks for NE function that can be used for the data from this chapter. First, the most consistent finding was a NE response to footshock US and U-US that were higher in magnitude and duration than auditory tones (e.g. Figs. 4.8, 4.11-4.16). This is consistent with painful stimuli triggering LC activity (e.g. Ozawa & Johansen, 2018; Sara & Bouret, 2012), which results in heightened NE levels in amygdala (Galvez et al., 1996; Hatfield et al., 1999; Quirarte et al., 1998).

Second, within a given recording session, the first presentation of a stimulus usually produced a stronger NE response than later presentations of the same stimulus (e.g. Figs. 4.11, 4.12, 4.15). This was true for footshocks and tone presentations. Interestingly, NE followed this pattern rather than correlating to conditioned freezing levels or other easily observable behaviors (data not shown). This is explainable by applying a view of NE as a signal of

unexpected uncertainty that arises from unexpected state changes or contextual changes (A. J. Yu & Dayan, 2005). A natural extension of this causal explanation is a conceptualization of the consequence of this, a “network reset” effect in which gamma band rhythms are transiently disrupted and then reset via the ventral frontoparietal network (Sara, 2016).

Third, although the gathered data is less clear on this front. The 6-month post-surgery sessions included multiple auditory tones, some of them conditioned and some of them neutral. A cursory visual analysis (Fig. 4.21, 4.22) suggests that NE responses habituate more quickly to neutral tones than conditioned tones, which would be in keeping with a conditioned arousal effect that preserves NE reactivity to conditioned stimuli (Sara & Bouret, 2012; Sokolov, 1963). However, the effective sample size for this comparison is very small (only $n=2$ rats showed robust NE responses to tones on these two days).

Overall, this fiber photometry method has identified multiple causal components of amygdalar NE activity relating to threat perceptions and unexpected stimuli. Importantly, there were no obvious difference between anatomical locations (LA versus CeA versus surrounding regions). This suggests the determinants of NE release might be generic and non-specific between amygdala subregions. Any functional specialization in NE effects that vary between subregions is likely to originate from the distinct and specialized circuitry underlying local ionotropic transmission, or from differences in adrenergic receptor distributions, rather than resulting from differing NE release dynamics.

In the future, fiber photometry studies of the amygdala with the neuromodulator GRAB sensors from Yulong Li’s Lab could be expanded to include acetylcholine alongside NE, as acetylcholine is hypothesized to signal expected uncertainty, which complements NE’s role as a signal of unexpected uncertainty (A. J. Yu & Dayan, 2005). Fiber photometry experiments could also be expanded by including optogenetic manipulations to add a manipulation toolkit or by

including calcium imaging in NE axon terminals to supplement and clarify the NE_GRAB signals like those observed in this current study.

Acknowledgments

I want to thank several collaborators and colleagues who made the work in this chapter possible. Dr. Dayu Lin provided the initial idea for a NE fiber photometry study and provided the initial NE_GRAB constructs for testing. Claudia Farb had the insight to use a GFP-targeted antibody to amplify NE_GRAB fluorescence in histological samples. Dr. Christine Constantinople and Andrew Mah provided access to fiber photometry equipment and engaged in helpful discussions regarding technical operations and data analysis methods. Dr. Yulong Li provided the NE2h construct used for the data presented in this chapter. Dr. Rob Sears and Dr. Erika Andrade assisted with and actively collaborated on the planning and coordination of this work. Dr. Rodrigo Triana-Del Río helped plan and assisted with the yohimbine NE2h-validation experiment. Dr. José Oliveira da Cruz introduced me to the DeepLabCut software that I used for automated animal tracking in video recordings of fiber photometry sessions. Lauren Branigan helped with early NE_GRAB construct testing. Dr. Lorenzo Díaz-Mataix was responsible for much of the empirical research and theoretical development in recent years that inspired this deep-dive into temporal dynamics of NE.

Finally, I want to thank my faculty committee members, Dr. Joseph LeDoux, Dr. Chiye Aoki, Dr. Dayu Lin, Dr. Cristina Alberini, and Dr. Sarina Rodrigues Saturn, for expanding my theoretical awareness of the norepinephrine system and its many roles.

CHAPTER 5

General Discussion

All together, these experiments and observational studies revealed norepinephrine (NE) response profiles consisting of well-characterized temporal dynamics, anatomically-distinct functional consequences, and generalized NE-release dynamics that were similar across amygdala subregions and may be triggered by multiple types of cognitive systems upstream from locus coeruleus (LC).

Characteristics of stimuli evoking amygdalar NE release

Fiber photometry recordings in Chapter 4 revealed at least two patterns that are consistent with major theoretical roles of NE and a third possible pattern that was hard to confirm due to small sample sizes.

Footshocks are known to trigger NE responses (Galvez et al., 1996; Hatfield et al., 1999; Quirarte et al., 1998). Fiber photometry-measured NE responses to footshock US (1-second, 0.7mA) and U-US (5-second, 1.0mA) were greater in magnitude than those to auditory tones (e.g. Figs. 4.8, 4.11-4.16). This is consistent with the idea that nociceptive stimuli trigger LC activity (e.g. Ozawa & Johansen, 2018; Sara & Bouret, 2012). Although the systemic β -adrenergic receptor (β -AR) antagonism experiments in Chapter 2 were not specific to amygdala, they nevertheless produced nuanced inferences regarding US- and U-US-evoked β -AR-enhancement of PTC memory formation. Based on these results, we can confirm that nociceptive stimuli are capable of producing robust surges of NE in the amygdala.

It must be noted that on occasion in the fiber photometry sessions (Chapter 4), an auditory tone (conditioned, novel, or neutral) triggered a strong NE response that approached

the magnitude of footshock-responses, but this was not a consistent pattern in any animal. Relating this to Chapter 2, this raises the question of why learning from single-trial PTC conditioning was not impaired by propranolol, even though amygdalar NE tone responses (Chapter 4) can sometimes be as strong as footshock responses. Our work in Chapter 2 repeatedly showed that isolated CS-US pairings do not engage β -ARs in time for enhancement of acquisition of that same pairing trial (Figs. 2.1-2.3). If novel auditory tones can trigger high NE levels in LA, theoretically engaging β -ARs, one would expect memory of isolated CS-US pairings to be sensitive to propranolol. Future work could explore individual variability in animals to determine the potential for an especially strong NE response to a novel stimulus to prime PTC learning through β -ARs.

Second, fiber photometry-measured NE reactions were usually most robust in response to the first presentations of each type of stimulus within a given session (Figs. 4.9, 4.11, 4.12, 4.22). This appeared to be true for all types of stimuli tested (i.e. footshock US or U-US and auditory CS or neutral (CS-) tone). The LC/NE system has long been expected to promote orienting to novelty, but this may be better explained by a conceptualization of NE as representing unexpected uncertainty (A. J. Yu & Dayan, 2005), being triggered by stimuli that produce the implicit inference that an unexpected context change or state change has taken place, and having the effect of producing a “network reset” by transiently (~200ms) interrupting network-level gamma rhythms and resetting attentional mechanisms via the ventral frontoparietal network (Bouret & Sara, 2005; Sara, 2016). While the passive nature of our Pavlovian conditioning paradigm differs from the more active instrumental or cognitive tasks used by some of these researchers (e.g. A. J. Yu & Dayan, 2005; Bouret & Sara, 2005), it is probably reasonable assume the lab rat is engaging in implicit inferences concerning its immediate environment, even though the animal does not have an active task while it is in the

recording session. The first presentation of a new type of stimulus could easily shift the animal's perceptions of context or of hidden states within the context.

Third, in the 2 best fiber photometry animals in the discriminative PTC (Fig 4.21) and discriminative LTM (Fig. 4.22) sessions, NE responses to neutral tone (CS⁻) habituated quickly, while NE responses to the conditioned tone (CS⁺) remained robust over 5 CS-US trials and 3 CS-alone trials on the following day. This pattern resembles the conditioned arousal effect described by Sokolov (1963), which can also be described as a type of truncated Pavlovian response (Sara & Bouret, 2012). Essentially, one of the conditioned physiological reactions directed by the CeA in response to the conditioned tone is to boost NE activity in the amygdala. This is clearly distinct from the novelty-related effect described earlier, as novelty-related responses habituate quickly. Logically, such a sustainable style of NE response would have more durability than novelty-related / "unexpected uncertainty"-signaling NE responses (A. J. Yu & Dayan, 2005), could theoretically become self-reinforcing given the plasticity-enhancing effects of NE, and therefore may have clinical relevance to disorders involving excessive rumination.

NE release dynamics appear similar across amygdala subregions

In general, all animals ($n=8$) appeared to have similar NE response patterns, regardless of the fiberoptic recording site's location. Fiber photometry recording sites (Appendix B) included 5 in LA, mostly located near or on LA's lateral edge (the internal capsule), ranging from the most dorsal part of LA to near its ventral border with BA. There were 3 sites in or near the medial part of CeA, with one on or near the ventromedial edge of CeA and one on or near the anterior edge of CeA. The amplitude and clarity (signal-to-noise and artifact considerations) of the putative NE signal varied between animals, but footshocks produced the largest responses in all animals. Responses to auditory tones were observed in most animals, including all animals that showed

clear responses to footshocks. While clarity and absolute amplitude of responses differed between animals, the relative amplitude between types of stimuli and the general were fairly consistent.

In general, the most robust and reliable NE responses across all animals were to the U-US (5-second, 1.0mA), typically with the first U-US trial in a session producing the strongest response. The typical NE response to U-US or to US (1-second, 0.7mA) was an immediate NE surge at footshock-onset combined with a steady increase for the duration of the footshock (Figs. 4.14, 4.16, 4.21). This is followed by a gradual and highly variable decay to baseline, with the duration of elevated NE persisting in the range of 15-120+ seconds.

Most animals showed NE responses to at least some auditory tone presentations. (e.g. Figs. 4.21, 4.22). In general, a rapid NE increase would accompany tone-onset, usually about $\frac{1}{4}$ to $\frac{1}{2}$ the amplitude of a NE response to footshock. This was sometimes followed by a more gradual climb over 5-10 seconds. These rapid and gradual components were sometimes observed multiple times within a tone presentation.

Given the presence of artifacts and substantial noise, it was not possible to draw inferences about spontaneous NE dynamics outside the time-marked trials. Once this method has been advanced and improved until the high noise and semi-regular artifacts are eliminated, it could play a valuable role in tracking endogenous neuromodulators during self-directed animal behavior.

The generalized NE response patterns in multiple regions of the amygdala is not too surprising considering the LC innervates both, with many LC neurons having axon collaterals that branch to both CeA and BA/LA (Uematsu et al., 2017).

Anatomically-specific functional consequences of NE release in LA and CeA

The LA and CeA are well-studied amygdala subnuclei with distinct specialized neural

circuitry (LeDoux, 2012). The LA (and to a lesser degree the CeA (Herry & Johansen, 2014)) receives a convergence of many types of sensory inputs and functions to acquire and consolidate CS-US associations in LA. The CeA recruits downstream regions across the forebrain, midbrain, and hindbrain in order to express conditioned reactions in response to the appearance of a CS (LeDoux, 2012).

These distinct functions are the same functions that can be bidirectionally modulated through β -ARs in the corresponding amygdala subnucleus. Bidirectional manipulations of β -ARs in LA can bidirectionally regulate the strength of PTC acquisition through interactions with Hebbian plasticity mechanisms (Bush et al., 2010; Dębiec & LeDoux, 2004; Johansen et al., 2014; Schiff et al., 2017). Our work in Chapter 2 shows that nociceptive US and U-US can trigger a similar PTC acquisition effect through β -ARs (Díaz-Mataix et al., 2017).

The PTC expression experiments in Chapter 3 established an ability of β -ARs in CeA to enhance conditioned reactions (Gu et al., 2020), affecting the same function CeA is optimized for. We also demonstrated these effects are not replicated by modulating NE in LA. The ability of β -ARs to stimulate the specific neural functions that are mediated by specific neural circuits is not surprising, given they are G_s-coupled receptors.

Consider the theoretical framework of conditioned arousal (Sara & Bouret, 2012; Sokolov, 1963), where the release of NE becomes part of a conditioned reaction. Future experiments could ascertain the potential for a functional positive feedback loop between the recruitment of the LC/NE system as part of a CeA-directed conditioned reaction, on one hand, and resultant β -AR activation in CeA or LA that could theoretically intensify that conditioned reaction or the memory it relates to. If such a positive feedback loop exists, it may represent a clinically interesting phenomenon.

NE temporal dynamics and downstream intracellular dynamics

Considering PTC memory formation, the systemic propranolol experiments in Chapter 2 generalized previous acquisition findings related to LA β -ARs (Bush et al., 2010; Dębiec & LeDoux, 2004; Johansen et al., 2014; Schiff et al., 2017) into the realm of naturalistic stimuli triggering β -ARs. Footshock-triggered β -AR activity primed animals to learn PTC associations. We determined the duration of this priming effect to be somewhere between 2 and 40 minutes (Díaz-Mataix et al., 2017). Interestingly, our fiber photometry observations of footshock-triggered NE release overlapped with this range, with some footshock-triggered NE still lingering after 2 minutes. However, many footshock trials produced a shorter elevation of NE, and even for the longer surges, most of the NE surge had faded by 2 minutes out.

Footshock-triggered β -AR activity opens up a time-limited window of NE-facilitated plasticity, and the duration of this window roughly matches the observed NE temporal dynamics in amygdala after U-US, as evidenced by our works in Chapter 2 and Chapter 4. The time limits on footshock-triggered amygdalar NE surges were found to range from 15-120+ seconds observed in fiber photometry measurements in Chapter 4 to at least 2-7 minutes estimated in Chapter 2 based on the intervals between trials or between U-US and CS-US administration. These also roughly match the temporal windows found by other labs in the past with low-resolution microdialysis (up to 15 minutes, possibly up to 30 minutes) (Galvez et al., 1996; Hatfield et al., 1999; Quirarte et al., 1998). The discrepancies in these numbers are not surprising given they were obtained with wildly different methods. They are all on the order of minutes, but they all terminate in less than 30 minutes.

It must be noted that β -ARs in LA recruit intracellular signaling pathways that enhance future acquisition and consolidation (Schiff et al., 2017), resulting in the trafficking of intracellular calcium-permeable AMPA receptors to the cell surface, closure of inward-rectifying potassium channels, and activation of gene expression and translation. These effects may linger for a time

after NE levels have declined, but how long is not known. However, our work in Chapter 2 found that all β -AR-dependent effects were gone by 40 minutes post-shock (Fig. 2.3).

Future directions

The fiber photometry work revealed NE temporal dynamics with some degree of clarity. As the method is further refined, that clarity can only increase. The neural basis of conditioned arousal (Sara & Bouret, 2012; Sokolov, 1963), in which NE responses to conditioned stimuli are more resistant to habituation than neutral stimuli, could be explored with similar protocols to those presented in Chapter 4 for discriminative PTC and discriminative LTM (Figs. 4.21, 4.22). Simply replicating this with a larger sample size of naïve animals could begin to generate new insight into conditioned arousal.

In addition to the NE_GRAB sensors (J. Feng et al., 2019), other GFP-conjugated GRAB sensors have already been developed for dopamine (Sun et al., 2018), acetylcholine (Jing et al., 2018), and others. The lab group led by Dr. Yulong Li is also developing GRAB sensors with a red-fluorescent protein domain, which would allow the simultaneous recording of multiple neuromodulators. Imaging NE and acetylcholine (ACh) together would allow specific testing of Yu and Dayan's (2005) hypotheses regarding the roles of NE in unexpected uncertainty and ACh in expected uncertainty. Such a research design could track learning processes within tasks as NE-represented unexpected uncertainty gives way to ACh-represented expected uncertainty as the animal gains experience with the conditions of the task.

Likewise, the parallel integration of other tools like optogenetics, calcium imaging, or other photon-mediated molecular techniques alongside the use of NE_GRAB sensors will allow precise control in parsing causes and consequences of observed neuromodulator dynamics. Future techniques could hypothetically track NE temporal dynamics in conjunction with observing or manipulating the temporal dynamics of NE-related intracellular processes.

Shrestha and colleagues (2020) recently developed a genetically-encoded tool for drug-inducible protein synthesis inhibition, which could be used to target specific cell types in LA or CeA during or immediately after conditioning or extinction sessions to probe organizational rules for PTC memory engrams and their possible modification by neuromodulator input.

Another future direction concerns the use of wireless fiber photometry implants (Lu et al., 2018) that may allow free social interactions between conspecifics or between species, possibly with long-term continuous data collection. This approach would be especially powerful when combined with computer vision techniques to track animal behavior (Mathis et al., 2018; Nath et al., 2019), which could analyze months of video recordings alongside months of neuromodulator recordings. This might allow fascinating studies on relationship building in mammalian species. Interesting combinations of neuromodulators to study in such circumstances could include oxytocin and serotonin, or oxytocin and dopamine. One interesting extension of this direction would be studying neuromodulatory dynamics in domestic pet species as they build social relationships with humans. Another interesting direction could be the development of naturalistic research paradigms that enable the recording of neuromodulator activity from many animals living in complex social structures and enriched environments.

Summary

Our experiments and observations in rats confirm that nociceptive stimuli trigger NE release and β -AR signaling, leading to a transient enhancement of acquisition for implicit memory of CS-US pairings in the following minutes. We also showed that stimulating or inhibiting NE release in CeA bidirectionally regulates the expression of conditioned reactions through β -AR-dependent signaling. Fiber photometry observations of extracellular NE concentrations in LA and CeA showed consistent robust increases during footshocks and inconsistent increases during auditory tones. Tones were most likely to trigger NE release the

first time they were presented in a session, possibly indicating a novelty or unexpected uncertainty effect. NE responses to conditioned tones may habituate more slowly than to neutral tones, possibly representing a conditioned arousal effect.

APPENDIX A

Figures begin on next page

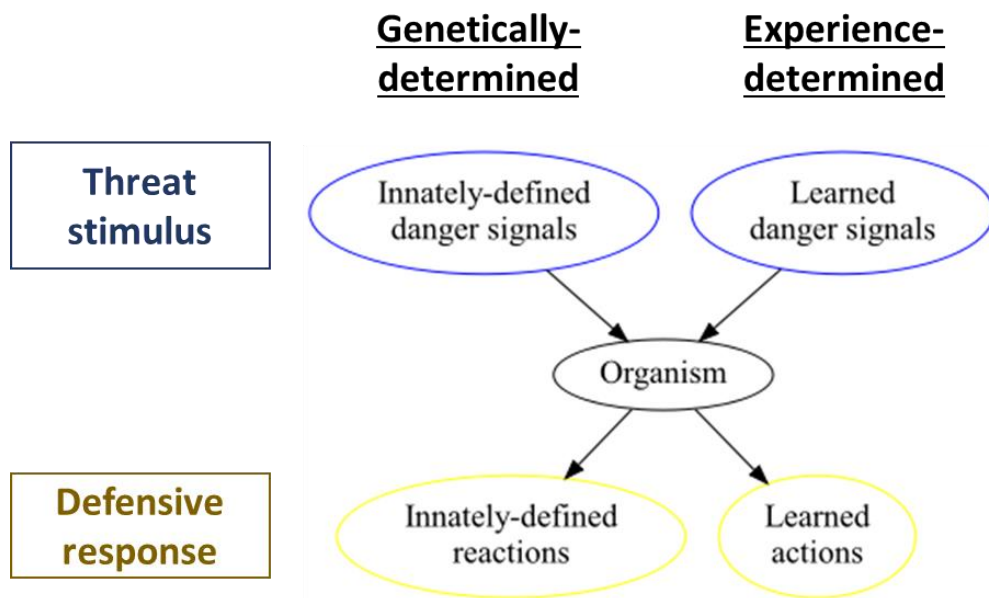


Figure 1.1. General configuration of active defense mechanisms, with or without learning.

Detection of danger (top) triggers deployment of a response (bottom). Nearly all species have innate capacity to recognize some threats (top left) and respond appropriately with innate reactions (bottom left). Many species have mechanisms to learn to recognize threats not innately recognized (top right), and some species have mechanisms to learn actions that successfully defend against threats (bottom right).

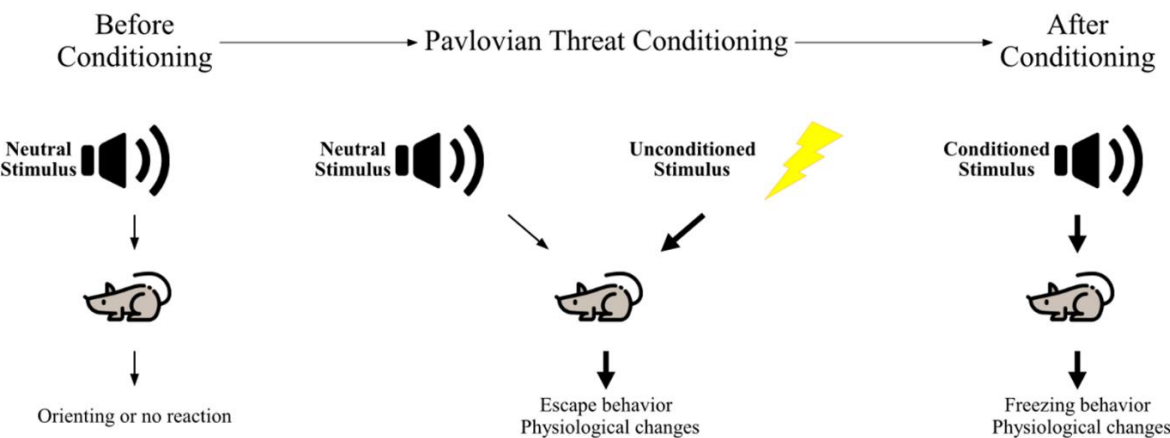


Figure 1.2. Pavlovian Threat Conditioning. Before conditioning, the soon-to-be conditioned stimulus has a neutral valence and is unlikely to elicit defensive behavior. On the first trial of Pavlovian Threat Conditioning, the neutral stimulus is presented immediately before or during an aversive unconditioned stimulus. The escape behavior and physiological changes in the first trial are triggered by the aversive unconditioned stimulus, in this case a footshock. After conditioning, the previously neutral stimulus is now a conditioned stimulus, which can trigger defensive freezing behavior and physiological changes without the presence of an unconditioned stimulus.

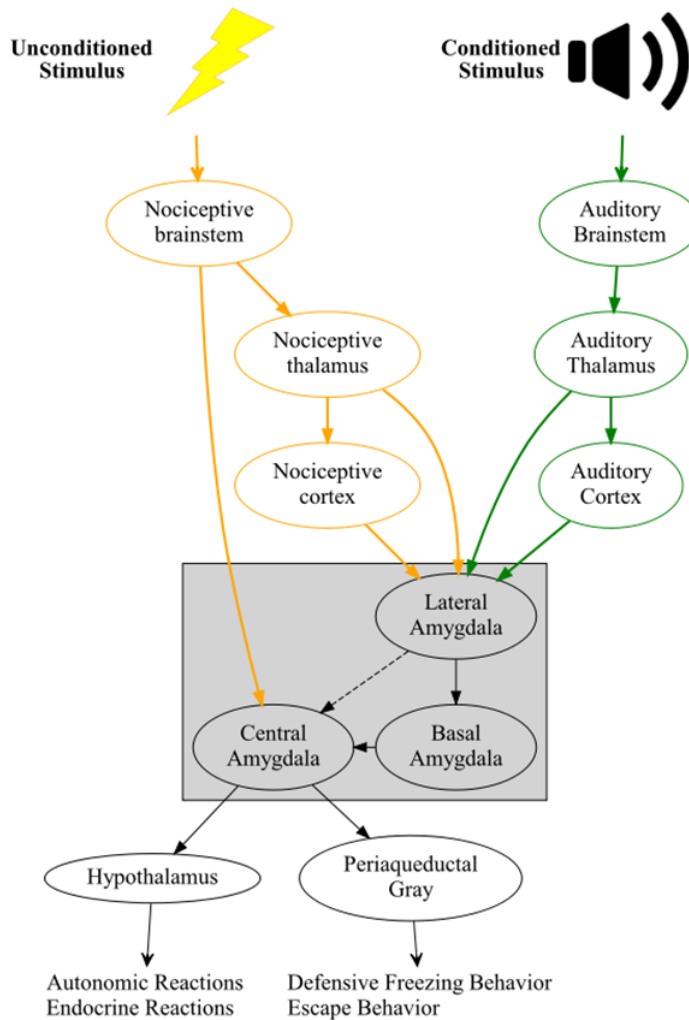


Figure 1.3. Circuits mediating acquisition of associative memory between a nociceptive unconditioned stimulus and an auditory conditioned stimulus. (orange) Nociception and somatosensory processing areas in brainstem, thalamus, and cortex transmit nociceptive signals to amygdala. Efferents from central amygdala trigger escape behavior in response to nociceptive input. (green) Auditory processing areas in the brainstem, thalamus, and cortex transmit auditory signals to lateral amygdala. If auditory stimulus has a neutral valence, the amygdala will show little response. However, after conditioning, afferent axon terminals from

thalamus and cortex to lateral amygdala experience long-term potentiation, enabling future presentations of the auditory stimulus to induce amygdala-triggered defensive reactions.

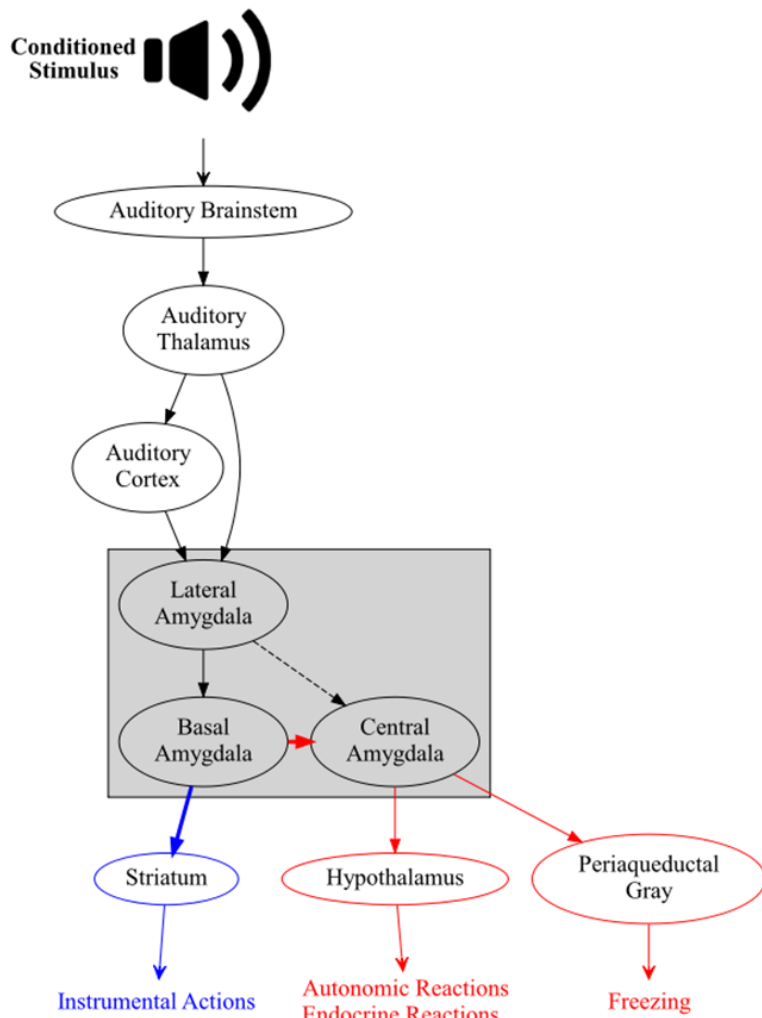


Figure 1.4. Circuits mediating expression of conditioned responses to an auditory conditioned stimulus. Low-level sensory processing areas in the brainstem, thalamus, and cortex ultimately interface with lateral amygdala via projections from auditory thalamus (broadly tuned to sensory features) and auditory cortex (narrowly tuned to sensory features). Basal amygdala receives signal from lateral amygdala and recruits one of two opposing response networks: (blue) Instrumental actions mediated by the striatum, or (red) Innate defensive reactions including freezing mediated by periaqueductal gray and autonomic/endocrine reactions mediated by various hypothalamic circuits.

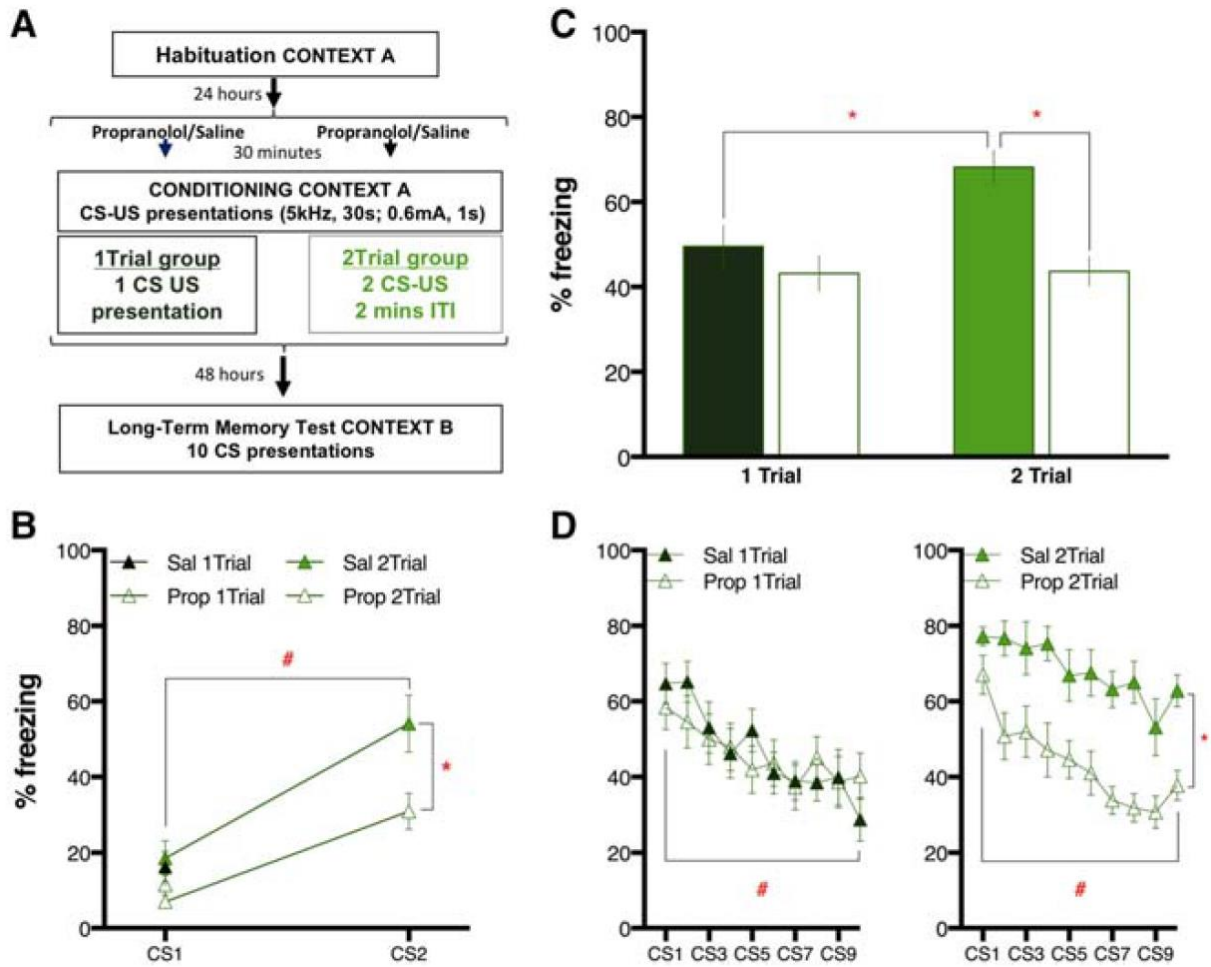


Figure 2.1. Long-term threat memory (LTM) is impaired by pretraining propranolol (10 mg/kg) in animals conditioned with 2 CS-US pairing trials but not in animals that received 1 CS-US trial.

(A) Schematic of the experimental design. Animals were habituated to the conditioning context for 30 min. Twenty-four hours later, rats received propranolol (10 mg/kg: Prop: empty symbols) or saline vehicle (1 mL/kg, Sal: filled symbols) 30 min before the conditioning session, which consisted of either 1 CS-US pairing trial (1Trial: dark green) or two trials (2Trial: light green) with a 2-min intertrial interval (ITI). Forty-eight hours later, LTM was tested in a modified context with 10 CS-alone presentations. **(B)** Graph showing the average percentage of freezing (mean

\pm SEM) to each CS presentations during threat conditioning session for each set of animals. In the group conditioned by presenting two CS-US pairings, the animals treated with propranolol froze less than their controls to the CS2. **(C)** Percentage of freezing (mean \pm SEM) averaged across all 10 CSs presented to test LTM. Post hoc tests after finding significant main Drug Treatment and Trial effects as well as Treatment by Trial interaction revealed that the saline animals conditioned with 2Trials froze more than the 1Trial ones. Propranolol reduced the amount of freezing only in the 2Trial group. **(D)** The percentage of freezing (mean \pm SEM) to each of the 10 CSs presented for LTM test divided by treatment. The 1Trial (left graph) and the 2Trial (right graph) groups showed main effects of CS presentation indicating normal within-session extinction learning. 2Trial animals also showed a main effect of the treatment.

(*) $P < 0.05$, (#) $P < 0.05$ for CS main effect.

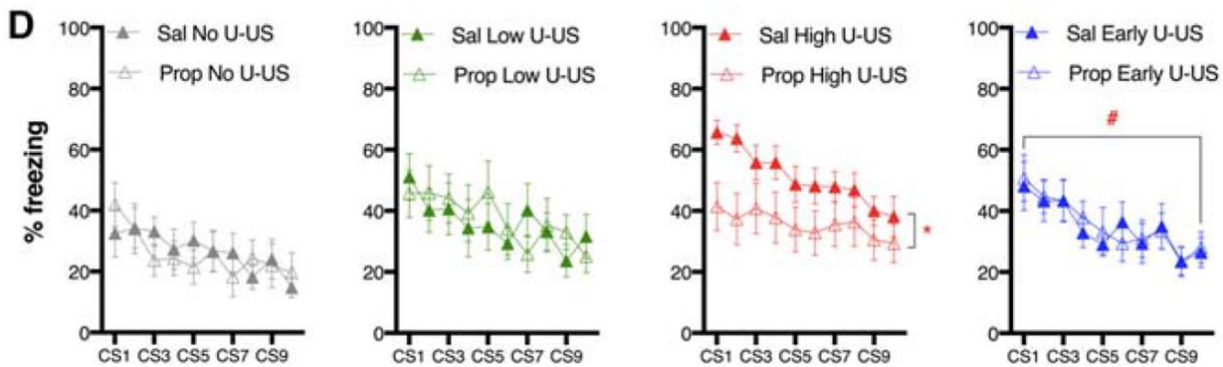
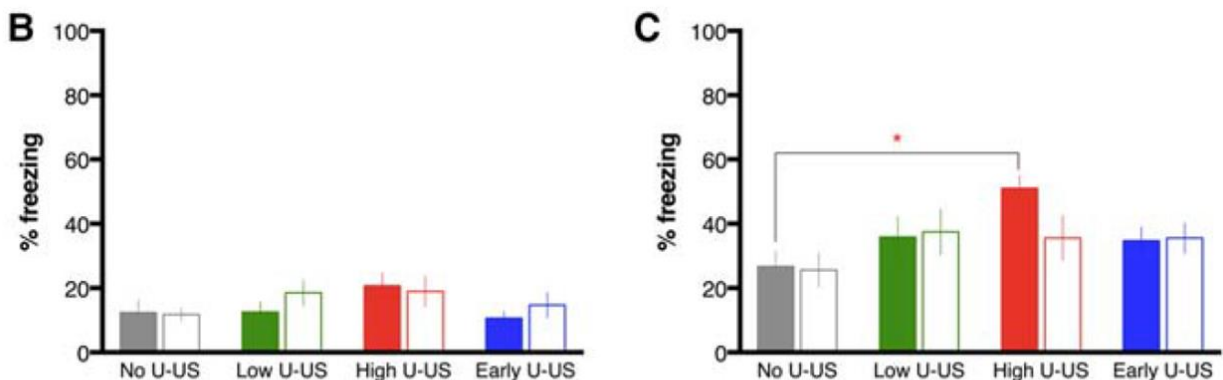
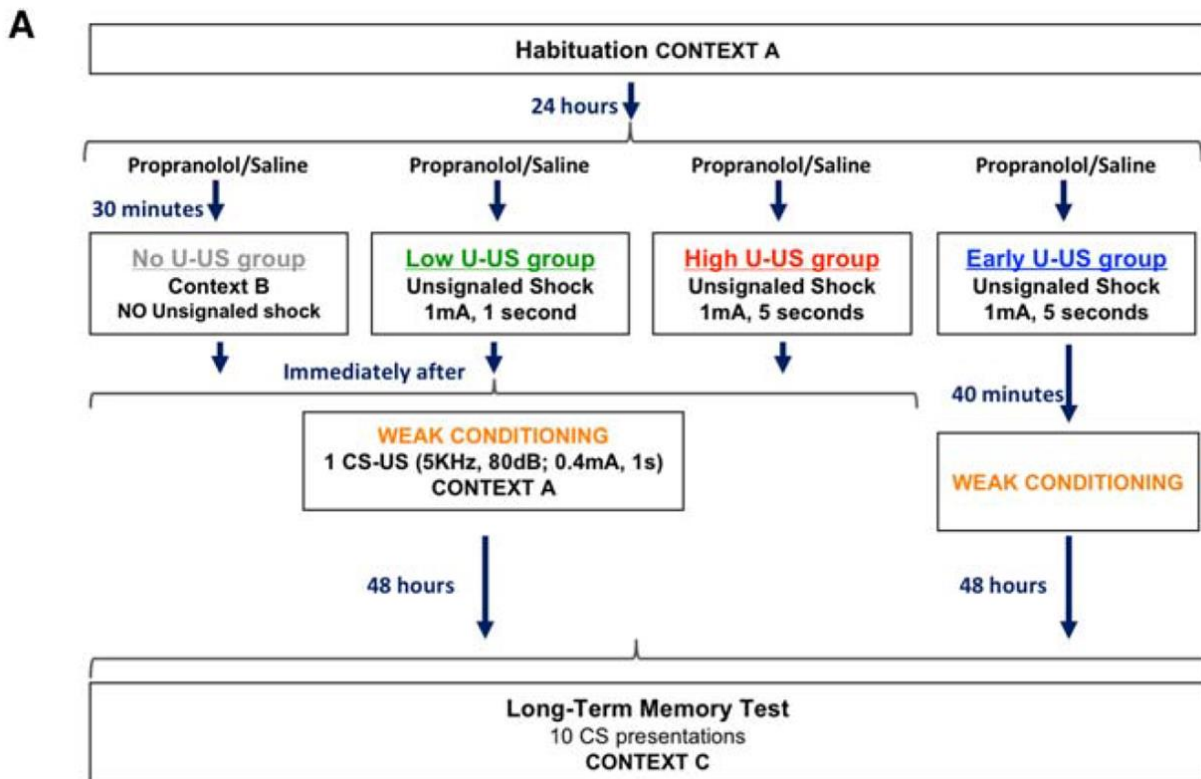


Figure 2.2. The enhancement of freezing during long-term memory test induced by the preexposure to an unsignaled footshock (U-US) before single-trial weak conditioning is prevented by pretraining propranolol.

(A) Schematic of experimental design. On the day following habituation to the conditioning context, animals received propranolol (10 mg/kg: Prop: empty symbols) or saline vehicle (1 mL/kg, Sal: filled symbols) 30 min before placement in a shuttlebox. Three seconds after the beginning of the shuttlebox protocol, rats received either no shock (No U-US: gray), a 1-sec shock (Low U-US: green), or a 5-sec shock (High U-US: red; or Early U-US: blue). All groups were immediately transferred to the conditioning context after offset of the U-US, except for the Early U-US group that instead waited in their home cages for 40 min before conditioning. Conditioning consisted of a single trial of tone–shock pairing with a weak shock (0.4 mA). Forty-eight hours later, an LTM test was done by giving 10 CS-alone presentations in a modified context. **(B)** Graph showing percentage of freezing (mean \pm SEM) during the CS presentation in the conditioning session for each group of animals. Note that this CS is a novel stimulus at this point, not having been paired with shock until the final second of this CS presentation. No significant effects or differences were observed on this measure. **(C)** Results from LTM test expressed as percentage freezing (mean \pm SEM) to CSs averaged across all 10 CS-alone presentations. A main effect of U-US condition was observed, and post hoc testing revealed that Sal High U-US froze more than the Sal No U-US control. **(D)** Percentage freezing (mean \pm SEM) to each CS in the LTM session. A main effect of drug treatment was seen only in the High U-US condition. A main effect of CS presentation was observed only for the Early U-US condition.

(*) $P < 0.05$, (#) $P < 0.05$ for CS main effect

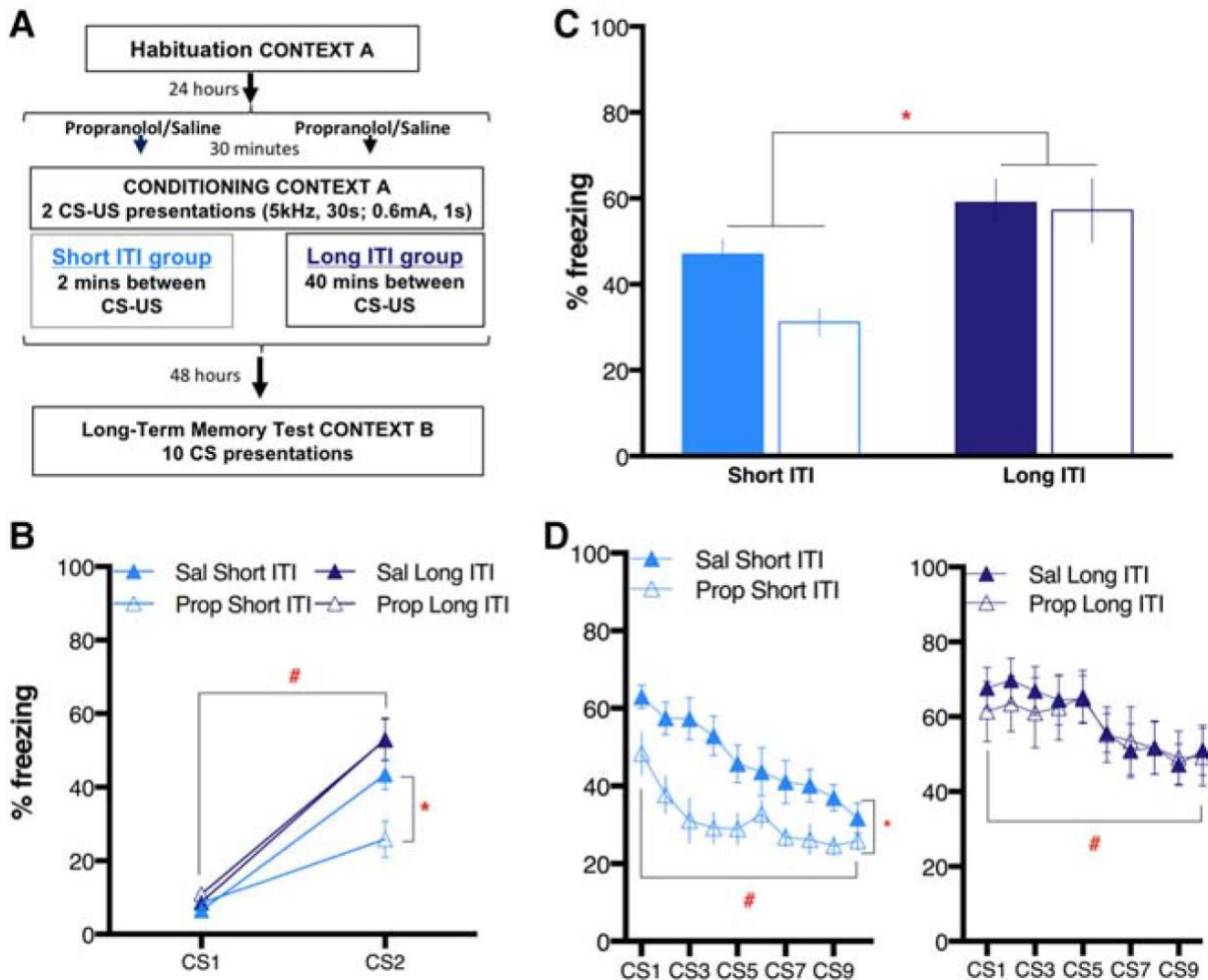


Figure 2.3. The norepinephrine enhancement of acquisition of long-term threat memory depends on the length of ITI during training. **(A)** Schematic of the experimental design. The conditioning session included two CS-US pairings, which were either 2 min apart (short ITI: light blue) or 40 min apart (long ITI: dark blue). All animals were injected with propranolol (10 mg/kg: Prop: empty symbols) or saline vehicle (1 mL/kg: Sal: filled symbols) 30 min before conditioning. Habituation and LTM test sessions were identical to the other experiments. **(B)** Percentage of freezing (mean \pm SEM) to each CS in the conditioning session for each condition. Post hoc pairwise comparisons showed Prop Short ITI animals froze less to CS2 than their saline

controls. **(C)** Graph showing freezing (mean \pm SEM) averaged across all 10 CS presentations in the LTM test. A main effect of group was observed. **(D)** Analysis of freezing in the LTM test to each CS within each group showed that pretraining propranolol reduced freezing only for the Short ITI group but not for Long ITI. Both conditions showed a main effect of CS, demonstrating within-session extinction learning.

(*) $P < 0.05$, (#) $P < 0.05$ for CS main effect.

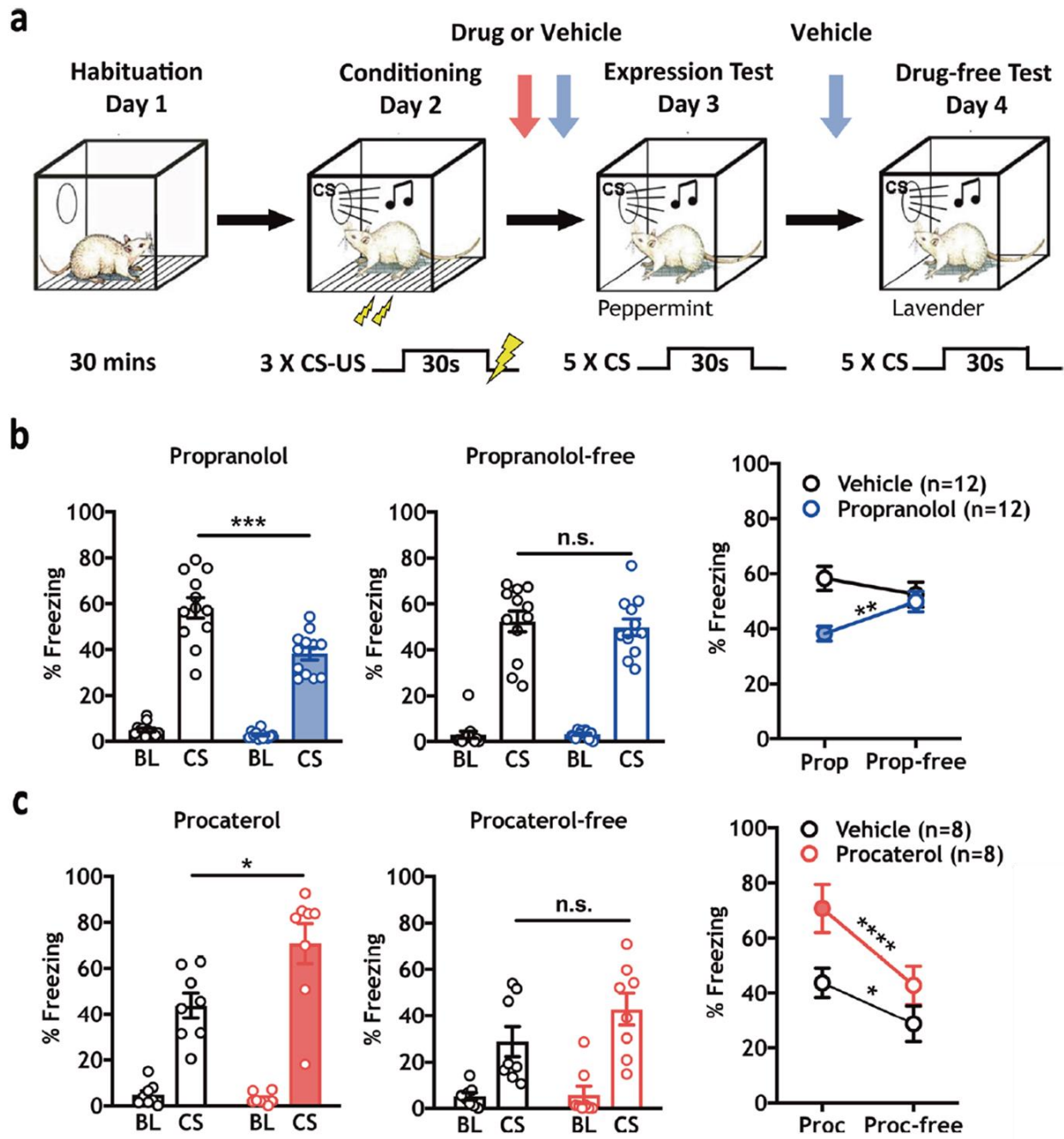


Figure 3.1 Norepinephrine β-AR activity is required for CS-elicited freezing responses. (a)
 Experimental timeline depicting habituation (Day 1), training (0.6 mA or 0.4 mA US) (Day 2), expression test (Day 3) and drug-free test (Day 4) phases. Vertical arrows indicate time of drug

(red arrow) or vehicle (blue arrow) injection for each manipulation. **(b)** Systemic injection of the β -AR antagonist propranolol (10 mg/kg) reduced baseline ($*p = 0.0283$) and CS-elicited ($***p = 0.0008$) freezing levels during the expression test compared with vehicle control animals (left panel), with no effect observed between groups during a drug-free test (center panel). A within-subject comparison of propranolol treatment versus propranolol-free treatment on CS-elicited freezing showed a significant difference for drug treatment (two-way RM ANOVA test, Interaction: $F(1, 22) = 15.79$, $***p = 0.0006$; Time (Drug versus Drug-free) $F(1, 22) = 1.678$, $p = 0.2086$; Drug versus Vehicle $F(1, 22) = 5.021$, $*p = 0.0355$; Sidak MCS, $**p < 0.01$ between days for propranolol treated animals, n.s. for vehicle-treated animals). **(c)** Systemic injection of the specific β_2 -AR agonist procaterol (300 μ g/kg) enhanced CS-elicited freezing during the expression test ($n = 8$ /group; left panel, $*p = 0.0200$), with no effect during a drug free test (center panel). Within subject analysis showed a main effect of procaterol on CS-elicited freezing between days in both groups (two-way RM ANOVA test, Interaction: $F(1, 14) = 3.991$, $p = 0.0655$; Drug: $F(1, 14) = 4.786$, $*p = 0.0462$; Time (Drug versus Drug-free), $F(1, 14) = 43.73$, $****p < 0.0001$; Sidak MCS, $****p < 0.0001$ between days for procaterol treated animals, $*p < 0.05$ for vehicle-treated animals).

All error bars indicate mean \pm SEM. $*p < 0.05$, $**p < 0.01$, $***p < 0.001$, $****p < 0.0001$

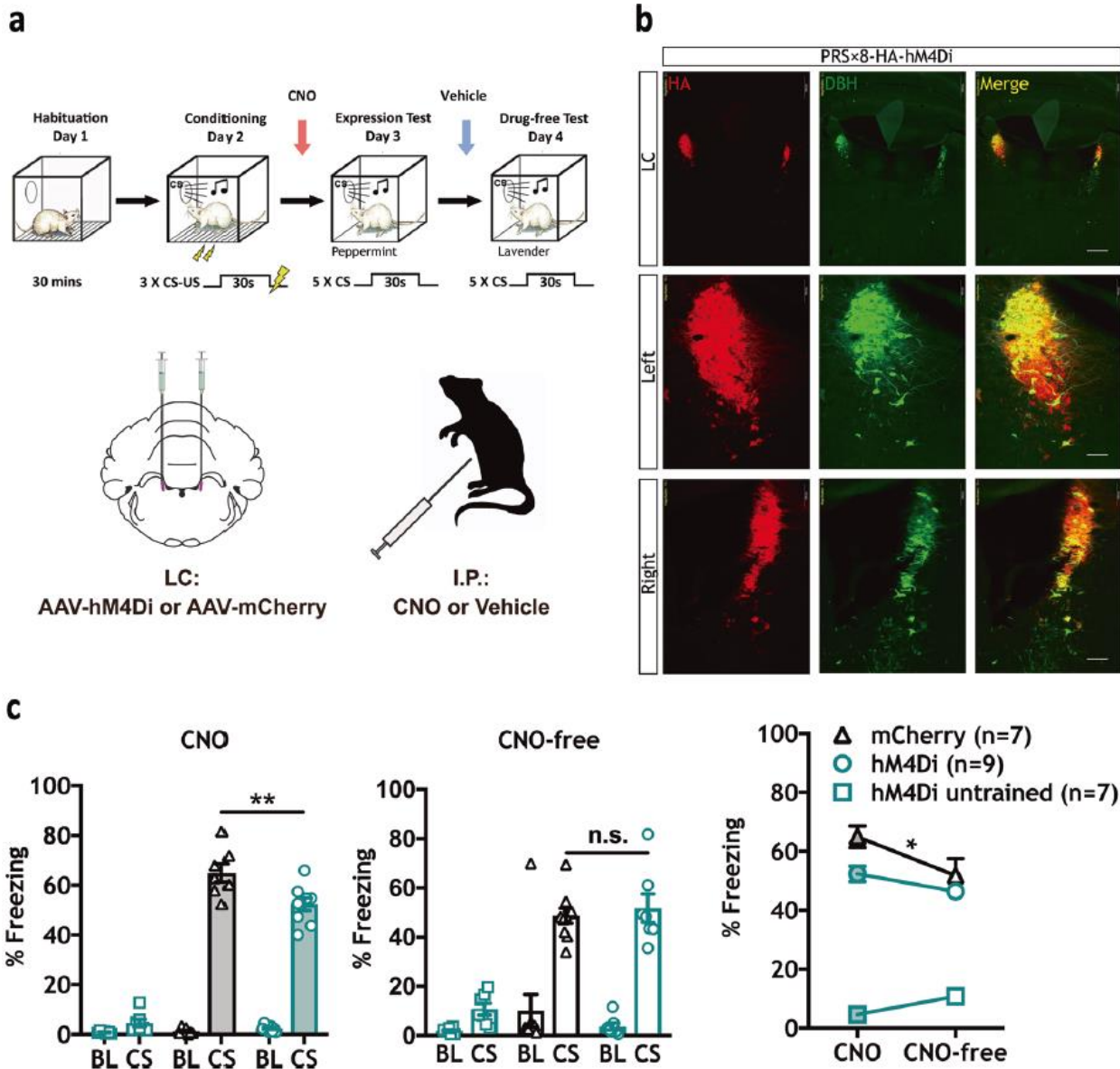


Figure 3.2 Chemogenetic inhibition of LC-NE signaling decreases CS-elicited freezing in threat-conditioned animals. (a) Top: Timeline indicating habituation (Day 1), conditioning (0.6 mA US) (Day 2), expression test (Day 3) and drug-free test (Day 4) phases. Bottom: Schematic depicting hM4Di or mCherry virus injection and CNO treatment strategy. (b) Representative IHC images show robust and selective targeting of hemagglutinin-tagged (HA) hM4Di receptors to DBH+ LC neurons. (Red = HA; Green = dopamine β hydroxylase (DBH); Yellow = indicates co-

localization. Scale bars: top three panels = 500 μ m, middle and bottom six panels = 100 μ m. **(c)** On conditioning day, hM4Di paired ($n = 9$) and mCherry paired groups ($n = 7$) were threat conditioned, and an unpaired hM4Di control group ($n = 7$) received three tones alone. CNO (5.0 mg/kg) inhibition of LC-NE neurons significantly decreased CS-elicited freezing in trained hM4Di animals compared with mCherry controls (one-way ANOVA, $F(2,20) = 126.4$, **** $P < 0.0001$; Tukey's MCS, ** $P < 0.01$), with no difference observed between hM4Di paired and mCherry paired groups during the drug-free test. Within subject analysis revealed a slight reduction in CS-elicited freezing between days in the mCherry group, with no significant reduction in the hM4Di paired group (two-way RM ANOVA test, Interaction: $F(2, 20) = 4.236$, * $p = 0.0292$; Training x virus: $F(2, 20) = 134.5$, **** $p < 0.0001$; Time (CNO versus CNO-free): $F(1,20) = 2.692$, $p = 0.1165$; Sidak MCS, CNO versus CNO-free: hM4Di untrained, $p = \text{n.s.}$, hM4Di trained, $p = \text{n.s.}$, mCherry * $p < 0.05$).

All error bars indicate mean \pm SEM. * $p < 0.05$, ** $p < 0.01$, **** $p < 0.0001$

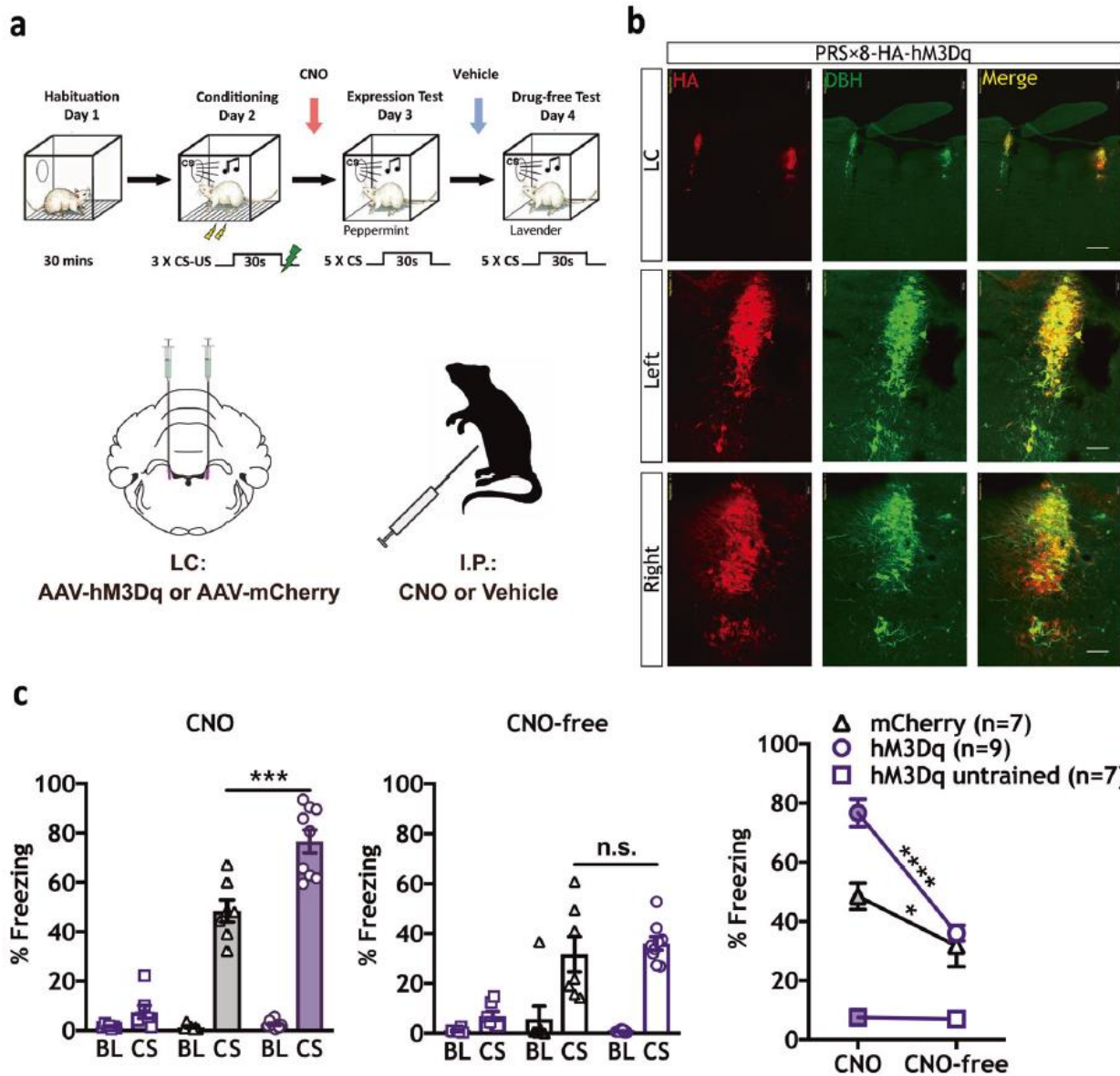


Figure 3.3 Chemogenetic activation of LC-NE signaling increases CS-elicited freezing in threat-conditioned animals. **(a)** Top: Timeline indicating habituation (Day 1), mild conditioning (0.4 mA US) (Day 2), expression test (Day 3), and drug-free test (Day 4) phases. Bottom: Schematic depicting hM3Dq or mCherry virus injection and CNO treatment strategy. **(b)** Representative IHC images show robust and selective targeting of hM3Dq-HA to DBH+ LC neurons. (Red = HA; Green = DBH; Yellow = co-localization). Scale bars: top three panels = 500 μ m, middle and

bottom six panels = 100 μ m. **(c)** Systemic injection of CNO (1.0 mg/kg) prior to the expression test significantly enhanced freezing in the trained hM3Dq group ($n = 9$) compared with the trained mCherry group ($n = 7$; left panel, one-way ANOVA, $F(2,20) = 69.54$, **** $P < 0.0001$, Tukey's MCS, *** $P < 0.001$). No differences were observed between groups during a CNO-free test (center panel). A difference in CS-elicited freezing was observed in trained animals between CNO- and CNO-free tests (two-way RM ANOVA test, Interaction: $F(2, 20) = 16.62$, **** $p < 0.0001$; Training X virus: $F(2, 20) = 55.64$, **** $p < 0.0001$, Time (CNO versus CNO-free): $F(1,20) = 43.45$, **** $p < 0.0001$; Sidak MCS, CNO versus CNO-free: hM4Di untrained, $p = \text{n.s.}$, hM3Dq trained, **** $p < 0.0001$, mCherry trained, * $p < 0.05$).

All error bars indicate mean \pm SEM. * $p < 0.05$, *** $p < 0.001$, **** $p < 0.0001$

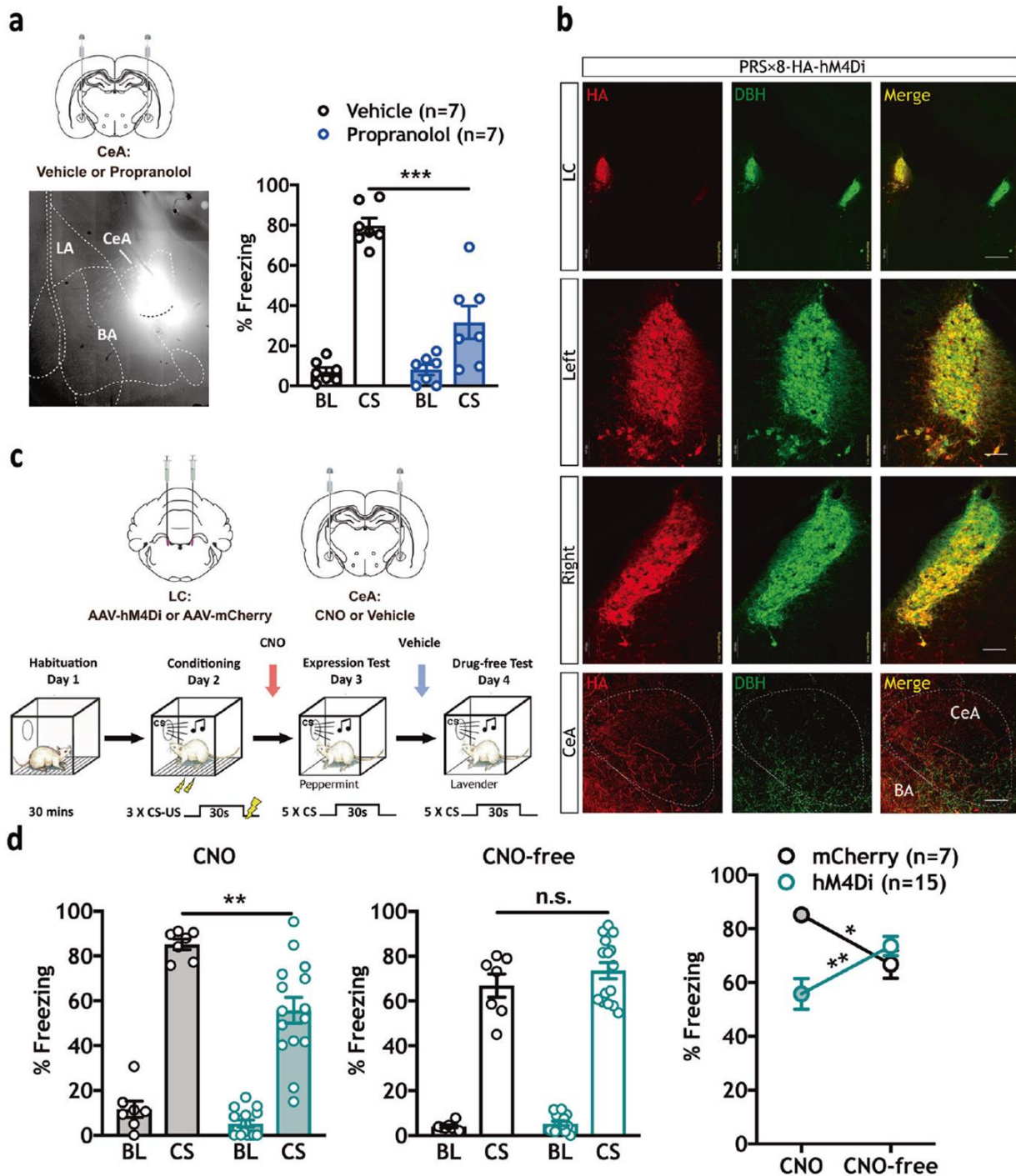


Figure 3.4 CeA blockade of β -ARs or chemogenetic inhibition of LC-NE axon terminals in the CeA decreases CS-elicited freezing. (a) Local propranolol infusions in CeA ($1.0 \mu\text{g}/0.3 \mu\text{l}/\text{side}$)

significantly reduced CS-elicited freezing ($***p = 0.0002$) in expression test as described above. A fluorophore-conjugated propranolol was infused to confirm the spread of the drug in CeA. **(b)** Robust and selective targeting of hM4Di-HA to DBH+ LC neurons and detectable expression in axons projecting to CeA after six weeks (Red = HA; Green = DBH; Yellow = co-localization). Scale bars: top three LC panels = 500 μm , middle six LC panels = 100 μm , bottom three CeA panels = 50 μm . **(c)** Virus and CNO infusion strategy and experimental timeline. **(d)** CNO infusions in CeA (1.0 mM/0.3 $\mu\text{l}/\text{side}$) significantly reduced CS-elicited freezing in hM4Di animals ($n = 15$) compared with the mCherry ($n = 7$) group, Mann–Whitney U, $**p = 0.0015$). No differences were observed between groups during the CNO-free test (center panel). Differences were observed in CS-elicited freezing in both groups between CNO- and CNO-free tests (two-way RM ANOVA test, Interaction: $F(1, 20) = 20.13$, $***p = 0.0002$; Virus: $F(1, 20) = 3.088$, $p = 0.0942$; Time (CNO versus CNO-free): $F(1, 20) = 0.005266$, $p = 0.9429$; Sidak MCS, CNO versus CNO-free: mCherry, $*p < 0.05$, hM4Di, $**p < 0.01$).

All error bars indicate mean \pm SEM. $*p < 0.05$, $**p < 0.01$, $***p < 0.001$.

Central amygdala (CeA), lateral amygdala (LA) basal amygdala (BA)

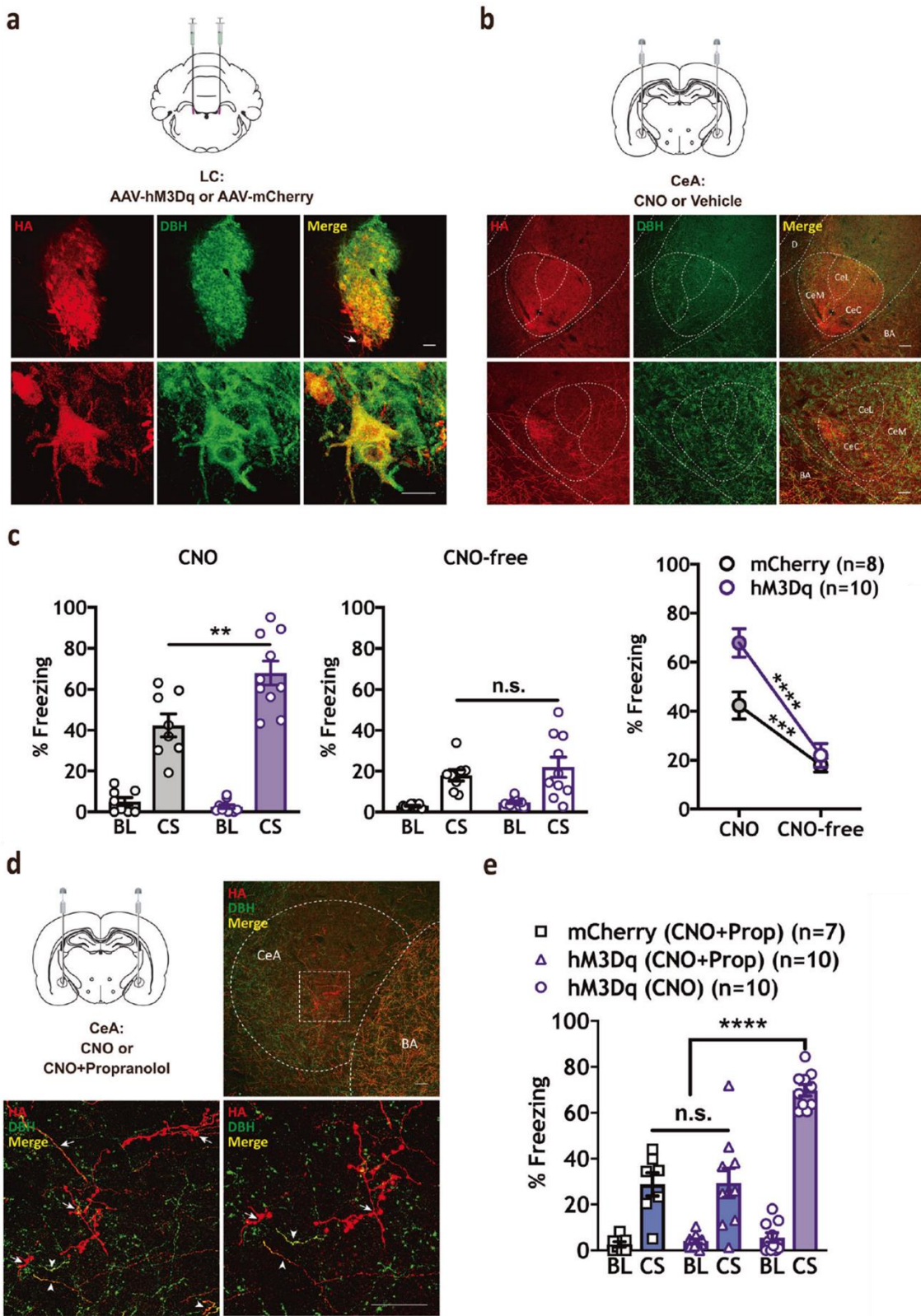
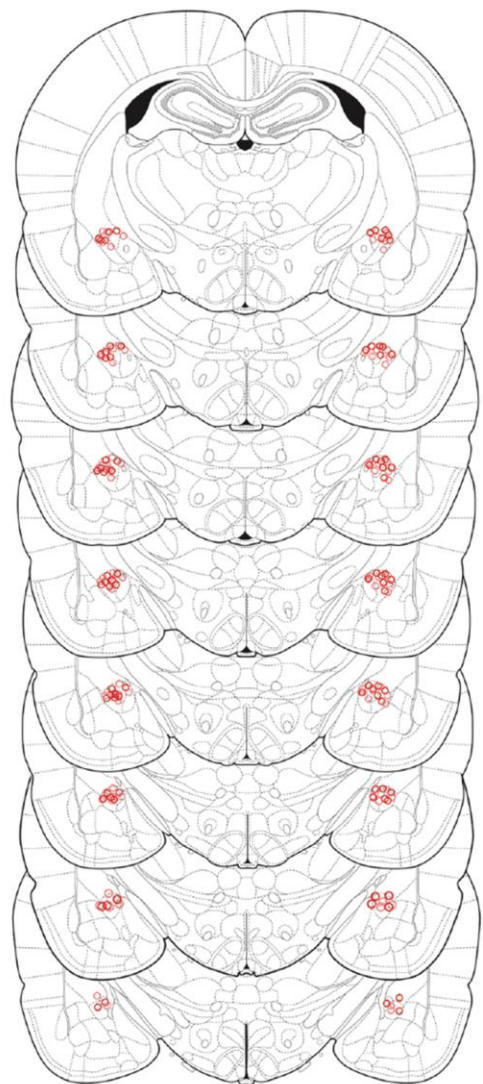


Figure 3.5 Chemogenetic activation of LC-NE terminals in CeA increases CS-elicited freezing behavior and is blocked by β-AR antagonist. **(a)** hM3Dq (HA) expression in LC (Red = HA; Green = DBH; Yellow = co-localization). Arrow indicates the magnification of the same LC neuron. Scale bars: LC panels = 50 μm. **(b)** HA-immunopositive terminals from LC were detected in CeA. Scale bars: CeA panels = 50 μm. **(c)** Infusions of CNO (1.0 mM/0.3 μl/side) led to a significant increase in CS-elicited freezing in hM3Dq ($n = 10$) animals compared with mCherry controls (left panel, $n = 8$, $t(16) = 3.114$, ** $p = 0.0067$), with no difference observed between groups during a CNO-free test (center panel). Differences were observed in CS-elicited freezing in both groups between CNO- and CNO-free tests (two-way RM ANOVA test, Interaction: $F(1, 16) = 11.78$, ** $p = 0.0034$; Virus: $F(1, 16) = 5.197$, * $p = 0.0367$; Time (CNO versus CNO-free): $F(1, 16) = 125.7$, **** $p < 0.0001$; Sidak MCS, CNO versus CNO-free: mCherry, *** $p < 0.001$, hM3Dq, **** $p < 0.0001$). **(d)** Prior to the expression test, animals received intra-CeA infusions of CNO alone (hM3Dq (CNO); ($n = 10$)), or a cocktail of CNO and propranolol (1.0 mM/0.3 μl/side + 1.0 μg/0.3 μl/side) in hM3Dq ($n = 10$) and mCherry ($n = 7$) animals. Representative IHC images show robust and selective targeting of hM3Dq-HA to DBH+ LC neurons and strong expression in CeA terminals. (Red = HA; Green = DBH; Yellow = overlapping indicates co-localization). Arrow indicates the magnification of the LC-NE terminals in CeA. Scale bars, CeA panels = 50 μm. **(e)** Propranolol significantly reduced the effect of CNO in hM3Dq-expressing animals (one-way ANOVA, $F(2, 24) = 23.77$, **** $p < 0.0001$, Tukey's MCS, mCherry (CNO + Prop) versus hM3Dq (CNO), **** $p < 0.0001$ and hM3Dq (CNO + Prop) versus hM3Dq (CNO), **** $p < 0.0001$).

All error bars indicate mean ± SEM. ** $p < 0.01$, **** $p < 0.0001$.

Central medial amygdala (CeM), Central lateral amygdala (CeL), Central capsular amygdala (Cec), Basal amygdala (BA), Central amygdala (CeA)

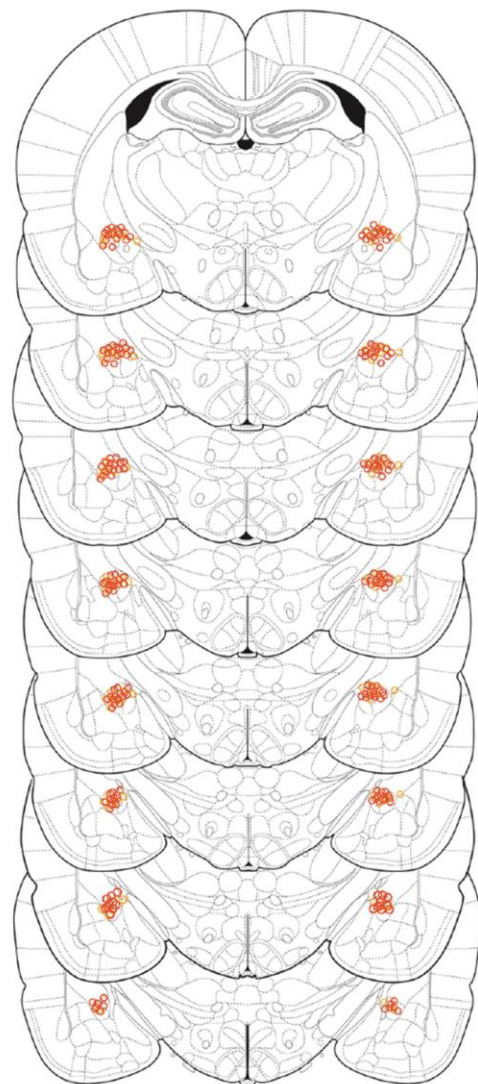
a



Propranolol group, CeA cannula placement (N=7)

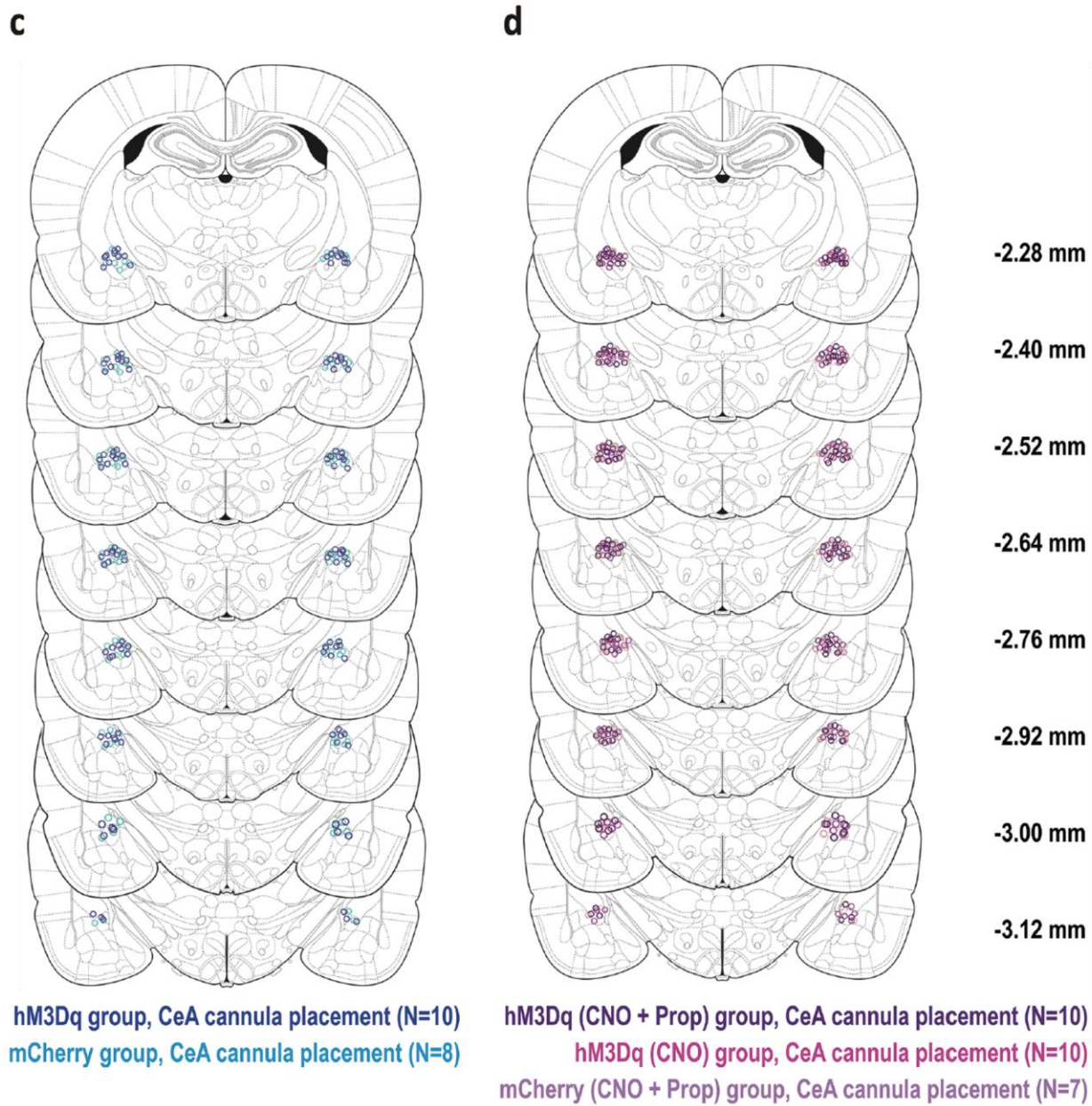
Vehicle group, CeA cannula placement (N=7)

b



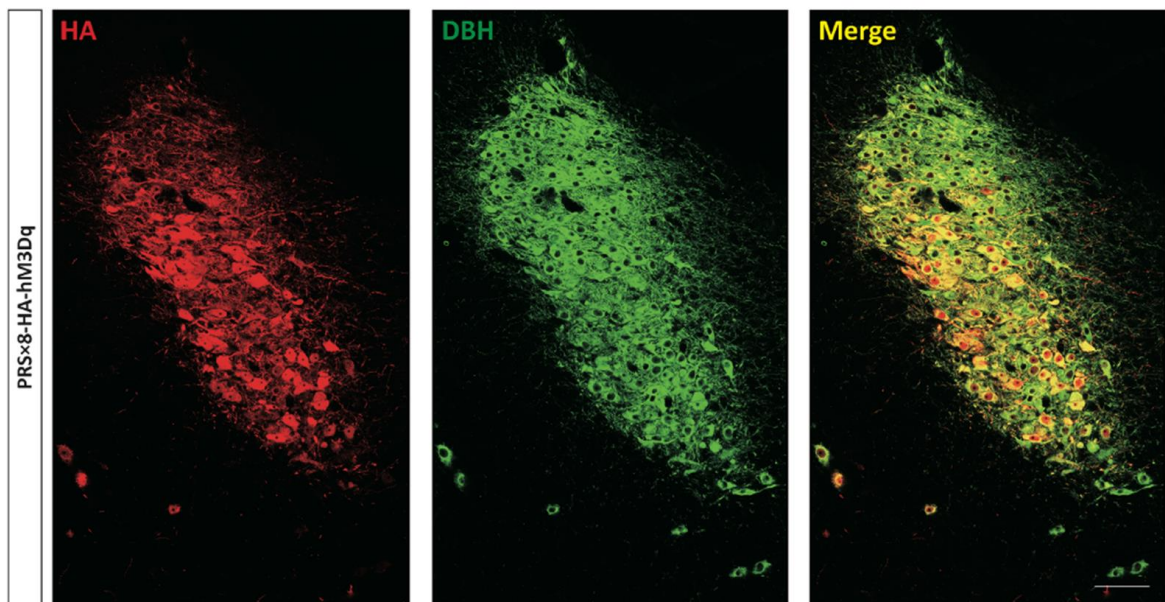
hM4Di group, CeA cannula placement (N=15)

mCherry group, CeA cannula placement (N=7)

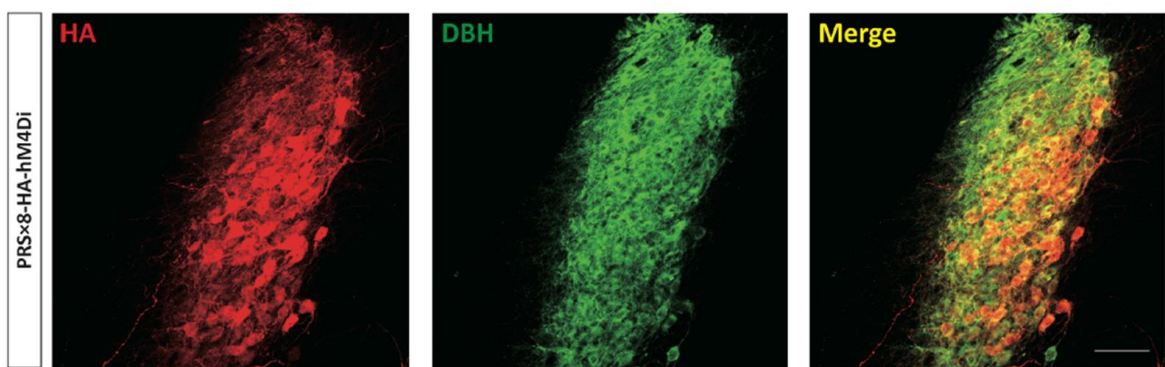


Supplementary Figure 3.1. Virus and CeA cannulation targeting for all experiments. Related to Figure 4 and 5.

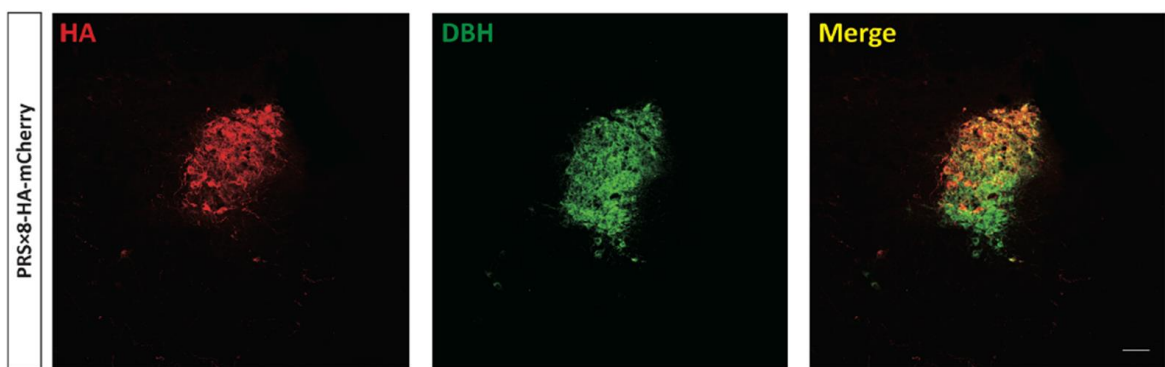
a



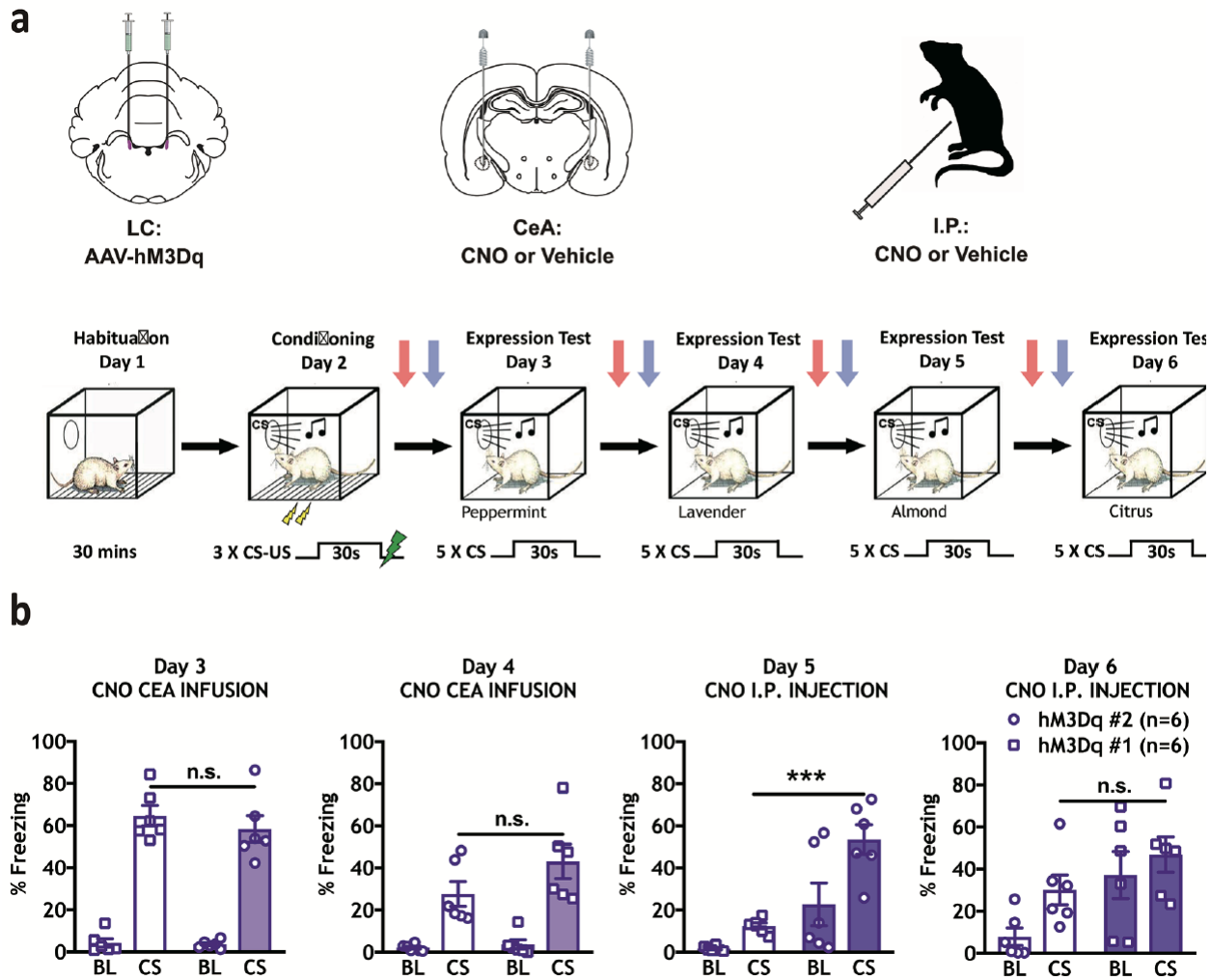
b



c



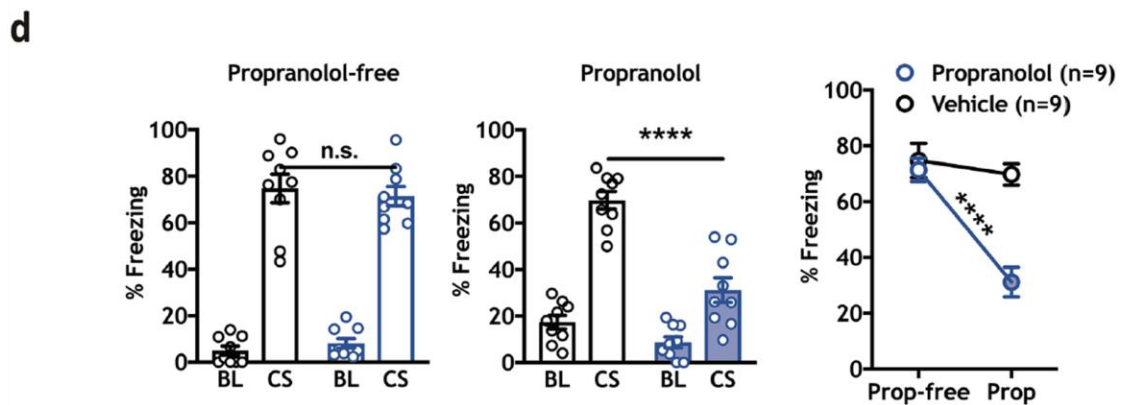
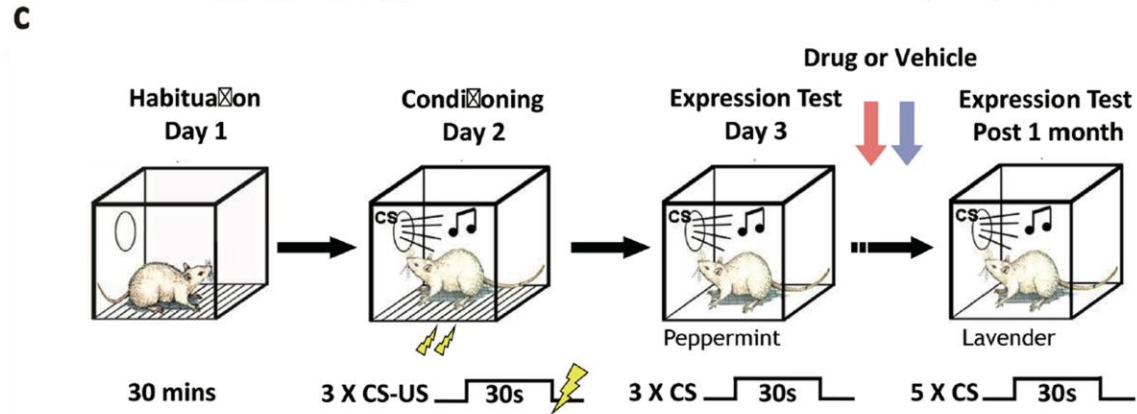
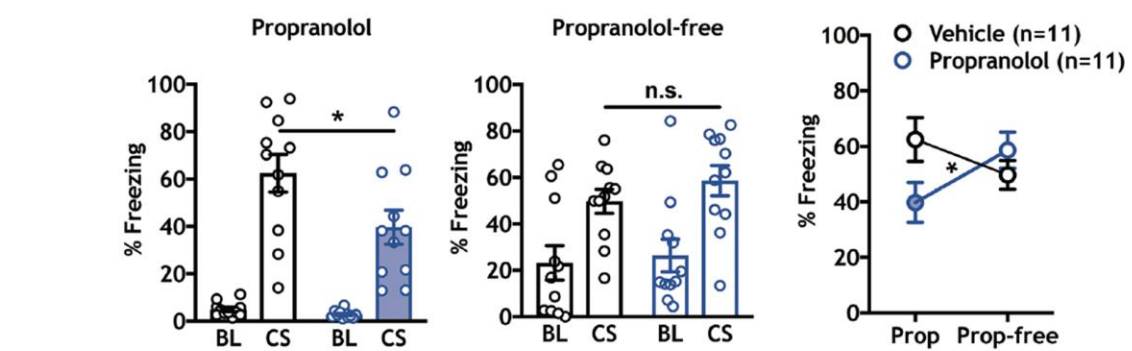
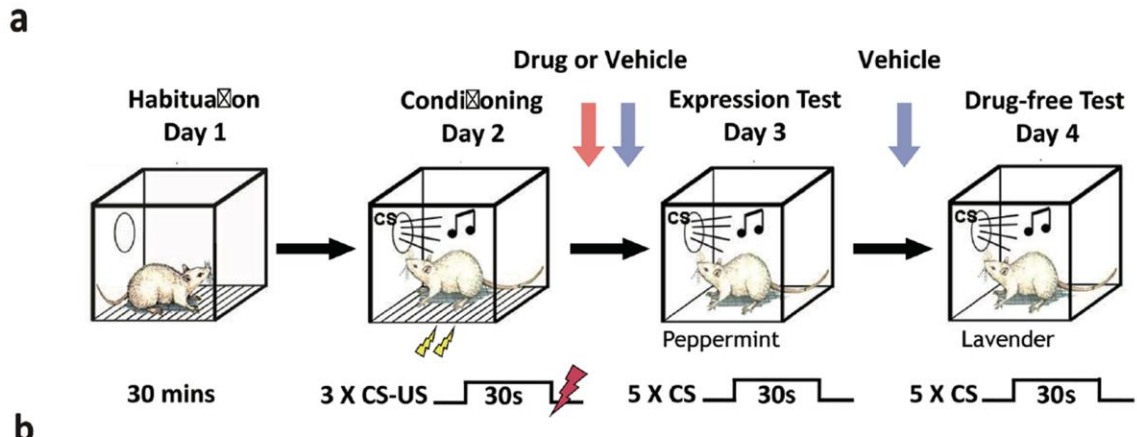
Supplementary Figure 3.2. Representative image of DBH+ and HA co-localization in hM3Dq/hM4Di LC rats. **(a)** Animals injected in LC with AAV-PRSx8-HA-hM3Dq and **(b)** PRSx8-HAhM4Di show immunoreactivity for HA exclusively in DBH+ neurons. **(c)** Animals injected with PRSx8-HA-mCherry (control virus) in LC show mCherry expression only in DBH+ neurons. Scale bars, LC panels = 50 μ m, respectively.



Supplementary Figure 3.3. Experiments using axon terminal manipulations require longer incubation periods. **(a)** Timeline indicating habituation (Day 1), mild conditioning (0.4 mA US) (Day 2), within subject expression test (CeA infusion) (Day 3, Day 4) and within subject expression test (i.p. injection) (Day 5, Day 6) phases. Three weeks following bilateral hM3Dq virus injection in LC, all rats ($n=6$ /group) were trained using a moderate protocol and vertical arrow indicates either CNO (red) or vehicle (blue) treatment strategy. **(b)** No significant difference between hM3Dq (CNO) vs. hM3Dq (vehicle) within CeA infusion on Day 3 and Day 4. Within-subject analysis showed a significant difference in freezing between hM3Dq (CNO) vs.

hM3Dq (vehicle) with systemic treatment (Day 5) ($t(10) = 5.694$, *** $p=0.0002$).

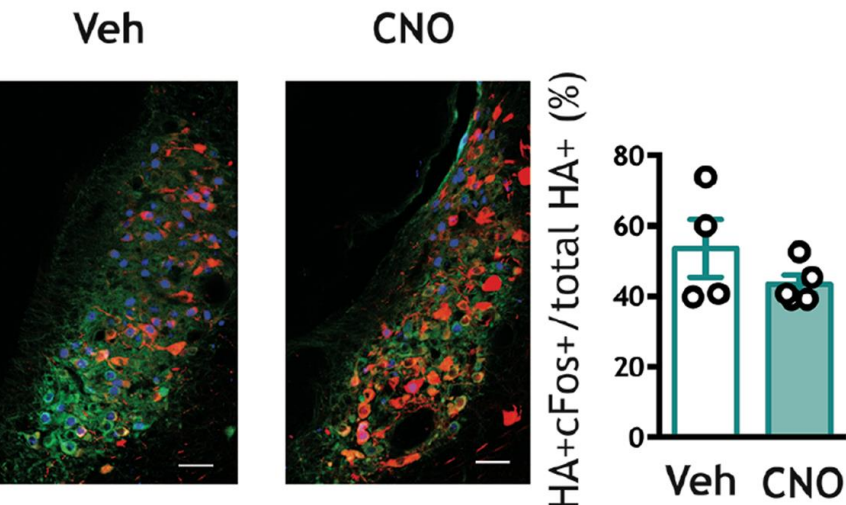
All error bars indicate mean \pm SEM. *** $p<0.001$



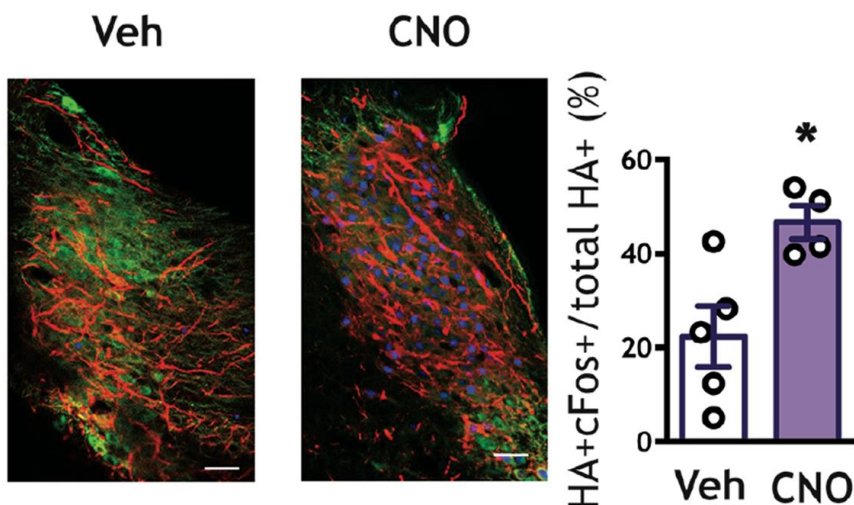
Supplementary Figure 3.4. β -ARs are required for Pavlovian defensive responses, regardless of US intensity or memory age. **(a)** Experimental timeline for strong conditioning paradigm (1.0 mA US). **(b)** Propranolol (10 mg/kg) reduced CS-elicited freezing levels during the expression tests compared to vehicle control animals (left panel: $n = 11/\text{group}$, $*p = 0.0459$), with no effect observed between groups during a drug-free test (center panel, $p = 0.2973$, n.s.). A within-subject comparison of propranolol versus propranolol-free treatment on CS freezing followed by a posthoc test revealed a significant difference in CS-elicited freezing for propranolol treatment day versus propranolol-free day (two-way RM ANOVA test, Interaction: $F(1, 20) = 9.669$, $**p = 0.0055$; Drug: $F(1, 20) = 0.7270$, $p = 0.4039$; Time (Drug vs. Drug-free): $F(1, 20) = 0.3610$, $p = 0.5547$; Sidak MCS, $*p < 0.05$ for propranolol treated animals, n.s. for vehicle-treated animals between days). **(c)** Timeline of remote Pavlovian threat conditioning (tested one month after conditioning (0.6 mA US)). **(d)** Animals showed memory retention after one day, with no difference between groups (left panel, Day 3, $n = 9/\text{group}$; $p = 0.6548$). Subsequent treatment with propranolol after one month (10 mg/kg, Post one month) significantly attenuated CS-elicited freezing ($****p < 0.0001$). Within-subject analysis showed a significant difference between a drug-free test (Day 3) freezing and freezing with propranolol treatment (Post one month); two-way RM ANOVA test, Interaction: $F(1, 16) = 14.06$, $**p = 0.0017$; Drug: $F(1, 16) = 16.55$, $***p = 0.0009$; Time (Drug-free vs. Drug): $F(1, 16) = 23.21$, $***p = 0.0002$; Sidak MCS, $****p < 0.0001$ for propranolol treated animals, n.s. for vehicle-treated animals between days.

All error bars indicate mean \pm SEM. $*p < 0.05$, $**p < 0.01$, $***p < 0.001$, $****p < 0.0001$.

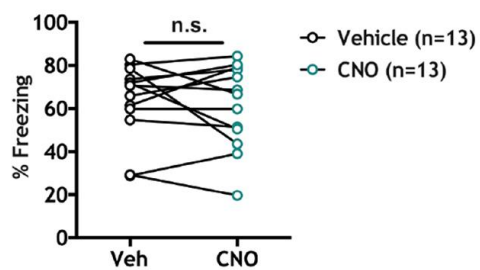
a LC hM4Di



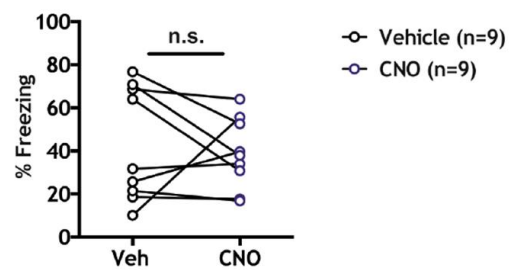
b LC hM3Dq



c LC hM4Di + BLA CNO/Veh infusion



d LC hM3Dq + BLA CNO/Veh infusion



Supplementary Figure 3.5. Control experiments to validate DREADD functionality and rule out noradrenergic BLA contributions to expression of conditioned freezing. **(a)** Representative images of LC in animals expressing hM4Di and receiving i.p. saline (“Veh”, Left) or 5.0 mg/kg CNO (Middle) 30 minutes prior to footshock and 120 minutes prior to sacrifice (Antibody pseudocolors: Red=HA-tag, Green=DBH, Blue=c-Fos; Scale bars = 50 μ m). Ratios of c-Fos+HA double labeled cells in LC over total HA cells in LC for saline and CNO conditions are shown (Right). **(b)** Representative images of LC in animals expressing hM3Dq and receiving i.p. saline (Left) or 1.0 mg/kg CNO (Middle) 90 minutes prior to sacrifice. Ratios are shown for c-Fos+HA double labeled cells in LC over total HA cells in LC (Right, * p = 0.018). **(c)** Expression of conditioned freezing during long-term memory testing for hM4Di-expressing animals receiving 0.3 μ L/side saline or 1.0 mM/0.3 μ L/side of CNO in basolateral amygdaloid complex (BLA). **(d)** Expression of conditioned freezing for hM3Dq-expressing animals receiving 0.3 μ L/side saline or 1.0 mM/0.3 μ L/side of CNO in BLA.

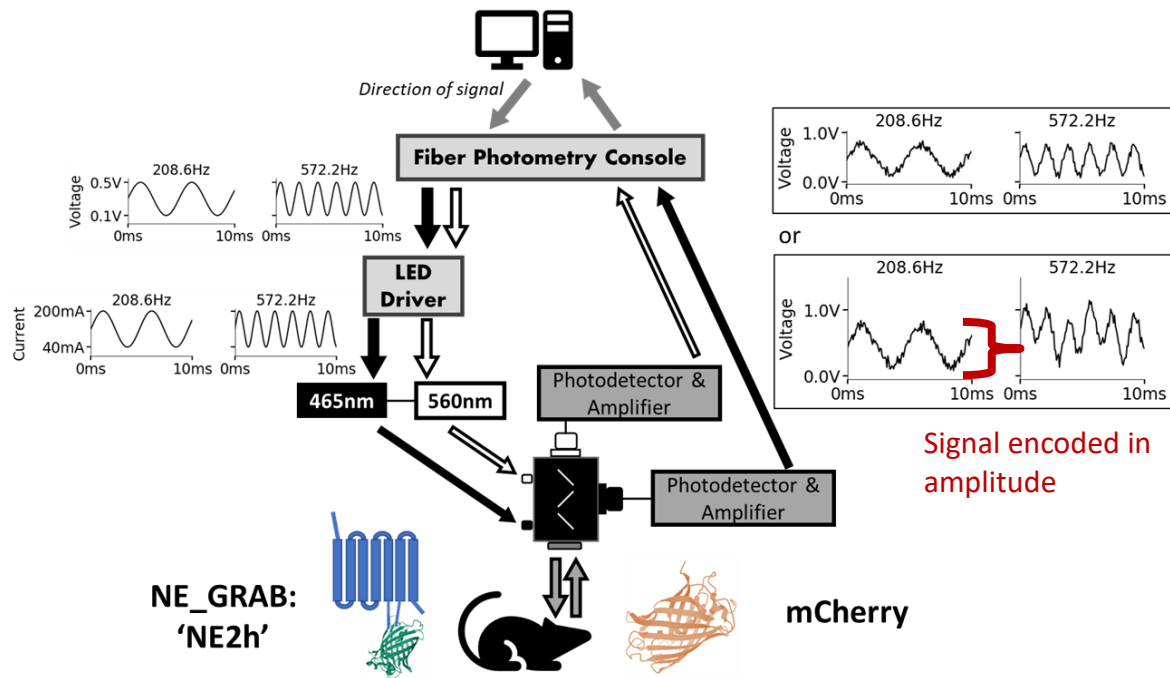


Figure 4.1. Schematic of fiber photometry system (dual-channel GFP+RFP, single-site; Doric Lenses Inc.). Arrows indicate direction of signal from software programming to Doric console, LED driver, LEDs, Doric minicube with 2 input ports, 1 input/output port to and from animal, 2 output ports with photodetectors, amplifiers, and back to the Doric console and software. Lock-in amplification was used to separate GFP-like from RFP-like emissions by encoding GFP-like signal in a 209Hz sine wave from the 465nm LED and RFP-like signal in a 572Hz sine wave from the 560nm LED. The GFP-like channel is used to detect changes in NE2h, a fluorescent norepinephrine sensor with a GFP domain. The RFP-like channel is used with mCherry as a control fluorophore.

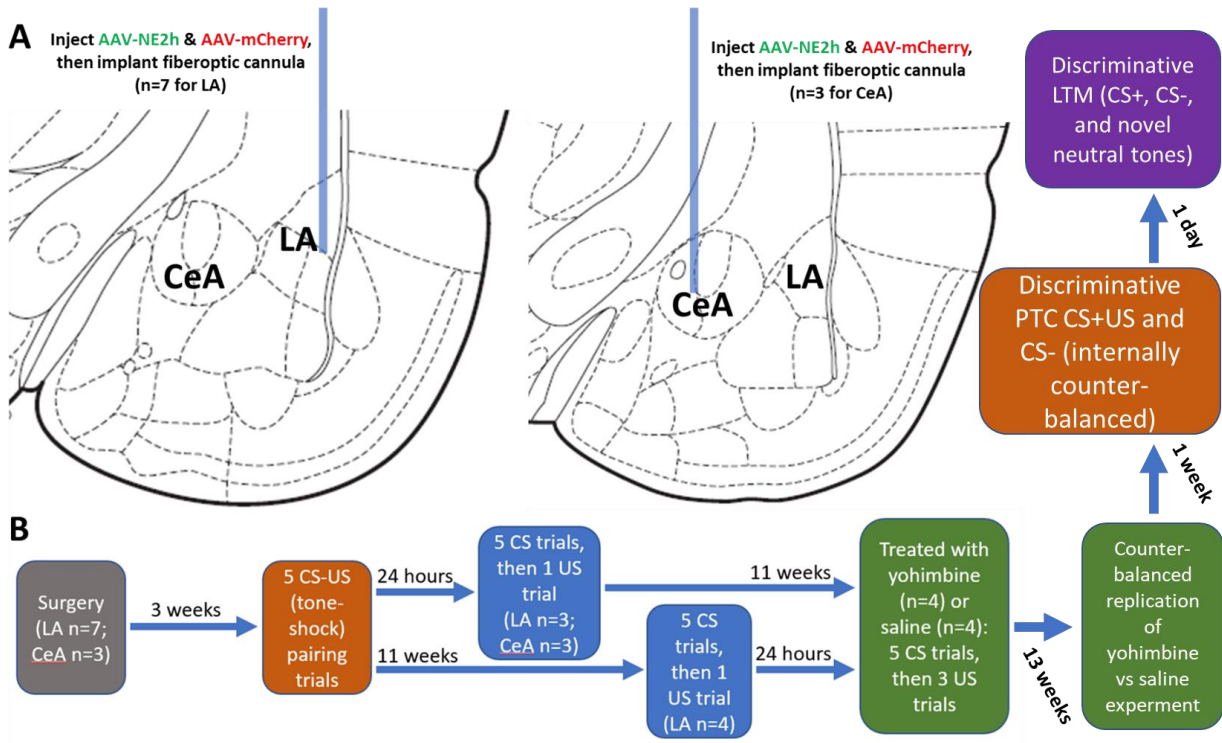


Figure 4.2. Surgical and experimental timeline. (A) Surgery consisted of unilaterally injecting a viral mixture of AAV9-hSyn-NE2h and AAV5-hSyn-mCherry, then implanting a fiberoptic cannula. The injected and implanted side (right or left) was alternated between animals. In some animals, the surgery targeted lateral amygdala (n=7), and in other animals the central amygdala was targeted (n=3). (B) Timeline of experiments. Rats recovered from surgery for 3 weeks before the first fiber photometry session, which was auditory Pavlovian threat conditioning (orange), consisting of 5 trials pairing CS (30 sec tone) with US (1 sec 0.7mA footshock). Either the next day or approximately 11 weeks later, a long-term memory test (blue) was administered with 5 CS presentations. About two minutes after the final CS, a more intense footshock was delivered (5 sec 1.0mA).

The delay of some animals for 11 weeks was due to weak NE2h signal in fiber

photometry sessions up to that point, possibly caused by an inadequate viral incubation period.

The long-term memory test was postponed for some animals to allow longer viral incubation.

After this delay, the signal was in fact stronger.

Finally (green), rats were injected i.p. with the α 2-adrenergic receptor antagonist yohimbine (2mg/kg) or saline vehicle in order to demonstrate that detected signals were in fact dependent on the NE2h NE sensor, which itself is a modified α 2-adrenergic receptor.

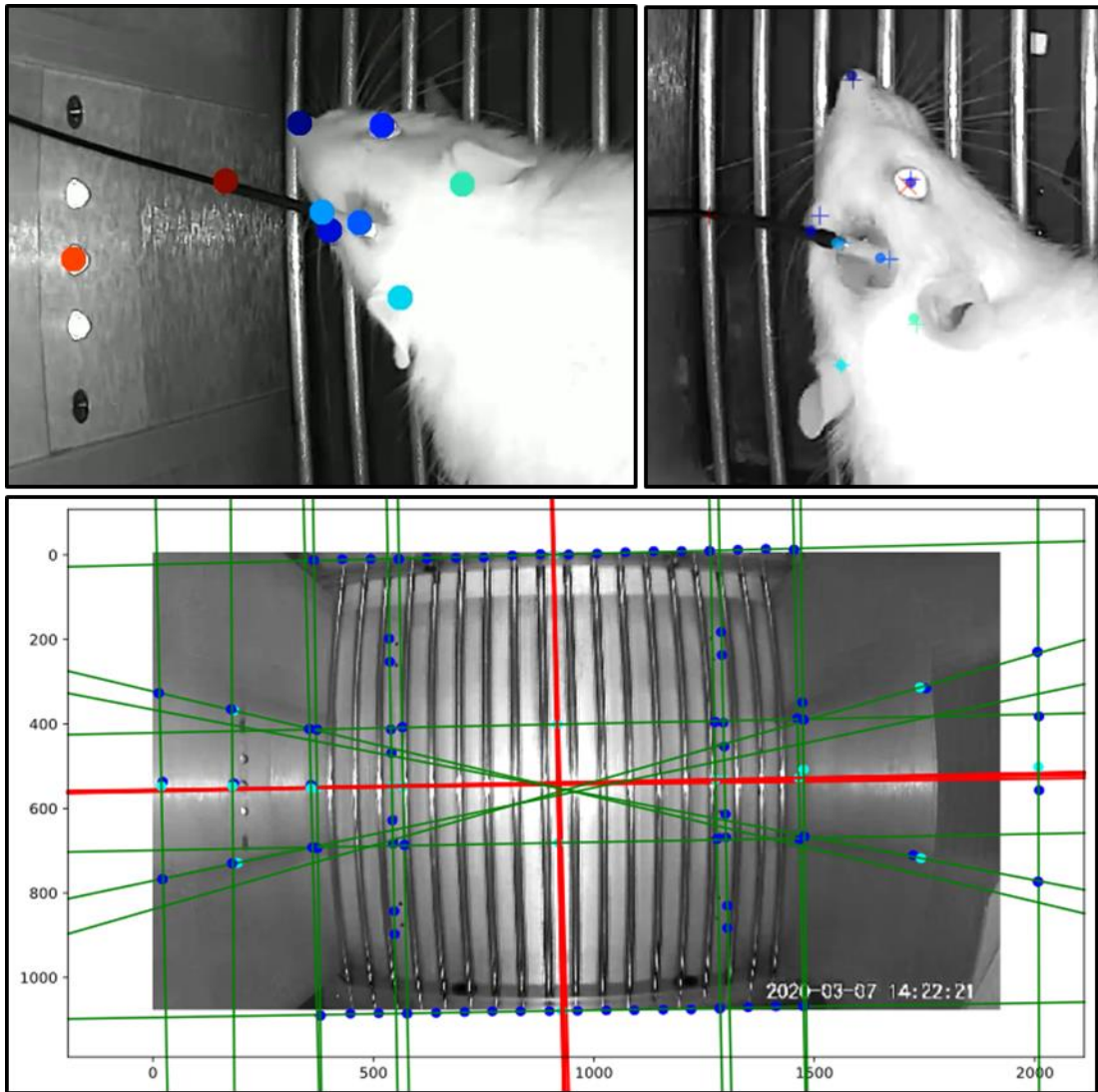


Figure 4.3. Visualization of the applied markers by DeepLabCut software. Upper left image shows the generated markers on an analyzed video. Upper right image shows a test image for a trained model, where the small circles are human-labeled points, and '+' crosses are computer labeled points. 'x' crosses are low-confidence markers, as all output data includes a Bayesian estimate of likelihood, which allows the experimenter to reject low-confidence markers below an arbitrary threshold. Bottom image demonstrates the use of DeepLabCut output as part of a lens distortion correction algorithm.

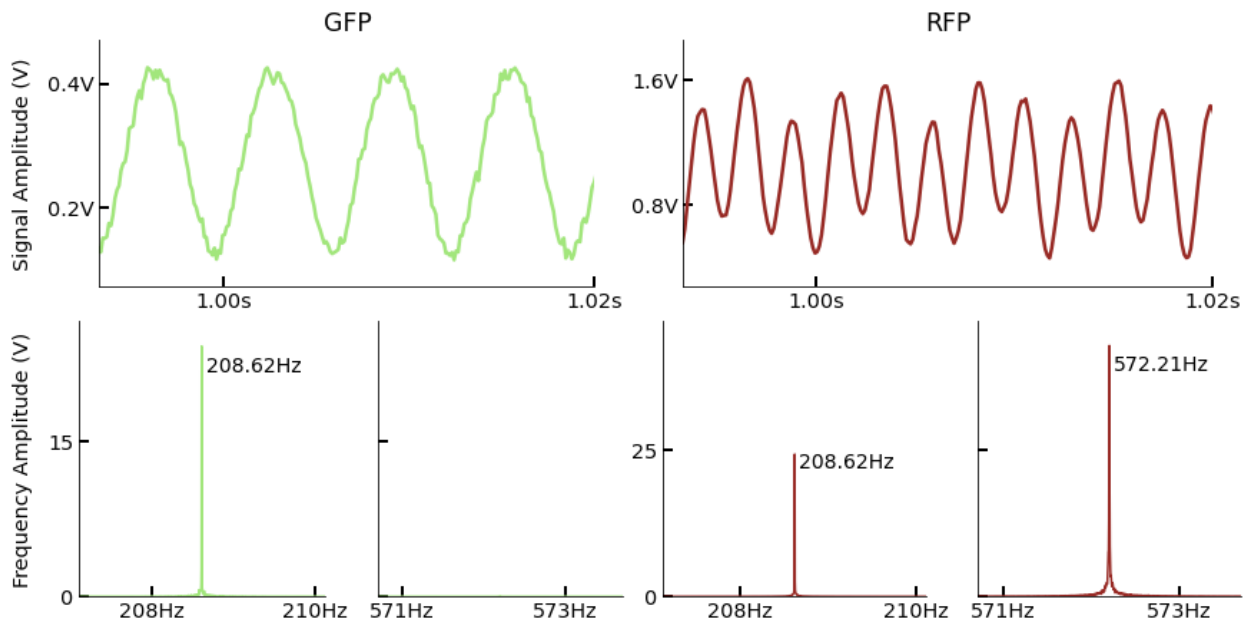


Figure 4.4. Representative recordings at photodetectors from (a.) the equipment without a tethered animal and (b.) with a tethered animal. Each set of plots shows the voltage signal at the photodetectors for the GFP channel (left) and RFP channel (right) in time domain (top) and frequency domain (bottom). Frequency amplitude was calculated via a Discrete Fast Fourier Transform using 2^{22} time points over 344 seconds at 12,190 Hz. Amplitude was normalized by dividing by the area under the curve of all frequencies greater than 1Hz and less than half the sampling rate.

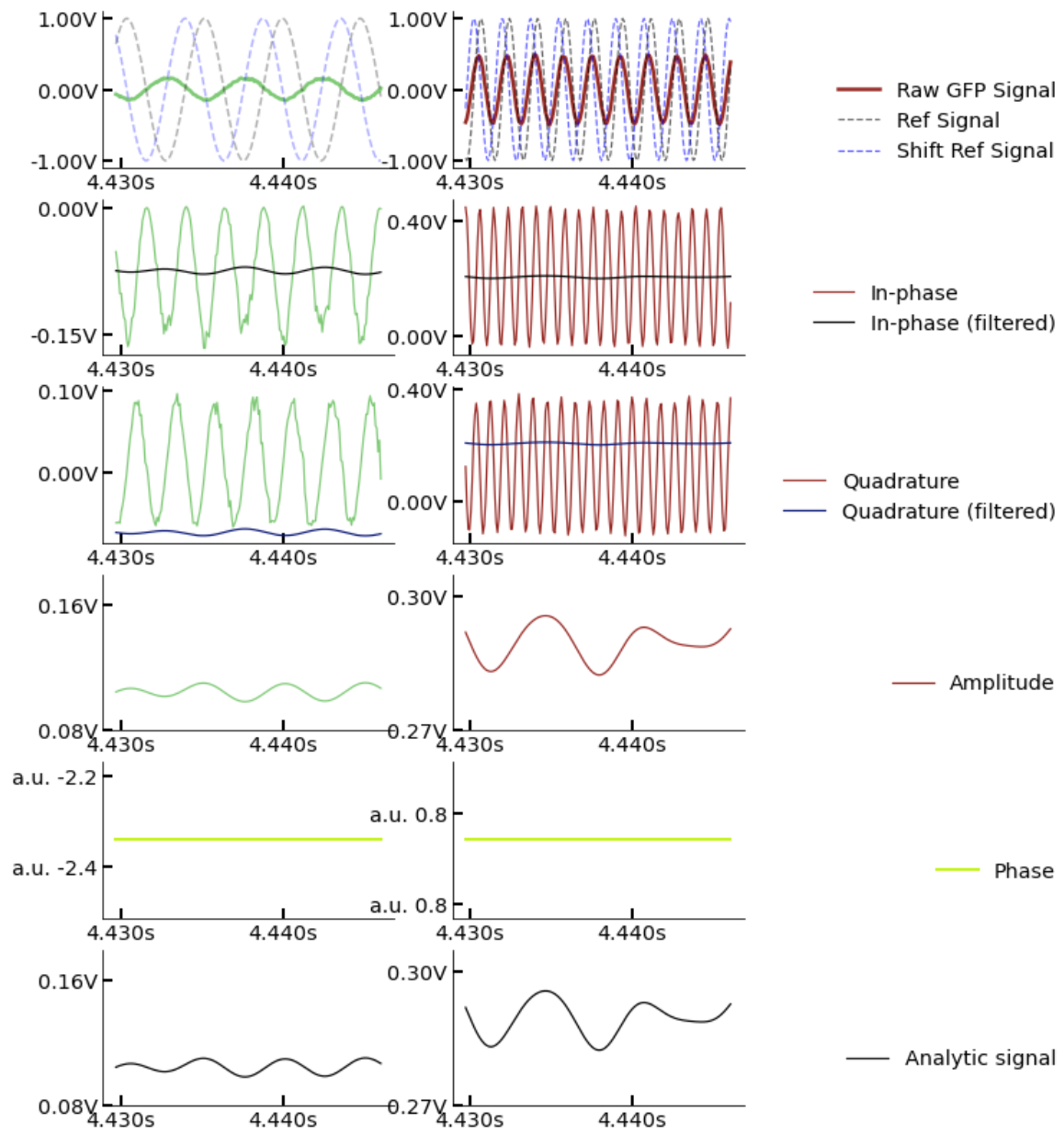


Figure 4.5. Demonstration of dual lock-in amplification, in which a reference signal is simulated and harnessed to dynamically compute the amplitude. First transformation centered the photodetector signal around zero by subtracting by a rolling mean window. Then a sine wave reference function (208.6Hz or 572.6Hz) was multiplied element-wise with the raw signal. An orthogonal cosine at the same frequency, called the quadrature, was also multiplied separately.

These sinusoids capture ‘in-phase’ and ‘quadrature’ components of the raw signal. Due to the multiplication of negative signs, the resulting frequencies of the product waves are effectively doubled. A low-pass filter is applied to reject these high frequency components, and the remaining signal indicates the amplitude of the original raw signal. In this case, the rolling mean window and filter window were 134ms and 110ms in width. The Euclidian norm of the two reference-times-raw product waves indicates amplitude of the original raw signal at the characteristic frequency. The phase of the wave is represented by arctangent of the quadrature over in-phase. Finally, the analytic signal is a multiplication of the amplitude by a complex representation of the phase: $\text{Amp} \cdot e^{j\text{phase}}$.

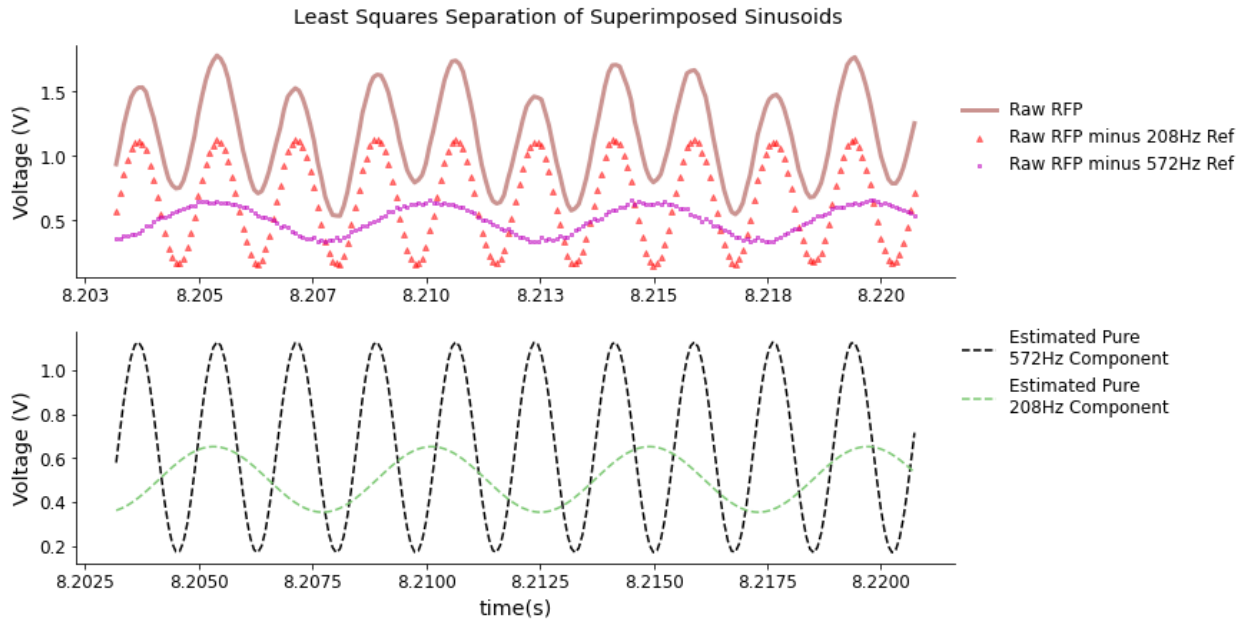


Figure 4.6. Least Squares optimization was effective for separating superimposed sinusoids and generating parameterized reference sinusoids. Raw RFP signal was a composite of two superimposed sinusoids, possibly due to residual autofluorescence. (Top) The raw RFP signal was modeled as a function of six parameters that simulated two distinct sinusoids of known frequency (208.616Hz, 572.205Hz), each with three trainable parameters: phase shift, amplitude, and DC-offset (mean Voltage).

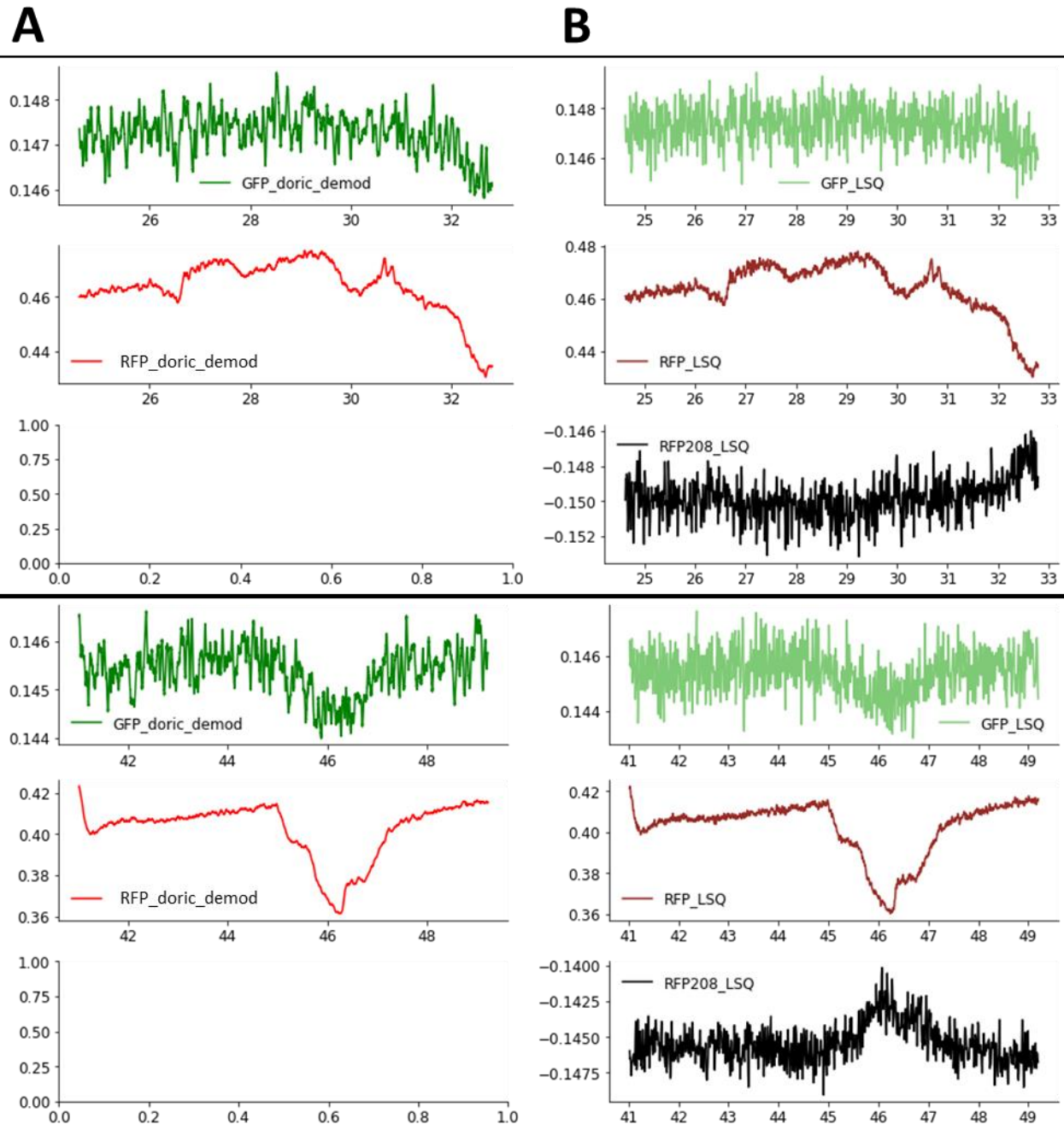
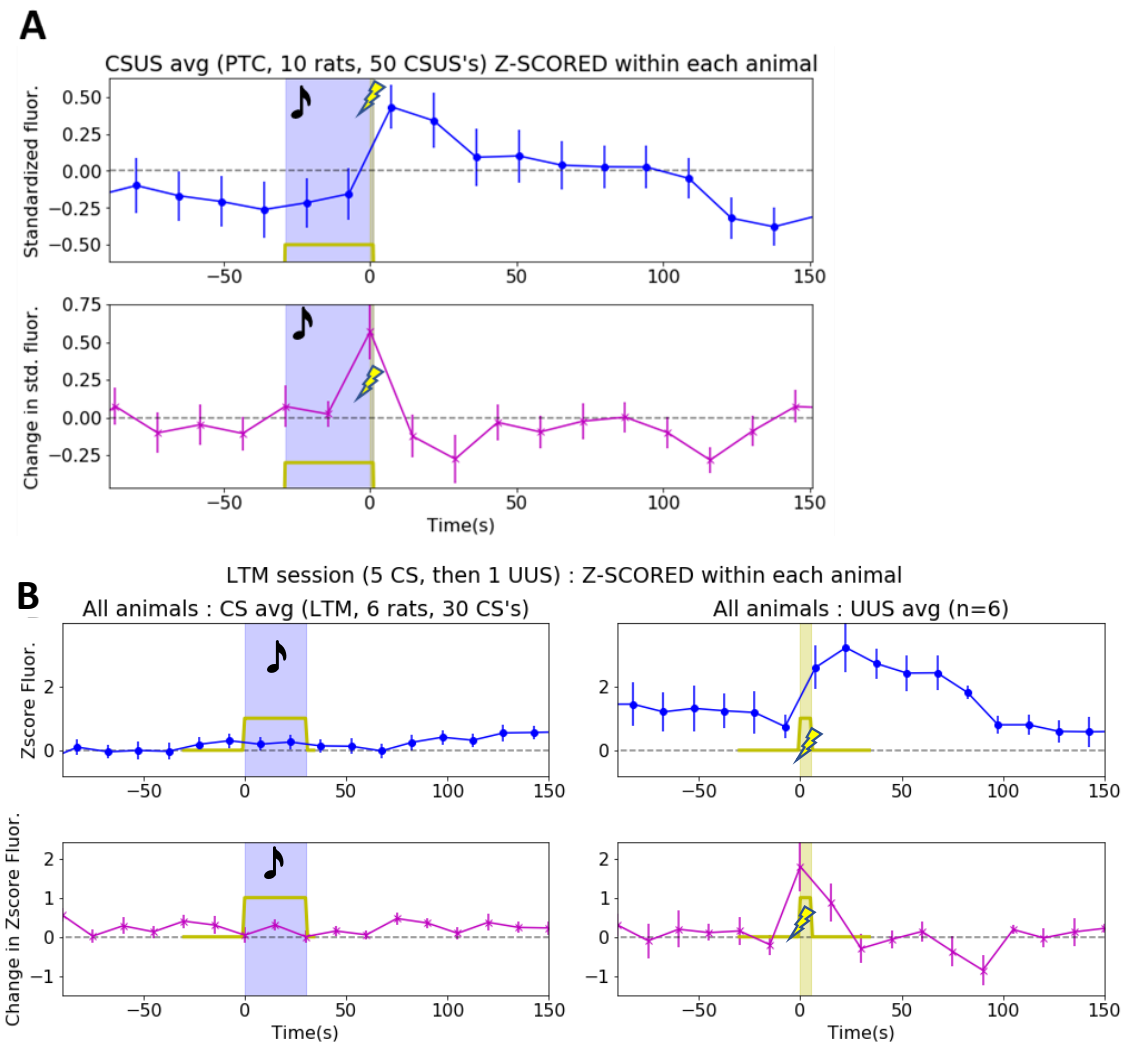


Figure 4.7. Examples of extracted amplitude signals, obtained by **(A)** Doric Lenses' built-in lock-in amplification algorithm, or **(B)** our least squares sinusoid fitting approach. The outputs appear to be virtually equivalent. However, we are free to adjust our approach to collect cross

contaminating signal (e.g. RFP208_LSQ in black) or shorter temporal windows.



*Figure 4.8. Preliminary analysis of sessions after only 3 weeks viral incubation. (A) Pavlovian Threat Conditioning session with 30-second tones as conditioned stimuli (CS) (blue shading) each co-terminated with a 1-second footshock unconditioned stimulus (US). These plots depict averaged signal from all trials from all animals (5 trials/rat * 10 rats). (Top line plot) AUC's from 'NE2h' channel are divided by the AUC's from the 'mCherry' control channel, then each value was Z-scored. (Bottom line plot) Z-scores of the differences between AUC values show a surge of putative norepinephrine release around the time of the footshock US. (B) Long-term memory test with first 6 rats. (Top) In the top two plots, blue circles represent 15-second segments, Z-*

scored. (Bottom) Purple stars represent changes between segments, Z-scored.

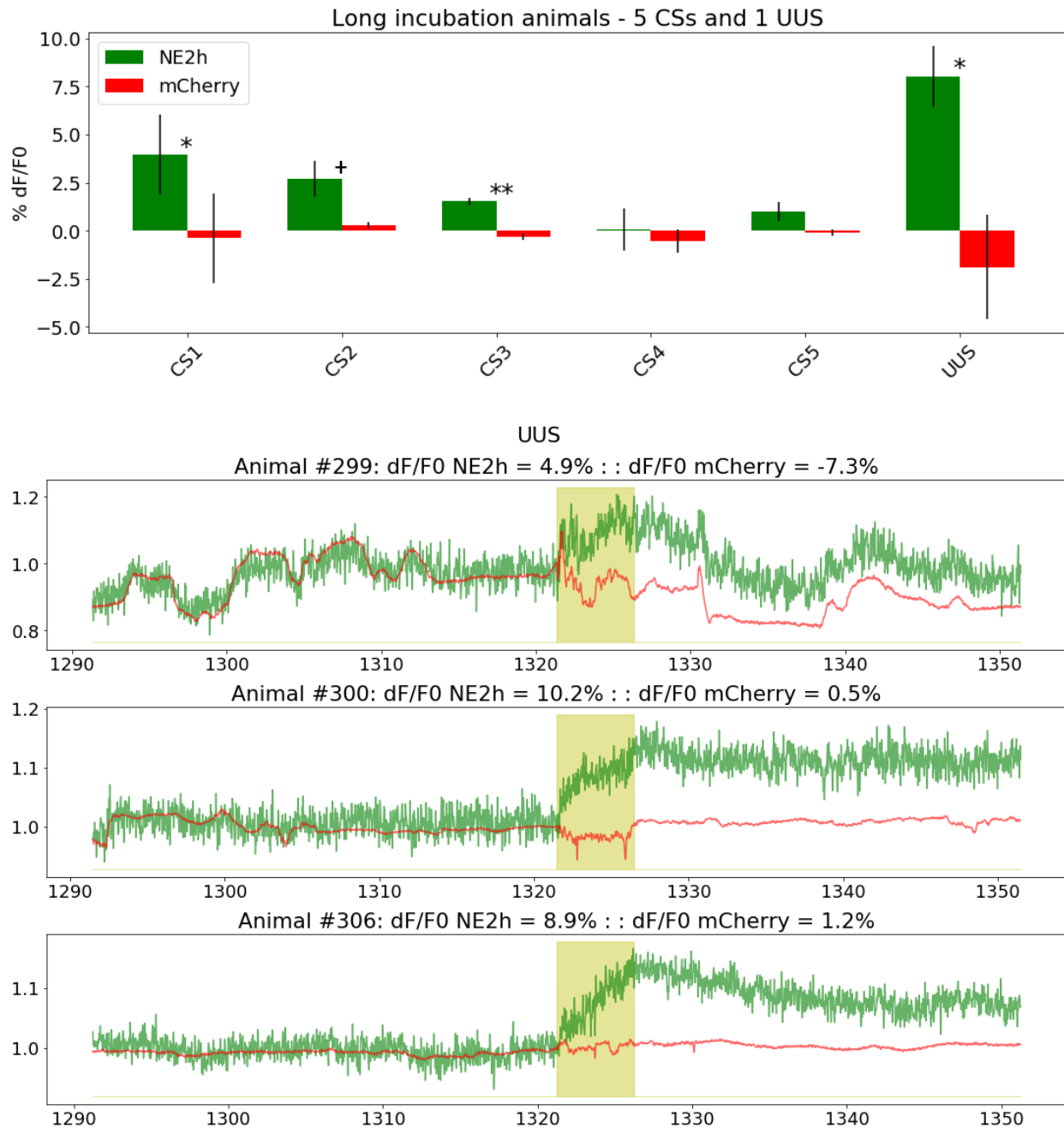


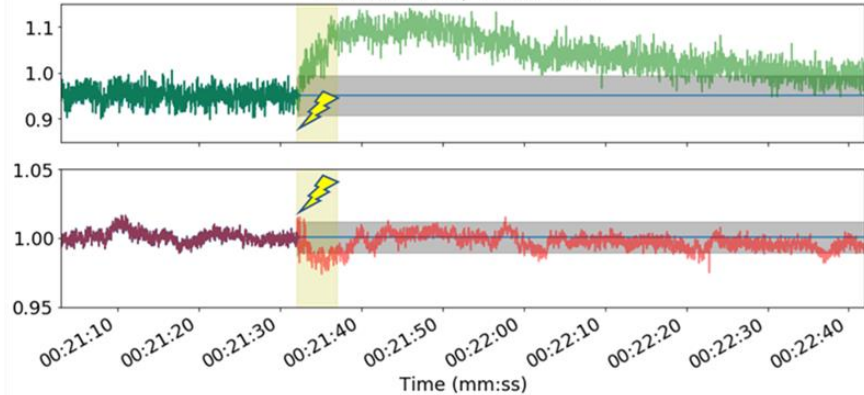
Figure 4.9. Demodulated data from UUS trial shows robust NE2h response. (top) Change in mean signal for NE2h (green) channel and mCherry (red) channel from the 30 seconds before stimulus onset to the 30 seconds after stimulus onset. The UUS trial triggered a response on the NE2h channel that was significantly different from the mCherry control channel. CS1-3 trials

also generated NE2h responses that were significantly or marginally significantly different from the mCherry control channel. (bottom 3) Representative traces to demonstrate the nature of relationship between NE2h channel (green) and mCherry channel (red thin line). Top plot (Animal #299) is a particularly good example of mCherry being a useful control for motion. While these channels are generally correlated to each other, they diverge markedly after onset of footshock (UUS; yellow shading), with NE2h consistently increasing relative to mCherry.

Paired t-tests: +p<0.10, *p<0.05, **p<0.01. (n=3)

Saline-treated rat

Footshock response compared to AR(2) forecast
Animal# 296, Trial# UUS1



Yohimbine-treated rat

Footshock response compared to AR(2) forecast
Animal# 295, Trial# UUS1

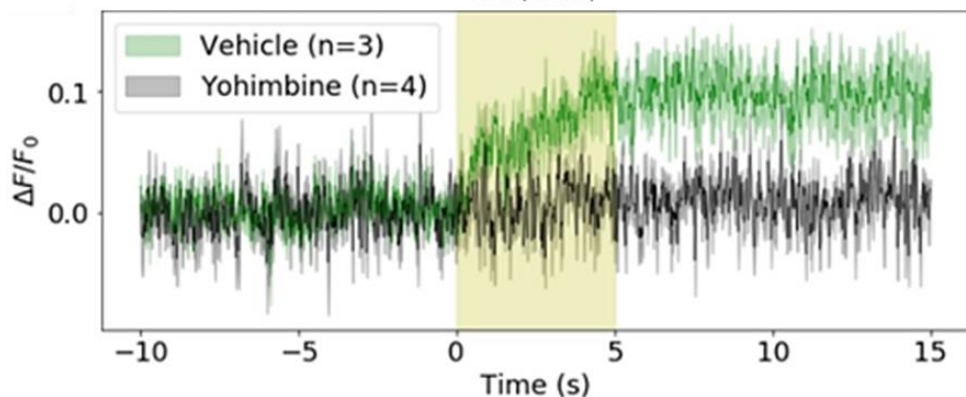
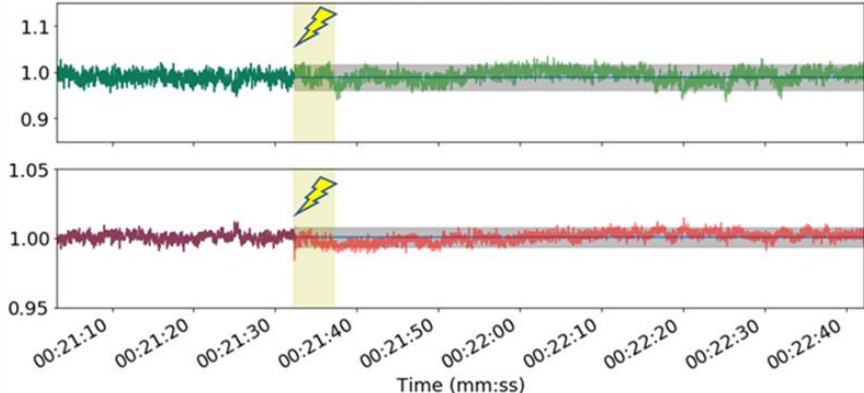


Figure 4.10. Representative recordings of Yohimbine- vs. Saline-treated animals. NE2h NE sensor channel (green) and mCherry control channel (red) before, during, and after unsignaled

unconditioned stimulus (UUS) (shaded yellow). An order=2 autoregressive model (AR(2)) was used with a 99% confidence interval to forecast the expected signal in absence of footshock. Saline-treated rats (top half of page) shows robust NE2h reaction to footshock, but rats treated with yohimbine to blockade NE2h do not show significant NE2h reaction.

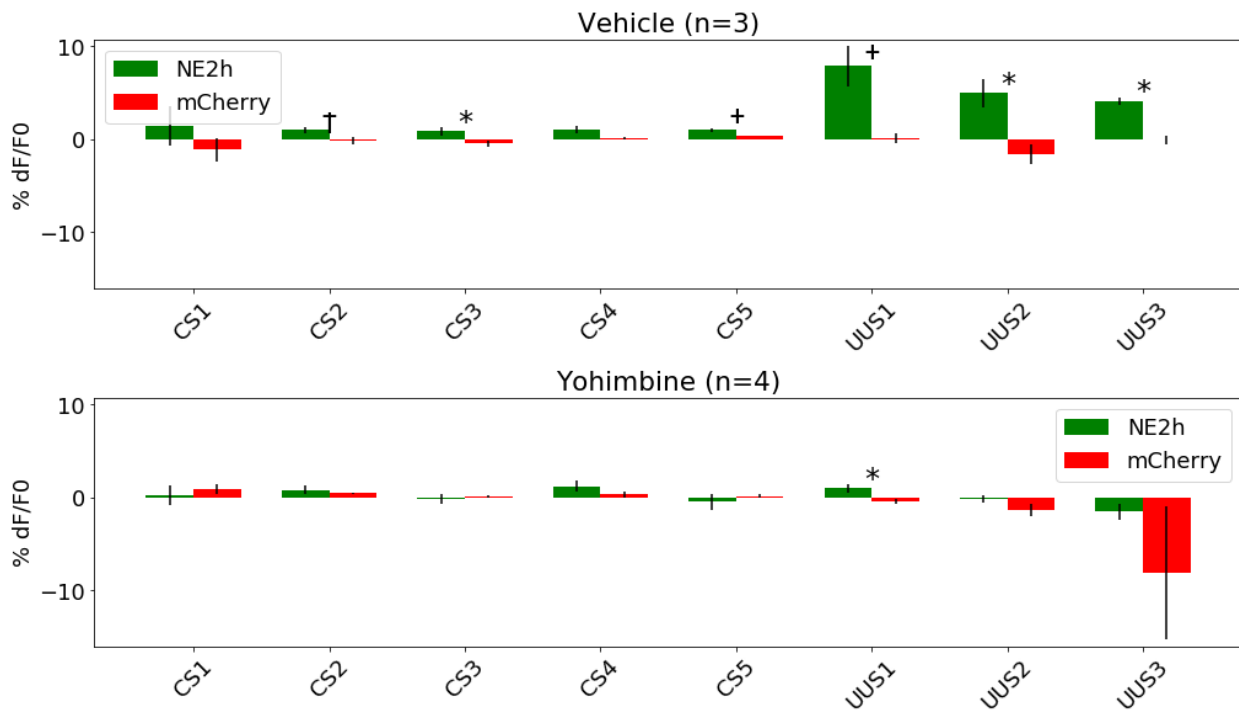


Figure 4.11. Yohimbine experiment comparison between channels within subjects. (top) In saline-treated rats, the NE2h channel increased more than the mCherry control channel during unsignaled footshocks (UUS) and some tone presentations (CS). (bottom) In yohimbine-treated rats, the NE2h channel only increased significantly more than mCherry during the first footshock.

+ $p<0.10$ * $p<0.05$

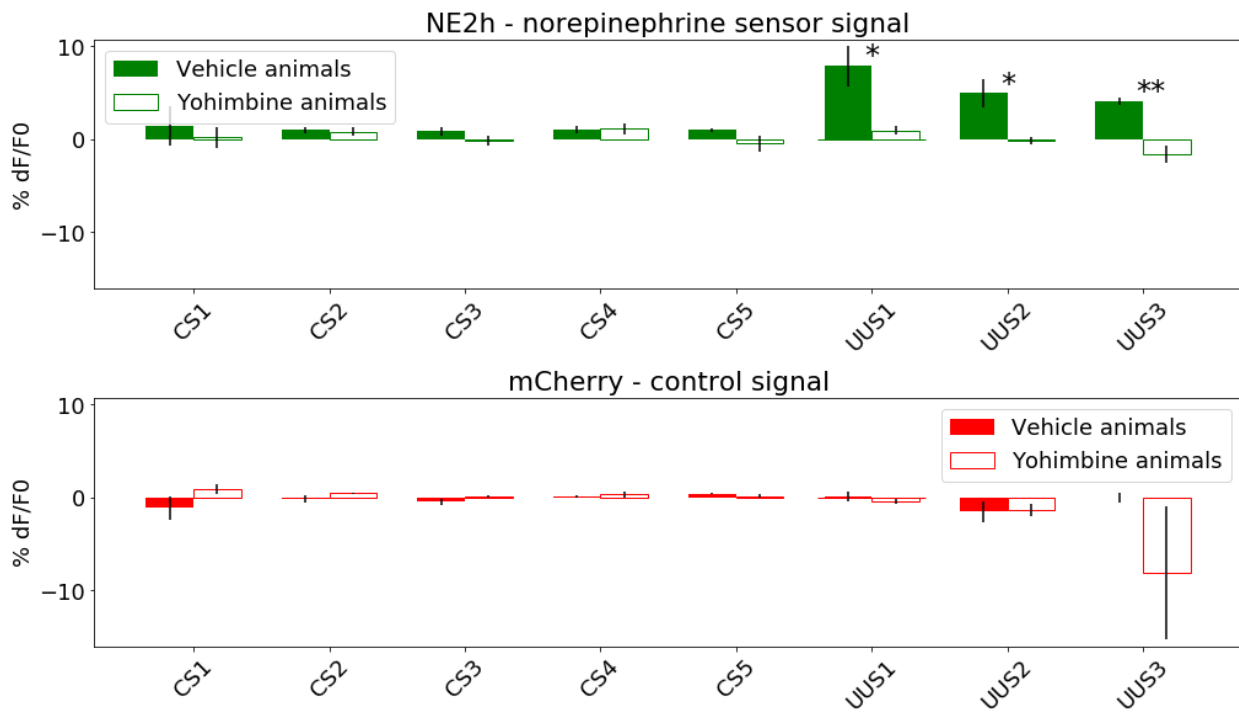


Figure 4.12. Yohimbine experiment comparison between treatments. (top) Footshock-evoked NE2h signal was blocked by yohimbine. (bottom) In contrast, mCherry control signal was unaffected.

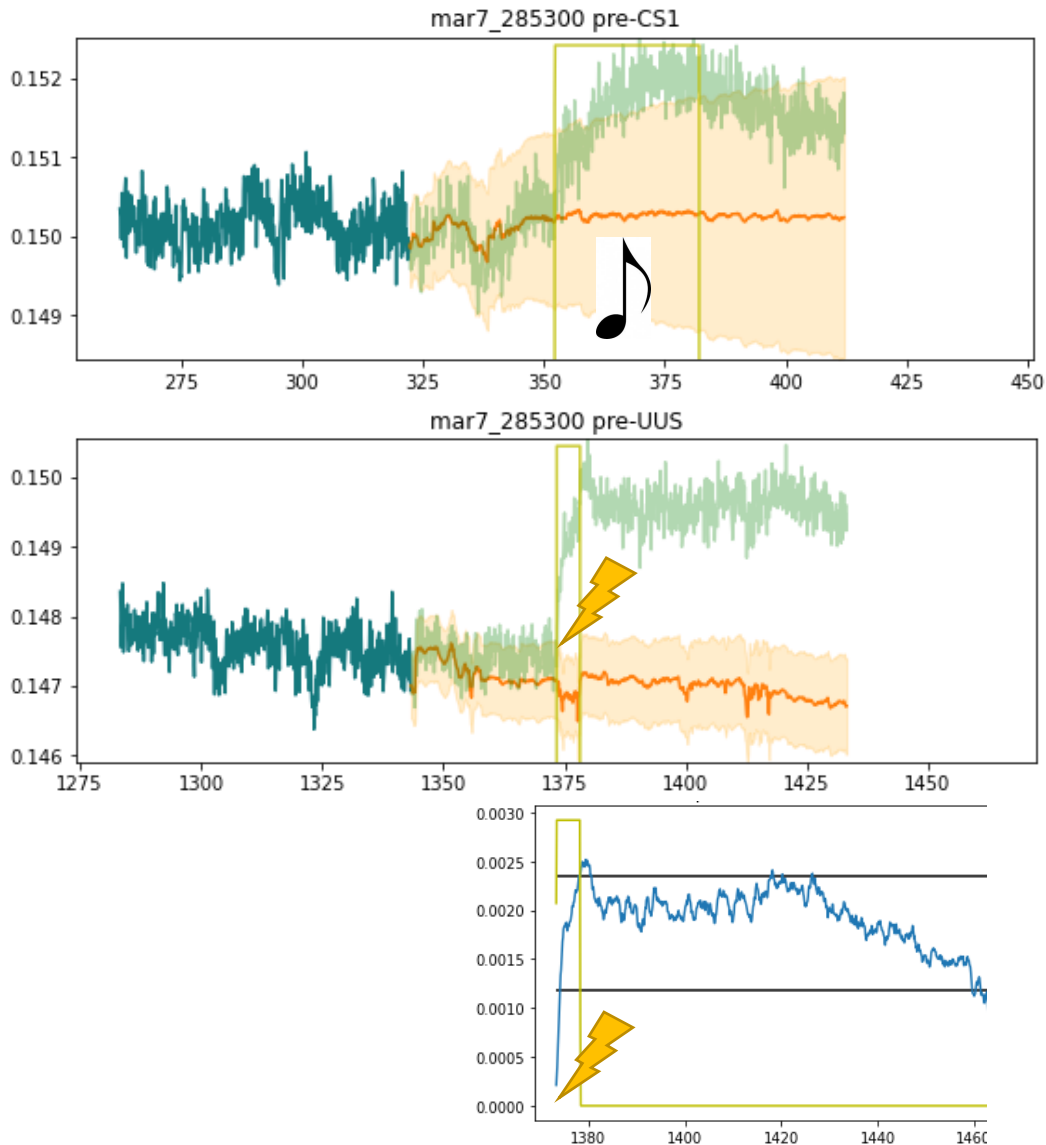


Figure 4.13. ARIMAX-model forecasted baseline (orange) with 95% confidence intervals plotted with the actual signal (green) during the first CS trial (top) and the U-US trial (middle). The difference between forecasted and actual signal was extracted as an NE estimate during U-US is shown in blue (bottom) with black horizontal lines illustrating peak height and half-height. These were recordings from the 3-month post-surgery LTM/U-US session.

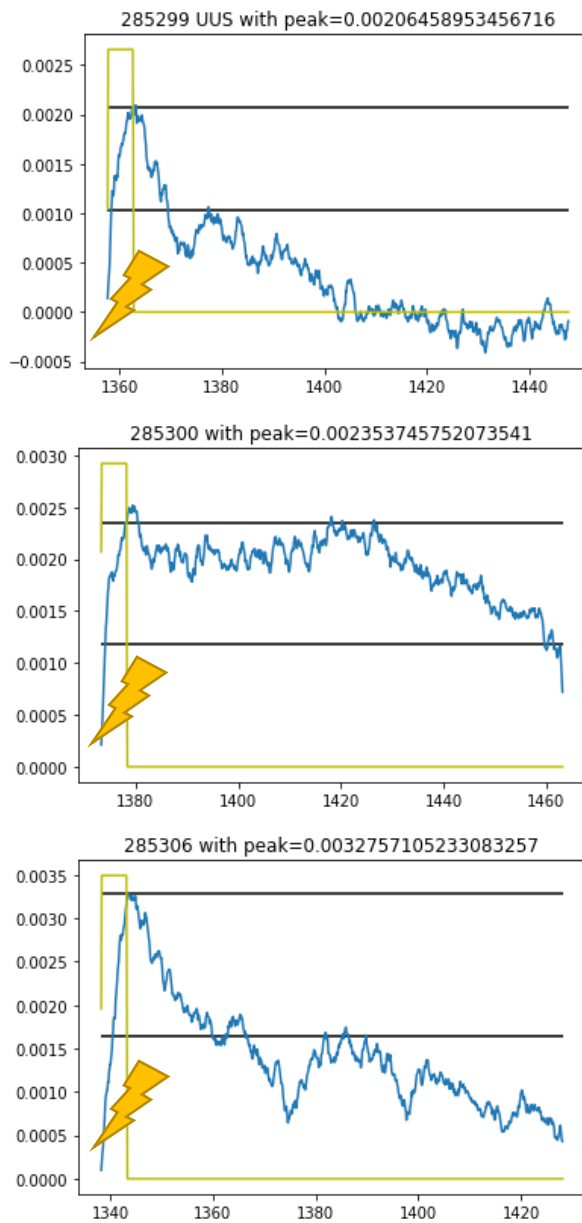
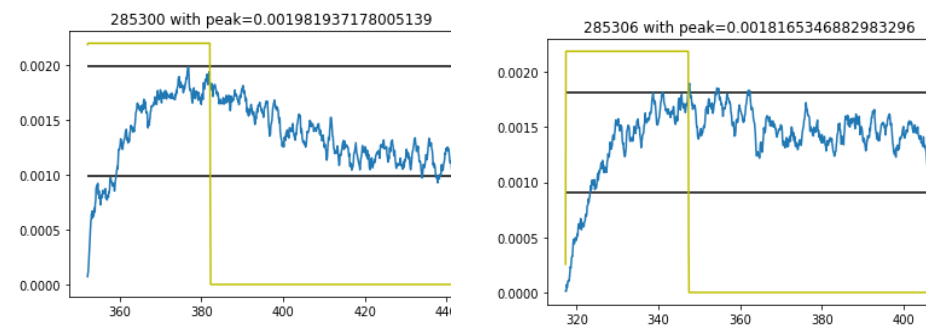


Figure 4.14. NE reactions to unsignaled footshocks. NE estimated signal during U-US is characterized by a steep, steady increase in NE during the entirety of the footshock, followed by a highly variable gradual decline after U-US offset. These were recordings from the 3-month post-surgery LTM/U-US session.

CS1
♩



CS5
♩

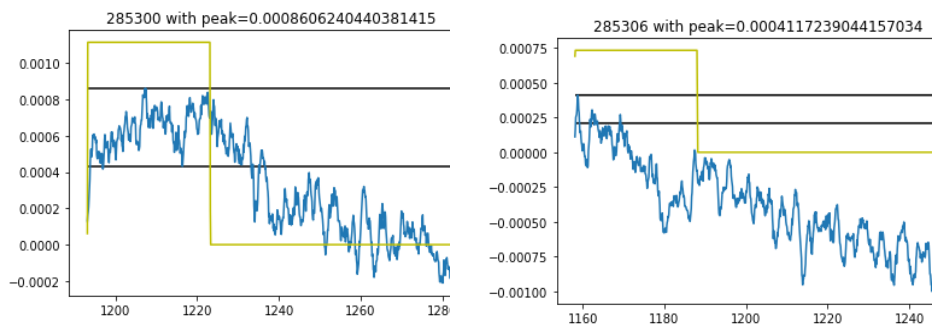


Figure 4.15. NE reactions to conditioned tones. NE responses appear to be much larger to first CS trials compared to later CS trials.

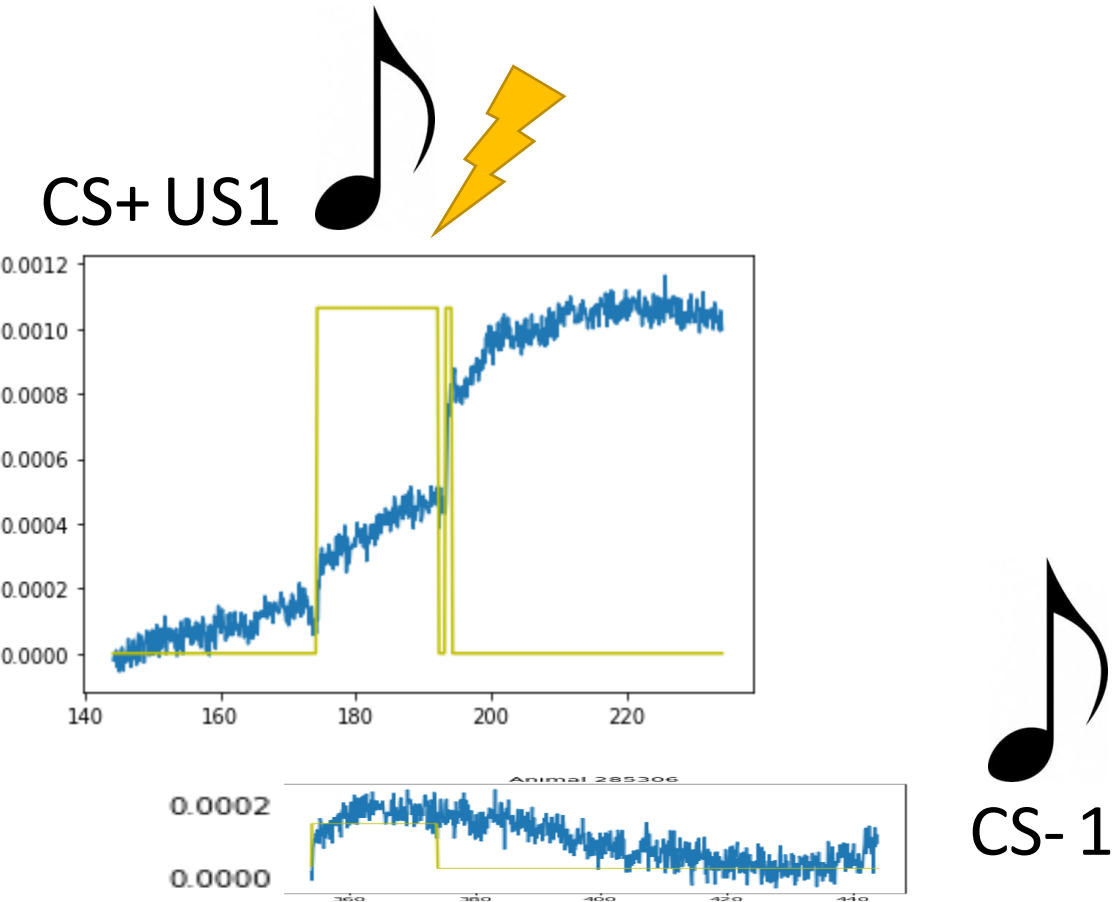


Figure 4.16. NE dynamics during discriminative PTC. NE appears to increase with the onset of a novel tone, then increases again during the paired footshock (top). NE signal to a novel tone not paired with footshock declines after the tone offset (bottom).

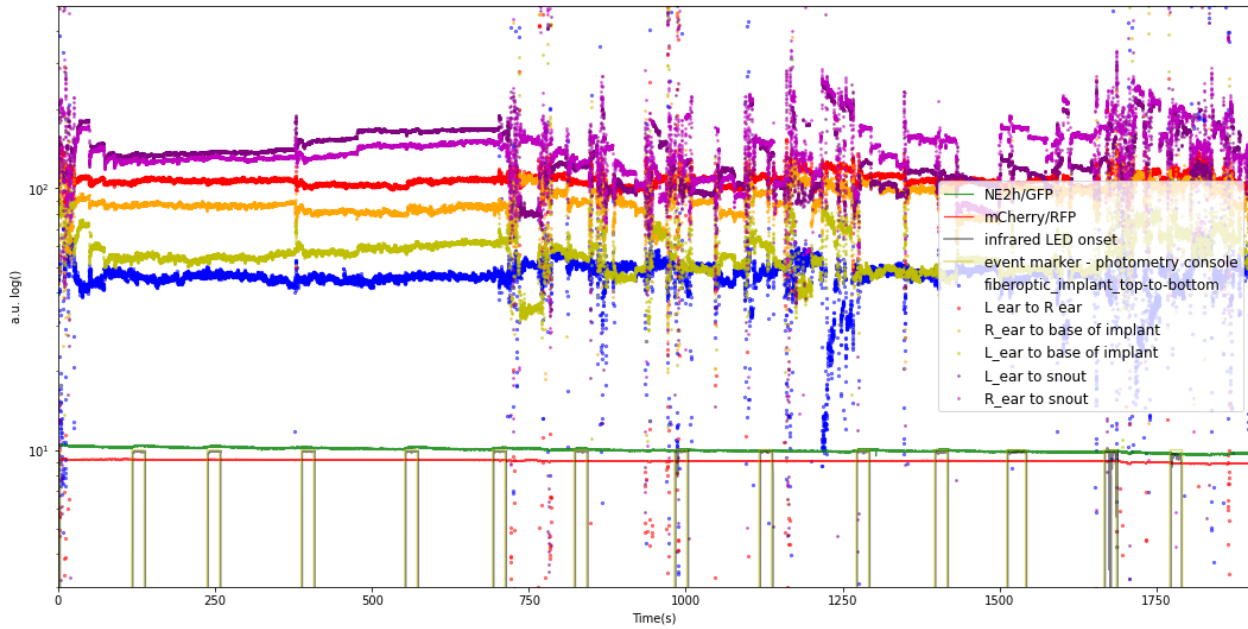


Figure 4.17. Output coordinates from DeepLabCut (DLC) are Bayesian-likelihood-weighted image coordinates that can be taken and entered into any kind of geometric transformation conditional on the Bayesian confidence of the automated scorer. The figure above shows a 30-minute fiber photometry session (thin green and red traces are photometry channels; yellow columns are Arduino-delivered time markers representing trials). DLC outputs represented in the figure include (in gray that overlaps the yellow columns) a Bayesian confidence that the cage's infrared LED is on, acting as the Arduino's time marker to the video dataset. The 6 brightly colored scatterplot sets represent the Euclidian distance (in pixels) between pairs of head points on the animal. Some behaviors can be interpreted simply by viewing this time series projection: After a brief period of activity upon entering the cage, the animal is mostly still by the first trial. The onset of the third trial triggers an orienting response, but the animal is otherwise mostly motionless until the fifth trial, then alternates between movement and stillness for the duration of the session.

Location in Conditioning Context over 35 minutes.

DeepLabCut estimated anatomical locations.

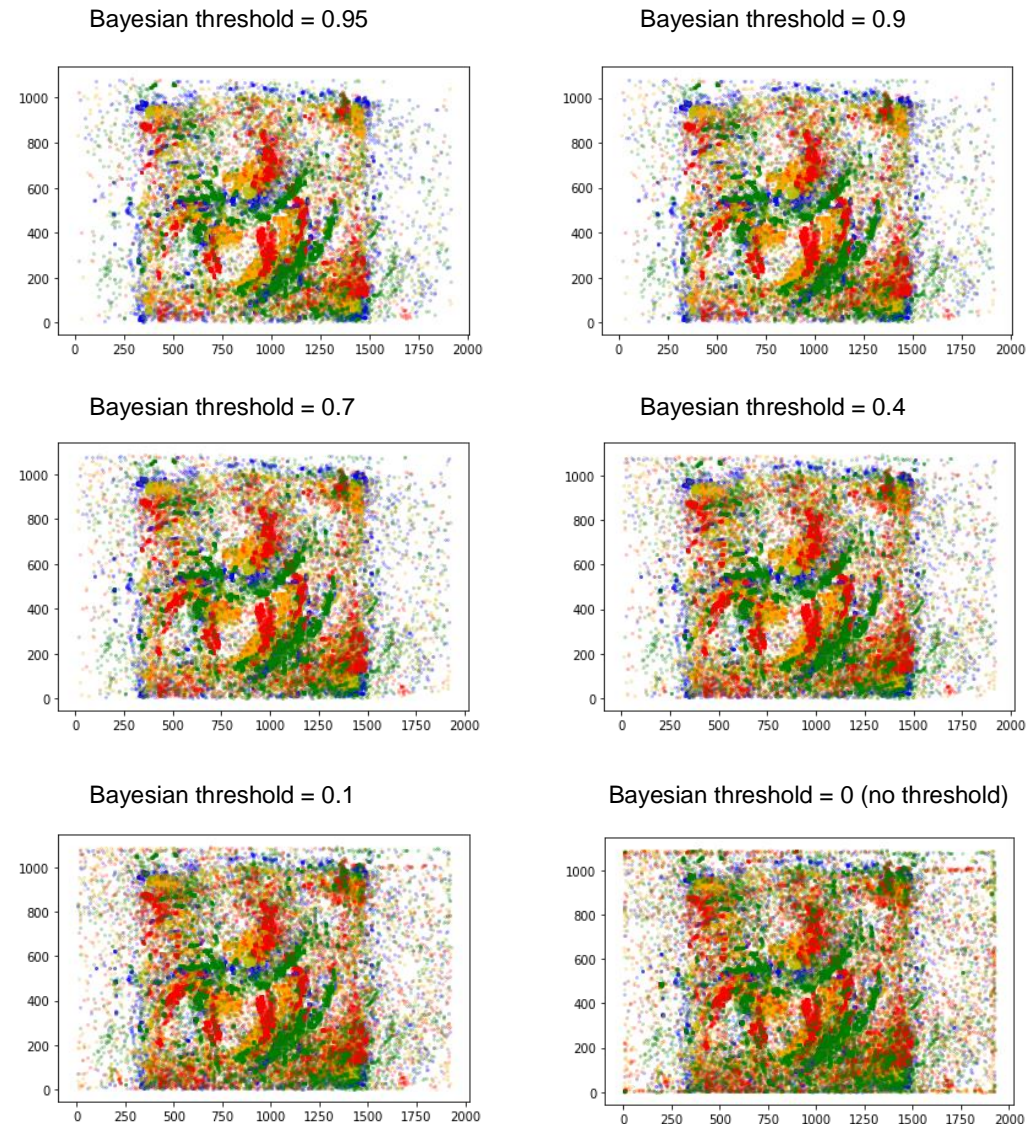


Figure 4.18. Estimated position of a single animal's head points in a 1080p resolution video of the conditioning context, summed over the entirety of the recording session. Bayesian threshold can be adjusted to control risk of reporting inaccurate positions.

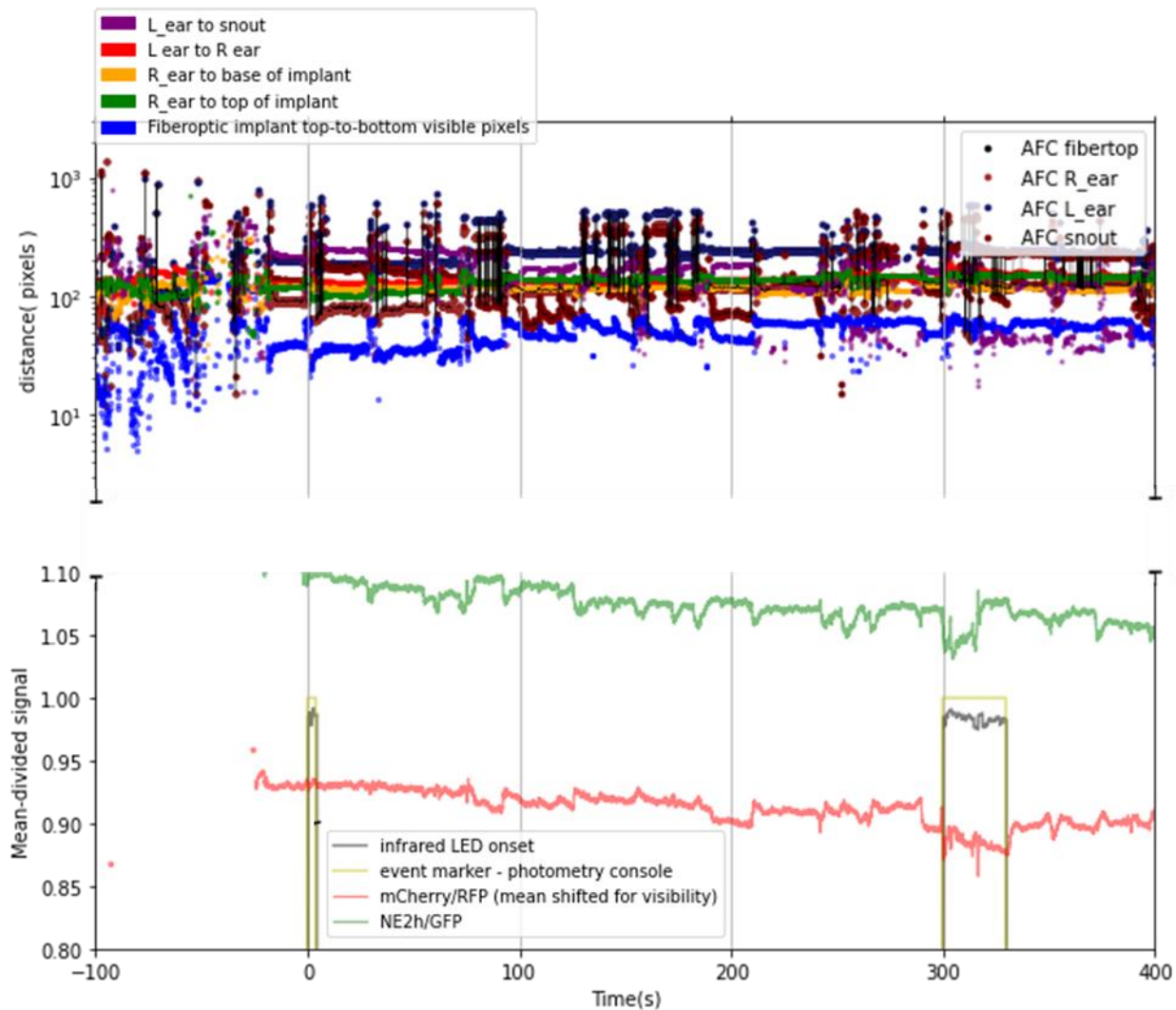


Figure 4.19. Correcting for asymmetric artifacts through identification of novel exogenous variables. The most dangerous artifacts for unsuspecting researchers are those that affect control data differently than the way they affect experimental data. The anticorrelated disturbances in the photometry channels in the lower portion of this figure were mysterious in origin until recently and threatened to undermine much of this research program. Their co-occurring companion, as can be seen by comparing the top portion of this figure, is the horizontal movement of a semi-flexible/semi-rigid section of the fiberoptic patch cord (denoted

'Above Fiber Connector' AFC in the legend). Precisely speaking, the variable plotted at the top is the Euclidian distance (in 2-dimensional image space) between AFC and various spots on the animal's head (snout, left ear, right ear, or the point of fiber connection with the animal's implant). The rapid changes in AFC's position relative to the head seem to drive the artifact that affects the photometry channels asymmetrically.

The movement of AFC is an ideal force meter for measuring horizontal pull under the domain that obeys Hooke's Law regarding spring-like dynamics (where displacement is directly proportional to force). It can be measured and plotted alongside photometry signals by taking advantage of computer vision techniques, which in our case was DeepLabCut's implementation of deep convolutional neural networks for visual feature recognition (Mathis et al., 2018; Nath et al., 2019). It would not be surprising if an equation related to Hooke's Law could be used to eliminate this class of artifact.

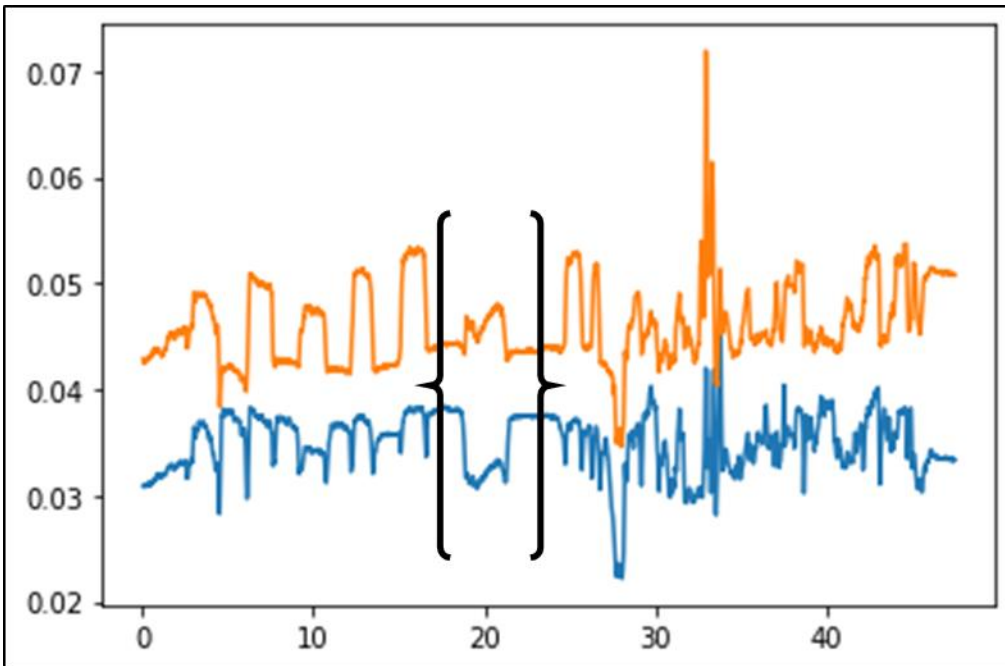
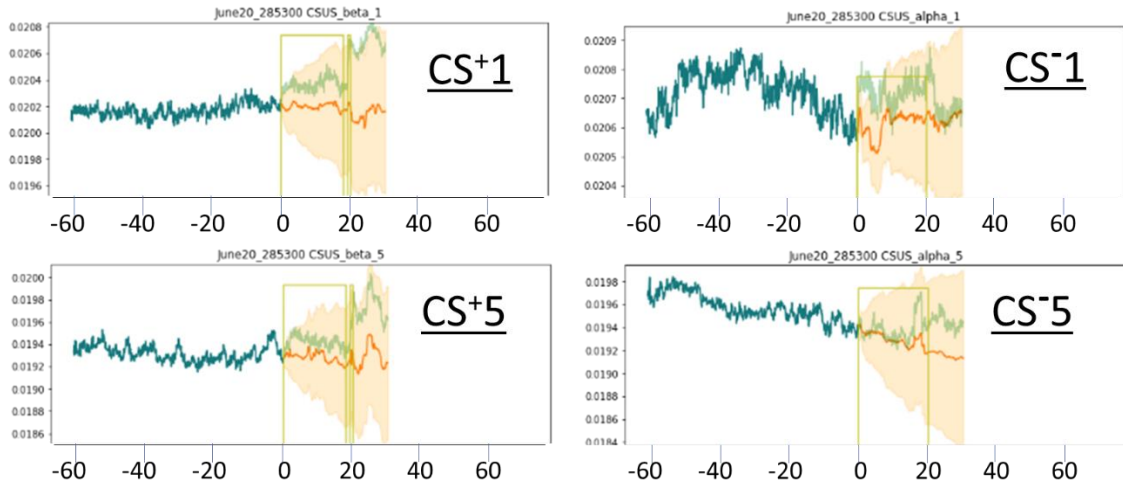


Figure 4.20. Manually generated anticorrelated artifact by holding the tip of a non-implanted fiberoptic cannula between fingers with loose latex gloves while pulling horizontally on the patch cord with the other hand, simulating the condition of an animal pulling on a patch cord that either has been caught on something at a shallow angle or an animal tilting its head forward and pulling down , or pushing the implant into a wall of the cage. Note that it is not easy to manually generate this artifact, as this ~50 second recording shown above only has one clearly anticorrelated segment. A fiber tip facing an orthogonal surface such as a palm of a hand will not generate such an artifact.

Discriminative PTC dorsal LA recording



Discriminative PTC Temporal cortex and basal amygdala

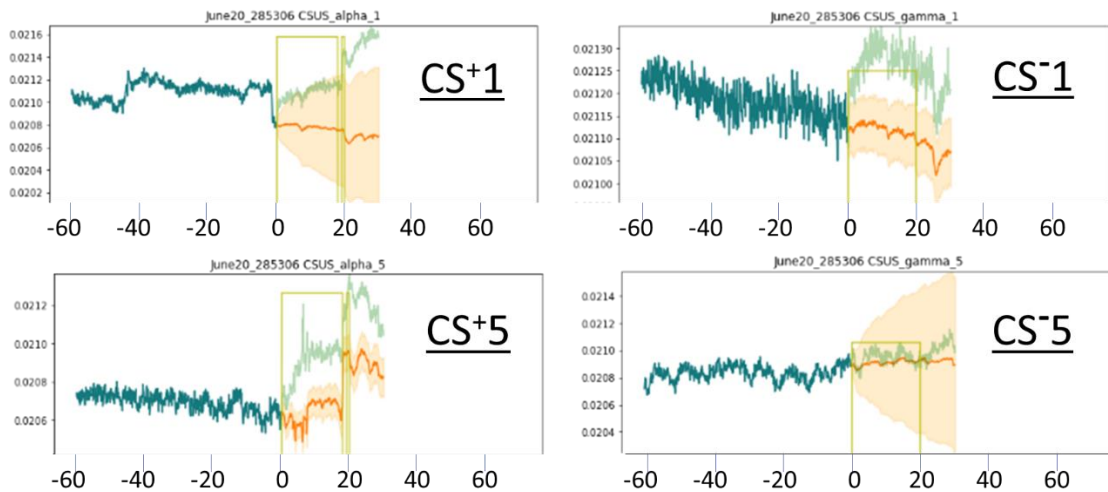
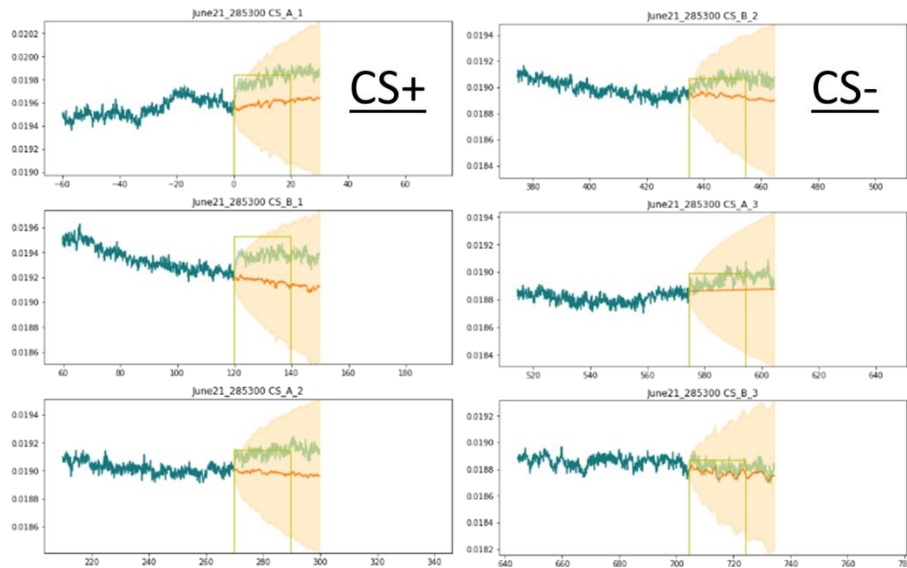


Figure 4.21. Discriminative PTC reveals conditioned-arousal-like effects in the dynamics of NE responses to tone over trials. NE reactions are robust to the first presentations of

two novel tones (2kHz or 10kHz, randomly assigned to CS⁺ or CS⁻), but by the fifth presentation of each tone, only the conditioned tone (CS⁺⁵) produces a robust NE response at tone onset.

Discriminative LTM dorsal LA recording



Discriminative LTM Temporal CTX & Basal Amygdala

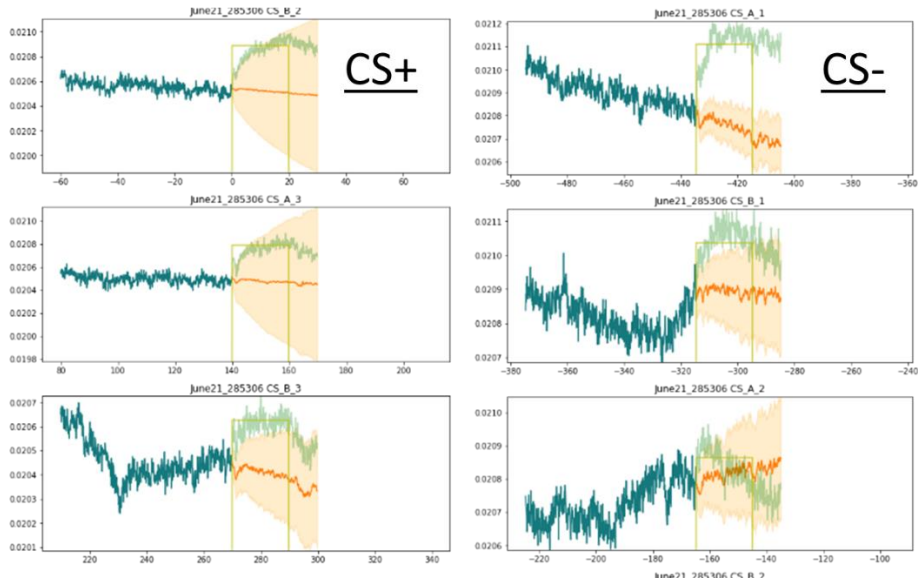


Figure 4.22. Discriminative LTM shows a continuation of conditioned-arousal-like effects. (left) NE reactions remain robust to the conditioned tone (CS⁺) over 3 trials, but (right) NE responses to the neutral tone habituate by the end of 3 trials.

APPENDIX B

Microscope Images for Fiber Photometry Animals
Expression Check for NE2h (with anti-GFP antibody)
and mCherry (native signal)

Table B.1

Summary of anatomical locations targeted by fiberoptic cannulas and viral expression.

| ID | Peak expression location | Approximate fiber tip location | Anatomical Group Assignment | Side (L/R) | Viral incubation time (Weeks after surgery) |
|--------|---|--------------------------------|-----------------------------|------------|---|
| 285295 | CeA | CeM | CeA animal | L | 30 |
| 285296 | CeA | CeM | CeA animal | L | 29 |
| 285298 | Anterior from CeA (and dorsomedial of internal capsule) | Anterior from CeA | CONTROL (OUTSIDE AMYG) | L | 30 |
| 285299 | LA (plus somata dorsal of CeA) | LAI | LA(l) animal | R | 16 |
| 285300 | LA | ~50µm above LAd | LA(d) animal | L | 30 |
| 285301 | LA | LAI | LA(l) animal | R | 16 |
| 285305 | LA & CeA | LAa | Anterior LA | R | 30 |
| 285306 | LA | LAI | LA(l) | L | 30 |

Abbreviations: Lateral Amygdala (LA), dorsal part of Lateral Amygdala (LAd), lateral edge of LA (LAI), anterior tip of LA (LAa), Central Amygdala (CeA), medial part of Central Amygdala (CeM)

N LA = 5, N CeA = 2, N Outside Amyg = 1

#95
CeA

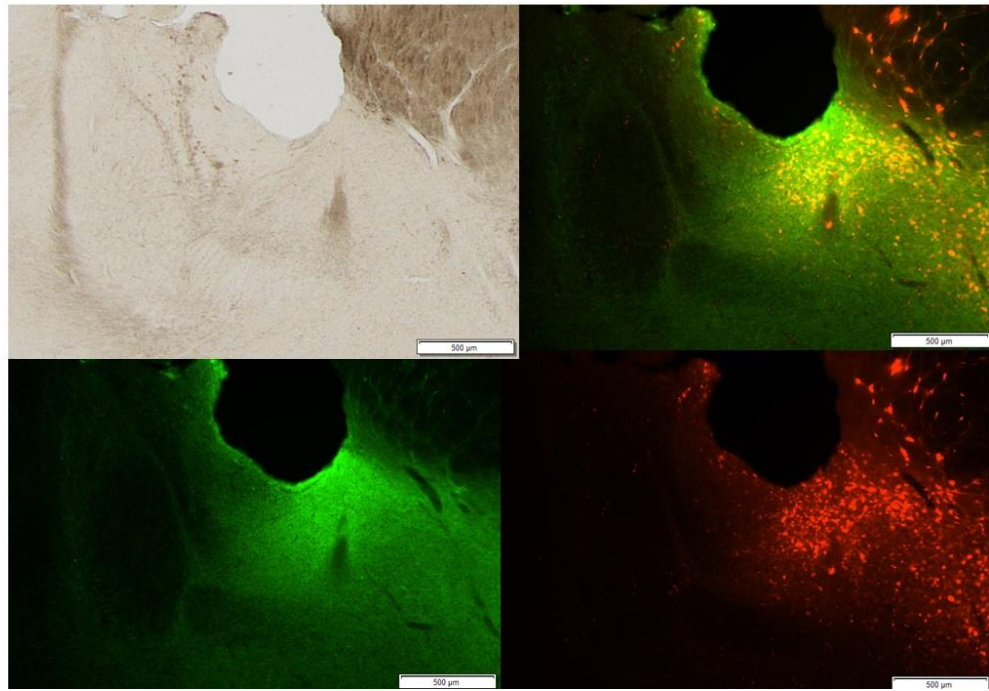


Figure B.1. Histological samples from animal #95. Targeted location is medial part of CeA. Brightfield image (upper left) shows gap in tissue where fiberoptic cannula was located. NE2h (lower left), mCherry (lower right), and merged (upper right) reveals fluorophore expression near the tip of the fiberoptic cannula.

#96
CeA

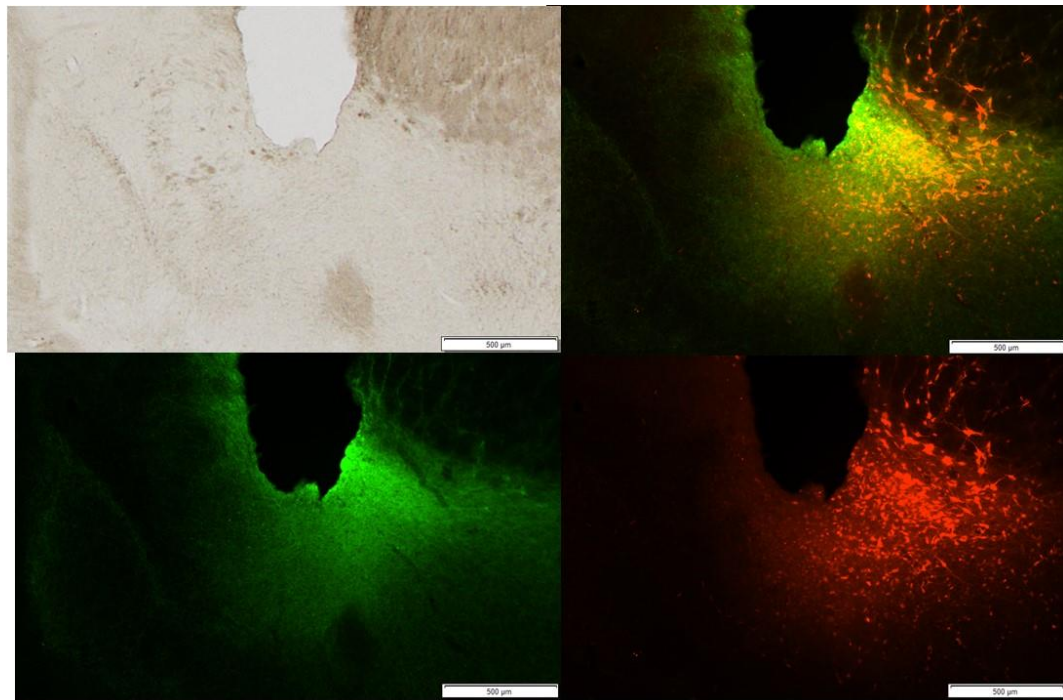


Figure B.2. Histological samples from animal #96. Targeted location is near the medial edge of CeA. Brightfield image (upper left) shows gap in tissue where fiberoptic cannula was located. NE2h (lower left), mCherry (lower right), and merged (upper right) reveals fluorophore expression near the tip of the fiberoptic cannula.

#98
Outside
Amyg
(too
anterior)

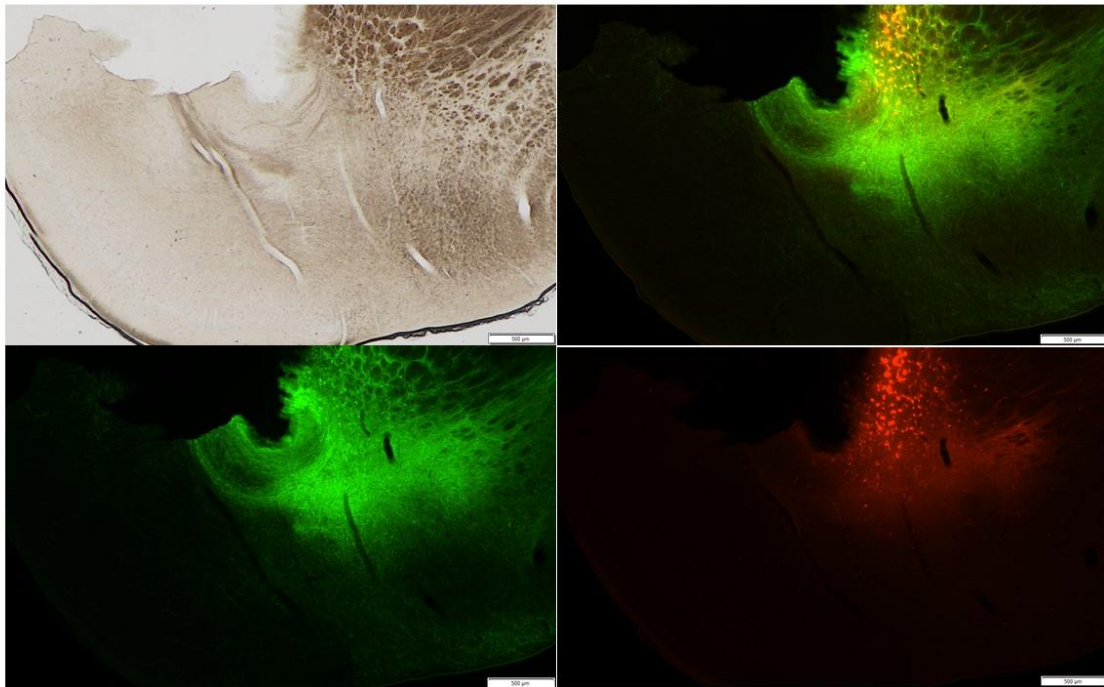


Figure B.3. Histological samples from animal #98. Targeted location is in or near anterior aspect of CeA. Brightfield image (upper left) shows gap in tissue where fiberoptic cannula was located. NE2h (lower left), mCherry (lower right), and merged (upper right) reveals fluorophore expression near the tip of the fiberoptic cannula.

#99
LA
(lateral
edge)

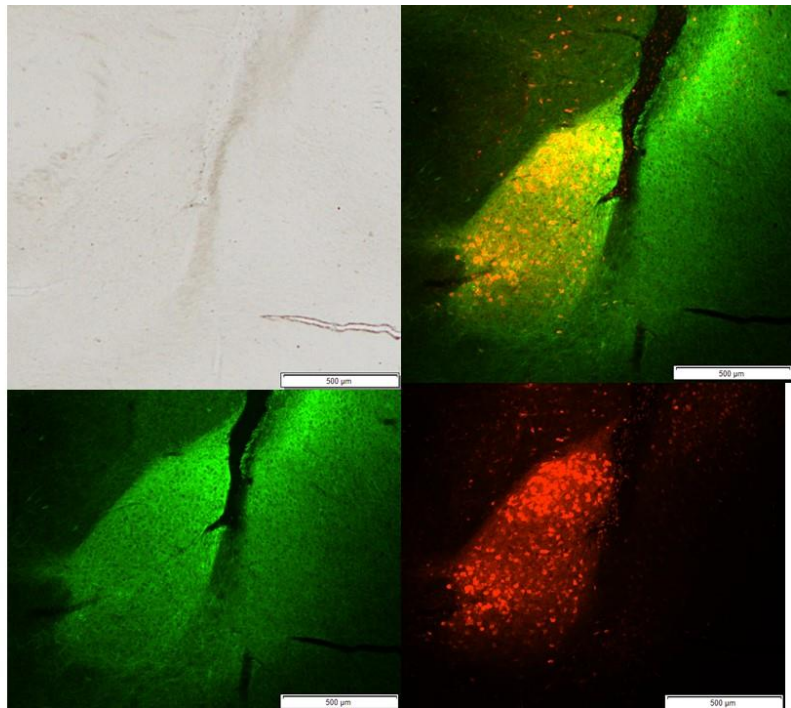


Figure B.4. Histological samples from animal #99. Targeted location is lateral aspect of LA. Brightfield image (upper left) shows track mark in tissue where fiberoptic cannula was located. NE2h (lower left), mCherry (lower right), and merged (upper right) reveals fluorophore expression near the tip of the fiberoptic cannula.

#00
LA
(50 μ m
above
LAd)

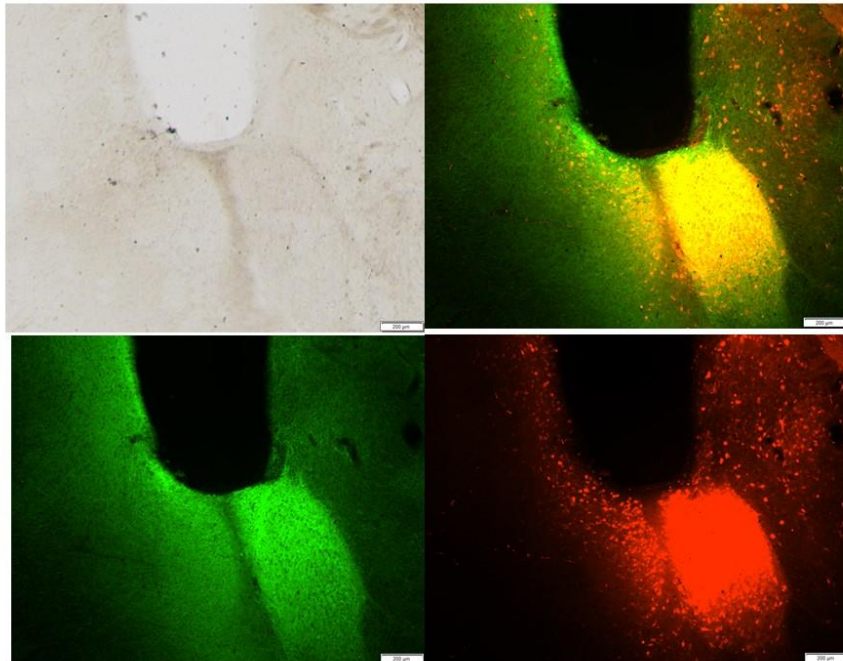


Figure B.5. Histological samples from animal #00. Targeted location is dorsal tip of LA. Brightfield image (upper left) shows gap in tissue where fiberoptic cannula was located. NE2h (lower left), mCherry (lower right), and merged (upper right) reveals fluorophore expression near the tip of the fiberoptic cannula.

#01
LA
(lateral
edge)

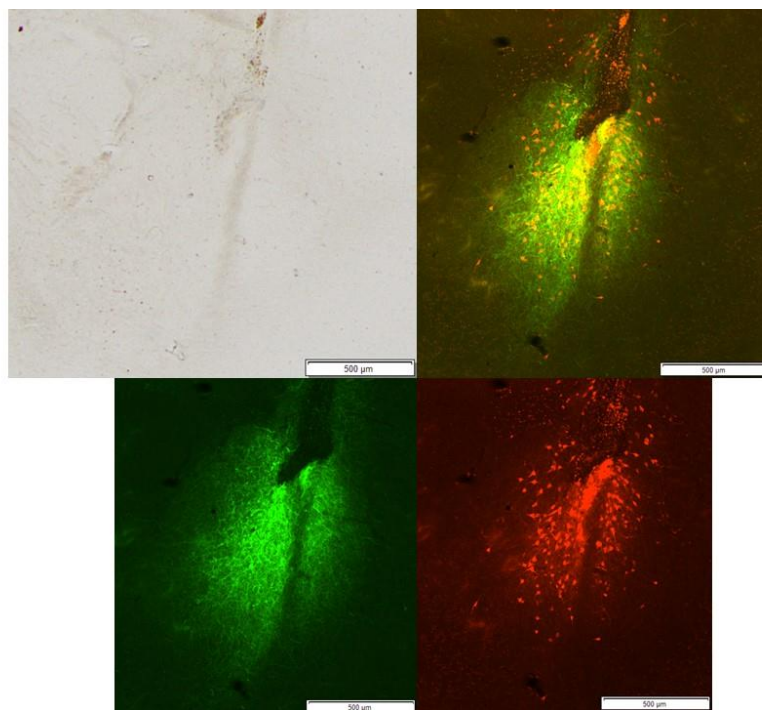


Figure B.6. Histological samples from animal #01. Targeted location is lateral aspect of LA. Brightfield image (upper left) shows track mark in tissue where fiberoptic cannula was located. NE2h (lower left), mCherry (lower right), and merged (upper right) reveals fluorophore expression near the tip of the fiberoptic cannula.

#05
anterior
tip of
LA

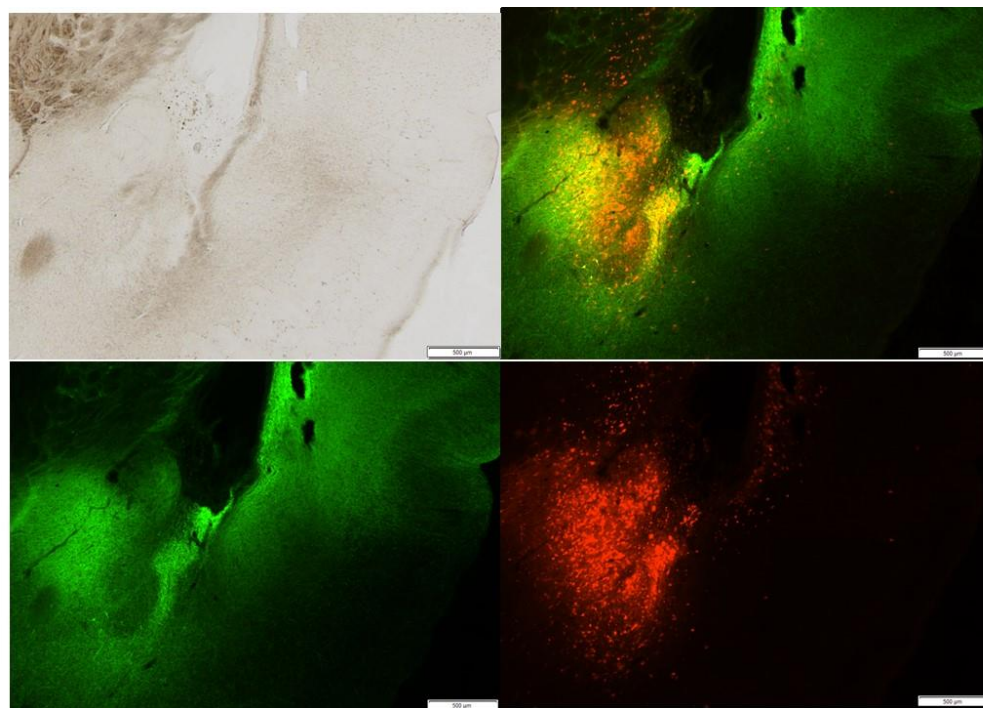


Figure B.7. Histological samples from animal #05. Targeted location is anterior aspect of LA. Brightfield image (upper left) shows gap and track mark in tissue where fiberoptic cannula was located. NE2h (lower left), mCherry (lower right), and merged (upper right) reveals fluorophore expression near the tip of the fiberoptic cannula.

#06
LA
(lateral
edge)

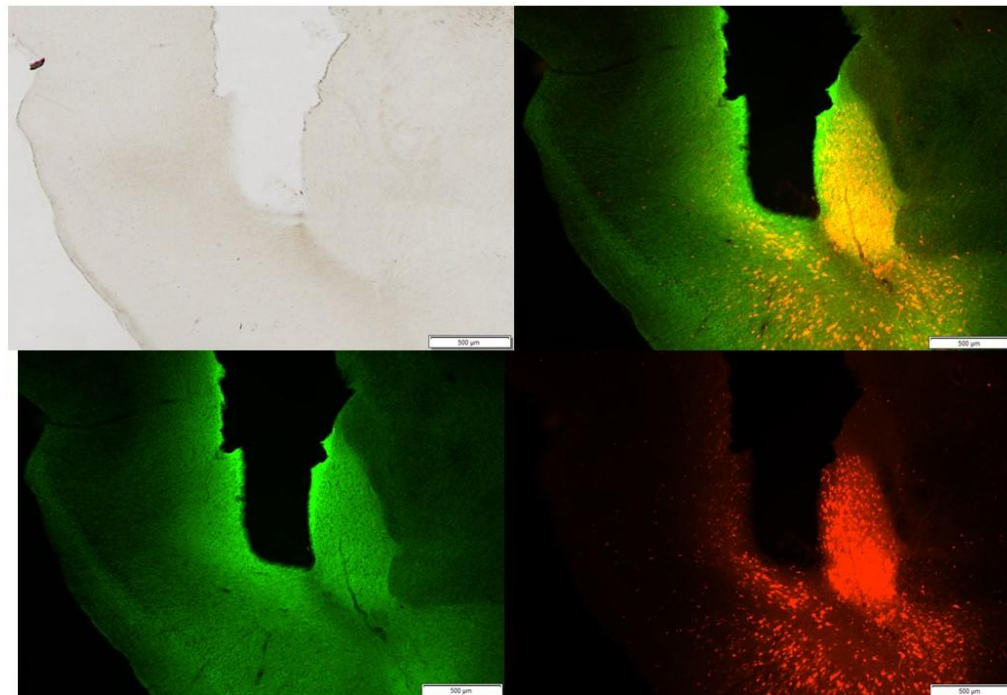


Figure B.8. Histological samples from animal #06. Targeted location is lateral edge of LA and BA. Brightfield image (upper left) shows gap in tissue where fiberoptic cannula was located. NE2h (lower left), mCherry (lower right), and merged (upper right) reveals fluorophore expression near the tip of the fiberoptic cannula.

APPENDIX C

Additional Works

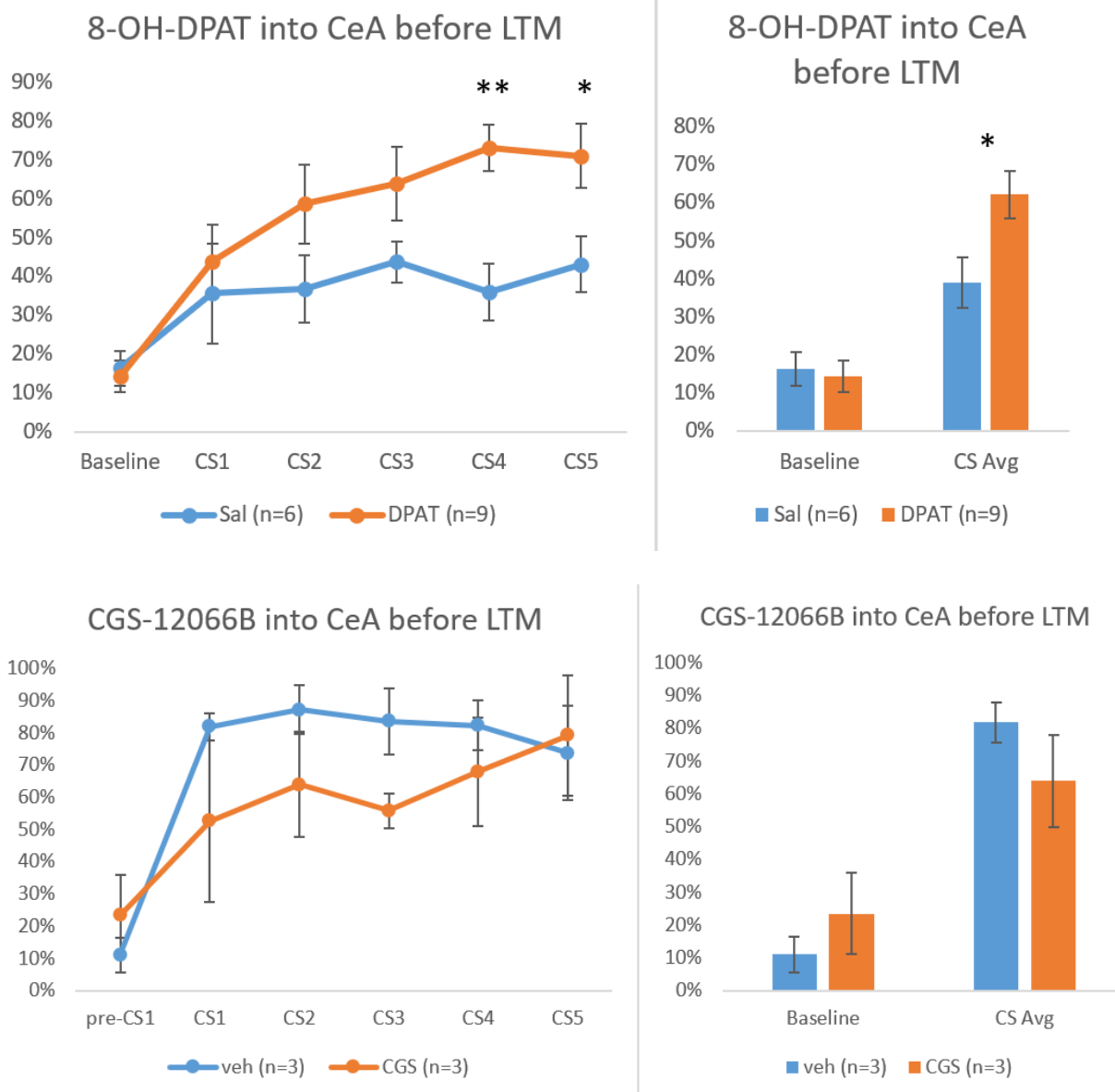


Figure C.1. Serotonergic 1A/1B agonism in CeA modulates conditioned freezing. Before a long-term memory (LTM) session, serotonin 1A and 1B receptors in central amygdala (CeA) were activated with agonists 8-hydroxy-DPAT and CGS-12066B, respectively. Freezing to conditioned tones (CS) in long-term memory test was significantly greater for animals infused intra-CeA with 8-hydroxy-DPAT animals than vehicle-treated animals. This was mainly due to the later trials, suggesting a delayed effect. This may be related to stimulus salience.

REFERENCES

- Abrari, K., Rashidy-Pour, A., Semnanian, S., & Fathollahi, Y. (2008). Administration of corticosterone after memory reactivation disrupts subsequent retrieval of a contextual conditioned fear memory: Dependence upon training intensity. *Neurobiology of Learning and Memory*, 89(2), 178–184. <https://doi.org/10.1016/j.nlm.2007.07.005>
- Anagnostaras, S. G., Gale, G. D., & Fanselow, M. S. (2001). Hippocampus and contextual fear conditioning: Recent controversies and advances. *Hippocampus*, 11(1), 8–17. [https://doi.org/10.1002/1098-1063\(2001\)11:1<8::AID-HIPO1015>3.0.CO;2-7](https://doi.org/10.1002/1098-1063(2001)11:1<8::AID-HIPO1015>3.0.CO;2-7)
- Andersen, P., Sundberg, S. H., Sveen, O., & Wigström, H. (1977). Specific long-lasting potentiation of synaptic transmission in hippocampal slices. *Nature*, 266(5604), 736–737. <https://doi.org/10.1038/266736a0>
- Argolo, F. C., Cavalcanti-Ribeiro, P., Netto, L. R., & Quarantini, L. C. (2015). Prevention of posttraumatic stress disorder with propranolol: A meta-analytic review. *Journal of Psychosomatic Research*, 79(2), 89–93. <https://doi.org/10.1016/j.jpsychores.2015.04.006>
- Armbruster, B. N., Li, X., Pausch, M. H., Herlitze, S., & Roth, B. L. (2007). Evolving the lock to fit the key to create a family of G protein-coupled receptors potently activated by an inert ligand. *Proceedings of the National Academy of Sciences*, 104(12), 5163–5168. <https://doi.org/10.1073/pnas.0700293104>
- Aston-Jones, G., & Bloom, F. (1981). Nonepinephrine-containing locus coeruleus neurons in behaving rats exhibit pronounced responses to non-noxious environmental stimuli. *The Journal of Neuroscience*, 1(8), 887–900. <https://doi.org/10.1523/JNEUROSCI.01-08-1981>

00887.1981

- Aston-Jones, G., & Cohen, J. D. (2005). An integrative theory of locus coeruleus-norepinephrine function: adaptive gain and optimal performance. *Annual Review of Neuroscience*, 28(1), 403–450. <https://doi.org/10.1146/annurev.neuro.28.061604.135709>
- Aston-Jones, G., Rajkowski, J., Kubiak, P., Valentino, R. J., & Shipley, M. T. (1996). Chapter 23 Role of the locus coeruleus in emotional activation. *Progress in Brain Research*, 107, 379–402. [https://doi.org/10.1016/S0079-6123\(08\)61877-4](https://doi.org/10.1016/S0079-6123(08)61877-4)
- Aston-Jones, G., & Waterhouse, B. (2016). Locus coeruleus: From global projection system to adaptive regulation of behavior. *Brain Research*, 1645, 75–78.
<https://doi.org/10.1016/j.brainres.2016.03.001>
- Bailey, C. H., Giustetto, M., Huang, Y.-Y., Hawkins, R. D., & Kandel, E. R. (2000). Is Heterosynaptic modulation essential for stabilizing hebbian plasticity and memory. *Nature Reviews Neuroscience*, 1(1), 11–20. <https://doi.org/10.1038/35036191>
- Ball, W., & Tronick, E. (1971). Infant Responses to Impending Collision: Optical and Real. *Science*, 171(3973), 818–820. <https://doi.org/10.1126/science.171.3973.818>
- Bangasser, D. A., Waxler, D. E., Santollo, J., & Shors, T. J. (2006). Trace conditioning and the hippocampus: The importance of contiguity. *Journal of Neuroscience*, 26(34), 8702–8706. <https://doi.org/10.1523/JNEUROSCI.1742-06.2006>
- Bauer, E. P., LeDoux, J. E., & Nader, K. (2001). Fear conditioning and LTP in the lateral amygdala are sensitive to the same stimulus contingencies. *Nature Neuroscience*, 4(7), 687–688. <https://doi.org/10.1038/89465>
- Bauer, E. P., Schafe, G. E., & LeDoux, J. E. (2002). NMDA Receptors and L-Type Voltage-

Gated Calcium Channels Contribute to Long-Term Potentiation and Different Components of Fear Memory Formation in the Lateral Amygdala. *Journal of Neuroscience*, 22(12), 5239–5249. <https://doi.org/10.1523/jneurosci.22-12-05239.2002>

Benarroch, E. E. (2009). The locus ceruleus norepinephrine system: Functional organization and potential clinical significance. *Neurology*, 73(20), 1699–1704.
<https://doi.org/10.1212/WNL.0b013e3181c2937c>

Berlau, D., & McGaugh, J. (2006). Enhancement of extinction memory consolidation: The role of the noradrenergic and GABAergic systems within the basolateral amygdala. *Neurobiology of Learning and Memory*, 86(2), 123–132. <https://doi.org/10.1016/j.nlm.2005.12.008>

Bertolim, M. A., Jacquemard, A., & Vago, G. (2016). Integration of a Dirac comb and the Bernoulli polynomials. *Bulletin Des Sciences Mathématiques*, 140(2), 119–139.
<https://doi.org/10.1016/j.bulsci.2015.11.001>

Blair, H. T., Schafe, G. E., Bauer, E. P., Rodrigues, S. M., & LeDoux, J. E. (2001). Synaptic plasticity in the lateral amygdala: A cellular hypothesis of fear conditioning. *Learning and Memory*, 8(5), 229–242. <https://doi.org/10.1101/lm.30901>

Bliss, T. V. P., & Lomo, T. (1973). Long-lasting potentiation of synaptic transmission in the dentate area of the anaesthetized rabbit following stimulation of the perforant path. *J Physiol*, 232, 331–356.

Bouret, S., & Sara, S. J. (2005). Network reset: a simplified overarching theory of locus coeruleus noradrenaline function. *Trends in Neurosciences*, 28(11), 574–582.
<https://doi.org/10.1016/j.tins.2005.09.002>

Brantigan, C. O., Brantigan, T. A., & Joseph, N. (1982). Effect of beta blockade and beta

- stimulation on stage fright. *The American Journal of Medicine*, 72(1), 88–94.
[https://doi.org/10.1016/0002-9343\(82\)90592-7](https://doi.org/10.1016/0002-9343(82)90592-7)
- Bremner, J. D., Krystal, J. H., Southwick, S. M., & Charney, D. S. (1996). Noradrenergic mechanisms in stress and anxiety: I. preclinical studies. *Synapse*, 23(1), 28–38.
[https://doi.org/10.1002/\(SICI\)1098-2396\(199605\)23:1<28::AID-SYN4>3.0.CO;2-J](https://doi.org/10.1002/(SICI)1098-2396(199605)23:1<28::AID-SYN4>3.0.CO;2-J)
- Buffalari, D. M., & Grace, A. A. (2007). Noradrenergic modulation of basolateral amygdala neuronal activity: Opposing influences of α -2 and β receptor activation. *Journal of Neuroscience*, 27(45), 12358–12366. <https://doi.org/10.1523/JNEUROSCI.2007-07.2007>
- Bush, D. E. A., Caparosa, E. M., Gekker, A., & LeDoux, J. E. (2010). Beta-Adrenergic Receptors in the Lateral Nucleus of the Amygdala Contribute to the Acquisition but Not the Consolidation of Auditory Fear Conditioning. *Frontiers in Behavioral Neuroscience*, 4(OCT), 1–7. <https://doi.org/10.3389/fnbeh.2010.00154>
- Buzsáki, G. (2006). Rhythms of the Brain. In *Rhythms of the Brain*. Oxford University Press.
<https://doi.org/10.1093/acprof:oso/9780195301069.001.0001>
- Cahill, L., Prins, B., Weber, M., & McGaugh, J. L. (1994). β -Adrenergic activation and memory for emotional events. *Nature*, 371(6499), 702–704. <https://doi.org/10.1038/371702a0>
- Cain, C. K., Maynard, G. D., & Kehne, J. H. (2012). Targeting memory processes with drugs to prevent or cure PTSD. *Expert Opinion on Investigational Drugs*, 21(9), 1323–1350.
<https://doi.org/10.1517/13543784.2012.704020>
- Campese, V. D., Kim, J., Lázaro-Muñoz, G., Pena, L., Ledoux, J. E., & Cain, C. K. (2014). Lesions of lateral or central amygdala abolish aversive Pavlovian-to-instrumental transfer in rats. *Frontiers in Behavioral Neuroscience*, 8(MAY), 1–7.

<https://doi.org/10.3389/fnbeh.2014.00161>

Campese, V. D., McCue, M., Lázaro-Muñoz, G., LeDoux, J. E., & Cain, C. K. (2013). Development of an aversive Pavlovian-to-instrumental transfer task in rat. *Frontiers in Behavioral Neuroscience*, 7(NOV), 1–10. <https://doi.org/10.3389/fnbeh.2013.00176>

Campese, V. D., Soroeta, J. M., Vazey, E. M., Aston-Jones, G., LeDoux, J. E., & Sears, R. M. (2017). Noradrenergic Regulation of Central Amygdala in Aversive Pavlovian-to-Instrumental Transfer. *Eneuro*, 4(5), ENEURO.0224-17.2017.

<https://doi.org/10.1523/ENEURO.0224-17.2017>

Carter, M. E., Yizhar, O., Chikahisa, S., Nguyen, H., Adamantidis, A., Nishino, S., Deisseroth, K., & de Lecea, L. (2010). Tuning arousal with optogenetic modulation of locus coeruleus neurons. *Nature Neuroscience*, 13(12), 1526–1533. <https://doi.org/10.1038/nn.2682>

Chen, D. Y., Bambah-Mukku, D., Pollonini, G., & Alberini, C. M. (2012). Glucocorticoid receptors recruit the CaMKIIα-BDNF-CREB pathways to mediate memory consolidation. *Nature Neuroscience*, 15(12), 1707–1714. <https://doi.org/10.1038/nn.3266>

Chen, F. J., & Sara, S. J. (2007). Locus coeruleus activation by foot shock or electrical stimulation inhibits amygdala neurons. *Neuroscience*, 144(2), 472–481.
<https://doi.org/10.1016/j.neuroscience.2006.09.037>

Chen, Y.-W., Das, M., Oyarzabal, E. A., Cheng, Q., Plummer, N. W., Smith, K. G., Jones, G. K., Malawsky, D., Yakel, J. L., Shih, Y.-Y. I., & Jensen, P. (2019). Genetic identification of a population of noradrenergic neurons implicated in attenuation of stress-related responses. *Molecular Psychiatry*, 24(5), 710–725. <https://doi.org/10.1038/s41380-018-0245-8>

Ciocchi, S., Herry, C., Grenier, F., Wolff, S. B. E., Letzkus, J. J., Vlachos, I., Ehrlich, I.,

- Sprengel, R., Deisseroth, K., Stadler, M. B., Müller, C., & Lüthi, A. (2010). Encoding of conditioned fear in central amygdala inhibitory circuits. *Nature*, 468(7321), 277–282. <https://doi.org/10.1038/nature09559>
- Clugnet, M. C., & LeDoux, J. E. (1990). Synaptic plasticity in fear conditioning circuits: Induction of LTP in the lateral nucleus of the amygdala by stimulation of the medial geniculate body. *Journal of Neuroscience*, 10(8), 2818–2824. <https://doi.org/10.1523/jneurosci.10-08-02818.1990>
- Cole, S., & McNally, G. P. (2007). Opioid receptors mediate direct predictive fear learning: Evidence from one-trial blocking. *Learning & Memory*, 14(4), 229–235. <https://doi.org/10.1101/lm.489507>
- Connor, D. F., Fletcher, K. E., & Swanson, J. M. (1999). A Meta-Analysis of Clonidine for Symptoms of Attention-Deficit Hyperactivity Disorder. *Journal of the American Academy of Child & Adolescent Psychiatry*, 38(12), 1551–1559. <https://doi.org/10.1097/00004583-199912000-00017>
- Damasio, A., & Carvalho, G. B. (2013). The nature of feelings: Evolutionary and neurobiological origins. *Nature Reviews Neuroscience*, 14(2), 143–152. <https://doi.org/10.1038/nrn3403>
- Davis, M. (1992). The Role of the Amygdala in Fear and Anxiety. *Annual Review of Neuroscience*, 15(1), 353–375. <https://doi.org/10.1146/annurev.ne.15.030192.002033>
- Dayan, P. (1993). Improving Generalization for Temporal Difference Learning: The Successor Representation. *Neural Computation*, 5(4), 613–624. <https://doi.org/10.1162/neco.1993.5.4.613>
- Dębiec, J., Bush, D. E. A., & LeDoux, J. E. (2011). Noradrenergic enhancement of

reconsolidation in the amygdala impairs extinction of conditioned fear in rats-a possible mechanism for the persistence of traumatic memories in PTSD. *Depression and Anxiety*, 28(3), 186–193. <https://doi.org/10.1002/da.20803>

Dębiec, J., & LeDoux, J. E. (2004). Disruption of reconsolidation but not consolidation of auditory fear conditioning by noradrenergic blockade in the amygdala. *Neuroscience*, 129(2), 267–272. <https://doi.org/10.1016/j.neuroscience.2004.08.018>

Dębiec, J., & LeDoux, J. E. (2006). Noradrenergic Signaling in the Amygdala Contributes to the Reconsolidation of Fear Memory: Treatment Implications for PTSD. *Annals of the New York Academy of Sciences*, 1071(1), 521–524. <https://doi.org/10.1196/annals.1364.056>

Derderian, C., & Tadi, P. (2020). Physiology, Withdrawal Response. In *StatPearls*.
<http://www.ncbi.nlm.nih.gov/pubmed/31335012>

Díaz-Mataix, L., Piper, W. T., Schiff, H. C., Roberts, C. H., Campese, V. D., Sears, R. M., & LeDoux, J. E. (2017). Characterization of the amplificatory effect of norepinephrine in the acquisition of Pavlovian threat associations. *Learning & Memory*, 24(9), 432–439.
<https://doi.org/10.1101/lm.044412.116>

Doyère, V., Schafe, G. E., Sigurdsson, T., & LeDoux, J. E. (2003). Long-term potentiation in freely moving rats reveals asymmetries in thalamic and cortical inputs to the lateral amygdala. *European Journal of Neuroscience*, 17(12), 2703–2715.
<https://doi.org/10.1046/j.1460-9568.2003.02707.x>

Dubovsky, S. L. (1990). Generalized anxiety disorder: new concepts and psychopharmacologic therapies. *The Journal of Clinical Psychiatry*, 51 Suppl, 3–10.
<http://www.ncbi.nlm.nih.gov/pubmed/1967248>

- Eichenbaum, H. (2000). A cortical–hippocampal system for declarative memory. *Nature Reviews Neuroscience*, 1(1), 41–50. <https://doi.org/10.1038/35036213>
- Estrade, L., Cassel, J. C., Parrot, S., Duchamp-Viret, P., & Ferry, B. (2019). Microdialysis Unveils the Role of the α 2 -Adrenergic System in the Basolateral Amygdala during Acquisition of Conditioned Odor Aversion in the Rat. *ACS Chemical Neuroscience*, 10(4), 1929–1934. <https://doi.org/10.1021/acschemneuro.8b00314>
- Faber, E. S. L., Delaney, A. J., Power, J. M., Sedlak, P. L., Crane, J. W., & Sah, P. (2008). Modulation of SK channel trafficking by beta adrenoceptors enhances excitatory synaptic transmission and plasticity in the amygdala. *Journal of Neuroscience*, 28(43), 10803–10813. <https://doi.org/10.1523/JNEUROSCI.1796-08.2008>
- Fadok, J. P., Markovic, M., Tovote, P., & Lüthi, A. (2018). New perspectives on central amygdala function. *Current Opinion in Neurobiology*, 49, 141–147. <https://doi.org/10.1016/j.conb.2018.02.009>
- Fallon, J. H., Koziell, D. A., & Moore, R. Y. (1978). Catecholamine innervation of the basal forebrain II. Amygdala, suprarhinal cortex and entorhinal cortex. *The Journal of Comparative Neurology*, 180(3), 509–531. <https://doi.org/10.1002/cne.901800308>
- Fanselow, M. S. (2018). The role of learning in threat imminence and defensive behaviors. *Current Opinion in Behavioral Sciences*, 24, 44–49. <https://doi.org/10.1016/j.cobeha.2018.03.003>
- Fanselow, M. S., & Pennington, Z. T. (2018). A return to the psychiatric dark ages with a two-system framework for fear. *Behaviour Research and Therapy*, 100(November 2017), 24–29. <https://doi.org/10.1016/j.brat.2017.10.012>

- Farb, C. R., Chang, W., & LeDoux, J. E. (2010). Ultrastructural Characterization of Noradrenergic Axons and Beta-Adrenergic Receptors in the Lateral Nucleus of the Amygdala. *Frontiers in Behavioral Neuroscience*, 4(OCT), 1–9.
<https://doi.org/10.3389/fnbeh.2010.00162>
- Feng, F., Samarth, P., Paré, D., & Nair, S. S. (2016). Mechanisms underlying the formation of the amygdalar fear memory trace: A computational perspective. *Neuroscience*, 322, 370–376. <https://doi.org/10.1016/j.neuroscience.2016.02.059>
- Feng, J., Zhang, C., Lischinsky, J. E., Jing, M., Zhou, J., Wang, H., Zhang, Y., Dong, A., Wu, Z., Wu, H., Chen, W., Zhang, P., Zou, J., Hires, S. A., Zhu, J. J., Cui, G., Lin, D., Du, J., & Li, Y. (2019). A Genetically Encoded Fluorescent Sensor for Rapid and Specific In Vivo Detection of Norepinephrine. *Neuron*, 102(4), 745-761.e8.
<https://doi.org/10.1016/j.neuron.2019.02.037>
- Fenster, R. J., Lebois, L. A. M., Ressler, K. J., & Suh, J. (2018). Brain circuit dysfunction in post-traumatic stress disorder: from mouse to man. *Nature Reviews Neuroscience*, 19(9), 535–551. <https://doi.org/10.1038/s41583-018-0039-7>
- Ferry, B., & McGaugh, J. L. (2000). Role of amygdala norepinephrine in mediating stress hormone regulation of memory storage. *Acta Pharmacologica Sinica*, 21(6), 481–493.
<http://www.ncbi.nlm.nih.gov/pubmed/11360681>
- Foote, S. L., Aston-Jones, G., & Bloom, F. E. (1980). Impulse activity of locus coeruleus neurons in awake rats and monkeys is a function of sensory stimulation and arousal. *Proceedings of the National Academy of Sciences*, 77(5), 3033–3037.
<https://doi.org/10.1073/pnas.77.5.3033>

Galvez, R., Mesches, M. H., & Mcgaugh, J. L. (1996). Norepinephrine Release in the Amygdala in Response to Footshock Stimulation. *Neurobiology of Learning and Memory*, 66(3), 253–257. <https://doi.org/10.1006/nlme.1996.0067>

Gendron, M., & Feldman Barrett, L. (2009). Reconstructing the Past: A Century of Ideas About Emotion in Psychology. *Emotion Review*, 1(4), 316–339.
<https://doi.org/10.1177/1754073909338877>

Geracioti, T. D., Baker, D. G., Ekhator, N. N., West, S. A., Hill, K. K., Bruce, A. B., Schmidt, D., Rounds-Kugler, B., Yehuda, R., Keck, P. E., & Kasckow, J. W. (2001). CSF Norepinephrine Concentrations in Posttraumatic Stress Disorder. *American Journal of Psychiatry*, 158(8), 1227–1230. <https://doi.org/10.1176/appi.ajp.158.8.1227>

Giustino, T. F., Fitzgerald, P. J., & Maren, S. (2016). Revisiting propranolol and PTSD: Memory erasure or extinction enhancement? *Neurobiology of Learning and Memory*, 130, 26–33.
<https://doi.org/10.1016/j.nlm.2016.01.009>

Giustino, T. F., & Maren, S. (2015). The role of the medial prefrontal cortex in the conditioning and extinction of fear. *Frontiers in Behavioral Neuroscience*, 9(NOVEMBER), 1–20.
<https://doi.org/10.3389/fnbeh.2015.00298>

Giustino, T. F., & Maren, S. (2018). Noradrenergic modulation of fear conditioning and extinction. *Frontiers in Behavioral Neuroscience*, 12(March), 1–20.
<https://doi.org/10.3389/fnbeh.2018.00043>

Gleick, J. (1988). *Chaos - Making a new science*. Penguin Books.

Gomez, J. L., Bonaventura, J., Lesniak, W., Mathews, W. B., Sysa-Shah, P., Rodriguez, L. A., Ellis, R. J., Richie, C. T., Harvey, B. K., Dannals, R. F., Pomper, M. G., Bonci, A., &

Michaelides, M. (2017). Chemogenetics revealed: DREADD occupancy and activation via converted clozapine. *Science*, 357(6350), 503–507.

<https://doi.org/10.1126/science.aan2475>

Goosens, K. A., & Maren, S. (2003). Pretraining NMDA receptor blockade in the basolateral complex, but not the central nucleus, of the amygdala prevents savings of the conditional fear. *Behavioral Neuroscience*, 117(4), 738–750. <https://doi.org/10.1037/0735-7044.117.4.738>

Grewen, B. F., Gründemann, J., Kitch, L. J., Lecoq, J. A., Parker, J. G., Marshall, J. D., Larkin, M. C., Jercog, P. E., Grenier, F., Li, J. Z., Lüthi, A., & Schnitzer, M. J. (2017). Neural ensemble dynamics underlying a long-term associative memory. *Nature*, 543(7647), 670–675. <https://doi.org/10.1038/nature21682>

Grillon, C., Cordova, J., Morgan, C. A., Charney, D. S., & Davis, M. (2004). Effects of the beta-blocker propranolol on cued and contextual fear conditioning in humans. *Psychopharmacology*, 175(3), 342–352. <https://doi.org/10.1007/s00213-004-1819-5>

Gu, Y., Piper, W. T., Branigan, L. A., Vazey, E. M., Aston-Jones, G., Lin, L., LeDoux, J. E., & Sears, R. M. (2020). A brainstem-central amygdala circuit underlies defensive responses to learned threats. *Molecular Psychiatry*, 25(3), 640–654. <https://doi.org/10.1038/s41380-019-0599-6>

Han, J. H., Yiu, A. P., Cole, C. J., Hsiang, H. L., Neve, R. L., Josselyn, S. A., Kushner, S. A., Matynia, A., Brown, R. A., Guzowski, J. F., & Silva, A. J. (2008). Increasing CREB in the auditory thalamus enhances memory and generalization of auditory conditioned fear. *Learn Mem*, 15(6), 443–453. <https://doi.org/10.1101/lm.993608.2007>

Han, S., Soleiman, M. T., Soden, M. E., Zweifel, L. S., & Palmiter, R. D. (2015). Elucidating an Affective Pain Circuit that Creates a Threat Memory. *Cell*, 162(2), 363–374.

<https://doi.org/10.1016/j.cell.2015.05.057>

Hatfield, T., Spanis, C., & McGaugh, J. L. (1999). Response of amygdalar norepinephrine to footshock and GABAergic drugs using in vivo microdialysis and HPLC. *Brain Research*, 835(2), 340–345. [https://doi.org/10.1016/S0006-8993\(99\)01566-8](https://doi.org/10.1016/S0006-8993(99)01566-8)

Hebb, D. O. (1949). *The organization of behavior; a neuropsychological theory*. Wiley.

Herry, C., & Johansen, J. P. (2014). Encoding of fear learning and memory in distributed neuronal circuits. *Nature Neuroscience*, 17(12), 1644–1654.

<https://doi.org/10.1038/nn.3869>

Huang, Y. Y., & Kandel, E. R. (1998). Postsynaptic induction and PKA-dependent expression of LTP in the lateral amygdala. *Neuron*, 21(1), 169–178. [https://doi.org/10.1016/S0896-6273\(00\)80524-3](https://doi.org/10.1016/S0896-6273(00)80524-3)

Huang, Y. Y., Martin, K. C., & Kandel, E. R. (2000). Both protein kinase A and mitogen-activated protein kinase are required in the amygdala for the macromolecular synthesis-dependent late phase of long-term potentiation. *Journal of Neuroscience*, 20(17), 6317–6325.
<https://doi.org/10.1523/JNEUROSCI.20-17-06317.2000>

Hurlemann, R., Walter, H., Rehme, A. K., Kukolja, J., Santoro, S. C., Schmidt, C., Schnell, K., Musshoff, F., Keysers, C., Maier, W., Kendrick, K. M., & Onur, O. A. (2010). Human amygdala reactivity is diminished by the β-noradrenergic antagonist propranolol. *Psychological Medicine*, 40(11), 1839–1848. <https://doi.org/10.1017/S0033291709992376>

Hwang, D.-Y., Carlezon, W. A., Isacson, O., & Kim, K.-S. (2001). A High-Efficiency Synthetic

Promoter That Drives Transgene Expression Selectively in Noradrenergic Neurons. *Human Gene Therapy*, 12(14), 1731–1740. <https://doi.org/10.1089/104303401750476230>

Jing, M., Zhang, P., Wang, G., Feng, J., Mesik, L., Zeng, J., Jiang, H., Wang, S., Looby, J. C., Guagliardo, N. A., Langma, L. W., Lu, J., Zuo, Y., Talmage, D. A., Role, L. W., Barrett, P. Q., Zhang, L. I., Luo, M., Song, Y., ... Li, Y. (2018). A genetically encoded fluorescent acetylcholine indicator for in vitro and in vivo studies. *Nature Biotechnology*, 36(8). <https://doi.org/10.1038/nbt.4184>

Joëls, M., Fernandez, G., & Roozendaal, B. (2011). Stress and emotional memory: a matter of timing. *Trends in Cognitive Sciences*, 15(6), 280–288. <https://doi.org/10.1016/j.tics.2011.04.004>

Johansen, J. P., Cain, C. K., Ostroff, L. E., & Ledoux, J. E. (2011). Molecular mechanisms of fear learning and memory. *Cell*, 147(3), 509–524. <https://doi.org/10.1016/j.cell.2011.10.009>

Johansen, J. P., Diaz-Mataix, L., Hamanaka, H., Ozawa, T., Ycu, E., Koivumaa, J., Kumar, A., Hou, M., Deisseroth, K., Boyden, E. S., & LeDoux, J. E. (2014). Hebbian and neuromodulatory mechanisms interact to trigger associative memory formation. *Proceedings of the National Academy of Sciences*, 111(51), E5584–E5592. <https://doi.org/10.1073/pnas.1421304111>

Johansen, J. P., Tarpley, J. W., Ledoux, J. E., & Blair, H. T. (2010). Neural substrates for expectation-modulated fear learning in the amygdala and periaqueductal gray. *Nature Neuroscience*, 13(8), 979–986. <https://doi.org/10.1038/nn.2594>

Jones, B. E., & Moore, R. Y. (1977). Ascending projections of the locus coeruleus in the rat. II. Autoradiographic study. *Brain Research*, 127(1), 25–53.

<http://www.ncbi.nlm.nih.gov/pubmed/301051>

Jones, B. E., & Yang, T.-Z. (1985). The efferent projections from the reticular formation and the locus coeruleus studied by anterograde and retrograde axonal transport in the rat. *The Journal of Comparative Neurology*, 242(1), 56–92. <https://doi.org/10.1002/cne.902420105>

Jones, E., Oliphant, T., & Peterson, P. (2001). *SciPy: Open Source Scientific Tools for Python*.

Jorge, R. E. (2015). Posttraumatic stress disorder. *CONTINUUM Lifelong Learning in Neurology*, 21(3), 789–805. <https://doi.org/10.1212/01.CON.0000466667.20403.b1>

Kane, G. A., Vazey, E. M., Wilson, R. C., Shenhav, A., Daw, N. D., Aston-Jones, G., & Cohen, J. D. (2017). Increased locus coeruleus tonic activity causes disengagement from a patch-foraging task. *Cognitive, Affective, & Behavioral Neuroscience*, 17(6), 1073–1083.
<https://doi.org/10.3758/s13415-017-0531-y>

Kapp, B. S., Frysinger, R. C., Gallagher, M., & Haselton, J. R. (1979). Amygdala central nucleus lesions: Effect on heart rate conditioning in the rabbit. *Physiology and Behavior*, 23(6), 1109–1117. [https://doi.org/10.1016/0031-9384\(79\)90304-4](https://doi.org/10.1016/0031-9384(79)90304-4)

Keifer, O. P., Hurt, R. C., Ressler, K. J., & Marvar, P. J. (2015). The Physiology of Fear: Reconceptualizing the Role of the Central Amygdala in Fear Learning. *Physiology*, 30(5), 389–401. <https://doi.org/10.1152/physiol.00058.2014>

Kim, W. Bin, & Cho, J.-H. (2017). Encoding of Discriminative Fear Memory by Input-Specific LTP in the Amygdala. *Neuron*, 95(5), 1129-1146.e5.
<https://doi.org/10.1016/j.neuron.2017.08.004>

Kim, W. Bin, & Cho, J.-H. (2020). Encoding of contextual fear memory in hippocampal–amygdala circuit. *Nature Communications*, 11(1), 1382. <https://doi.org/10.1038/s41467-019-12540-w>

020-15121-2

- Krabbe, S., Gründemann, J., & Lüthi, A. (2018). Amygdala Inhibitory Circuits Regulate Associative Fear Conditioning. *Biological Psychiatry*, 83(10), 800–809.
<https://doi.org/10.1016/j.biopsych.2017.10.006>
- Kroes, M. C. W., Strange, B. A., & Dolan, R. J. (2010). β -Adrenergic Blockade during Memory Retrieval in Humans Evokes a Sustained Reduction of Declarative Emotional Memory Enhancement. *Journal of Neuroscience*, 30(11), 3959–3963.
<https://doi.org/10.1523/JNEUROSCI.5469-09.2010>
- LeDoux, J. E. (1996). *The emotional brain: the mysterious underpinnings of emotional life*. Simon & Schuster Paperbacks.
- LeDoux, J. E. (2000). Emotion Circuits in the Brain. *Annual Review of Neuroscience*, 23(1), 155–184. <https://doi.org/10.1146/annurev.neuro.23.1.155>
- LeDoux, J. E. (2007). The amygdala. *Current Biology*, 17(20), R868–R874.
<https://doi.org/10.1016/j.cub.2007.08.005>
- LeDoux, J. E. (2012). Rethinking the Emotional Brain. *Neuron*, 73(4), 653–676.
<https://doi.org/10.1016/j.neuron.2012.02.004>
- LeDoux, J. E. (2014). Coming to terms with fear. *Proceedings of the National Academy of Sciences of the United States of America*, 111(8), 2871–2878.
<https://doi.org/10.1073/pnas.1400335111>
- LeDoux, J. E. (2017). Semantics, Surplus Meaning, and the Science of Fear. *Trends in Cognitive Sciences*, 21(5), 303–306. <https://doi.org/10.1016/j.tics.2017.02.004>
- LeDoux, J. E. (2019). *The deep history of ourselves: the four-billion-year story of how we got here*.

conscious brains. Viking.

LeDoux, J. E. (2020). How does the non-conscious become conscious? *Current Biology*, 30(5), R196–R199. <https://doi.org/10.1016/j.cub.2020.01.033>

LeDoux, J. E., Cicchetti, P., Xagoraris, A., & Romanski, L. (1990). The lateral amygdaloid nucleus: sensory interface of the amygdala in fear conditioning. *The Journal of Neuroscience*, 10(4), 1062–1069. <https://doi.org/10.1523/JNEUROSCI.10-04-01062.1990>

LeDoux, J. E., Farb, C., & Ruggiero, D. (1990). Topographic organization of neurons in the acoustic thalamus that project to the amygdala. *The Journal of Neuroscience*, 10(4), 1043–1054. <https://doi.org/10.1523/JNEUROSCI.10-04-01043.1990>

LeDoux, J. E., Iwata, J., Cicchetti, P., & Reis, D. (1988). Different projections of the central amygdaloid nucleus mediate autonomic and behavioral correlates of conditioned fear. *The Journal of Neuroscience*, 8(7), 2517–2529. <https://doi.org/10.1523/JNEUROSCI.08-07-02517.1988>

LeDoux, J. E., & Pine, D. S. (2016). Using neuroscience to help understand fear and anxiety: A two-system framework. *American Journal of Psychiatry*, 173(11), 1083–1093. <https://doi.org/10.1176/appi.ajp.2016.16030353>

LeDoux, J. E., Sakaguchi, A., Iwata, J., & Reis, D. J. (1986). Interruption of projections from the medial geniculate body to an archi-neostriatal field disrupts the classical conditioning of emotional responses to acoustic stimuli. *Neuroscience*, 17(3), 615–627. [https://doi.org/10.1016/0306-4522\(86\)90034-5](https://doi.org/10.1016/0306-4522(86)90034-5)

LeDoux, J. E., Sakaguchi, A., & Reis, D. (1984). Subcortical efferent projections of the medial geniculate nucleus mediate emotional responses conditioned to acoustic stimuli. *The*

Journal of Neuroscience, 4(3), 683–698. <https://doi.org/10.1523/JNEUROSCI.04-03-00683.1984>

Lee, H. J., Berger, S. Y., Stiedl, O., Spiess, J., & Kim, J. J. (2001). Post-training injections of catecholaminergic drugs do not modulate fear conditioning in rats and mice. *Neuroscience Letters*, 303(2), 123–126. [https://doi.org/10.1016/S0304-3940\(01\)01733-5](https://doi.org/10.1016/S0304-3940(01)01733-5)

Lee, S., Kim, S. J., Kwon, O. Bin, Lee, J. H., & Kim, J. H. (2013). Inhibitory networks of the amygdala for emotional memory. *Frontiers in Neural Circuits*, 7(JUL), 1–10. <https://doi.org/10.3389/fncir.2013.00129>

Li, B. (2019). Central amygdala cells for learning and expressing aversive emotional memories. *Current Opinion in Behavioral Sciences*, 26, 40–45. <https://doi.org/10.1016/j.cobeha.2018.09.012>

Li, H., Penzo, M. A., Taniguchi, H., Kopec, C. D., Huang, Z. J., & Li, B. (2013). Experience-dependent modification of a central amygdala fear circuit. *Nature Neuroscience*, 16(3), 332–339. <https://doi.org/10.1038/nn.3322>

Lonergan, M., Olivera-Figueroa, L., Pitman, R., & Brunet, A. (2013). Propranolol's effects on the consolidation and reconsolidation of long-term emotional memory in healthy participants: a meta-analysis. *Journal of Psychiatry & Neuroscience*, 38(4), 222–231. <https://doi.org/10.1503/jpn.120111>

Lu, L., Gutruf, P., Xia, L., Bhatti, D. L., Wang, X., Vazquez-Guardado, A., Ning, X., Shen, X., Sang, T., Ma, R., Pakeltis, G., Sobczak, G., Zhang, H., Seo, D. oh, Xue, M., Yin, L., Chanda, D., Sheng, X., Bruchas, M. R., & Rogers, J. A. (2018). Wireless optoelectronic photometers for monitoring neuronal dynamics in the deep brain. *Proceedings of the*

National Academy of Sciences of the United States of America, 115(7), E1374–E1383.

<https://doi.org/10.1073/pnas.1718721115>

Luppi, P.-H., Aston-Jones, G., Akaoka, H., Chouvet, G., & Jouvet, M. (1995). Afferent projections to the rat locus coeruleus demonstrated by retrograde and anterograde tracing with cholera-toxin B subunit and Phaseolus vulgaris leucoagglutinin. *Neuroscience*, 65(1), 119–160. [https://doi.org/10.1016/0306-4522\(94\)00481-J](https://doi.org/10.1016/0306-4522(94)00481-J)

Lynch, G. S., Dunwiddie, T., & Gribkoff, V. (1977). Heterosynaptic depression: a postsynaptic correlate of long-term potentiation. *Nature*, 266(5604), 737–739.
<https://doi.org/10.1038/266737a0>

Mackintosh, N. J. (1975). A theory of attention: Variations in the associability of stimuli with reinforcement. *Psychological Review*, 82(4), 276–298. <https://doi.org/10.1037/h0076778>

MacLaren, D. A. A., Browne, R. W., Shaw, J. K., Krishnan Radhakrishnan, S., Khare, P., España, R. A., & Clark, S. D. (2016). Clozapine N-Oxide Administration Produces Behavioral Effects in Long-Evans Rats: Implications for Designing DREADD Experiments. *Eneuro*, 3(5), ENEURO.0219-16.2016. <https://doi.org/10.1523/ENEURO.0219-16.2016>

Mahan, A. L., & Ressler, K. J. (2012). Fear conditioning, synaptic plasticity and the amygdala: implications for posttraumatic stress disorder. *Trends in Neurosciences*, 35(1), 24–35.
<https://doi.org/10.1016/j.tins.2011.06.007>

Mahler, S. V., & Aston-Jones, G. (2018). CNO Evil? Considerations for the Use of DREADDs in Behavioral Neuroscience. *Neuropsychopharmacology*, 43(5), 934–936.
<https://doi.org/10.1038/npp.2017.299>

Mahler, S. V., Vazey, E. M., Beckley, J. T., Keistler, C. R., McGlinchey, E. M., Kaufling, J.,

- Wilson, S. P., Deisseroth, K., Woodward, J. J., & Aston-Jones, G. (2014). Designer receptors show role for ventral pallidum input to ventral tegmental area in cocaine seeking. *Nature Neuroscience*, 17(4), 577–585. <https://doi.org/10.1038/nn.3664>
- Manns, J. R., & Eichenbaum, H. (2006). Evolution of declarative memory. *Hippocampus*, 16(9), 795–808. <https://doi.org/10.1002/hipo.20205>
- Maren, S., & Quirk, G. J. (2004). Neuronal signalling of fear memory. *Nature Reviews Neuroscience*, 5(11), 844–852. <https://doi.org/10.1038/nrn1535>
- Martins, A. R. O., & Froemke, R. C. (2015). Coordinated forms of noradrenergic plasticity in the locus coeruleus and primary auditory cortex. *Nature Neuroscience*, 18(10), 1483–1492. <https://doi.org/10.1038/nn.4090>
- Mathis, A., Manimanna, P., Cury, K. M., Abe, T., Murthy, V. N., Mathis, M. W., & Bethge, M. (2018). DeepLabCut: markerless pose estimation of user-defined body parts with deep learning. *Nature Neuroscience*, 21(9), 1281–1289. <https://doi.org/10.1038/s41593-018-0209-y>
- McAllister, W. R., McAllister, D. E., & Douglass, W. K. (1971). The inverse relationship between shock intensity and shuttle-box avoidance learning in rats: A reinforcement explanation. *Journal of Comparative and Physiological Psychology*, 74(3), 426–433. <https://doi.org/10.1037/h0030579>
- McCall, J. G., Al-Hasani, R., Siuda, E. R., Hong, D. Y., Norris, A. J., Ford, C. P., & Bruchas, M. R. (2015). CRH Engagement of the Locus Coeruleus Noradrenergic System Mediates Stress-Induced Anxiety. *Neuron*, 87(3), 605–620. <https://doi.org/10.1016/j.neuron.2015.07.002>

- McCall, J. G., Siuda, E. R., Bhatti, D. L., Lawson, L. A., McElligott, Z. A., Stuber, G. D., & Bruchas, M. R. (2017). Locus coeruleus to basolateral amygdala noradrenergic projections promote anxiety-like behavior. *eLife*, 6. <https://doi.org/10.7554/eLife.18247>
- McEchron, M. D., Green, E. J., Winters, R. W., Nolen, T. G., Schneiderman, N., & McCabe, P. M. (1996). Changes of synaptic efficacy in the medial geniculate nucleus as a result of auditory classical conditioning. *Journal of Neuroscience*, 16(3), 1273–1283.
<https://doi.org/10.1523/jneurosci.16-03-01273.1996>
- McEwen, B. S. (2012). Brain on stress: How the social environment gets under the skin. *Proceedings of the National Academy of Sciences*, 109(Supplement_2), 17180–17185.
<https://doi.org/10.1073/pnas.1121254109>
- McGaugh, J. L. (2000). Memory--a Century of Consolidation. *Science*, 287(5451), 248–251.
<https://doi.org/10.1126/science.287.5451.248>
- McGaugh, J. L. (2015). Consolidating Memories. *Annual Review of Psychology*, 66(1), 1–24.
<https://doi.org/10.1146/annurev-psych-010814-014954>
- McGaugh, J. L., McIntyre, C. K., & Power, A. E. (2002). Amygdala Modulation of Memory Consolidation: Interaction with Other Brain Systems. *Neurobiology of Learning and Memory*, 78(3), 539–552. <https://doi.org/10.1006/nlme.2002.4082>
- Mcnaughton, B. L., Douglas, R. M., & Goddard, G. V. (1978). Synaptic enhancement in fascia dentata: cooperativity among coactive afferents. *Brain Research*, 157, 277–293.
- Michely, J., Rigoli, F., Rutledge, R. B., Hauser, T. U., & Dolan, R. J. (2020). Distinct Processing of Aversive Experience in Amygdala Subregions. *Biological Psychiatry: Cognitive Neuroscience and Neuroimaging*, 5(3), 291–300.

<https://doi.org/10.1016/j.bpsc.2019.07.008>

Miserendino, M. J. D., Sananes, C. B., Melia, K. R., & Davis, M. (1990). Blocking of acquisition but not expression of conditioned fear-potentiated startle by NMDA antagonists in the amygdala. *Nature*, 345(6277), 716–718. <https://doi.org/10.1038/345716a0>

Mobbs, D., Adolphs, R., Fanselow, M. S., Barrett, L. F., LeDoux, J. E., Ressler, K., & Tye, K. M. (2019). Viewpoints: Approaches to defining and investigating fear. *Nature Neuroscience*, 22(8), 1205–1216. <https://doi.org/10.1038/s41593-019-0456-6>

Mobbs, D., & LeDoux, J. E. (2018). Editorial overview: Survival behaviors and circuits. *Current Opinion in Behavioral Sciences*, 24(April 2017), 168–171.

<https://doi.org/10.1016/j.cobeha.2018.10.004>

Moore, B. R. (2004). The evolution of learning. *Biological Reviews*, 79(2), 301–335.

<https://doi.org/10.1017/S1464793103006225>

Moore, R. Y., & Bloom, F. E. (1979). Central Catecholamine Neuron Systems: Anatomy and Physiology of the Norepinephrine and Epinephrine Systems. *Annual Review of Neuroscience*, 2(1), 113–168. <https://doi.org/10.1146/annurev.ne.02.030179.000553>

Morgan, M. A., Romanski, L. M., & LeDoux, J. E. (1993). Extinction of emotional learning: Contribution of medial prefrontal cortex. *Neuroscience Letters*, 163(1), 109–113.

[https://doi.org/10.1016/0304-3940\(93\)90241-C](https://doi.org/10.1016/0304-3940(93)90241-C)

Morilak, D. A., Barrera, G., Echevarria, D. J., Garcia, A. S., Hernandez, A., Ma, S., & Petre, C. O. (2005). Role of brain norepinephrine in the behavioral response to stress. *Progress in Neuro-Psychopharmacology and Biological Psychiatry*, 29(8), 1214–1224.

<https://doi.org/10.1016/j.pnpbp.2005.08.007>

Muravieva, E. V., & Alberini, C. M. (2010). Limited efficacy of propranolol on the reconsolidation of fear memories. *Learning and Memory*, 17(6), 306–313.

<https://doi.org/10.1101/lm.1794710>

Nader, K., Schafe, G. E., & LeDoux, J. E. (2000). Fear memories require protein synthesis in the amygdala for reconsolidation after retrieval. *Nature*, 406(6797), 722–726.

<https://doi.org/10.1038/35021052>

Naegeli, C., Zeffiro, T., Piccirelli, M., Jaillard, A., Weilenmann, A., Hassanpour, K., Schick, M., Rufer, M., Orr, S. P., & Mueller-Pfeiffer, C. (2018). Locus Coeruleus Activity Mediates Hyperresponsiveness in Posttraumatic Stress Disorder. *Biological Psychiatry*, 83(3), 254–262. <https://doi.org/10.1016/j.biopsych.2017.08.021>

Nath, T., Mathis, A., Chen, A. C., Patel, A., Bethge, M., & Mathis, M. W. (2019). Using DeepLabCut for 3D markerless pose estimation across species and behaviors. *Nature Protocols*, 14(7), 2152–2176. <https://doi.org/10.1038/s41596-019-0176-0>

O'Donnell, J., Zeppenfeld, D., McConnell, E., Pena, S., & Nedergaard, M. (2012). Norepinephrine: A Neuromodulator That Boosts the Function of Multiple Cell Types to Optimize CNS Performance. *Neurochemical Research*, 37(11), 2496–2512.
<https://doi.org/10.1007/s11064-012-0818-x>

Oliphant, T. (2006). *A guide to Numpy*. Trelgol Publishing USA.

Olsson, A., & Phelps, E. A. (2007). Social learning of fear. *Nature Neuroscience*, 10(9), 1095–1102. <https://doi.org/10.1038/nn1968>

Ostroff, L. E., Cain, C. K., Bedont, J., Monfils, M. H., & LeDoux, J. E. (2010). Fear and safety learning differentially affect synapse size and dendritic translation in the lateral amygdala.

Proceedings of the National Academy of Sciences, 107(20), 9418–9423.

<https://doi.org/10.1073/pnas.0913384107>

Ota, K. T., Monsey, M. S., Wu, M. S., Young, G. J., & Schafe, G. E. (2010). Synaptic plasticity and NO-cGMP-PKG signaling coordinately regulate ERK-driven gene expression in the lateral amygdala and in the auditory thalamus following Pavlovian fear conditioning.

Learning & Memory (Cold Spring Harbor, N.Y.), 17(4), 221–235.

<https://doi.org/10.1101/lm.1592510>

Ozawa, T., & Johansen, J. P. (2018). Learning rules for aversive associative memory formation.

Current Opinion in Neurobiology, 49, 148–157. <https://doi.org/10.1016/j.conb.2018.02.010>

Ozawa, T., Ycu, E. A., Kumar, A., Yeh, L. F., Ahmed, T., Koivumaa, J., & Johansen, J. P. (2017). A feedback neural circuit for calibrating aversive memory strength. *Nature Neuroscience*, 20(1), 90–97. <https://doi.org/10.1038/nn.4439>

Packard, M. G., & Wingard, J. C. (2004). Amygdala and “emotional” modulation of the relative use of multiple memory systems. *Neurobiology of Learning and Memory*, 82(3), 243–252. <https://doi.org/10.1016/j.nlm.2004.06.008>

Paré, D., Quirk, G. J., & Ledoux, J. E. (2004). New vistas on amygdala networks in conditioned fear. *Journal of Neurophysiology*, 92(1), 1–9. <https://doi.org/10.1152/jn.00153.2004>

Parsons, R. G., & Ressler, K. J. (2013). Implications of memory modulation for post-traumatic stress and fear disorders. *Nature Neuroscience*, 16(2), 146–153. <https://doi.org/10.1038/nn.3296>

Pavlov, I. P. (1927). *Conditional reflexes*. Dover.

Pawlak, V., Wickens, J. R., Kirkwood, A., & Kerr, J. N. D. (2010). Timing is not everything:

neuromodulation opens the STDP gate. *Frontiers in Synaptic Neuroscience*, 2.

<https://doi.org/10.3389/fnsyn.2010.00146>

Paxinos, G., & Watson, C. (2005). *The rat brain in stereotaxic coordinates* (5th edn). Elsevier Academic Press: Amsterdam.

Phelps, E. A., & LeDoux, J. E. (2005). Contributions of the amygdala to emotion processing: From animal models to human behavior. *Neuron*, 48(2), 175–187.

<https://doi.org/10.1016/j.neuron.2005.09.025>

Phillips, R. G., & LeDoux, J. E. (1992). Differential Contribution of Amygdala and Hippocampus to Cued and Contextual Fear Conditioning. *Behavioral Neuroscience*, 106(2), 274–285.

<https://doi.org/10.1037/0735-7044.106.2.274>

Pierson, L. M., & Trout, M. (2017). What is consciousness for? *New Ideas in Psychology*, 47, 62–71. <https://doi.org/10.1016/j.newideapsych.2017.05.004>

Pitkänen, A., Savander, V., & LeDoux, J. E. (1997). Organization of intra-amygdaloid circuitries in the rat: An emerging framework for understanding functions of the amygdala. *Trends in Neurosciences*, 20(11), 517–523. [https://doi.org/10.1016/S0166-2236\(97\)01125-9](https://doi.org/10.1016/S0166-2236(97)01125-9)

Pitman, R. K., Sanders, K. M., Zusman, R. M., Healy, A. R., Cheema, F., Lasko, N. B., Cahill, L., & Orr, S. P. (2002). Pilot study of secondary prevention of posttraumatic stress disorder with propranolol. *Biological Psychiatry*, 51(2), 189–192. [https://doi.org/10.1016/S0006-3223\(01\)01279-3](https://doi.org/10.1016/S0006-3223(01)01279-3)

Quirarte, G. L., Galvez, R., Roozendaal, B., & McGaugh, J. L. (1998). Norepinephrine release in the amygdala in response to footshock and opioid peptidergic drugs. *Brain Research*, 808(2), 134–140. [https://doi.org/10.1016/S0006-8993\(98\)00795-1](https://doi.org/10.1016/S0006-8993(98)00795-1)

- Quirk, G. J., Armony, J. L., & LeDoux, J. E. (1997). Fear conditioning enhances different temporal components of tone-evoked spike trains in auditory cortex and lateral amygdala. *Neuron*, 19(3), 613–624. [https://doi.org/10.1016/S0896-6273\(00\)80375-X](https://doi.org/10.1016/S0896-6273(00)80375-X)
- Raio, C. M., & Phelps, E. A. (2015). The influence of acute stress on the regulation of conditioned fear. *Neurobiology of Stress*, 1(1), 134–146. <https://doi.org/10.1016/j.ynstr.2014.11.004>
- Ramirez, F., Moscarello, J. M., LeDoux, J. E., & Sears, R. M. (2015). Active avoidance requires a serial basal amygdala to nucleus accumbens shell circuit. *Journal of Neuroscience*, 35(8), 3470–3477. <https://doi.org/10.1523/JNEUROSCI.1331-14.2015>
- Rau, V., & Fanselow, M. S. (2009). Exposure to a stressor produces a long lasting enhancement of fear learning in rats. *Stress*, 12(2), 125–133. <https://doi.org/10.1080/10253890802137320>
- Rescorla, R. A. (1988). Pavlovian conditioning: It's not what you think it is. *American Psychologist*, 43(3), 151–160. <https://doi.org/10.1037/0003-066X.43.3.151>
- Rescorla, R. A., & Wagner, A. R. (1972). A theory of Pavlovian conditioning: Variations in the effectiveness of reinforcement and nonreinforcement. *Classical Conditioning II: Current Research and Theory*, 64–99. <http://scholar.google.com/scholar?hl=en&btnG=Search&q=intitle:A+theory+of+Pavlovian+Conditioning:+variations+in+the+effectiveness+of+reinforcement+and+nonreinforcement#2>
- Ressler, R. L., & Maren, S. (2019). Synaptic encoding of fear memories in the amygdala. *Current Opinion in Neurobiology*, 54, 54–59. <https://doi.org/10.1016/j.conb.2018.08.012>
- Rinaman, L. (2011). Hindbrain noradrenergic A2 neurons: diverse roles in autonomic,

endocrine, cognitive, and behavioral functions. *American Journal of Physiology-Regulatory, Integrative and Comparative Physiology*, 300(2), R222–R235.

<https://doi.org/10.1152/ajpregu.00556.2010>

Robertson, S. D., Plummer, N. W., de Marchena, J., & Jensen, P. (2013). Developmental origins of central norepinephrine neuron diversity. *Nature Neuroscience*, 16(8), 1016–1023.
<https://doi.org/10.1038/nn.3458>

Rodrigues, S. M., Farb, C. R., Bauer, E. P., LeDoux, J. E., & Schafe, G. E. (2004). Pavlovian Fear Conditioning Regulates Thr286 Autophosphorylation of Ca²⁺ /Calmodulin-Dependent Protein Kinase II at Lateral Amygdala Synapses. *Journal of Neuroscience*, 24(13), 3281–3288. <https://doi.org/10.1523/JNEUROSCI.5303-03.2004>

Rodrigues, S. M., LeDoux, J. E., & Sapolsky, R. M. (2009). The Influence of Stress Hormones on Fear Circuitry. *Annual Review of Neuroscience*, 32(1), 289–313.
<https://doi.org/10.1146/annurev.neuro.051508.135620>

Rodrigues, S. M., Schafe, G. E., & Ledoux, J. E. (2004). Molecular mechanisms underlying emotional learning and memory in the lateral amygdala. *Neuron*, 44(1), 75–91.
<https://doi.org/10.1016/j.neuron.2004.09.014>

Rodrigues, S. M., Schafe, G. E., & LeDoux, J. E. (2001). Intra-amygdala blockade of the NR2B subunit of the NMDA receptor disrupts the acquisition but not the expression of fear conditioning. *Journal of Neuroscience*, 21(17), 6889–6896.
<https://doi.org/10.1523/jneurosci.21-17-06889.2001>

Rodriguez-Romaguera, J., Sotres-Bayon, F., Mueller, D., & Quirk, G. J. (2009). Systemic Propranolol Acts Centrally to Reduce Conditioned Fear in Rats Without Impairing

Extinction. *Biological Psychiatry*, 65(10), 887–892.

<https://doi.org/10.1016/j.biopsych.2009.01.009>

Rogan, M. T., & LeDoux, J. E. (1995). LTP is accompanied by commensurate enhancement of auditory-evoked responses in a fear conditioning circuit. *Neuron*, 15(1), 127–136.
[https://doi.org/10.1016/0896-6273\(95\)90070-5](https://doi.org/10.1016/0896-6273(95)90070-5)

Rogan, M. T., Stäubli, U. V., & LeDoux, J. E. (1997). Fear conditioning induces associative long-term potentiation in the amygdala. *Nature*, 390(6660), 604–607.
<https://doi.org/10.1038/37601>

Ronzoni, G., del Arco, A., Mora, F., & Segovia, G. (2016). Enhanced noradrenergic activity in the amygdala contributes to hyperarousal in an animal model of PTSD. *Psychoneuroendocrinology*, 70, 1–9. <https://doi.org/10.1016/j.psyneuen.2016.04.018>

Roozendaal, B., McEwen, B. S., & Chattarji, S. (2009). Stress, memory and the amygdala. *Nature Reviews Neuroscience*, 10(6), 423–433. <https://doi.org/10.1038/nrn2651>

Roozendaal, B., & McGaugh, J. L. (2011). Memory modulation. *Behavioral Neuroscience*, 125(6), 797–824. <https://doi.org/10.1037/a0026187>

Saha, S, Henderson, Z., & Batten, T. F. . (2002). Somatostatin immunoreactivity in axon terminals in rat nucleus tractus solitarii arising from central nucleus of amygdala: coexistence with GABA and postsynaptic expression of sst2A receptor. *Journal of Chemical Neuroanatomy*, 24(1), 1–13. [https://doi.org/10.1016/S0891-0618\(02\)00013-3](https://doi.org/10.1016/S0891-0618(02)00013-3)

Saha, Sikha, Drinkhill, M. J., Moore, J. P., & Batten, T. F. C. (2005). Central nucleus of amygdala projections to rostral ventrolateral medulla neurones activated by decreased blood pressure. *European Journal of Neuroscience*, 21(7), 1921–1930.

<https://doi.org/10.1111/j.1460-9568.2005.04023.x>

Sara, S. J. (2009). The locus coeruleus and noradrenergic modulation of cognition. *Nature Reviews Neuroscience*, 10(3), 211–223. <https://doi.org/10.1038/nrn2573>

Sara, S. J. (2016). Locus coeruleus reports changes in environmental contingencies. *The Behavioral and Brain Sciences*, 39, e223. <https://doi.org/10.1017/S0140525X15001946>

Sara, S. J., & Bouret, S. (2012). Orienting and Reorienting: The Locus Coeruleus Mediates Cognition through Arousal. *Neuron*, 76(1), 130–141.

<https://doi.org/10.1016/j.neuron.2012.09.011>

Sauter, D. A., Eisner, F., Ekman, P., & Scott, S. K. (2010). Cross-cultural recognition of basic emotions through nonverbal emotional vocalizations. *Proceedings of the National Academy of Sciences*, 107(6), 2408–2412. <https://doi.org/10.1073/pnas.0908239106>

Scarantino, A. (2018). Are LeDoux's survival circuits basic emotions under a different name? *Current Opinion in Behavioral Sciences*, 24, 75–82.

<https://doi.org/10.1016/j.cobeha.2018.06.001>

Schafe, G. E., Atkins, C. M., Swank, M. W., Bauer, E. P., Sweatt, J. D., & LeDoux, J. E. (2000). Activation of ERK/MAP kinase in the amygdala is required for memory consolidation of Pavlovian fear conditioning. *Journal of Neuroscience*, 20(21), 8177–8187.

<https://doi.org/10.1523/jneurosci.20-21-08177.2000>

Schiff, H. C., Johansen, J. P., Hou, M., Bush, D. E. A., Smith, E. K., Klein, J. A. E., LeDoux, J. E., & Sears, R. M. (2017). β -Adrenergic Receptors Regulate the Acquisition and Consolidation Phases of Aversive Memory Formation Through Distinct, Temporally Regulated Signaling Pathways. *Neuropsychopharmacology*, 42(4), 895–903.

<https://doi.org/10.1038/npp.2016.238>

Schiller, D., Kanen, J. W., LeDoux, J. E., Monfils, M. H., & Phelps, E. A. (2013). Extinction during reconsolidation of threat memory diminishes prefrontal cortex involvement.

Proceedings of the National Academy of Sciences of the United States of America, 110(50), 20040–20045. <https://doi.org/10.1073/pnas.1320322110>

Schönberg, T., Daw, N. D., Joel, D., & O'Doherty, J. P. (2007). Reinforcement learning signals in the human striatum distinguish learners from nonlearners during reward-based decision making. *Journal of Neuroscience*, 27(47), 12860–12867.

<https://doi.org/10.1523/JNEUROSCI.2496-07.2007>

Schreiber, A., & Gimbel, S. (2010). Evolution and the Second Law of Thermodynamics: Effectively Communicating to Non-technicians. *Evolution: Education and Outreach*, 3(1), 99–106. <https://doi.org/10.1007/s12052-009-0195-3>

Schwabe, L., Joëls, M., Roozendaal, B., Wolf, O. T., & Oitzl, M. S. (2012). Stress effects on memory: An update and integration. *Neuroscience & Biobehavioral Reviews*, 36(7), 1740–1749. <https://doi.org/10.1016/j.neubiorev.2011.07.002>

Seabold, S., & Perktold, J. (2010). 9th Python in Science Conference. *Statsmodels: Econometric and Statistical Modeling with Python*.

Sears, R. M., Fink, A. E., Wigestrland, M. B., Farb, C. R., De Lecea, L., & LeDoux, J. E. (2013). Orexin/hypocretin system modulates amygdala-dependent threat learning through the locus coeruleus. *Proceedings of the National Academy of Sciences of the United States of America*, 110(50), 20260–20265. <https://doi.org/10.1073/pnas.1320325110>

Seda, G., Sanchez-Ortuno, M. M., Welsh, C. H., Halbower, A. C., & Edinger, J. D. (2015).

Comparative Meta-Analysis of Prazosin and Imagery Rehearsal Therapy for Nightmare Frequency, Sleep Quality, and Posttraumatic Stress. *Journal of Clinical Sleep Medicine*, 11(01), 11–22. <https://doi.org/10.5664/jcsm.4354>

Shrestha, P., Ayata, P., Herrero-Vidal, P., Longo, F., Gastone, A., LeDoux, J. E., Heintz, N., & Klann, E. (2020). Cell-type-specific drug-inducible protein synthesis inhibition demonstrates that memory consolidation requires rapid neuronal translation. *Nature Neuroscience*, 23(2), 281–292. <https://doi.org/10.1038/s41593-019-0568-z>

Silva, B. A., Gross, C. T., & Gräff, J. (2016). The neural circuits of innate fear: Detection, integration, action, and memorization. *Learning and Memory*, 23(10), 544–555. <https://doi.org/10.1101/lm.042812.116>

Sokolov, E. N. (1963). Higher Nervous Functions: The Orienting Reflex. *Annual Review of Physiology*, 25(1), 545–580. <https://doi.org/10.1146/annurev.ph.25.030163.002553>

Southwick, S. M., Krystal, J. H., Bremner, J. D., Morgan 3rd, C. A., Nicolaou, A. L., Nagy, L. M., Johnson, D. R., Heninger, G. R., & Charney, D. S. (1997). Noradrenergic and Serotonergic Function in Posttraumatic Stress Disorder. *Archives of General Psychiatry*, 54(8), 749. <https://doi.org/10.1001/archpsyc.1997.01830200083012>

Squire, L., Berg, D., Bloom, F. E., du Lac, S., Ghosh, A., & Spitzer, N. C. (Eds.). (2012). *Fundamental Neuroscience* (4th ed.). Academic Press.

Stachenfeld, K. L., Botvinick, M. M., & Gershman, S. J. (2017). The hippocampus as a predictive map. *Nature Neuroscience*, 20(11), 1643–1653. <https://doi.org/10.1038/nn.4650>

Sun, F., Zeng, J., Jing, M., Zhou, J., Feng, J., Owen, S. F., Luo, Y., Li, F., Wang, H., Yamaguchi, T., Yong, Z., Gao, Y., Peng, W., Wang, L., Zhang, S., Du, J., Lin, D., Xu, M.,

Kreitzer, A. C., ... Li, Y. (2018). A Genetically Encoded Fluorescent Sensor Enables Rapid and Specific Detection of Dopamine in Flies, Fish, and Mice. *Cell*, 174(2), 481-496.e19. <https://doi.org/10.1016/j.cell.2018.06.042>

Swanson, L. W., & Hartman, B. K. (1975). The central adrenergic system. An immunofluorescence study of the location of cell bodies and their efferent connections in the rat utilizing dopamine-B-hydroxylase as a marker. *The Journal of Comparative Neurology*, 163(4), 467–505. <https://doi.org/10.1002/cne.901630406>

Swanson, L. W., & Petrovich, G. D. (1998). What is the amygdala? *Trends in Neurosciences*, 21(8), 323–331. [https://doi.org/10.1016/S0166-2236\(98\)01265-X](https://doi.org/10.1016/S0166-2236(98)01265-X)

Thompson, R. F., & Steinmetz, J. E. (2009). The role of the cerebellum in classical conditioning of discrete behavioral responses. *Neuroscience*, 162(3), 732–755. <https://doi.org/10.1016/j.neuroscience.2009.01.041>

Tovote, P., Esposito, M. S., Botta, P., Chaudun, F., Fadok, J. P., Markovic, M., Wolff, S. B. E., Ramakrishnan, C., Fenno, L., Deisseroth, K., Herry, C., Arber, S., & Lüthi, A. (2016). Midbrain circuits for defensive behaviour. *Nature*, 534(7606), 206–212. <https://doi.org/10.1038/nature17996>

Tully, K., & Bolshakov, V. Y. (2010). Emotional enhancement of memory: How norepinephrine enables synaptic plasticity. *Molecular Brain*, 3(1), 1–9. <https://doi.org/10.1186/1756-6606-3-15>

Tully, K., Li, Y., Tsvetkov, E., & Bolshakov, V. Y. (2007). Norepinephrine enables the induction of associative long-term potentiation at thalamo-amygdala synapses. *Proceedings of the National Academy of Sciences of the United States of America*, 104(35), 14146–14150.

<https://doi.org/10.1073/pnas.0704621104>

Uematsu, A., Tan, B. Z., & Johansen, J. P. (2015). Projection specificity in heterogeneous locus coeruleus cell populations: Implications for learning and memory. *Learning and Memory*, 22(9), 444–451. <https://doi.org/10.1101/lm.037283.114>

Uematsu, A., Tan, B. Z., Ycu, E. A., Cuevas, J. S., Koivumaa, J., Junyent, F., Kremer, E. J., Witten, I. B., Deisseroth, K., & Johansen, J. P. (2017). Modular organization of the brainstem noradrenaline system coordinates opposing learning states. *Nature Neuroscience*, 20(11), 1602–1611. <https://doi.org/10.1038/nn.4642>

Valentino, R. J., & Van Bockstaele, E. (2008). Convergent regulation of locus coeruleus activity as an adaptive response to stress. *European Journal of Pharmacology*, 583(2–3), 194–203. <https://doi.org/10.1016/j.ejphar.2007.11.062>

Vazey, E. M., & Aston-Jones, G. (2014). Designer receptor manipulations reveal a role of the locus coeruleus noradrenergic system in isoflurane general anesthesia. *Proceedings of the National Academy of Sciences*, 111(10), 3859–3864.

<https://doi.org/10.1073/pnas.1310025111>

Vazey, E. M., Moorman, D. E., & Aston-Jones, G. (2018). Phasic locus coeruleus activity regulates cortical encoding of salience information. *Proceedings of the National Academy of Sciences*, 115(40), E9439–E9448. <https://doi.org/10.1073/pnas.1803716115>

Vetere, G., Piserchia, V., Borreca, A., Novembre, G., Aceti, M., & Ammassari-Teule, M. (2013). Reactivating fear memory under propranolol resets pre-trauma levels of dendritic spines in basolateral amygdala but not dorsal hippocampus neurons. *Frontiers in Behavioral Neuroscience*, 7. <https://doi.org/10.3389/fnbeh.2013.00211>

- Walker, D. L., & Davis, M. (2002). Light-enhanced startle: further pharmacological and behavioral characterization. *Psychopharmacology*, 159(3), 304–310.
<https://doi.org/10.1007/s002130100913>
- Weisskopf, M. G., Bauer, E. P., & LeDoux, J. E. (1999). L-type voltage-gated calcium channels mediate NMDA-independent associative long-term potentiation at thalamic input synapses to the amygdala. *Journal of Neuroscience*, 19(23), 10512–10519.
<https://doi.org/10.1523/JNEUROSCI.19-23-10512.1999>
- Wilensky, A. E., Schafe, G. E., Kristensen, M. P., & LeDoux, J. E. (2006). Rethinking the Fear Circuit: The Central Nucleus of the Amygdala Is Required for the Acquisition, Consolidation, and Expression of Pavlovian Fear Conditioning. *Journal of Neuroscience*, 26(48), 12387–12396. <https://doi.org/10.1523/JNEUROSCI.4316-06.2006>
- Yehuda, R., Joëls, M., & Morris, R. G. M. (2010). The memory paradox. *Nature Reviews Neuroscience*, 11(12), 837–839. <https://doi.org/10.1038/nrn2957>
- Yokoyama, M., Suzuki, E., Sato, T., Maruta, S., Watanabe, S., & Miyaoka, H. (2005). Amygdalic levels of dopamine and serotonin rise upon exposure to conditioned fear stress without elevation of glutamate. *Neuroscience Letters*, 379(1), 37–41.
<https://doi.org/10.1016/j.neulet.2004.12.047>
- Yu, A. J., & Dayan, P. (2005). Uncertainty, neuromodulation, and attention. *Neuron*, 46(4), 681–692. <https://doi.org/10.1016/j.neuron.2005.04.026>
- Yu, K., Ahrens, S., Zhang, X., Schiff, H., Ramakrishnan, C., Fenno, L., Deisseroth, K., Zhao, F., Luo, M.-H. H., Gong, L., He, M., Zhou, P., Paninski, L., & Li, B. (2017). The central amygdala controls learning in the lateral amygdala. *Nature Neuroscience*, 20(12), 1680–

1685. <https://doi.org/10.1038/s41593-017-0009-9>

Yu, K., Garcia da Silva, P., Albeanu, D. F., & Li, B. (2016). Central Amygdala Somatostatin Neurons Gate Passive and Active Defensive Behaviors. *The Journal of Neuroscience*, 36(24), 6488–6496. <https://doi.org/10.1523/JNEUROSCI.4419-15.2016>

Zhu, L., & Onaka, T. (2002). Involvement of medullary A2 noradrenergic neurons in the activation of oxytocin neurons after conditioned fear stimuli. *European Journal of Neuroscience*, 16(11), 2186–2198. <https://doi.org/10.1046/j.1460-9568.2002.02285.x>

Zurich Instruments. (2016). *Principles of lock-in detection and the state of the art*.